Odudu, Aghogho (2013) Characterising haemodialysis-associated cardiomyopathy using deformation imaging by cardiovascular magnetic resonance tagging and speckle-tracking echocardiography. PhD thesis, University of Nottingham.

Characterising haemodialysis-associated cardiomyopathy using deformation imaging by cardiovascular magnetic resonance tagging and speckle-tracking echocardiography

Aghogho Odudu

MB ChB, MRCP (UK)

Thesis submitted to the Division of Medical Sciences and Graduate Entry Medicine,

University of Nottingham

for the degree of Doctor of Philosophy

November 2013

"Everything should be made as simple as possible, but no simpler."

Albert Einstein

Table of Contents

Table of Figures

Except where acknowledged, I declare that this thesis is entirely my own work and is based upon research carried out in the School of Graduate Entry Medicine and Health, University of Nottingham and four NHS research sites within a 40 mile radius between January 2009 and January 2013. Ethical and local approval for this work was sought and gained by myself with the exception of a single protocol amendment which was obtained by Dr Tarek Eldehni. The main study funding application was made by Prof Chris McIntyre to the National Institute of Health Research. I also obtained personal funding in the form of a British Heart Foundation Clinical Research Training Fellowship Grant. All patients were recruited by myself and Dr Eldehni. All cardiac magnetic resonance (CMR) scans were performed by radiographers in 2 research sites under the supervision of myself or Dr Tarek Eldehni. All dialysis data including echocardiography was collected by myself or Dr Tarek Eldehni. This involved travelling to all four dialysis centres with the haemodynamic monitoring equipment to study patients on dialysis at their usual dialysis times. Either Dr Eldehni or I arranged participant transport for study visits to ensure patients' safety. Both Dr Eldehni and I attended courses in cardiac magnetic resonance and cardiac ultrasound image acquisition. I personally analysed all cardiac imaging. I was trained in CMR analysis by a senior cardiologist with expertise in CMR, Dr Gerry McCann of Leicester NIHR Cardiovascular Biomedical Research Unit. I also reanalysed a proportion of blinded data analyses from a training data set previously analysed by Gerry McCann and then had a series of meetings to review

discrepancies to the unblinded analyses until such time that I achieved a formally calculated inter-observer variability within that of other trained analysers in the CMR service which Dr McCann leads. Biochemical and haematological data were provided by the laboratories at Derby Hospitals NHS Foundation Trust or Sheffield teaching Hospitals NHS Foundation Trust. All statistical analysis were performed by me and then verified prior to publication by Mr Apostolos Fakis, an independent statistician, especially in the case of more complex statistical models.

Aghogho Odudu

January 2013

Publications and abstracts arising from this thesis

Peer-reviewed publications

1. **Odudu A**, Francis ST, McIntyre CW. MRI for the assessment of organ perfusion in patients with chronic kidney disease *Curr Opin Nephrol Hypertens* 2012 Sep 24.

2. **Odudu A**, McIntyre CW. Volume is not the only key to hypertension control in dialysis patients. *Nephron Clin Pract* 2012;120(3):c173-c177

3. **Odudu A**, Eldehni MT, Fakis A, McIntyre C. Rationale and design of a multi-centre randomised controlled trial of individualised cooled dialysate to prevent left ventricular systolic dysfunction in haemodialysis patients. *BMC Nephrol.* 2012 Jun 21;13(1):45.

4. **Odudu A,** McIntyre CW Influence of dialysis therapies in the development of cardiac disease in CKD. *Journal of Renal Care.* 2010: 36(Suppl. 3):47-54

5. McIntyre CW, **Odudu A**, Eldehni MT. Cardiac assessment in chronic kidney disease. *Curr Opin Nephrol Hypertens*. 2009;18(6):501-6.

Oral presentations

- **A Odudu**, MT Eldehni, and CW McIntyre. Circumferential strain is globally reduced in incident haemodialysis patients despite normal left ventricular ejection fraction: insights from a cardiac magnetic resonance tagging study. **ISBP Trustees best abstract prize,** *International Society of Blood Purification, Los Angeles, September 2010.*

- **Aghogho Odudu**, Mohamed Tarek Eldehni and Christopher W. McIntyre. Left ventricular systolic strain and rotation is reduced in incident haemodialysis patients despite normal ejection fraction: insights from a cardiac magnetic resonance tagging study. *Renal Association, Birmingham, June 2011.*

- **Aghogho Odudu**, Mohamed Tarek Eldehni, Laura Leighton, Shvan Korsheed and Christopher W. McIntyre. Investigation of the effects of arteriovenous fistula formation on left ventricular function. *Renal Association, Birmingham, June 2011.*

- **A Odudu.** Cardiac imaging in CKD. **Invited speaker** to a plenary session of the *1st meeting of the European Cardionephrology Association, Assisi, Italy,* March 2010*.*

- **A Odudu**. Characterising Organ Insults in Haemodialysis. **Invited speaker,** *Renal Association SpR Club Meeting, Bristol, March 2012.*

Poster presentations

- Mohamed Tarek Eldehni, **Aghogho Odudu** and Christopher McIntyre. Reduced early diastolic left ventricular circumferential strain in haemodialysis patients: insights from a cardiac magnetic resonance tagging study. *UK Renal Association, Birmingham, June 2011.*

- Laura Leighton, **Aghogho Odudu**, Mohamed Tarek Eldehni, Shvan Korsheed and Christopher W. McIntyre. Investigation of the effects of arteriovenous fistula formation on left ventricular function. *Oral presentation. UK Renal Association, Birmingham, June 2011.*

- Laura Leighton, Mohamed Tarek Eldehni, **Aghogho Odudu**, Shvan Korsheed and Christopher McIntyre. Formation of an arteriovenous fistula does not adversely impact on cardiac function: insights from a study utilising serial speckle tracking echocardiography. *ISN Meeting Vancouver April 2011*

- **Aghogho Odudu**, Mohamed Tarek Eldehni and Christopher W. McIntyre. Left ventricular systolic strain and rotation is reduced in incident haemodialysis patients despite normal ejection fraction: insights from a cardiac magnetic resonance tagging study. *ISN Meeting Vancouver April 2011*

- **A Odudu,** MT Eldehni, CW McIntyre. Left ventricular torsion is an early marker of myocardial dysfunction in incident haemodialysis patients. American Society of Nephrology*, Denver,* November 2010.

Introduction

1. Introduction

1.1.   Normal functions of the kidney

The kidneys are two intra-abdominal organs found in all mammals. In humans, they are relatively small measuring 9-13 centimetres in length. Despite their small size they receive 25% of cardiac output, and have the highest perfusion rate per-unit mass of all organs. Their principal function is excretion of excess fluid and electrolytes. In addition the kidneys also provide acid-base homeostasis, regulation of blood pressure, and production of hormones involved in red blood cell production and vitamin D metabolism. Therefore, kidney disease has wide ranging consequences and complications.

1.2.   Definition of chronic kidney disease

The definition of chronic kidney disease is currently based on impairment of renal excretory function and chronicity, being diagnosed if there is evidence of kidney damage for more than 3 months. Measurement of renal excretory function involves blood testing for measurement of serum creatinine which is corrected in a formula that includes terms for age, gender and ethnicity to derive an estimation of the glomerular filtration rate (GFR). In health, the GFR approximates 100-120 ml/min/1.73m^2. CKD is divided into five stages depending on the GFR (Table 1-1). When the GFR declines to less than 15 the term End Stage Renal Disease (ESRD) is used. This is synonymous with

the terms End Stage Renal Failure (ESRD) and Established Renal Failure (ERF).

Table 1-1 National Institute of Clinical Excellence Classification of CKD (2008) [1]

Stage	GFR	Description
1	90	Normal kidney function but urine findings or structural abnormalities or genetic trait point to kidney disease
2	60-89	Mildly reduced kidney function, and other findings (as for stage 1) point to kidney disease
3A 3B	45-59 30-44	Moderately reduced kidney function
4	15-29	Severely reduced kidney function
5	< 15	Very severe, or end stage kidney disease (sometimes call established renal failure)

1.3. Epidemiology of Chronic Kidney Disease

Chronic Kidney Disease (CKD) is an increasingly recognised global public health problem. As it is asymptomatic, estimates of prevalence rely on community screening studies. As methodology and populations vary there is wide variation (Table 1-2).

Table 1-2 CKD prevalence in a range of populations [2]

Country	Study	Number of subjects	Age of subjects	Definition of CKD	Prevalence of CKD
Australia	AUSDIAB	11247	≥25	CKD 1-5	16%
D.R of Congo	Sumaili et al.	503	≥20	CKD 1-5	12.40%
Netherlands	PREVEND	8459	28-75	CKD 1-5	12%
Norway	HUNT 2	65604	≥20	CKD 3-5	4.70%
South China	Chen et al.	6311	>20	CKD 1-5	12.10%
Spain	EPIRCE	2746	≥20	CKD 3-5	6.80%
Thailand	THAI SEEK	3459	≥8	CKD 1-4	17.50%
Tibet	Chen et al.	1289	≥18	CKD 1-5	19.10%
UK	CKD-QI	930997	Any	CKD 3-5	5.41%
UK	NEOERICA	38262	≥18	CKD 3-5	8.50%
USA	NHANES IV	13233	≥20	CKD 1-4	13.10%

In the UK, prevalence of CKD stage 3-5 is estimated at 5-8.5% and prevalence increases with age [3, 4]. The majority of these people have stage 3 CKD and are followed up in primary care. The prevalence of CKD in the UK is predicted to rise sharply due to the combined effects of an ageing population, and epidemics of obesity, diabetes and cardiovascular disease [5, 6]. Currently, diabetes and cardiovascular disease are the two biggest causes of ESRD in the UK [7]. It is notable that most people with CKD will not reach ESRD and are far more likely to die from cardiovascular disease [8]. Preliminary data suggest that cardiovascular disease may also be a risk

factor for CKD progression. Thus kidney and cardiovascular disease may exacerbate each other, leading to a vicious circle of progressive cardiovascular and renal decline [9].

1.4. Renal replacement therapy

CKD stage 5 or ESRD is treated by renal replacement therapy or actively managed with conservative non-dialytic care in a pathway that includes palliative care. Renal replacement therapy (RRT) aims to replace the functions of the kidney. The gold standard is renal transplantation as if successful this will replace all the functions of the kidney and patients are not tied to a regime of regular dialysis. However there is a limited pool of donors and the majority of incident patients have a choice between haemodialysis and peritoneal dialysis. Haemodialysis (HD) is a process which involves removal of blood into a machine where the blood is purified by filtration across a semi-permeable membrane and then returned to the patient (Figure 1-1).

Figure 1-1- Haemodialysis
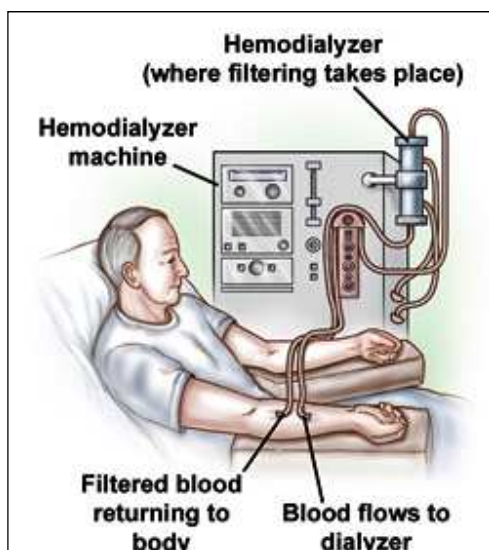
HD requires access to a large vein and this is usually in the form of an arteriovenous fistula. It is a resource intensive treatment typically using 120 litres of highly purified water per patient-treatment session, which is further heated to between 35 and 37°C to prevent excessive blood heat loss. It also requires a dialysis monitor and technical expertise. It only replaces the excretory function of the kidney. HD is usually in hospital and typically occurs 3 times per week for 4 hours per session. A minority of patients and their carers have been trained to deliver the treatment at home. Peritoneal dialysis (PD) involves insertion of a synthetic tube into the peritoneal space which lies within the abdomen surrounding the bowel and intra-abdominal organs. It uses the peritoneum as the semi-permeable membrane across which waste products diffuse (Figure 1-2). Fluid is drained into the abdomen and after a few hours, fluid and the waste products are drained out. It is primarily a self-delivered treatment and so can be performed at home.

Figure 1-2- Principle of peritoneal dialysis
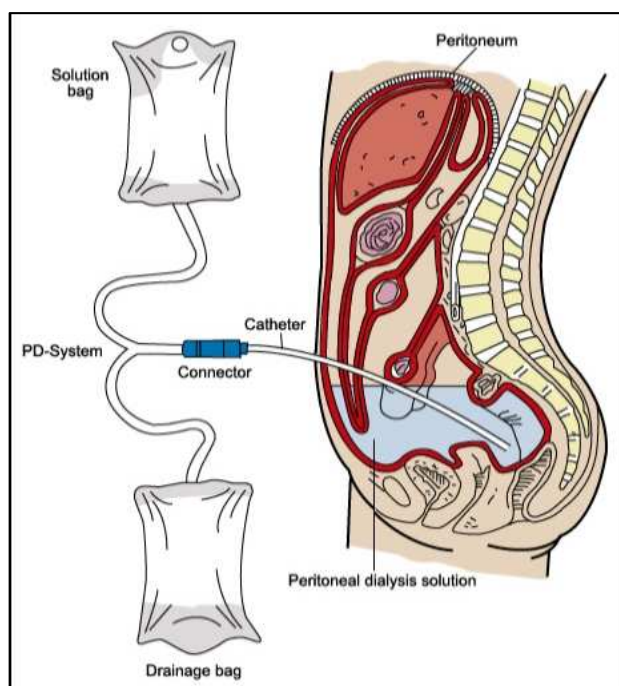
Currently there are 51,000 patients in the UK receiving RRT (Figure 1-3). Renal transplantation is the most prevalent form of RRT accounting for 49%, in-centre HD accounts for 43% and 8% have PD [10].

Figure 1-3 Treatment modality in prevalent RRT patients in the UK on 31/12/2010 [10]
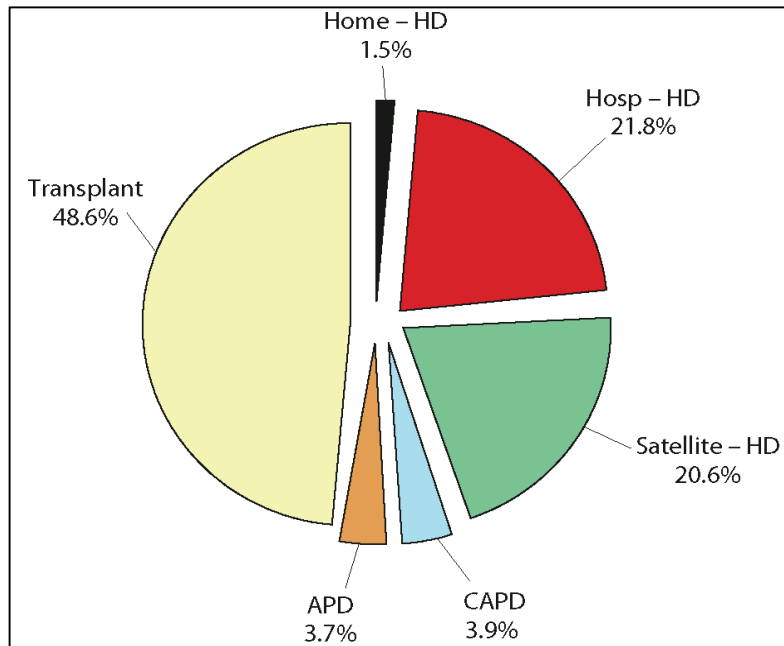
The projected 5-7% annual increase in RRT patients will predominantly be in the in-centre HD population and this is reflected in Figure 1-4 [10].

Figure 1-4   Growth in prevalent RRT patients by treatment modality in the UK 1997-2010 [10]
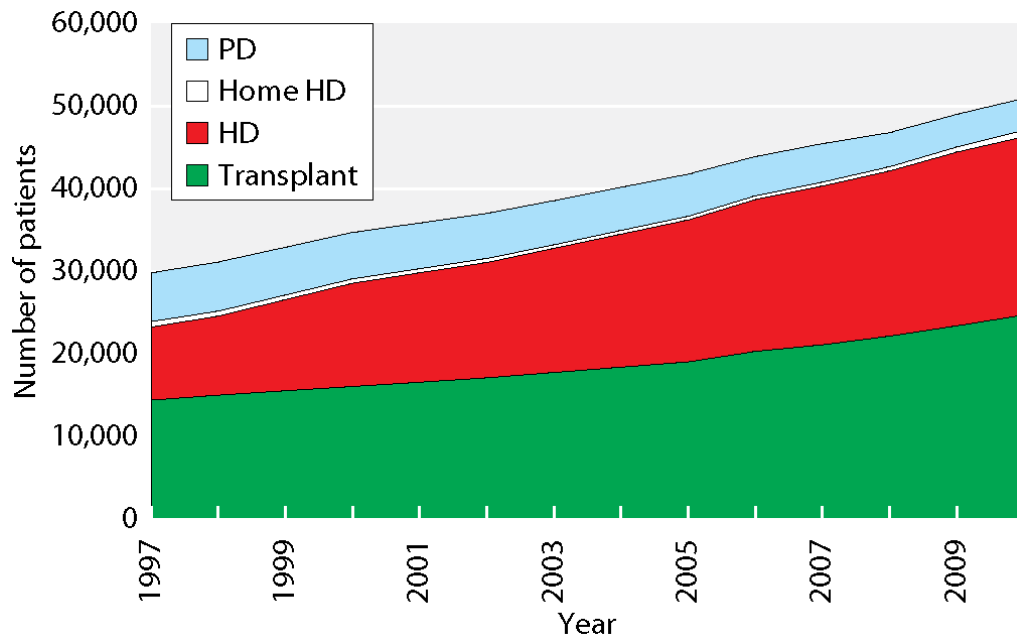
Background

2. Background

2.1. Risk factors for cardiovascular disease in dialysis patients

The aim of this section is to describe the background to the development of my study hypothesis. This requires an appreciation that cardiovascular risk in HD patients cannot be fully explained by traditional risk factors. I will describe the influence of non-traditional risk factors, reverse causality and the possibility that HD may itself promulgate some of the excessive rates of cardiovascular morbidity and mortality. Thus, modifications to the process of HD may be the key to improving outcomes. It is well recognised that dialysis patients suffer excess cardiac morbidity and mortality [11, 12]. Figure 2-1 shows US derived data for the cardiovascular mortality rates by age and ethnicity for dialysis patients and healthy controls. The y-axis is a logarithmic scale, emphasising the excess of cardiovascular death. It is also appreciated that the causes of mortality have a distinctly different pattern to the general population [13]. Increased mortality is driven by a combination of sudden cardiac death and heart failure as can be seen in Figure 2-2 from 2011 US Renal Data System Report [14].

Figure 2-1 : Graph showing the cardiovascular mortality rates by age and ethnicity for dialysis patients and healthy controls from US registry data [11].
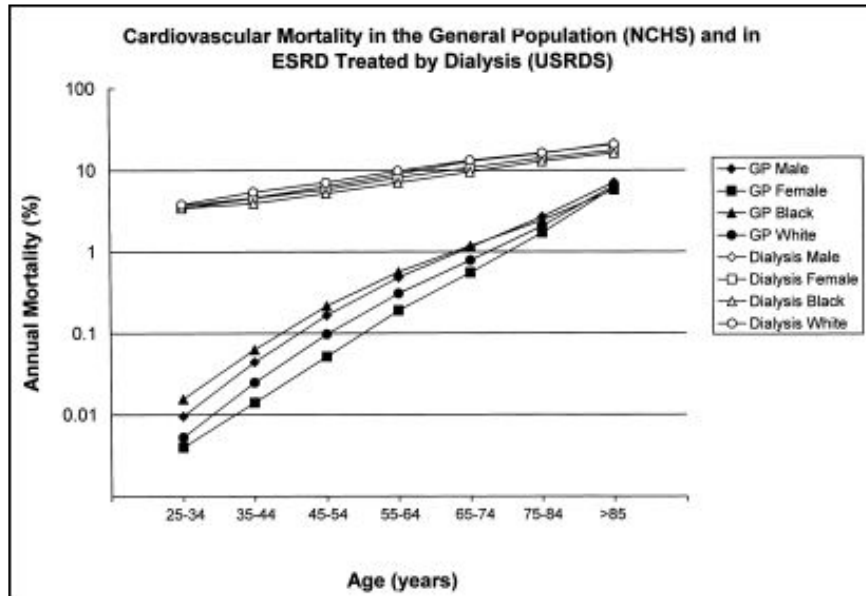
Figure 2-2- Causes of death in prevalent US dialysis patients from 2011 US Renal Data System annual report; AMI, acute myocardial infarction; CHF, congestive heart failure; CVA, cerebrovascular accident[14].
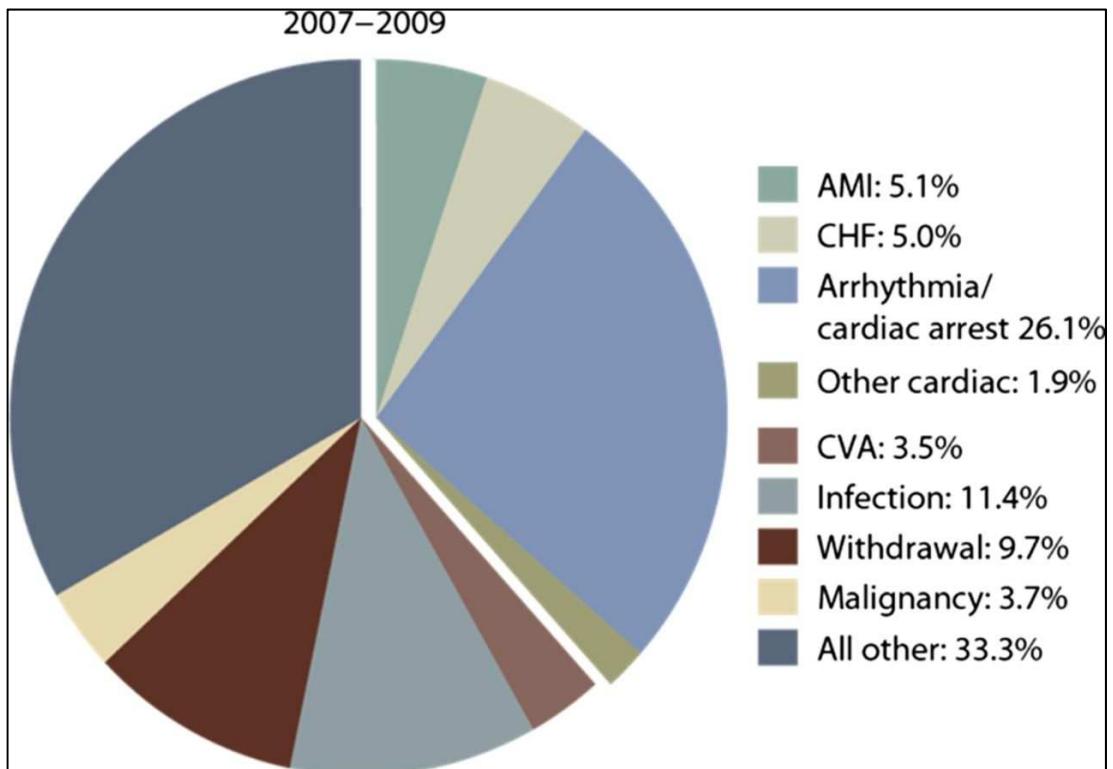
Since the widespread use of weight independent formulae to estimate GFR, there is accumulating data that this excess cardiovascular risk occurs in earlier stages of CKD and has a graded and linear association of GFR [15]. Increased mortality in CKD cannot solely be explained by accumulation of traditional risk factors for atherosclerosis and cardiovascular disease (Table 2-1, Table 2-2). Indeed many traditional risk factors display 'reverse causality' a termed coined to describe their paradoxical behaviour compared to the general population.

Table 2-1 Predicted 5 year cardiovascular risk and the observed 5 year cardiovascular risk using the New Zealand Cardiovascular Risk Calculator (n = 274)[16]

No. of patients	Predicted 5 years CVD risk	Observed 5 years CVD
6	>30%	66.6%
7	25–30%	71.4%
13	20–25%	61.5%
14	15–20%	50%
52	10–15%	36.5%
92	5–10%	27.1%
39	2.5–5%	10.2%
51	<2.5%	3.9%

Table 2-2- Cardiovascular risk factors in CKD patients

Traditional risk factors	Non-traditional risk factors
Hypertension	Albuminuria
Diabetes	Abnormal calcium/phosphate metabolism
Smoking	Hypervolaemia/Over-hydration
Hypercholesterolaemia	Oxidative stress
Male sex	Malnutrition
Age	Inflammation
Family history	Anaemia
Obesity	Vascular calcification
Hyperglycaemia	Arterial stiffness
Left ventricular hypertrophy	Advanced-Glycation End Product deposition

2.1.1. Hypertension

There is a strong and linear risk association of BP to cardiovascular morbidity and mortality in the general population. A recent- meta-analysis including one million adults confirmed this risk is reduced by anti-hypertensive drug therapy with no evidence of a threshold at which risk reduction stops down to at least 115/75 mm Hg [17]. Hypertension is an independent risk factor for left ventricular hypertrophy, ischaemic heart disease, cardiac failure, stroke, and cardiovascular mortality [18]. Cardiovascular mortality is increased three-fold in patients starting dialysis therapy with uncontrolled hypertension [19]. However, the relationship of risk to hypertension is fundamentally more complicated in ESRD. Large observational studies of HD patients consistently show a J or U-shaped association, with a paradoxical survival advantage in hypertensive patients and the highest mortality in hypotensive patients after multivariable adjustment depicted in Figure 2-3 [20, 21]. Based on this some have cautioned against using drug therapy to lower blood pressure in hypertensive dialysis patients. Meta-analyses have suggested benefit of using drugs [22]. However the meta-analyses themselves were criticised for the wide heterogeneity of studies included and whether lowering blood pressure in HD patients reduces mortality is far from clear [23]. The cause of the J-curve has been widely debated and its existence has been questioned. However it has been clearly demonstrated in other high-risk populations such as coronary artery disease, and the most commonly cited explanations include a confounding effect of co-morbidity such as heart failure, malnutrition or cancer and decreased coronary flow reserve due to arterial stiffness [24].

Figure 2-3 - J shaped association of systolic BP to 15 month cardiovascular mortality in 40,933 HD patients [20].

Post-Dialysis Systolic BP (mmHg)
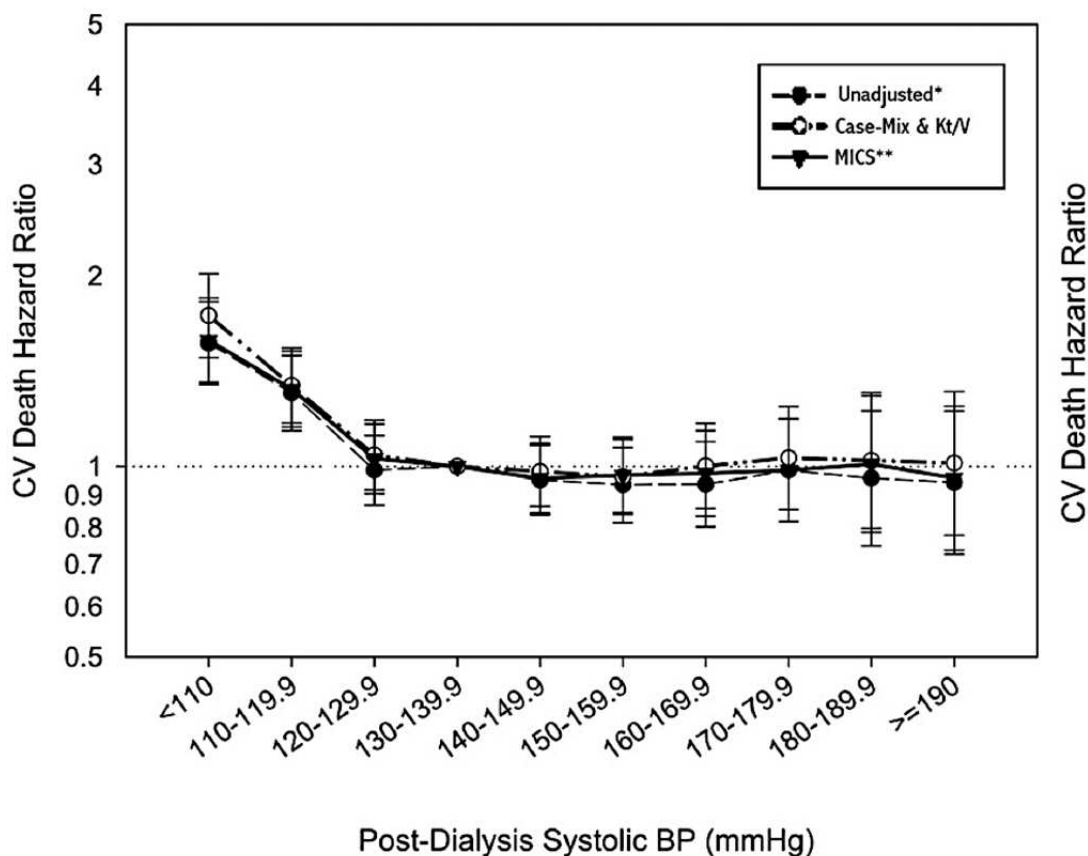
2.1.2. Hypervolaemia

The mechanisms underlying hypertension in HD patients are complex and include overactivity of the renin-angiotensin-aldosterone system, abnormal endothelial function and iatrogenic factors such as use of erythropoiesis stimulating agents. However in ESRD the principal reason for hypertension is the loss of renal regulation of salt and water excretion [25]. This leads to extra-cellular volume overload (synonymous with hypervolaemia or overhydration) with consequent adverse cardiac remodelling and higher inter-dialytic weight gain [18, 26]. As such, the principle approach is to use a

combination of ultrafiltration by dialysis to dry-weight and antihypertensive therapy to control BP.

2.1.2.1.　Methods to determine and optimise volume status

Whilst achieving euvolaemia or dry weight is an uncontroversial target, the best way to determine this is unclear. Dry weight is currently based on imprecise empirical observations in most centres and commonly defined as the lowest body weight a patient can tolerate without developing intra-dialytic or inter-dialytic hypotension. The frequent risk of dialysis related hypo-perfusion is due to imprecision in the assessment of dry weight. If dry weight could be accurately, reliably and practicably determined then we would not have to resort to 'probing' for this by trial and error with the risks outlined. Two developments in the assessment of dry weight are worthy of mention. Intradialytic relative blood volume (RBV) monitoring uses a photo-optical technique to noninvasively measure real-time absolute hematocrit through equipment attached at the arterial end of the dialyser. Graphs of RBV against time have been proven to predict interdialytic reductions in blood pressure [27]. RBV changes are closely related to ultrafiltration and plasma-refill rate. However plasma refilling is impaired in autonomic dysfunction, which is common in HD patients. This reduces the specificity of RBV change to direct HD prescription and there is no data that its use can improve outcomes [28]. One of the most promising methods is bioelectrical impedance analysis (BIA). It measures resistance which is proportional to tissue water and reactance which is proportional to cell mass providing an index of volume status which can be longitudinally monitored. The difficulty arises in

converting this measure of relative hydration into absolute volumes of fluid as they require algorithms using assumptions from studies of healthy volunteers that perform poorly when applied to populations with disordered hydration. We conducted a study showing the added value of combining the relative hydration data from bioimpedance with absolute hydration data from a novel deuterium breath-test by portable mass spectrometer [29]. This highlighted that higher co-morbidity scores led to increasing underestimation of extracellular volume by bioimpedance [29]. Recently two novel approaches to quantify excess hydration by bioimpedance have been proposed. Assessment of continuous intra-dialytic calf bioimpedance ratios does not rely on geometric assumptions or comparison to population averages typical of whole-body methods [24]. Chamney et al proposed a three compartment physiological tissue model allowing quantification of excess fluid compared to normal controls [30]. Whilst requiring a population reference standard, the unique separation of extracellular volume into that due to excess and normal hydration is an important conceptual advance and has been shown to be of prognostic value in predicting mortality in a HD population [31]. Machek et al have used this new approach to perform bioimpedance guided prescription of dry weight in 52 HD patients. They showed that not only did this assist in dealing with hypertension in the overhydrated but it enabled a 73% reduction in intradialytic adverse events by increasing the target weight in the under-hydrated group [32]. These preliminary data are promising but whether this will be of a discernible long-term value requires studies randomising clinicians to be blinded or have access to bioimpedance data and such studies have commenced (ISRCTN 95439739).

2.1.2.2. Complex relationship of hypertension to hypervolaemia

The existence of overhydration in hypertensive dialysis patients is far from universal. Wabel and co-workers measured pre-dialysis systolic BP and fluid status in 500 HD patients by bioimpedance monitoring (compared to a matched healthy population). Only 15% of patients fitted the stereotype of overhydration with hypertension. 13% of patients had hypertension despite under-hydration and 10% had overhydration despite normal or low BP [33]. Similar findings were seen in a another study using the same methodology in 639 patients using peritoneal dialysis (PD) Figure 2-4 [34]. These studies highlight that although physicians often estimate hydration status by blood pressure, the two factors are often dissociated in the setting of the physiological derangements characteristic of ESRD. A wide variety of pathophysiological mechanisms may contribute to this dissociation.

Figure 2-4- Scatter plot of the relation between absolute delta tissue hydration (litres) in the X-axis and systolic BP (mmHg) in the Y-axis in patients of the EuroBCM study cohort of 639 dialysis patients. Different zones of patients can be seen in the plot. Zone A patients (27%) are both normohydrated and normotensive. Zone B (26%) are both fluid overloaded and hypertensive. Zone C (13%), are hypertensive despite being normal or underhydrated Zone D, (28%) are normo- and hypotensive despite being fluid overloaded. Zone E (7%) are hypotensive and normohydrated or normotensive and underhydrated [34].
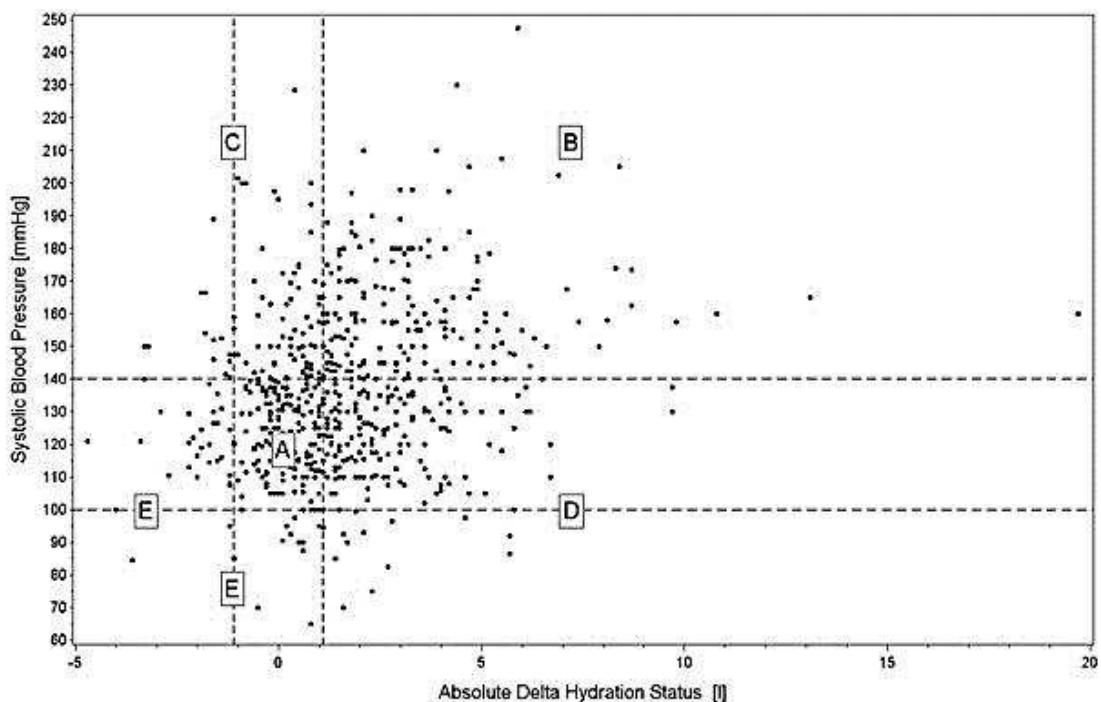
2.1.2.3. Over-activity of the renin-angiotensin system

Volume-independent factors contribute to hypertension in ESRD. Despite loss of renal excretory function, dialysis patients have inappropriately high renin levels relative to their salt and volume status [35]. A subgroup of patients with volume independent hypertension do not respond to salt or volume removal but are sensitive to ACE-inhibitors [35]. This subgroup can have hypertension despite low volume. (Zone C in Figure 2-4).

2.1.2.4. Increased arterial stiffness

Arterial stiffness measured by pulse wave velocity is independently associated with increased risk of cardiovascular disease in HD patients, (Figure 2-5). Sigrist et al assessed the relationship of vascular calcification to arterial stiffness and its progression with time in 134 patients (60 on HD, 28

Figure 2-5- Probabilities of overall survival in 241 HD patients according to tertiles of Pulse Wave Velocity (PWV) [36].
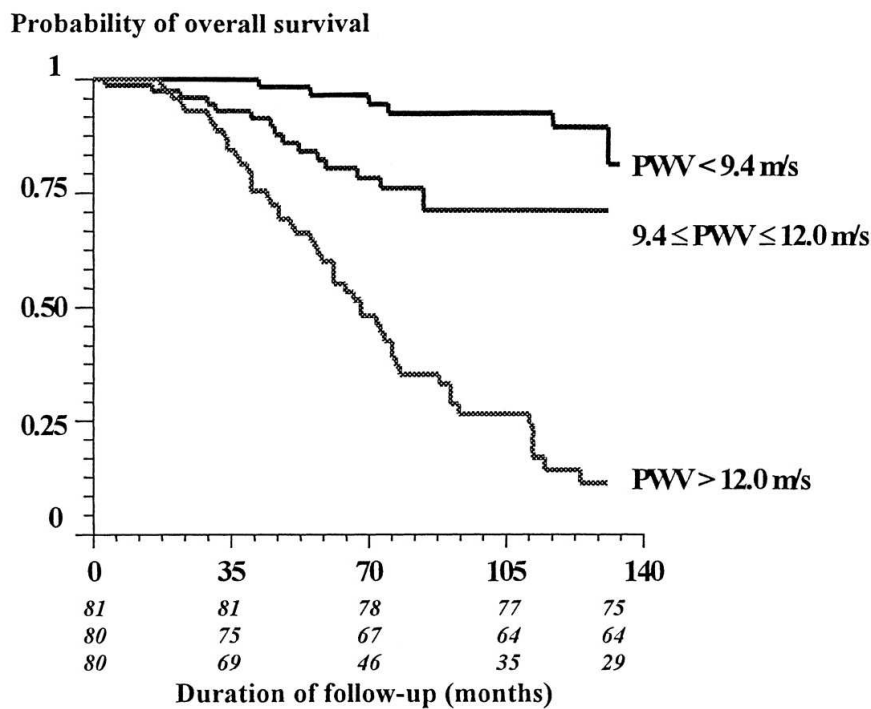
on PD, 46 stage 4 CKD) assessed at baseline and 2 years by femoral artery computed tomography and pulse wave velocity (PWV) [37]. Increased PWV correlated with vascular calcification and increased with progressive stage of CKD. Vascular calcification was strongly predictive of death, being present in 20 of the 21 patients who died [37]. This was highly correlated with decreasing diastolic BP and increasing pulse pressure [37]. In this setting the principal driver of hypertension is not hypervolaemia but increased arterial stiffness. This allows hypertension to occur despite normal or under-

hydration. Arterial stiffness will also further aggravate hypertension in those with overhydration.

2.1.2.5. Advanced glycation end-product tissue deposition

A relatively novel risk factor in increasing arterial stiffness is the formation and tissue deposition of advanced glycation end-products (AGEs). These heterogeneous compounds were classically described as end-products of a complex non-enzymatic reaction between glucose and proteins with a long half-life such as collagen. It is now known that AGEs accumulate by a variety of non-glucose mediated methods including ingested processed food, hyperlipidaemia, oxidative stress, carbonyl stress and reduced renal clearance. AGE formation has therefore been proposed to be a direct result of cumulative metabolic stress [38]. AGE accumulation causes cross-linking of collagen fibres directly increasing arterial stiffness. AGE levels are markedly increased in dialysis patients and predictive of mortality [38]. This may be as a result of increased arterial stiffness and increased endothelial dysfunction.

2.1.2.6. The lag phenomenon and buffering of water-free sodium

The Tassin group coined the term 'lag phenomenon' to explain a well described time delay between normalization of extracellular volume in HD patients by ultrafiltration and a sustained further reduction in blood pressure. This lag lasted several months, highlighting a dissociation between hypertension and hydration state [39]. The explanation for this may be linked to Jens Titze's work showing that large amounts of sodium can be buffered in

the interstitial space without commensurate water retention [40]. Accumulation within resistance vessels may also contribute to increased tonic vasoconstriction, further favouring the development of hypertension. This extension to the traditional model of fluid homeostasis is supported by data showing that sodium is pro-inflammatory and is capable of direct adverse cardiovascular consequences independent of its effect on BP [40, 41].

Figure 2-6 The lag phenomenon. A delayed reduction in mean arterial pressure occurred several months after the exchangeable sodium and body weight had stabilized [42]
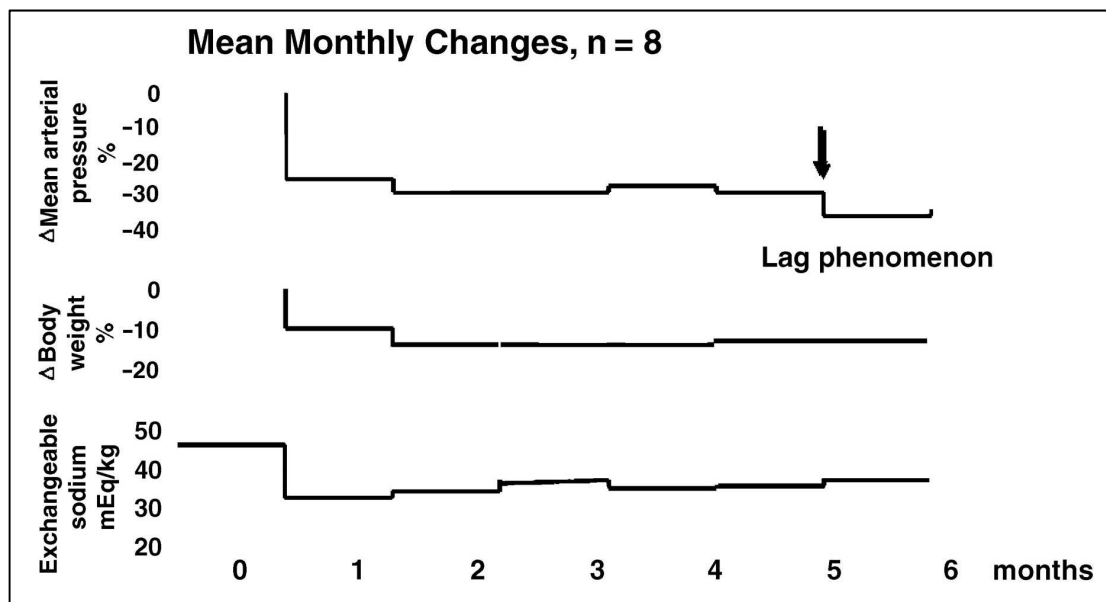
2.1.2.7. The role of hyperglycaemia in hypervolaemia

Hyperglycaemia may be another factor in the dissociation of BP and hydration status. Patients with diabetes ingest water as a result of glucose driven hypertonicity. Ramdeen et al performed a one year balance study in 9 diabetic and 7 non-diabetic HD patients. This demonstrated sodium intake with commensurate water retention accounted for the entire inter-dialytic fluid gains in non-diabetic patients but only half the fluid gains in diabetic patients.

20

The other half was pure water intake presumably driven by hyperglycaemia [43]. In this setting free water ingestion is not being driven by the conventional salt and water paradigm and overhydration may even occur without hypertension. Acute hyperglycaemia and hyperinsulinemia can directly cause hypertension via vasopressor effects [44]. We have previously demonstrated that PD exchanges with hypertonic glucose based dialysate causes sustained hyperglycaemia and hyperinsulinaemia with resultant hypertension in both the fed and starved state [45]. In this setting hypertension can occur despite the dehydrating effect of peritoneal ultrafiltration and is abrogated by the use of glucose-sparing dialysate.

2.1.2.8. Potential risks of probing for dry weight

Probing for dry weight may also be at the risk of under-perfusing other vascular beds including those of the kidney, gut and brain. Although it might seem counter-intuitive to be concerned about renal perfusion in a dialysis patient it is well recognised that maintenance of residual renal function confers a survival advantage and improves volume control. Gunal and co-workers targeted normal BP as a surrogate for normal volume status in 78 PD patients by increasing ultrafiltration volumes with 3.86% glucose dialysate, and salt-restriction. They showed an impressive reduction in BP to a normotensive range at the expense of a 28% decrease in urine volume in the 19 patients with significant residual renal function [46]. The gut is also an important vascular bed, extracting 25% of resting cardiac output to maintain nutrition. 70% of gut bacteria possess pro-inflammatory endotoxin. In health, protection from endotoxin is afforded by energy-dependent tight-junctions in

the gut wall. In disease states with aberrant perfusion such as advanced heart failure and septic shock, endotoxin translocation across leaking tight-junctions is well described [47]. We hypothesised that dialysis might also lead to aberrant gut perfusion and endotoxaemia and performed a study in 249 subjects without heart failure across the spectrum of CKD. Serum endotoxin levels were 1000 times greater in HD patients compared to non-CKD patients, with a four-fold increase between pre-dialysis CKD stage 5 and commencing HD or PD [48]. These elevated levels correlated with intradialytic hypotension, systemic inflammation, and troponin T levels. Whether dialysis-associated endotoxaemia is a culprit or bystander in the pathophysiology of inflammation, malnutrition and adverse cardiovascular outcomes in this setting is subject to current studies. We have further proposed and are investigating the hypothesis that the cerebral microcirculation is also sensitive to dialysis-induced circulatory stress potentially explaining specific patterns of brain injury highly prevalent in the dialysis setting [49].

2.1.3. Left ventricular hypertrophy

LVH is a well-recognised risk factor for cardiovascular morbidity and mortality in the haemodialysis population, and the risk of complications can be stratified according to the differential patterns of left ventricular geometry (Figure 2-7).

Figure 2-7 Time in months after starting dialysis to the first episode of heart failure, in 245 patients stratified by left ventricular geometry on echocardiography [50]
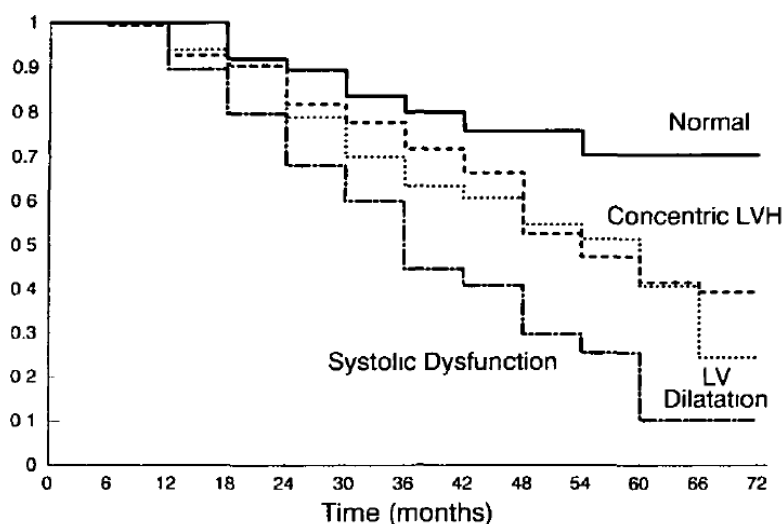
The link to LV hypertrophy (determined by LV mass) is well established in HD patients. LVH is thought to be an adaptive response that allows for normal LVEF despite abnormal pressure or volume load. Multiple risk factors are thought to be contributory including aortic stiffness, volume and pressure overload, hyperphosphatemia and neurohormonal activation [51]. Recent work has extended this picture with the implication of endogenous digitalis glycosides and fibroblast growth factor 23, both known to have higher concentrations in ESRD [52, 53]. In particular, sodium has been shown to

induce adrenal gland secretion of endogenous digitalis glycosides and in vitro studies have shown they directly induce myocyte hypertrophy thus providing a novel mechanism linking high dietary salt intake and impaired sodium excretion to hypertension and LVH in HD patients [54].

2.1.4. Dyslipideamia

In the general population, meta-analyses of over 50,000 patients have confirmed there is a linear association between total and low-density lipoprotein-cholesterol (LDL-C) levels and cardiovascular morbidity and mortality [55]. Their reduction by drug therapy causes large reductions in cardiovascular risk of at least 20%. This relative risk reduction is independent of blood pressure and is complex in nature, with a greater impact on coronary event rates than stroke [55]. Recent meta-analyses have suggested the benefits of reducing total cholesterol and LDL-C using HMG-CoA reductase inhibitors (statins) are extended to those with low baseline risk [56]. In the absence of nephrotic syndrome, CKD is characterized by a distinctly different pattern of dyslipidaemia than the general population. Total cholesterol and LDL-C, the principle targets of statins, tend to be normal or low. High-density lipoprotein cholesterol (HDL-C) concentrations tend to be low and triglycerides tend to be increased [57]. The pattern is further complicated by variations in lipoprotein abnormalities depending on the stage of CKD, the modality of dialysis and the primary renal disease. As such epidemiological studies in HD have often shown paradoxical patterns of reverse causality with low cholesterol being associated with high mortality. Liu et al demonstrated in a study of 823 HD patients that this inverse relationship

reverted to a conventional relationship if the patients had low levels of C-reactive protein (CRP)[58]. This suggested that the inverse relationship might be explained by comorbidity associated with inflammation (Figure 2-8).

Figure 2-8- Association Between Cholesterol Level and Mortality in Dialysis Patients: Role of Inflammation and Malnutrition [58]
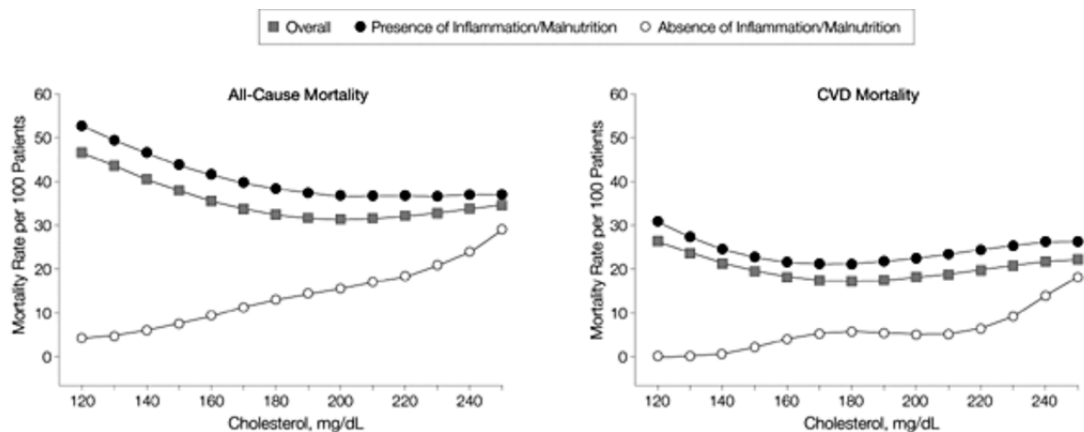
Recent large randomised trials of statins in CKD and HD have shown the beneficial effects of reducing total and HDL cholesterol seen in the general population are either diminished or absent. The Die Deutsche Diabetes Dialyse (4D) study achieved a 40% reduction in LDL-C in 1225 HD patients with type 2 diabetes [59]. Despite this there was no reduction in the composite endpoint of cardiovascular and all-cause mortality [59]. Further analyses confirmed the distinctly different causes of mortality in HD patients with adjudicated deaths from coronary artery disease accounting for only 9%, whilst 33% died of sudden death or heart failure (Figure 2-9). Other explanations for the negative finding include the study probably being underpowered for the primary endpoint.

Figure 2-9 Causes of death in the 4D (Die Deutsche Diabetes Dialyse) study [57].+-
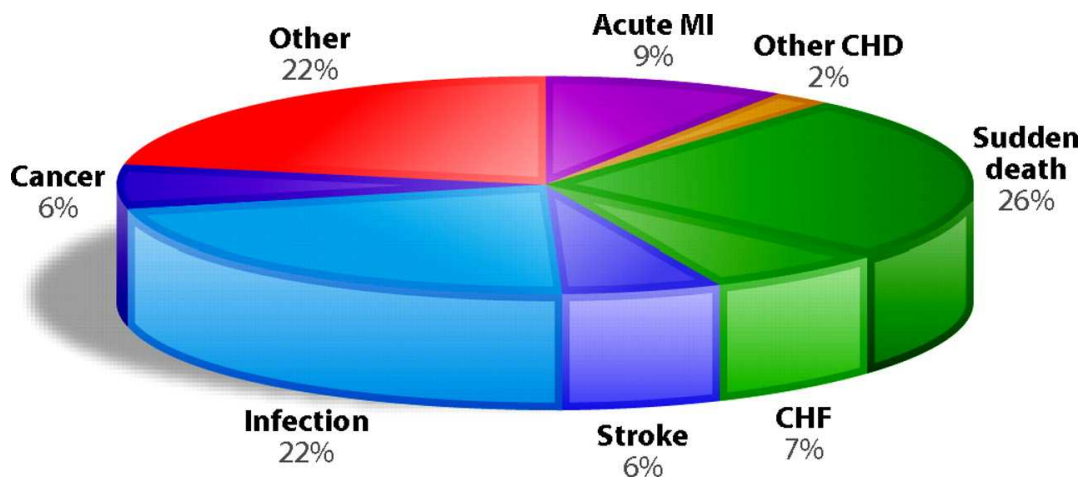
The AURORA trial randomized 2776 patients to rosuvastatin or placebo achieving a 43% reduction in LDL cholesterol. Despite this there was no effect on the primary composite endpoint of cardiovascular mortality and cardiovascular events [60]. The SHARP (Study of Heart And Renal Protection) trial in 9270 CKD patients including 3023 on dialysis, showed LDL-C reduction caused a significant decrease in major atherosclerotic events, but no reduction in cardiovascular or all-cause mortality [61]. Therefore, in dialysis patients, particularly without ischemic heart disease, the benefits of lowering cholesterol remain uncertain.

2.1.5. Smoking

Cigarette smoking is associated with increased cardiovascular morbidity and mortality in the general population. In CKD smoking is associated with more rapid progression of renal disease, but the effect of smoking in the dialysis population is less well studied [62]. Registry data typically underestimate true smoking prevalence [63]. A recent meta-analysis of studies including over

6000 dialysis patients, showed active smoking is associated with a significant increase in all-cause mortality (hazard ratio 1.65, 95% CI 1.26-2.14; p<0.001) although there was no corresponding increased risk of incident cardiovascular events [64]. The data were limited by heterogeneity and few studies assessed smoking as the primary endpoint.

2.1.6. Glycaemic control in diabetic HD patients

Diabetes is a potent cardiovascular risk factor in the general population as well as the the most common cause of CKD requiring HD in the Western world [65]. Indeed there are increasing data demonstrating that even in non-diabetic subjects hyperglycaemia *per se* is an independent cardiovascular risk factor [66-68]. Compared with non-diabetic HD patients, diabetic HD patients are characterised by having approximately double the mortality rate but the reasons for this are poorly defined [69, 70]. Certainly those with diabetes have a clustering of traditional and non-traditional risk factors but as with other risk factors in ESRD there is incredible complexity relating hyperglycaemia to stage of CKD, drug effects, co-morbidity and treatment-related factors. These combine to ensure findings and guidelines developed in the general population cannot simply be extrapolated. Nevertheless, current UK Renal Association guidelines suggest a target of HbA1C of 6.5-7.5% irrespective of stage of CKD. This is based on non-CKD trials and observational data. Observational studies consistently show a J or U-shaped association of HbA1C to mortality in CKD or ESRD, contrasting with the linear association seen in the general population (Figure 2-10).

Figure 2-10 Hazard Ratios of all-cause mortality against HbA1C in 54,757 HD patients using time-averaged Cox proportional hazards regression [71].
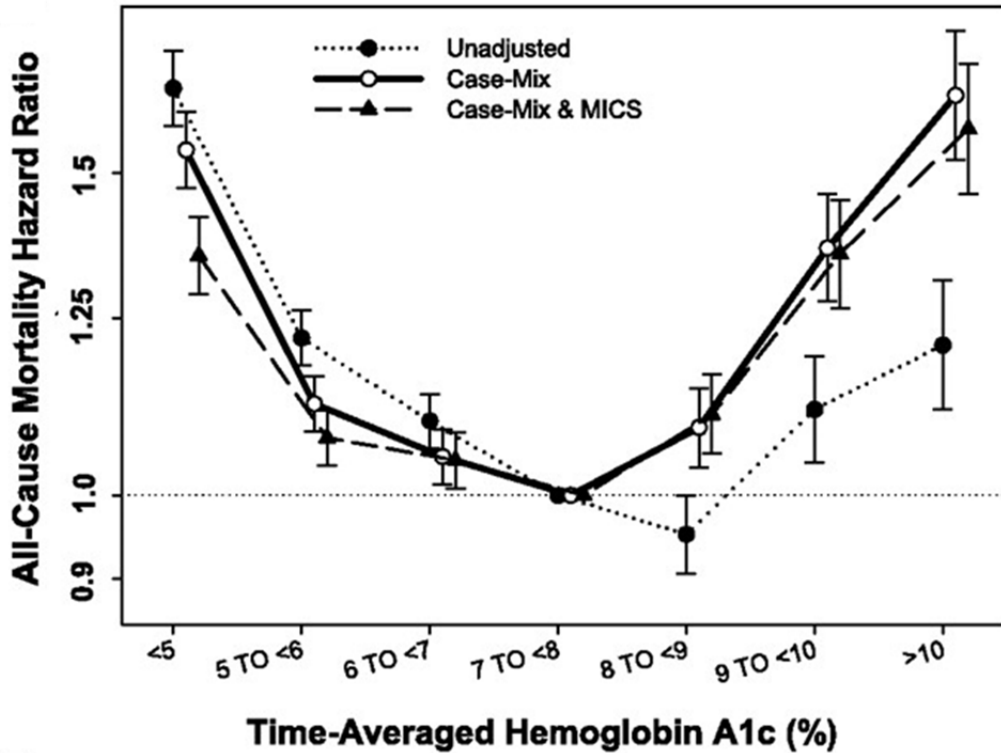
The Diabetes Control and Complications Trial (DCCT) of 1441 patients with type 1 diabetes and no other co-morbidities showed that intensified glycaemic control delayed the onset of microvascular complications [72]. The UK Prospective Diabetes Study in newly diagnosed type 2 diabetes showed strict glycaemic control delayed the onset of proteinuria and microvascular complications [73]. However, insulin and glucose homeostasis is markedly dysregulated in CKD (Figure 2-11). Assessment of glycaemic control is further complicated as erythrocyte survival is altered by use of erythropoeisis-stimulating agents and glycated albumin may be a more appropriate marker [74].

Figure 2-11 Dysregulation of glycaemic control in advanced CKD [75]
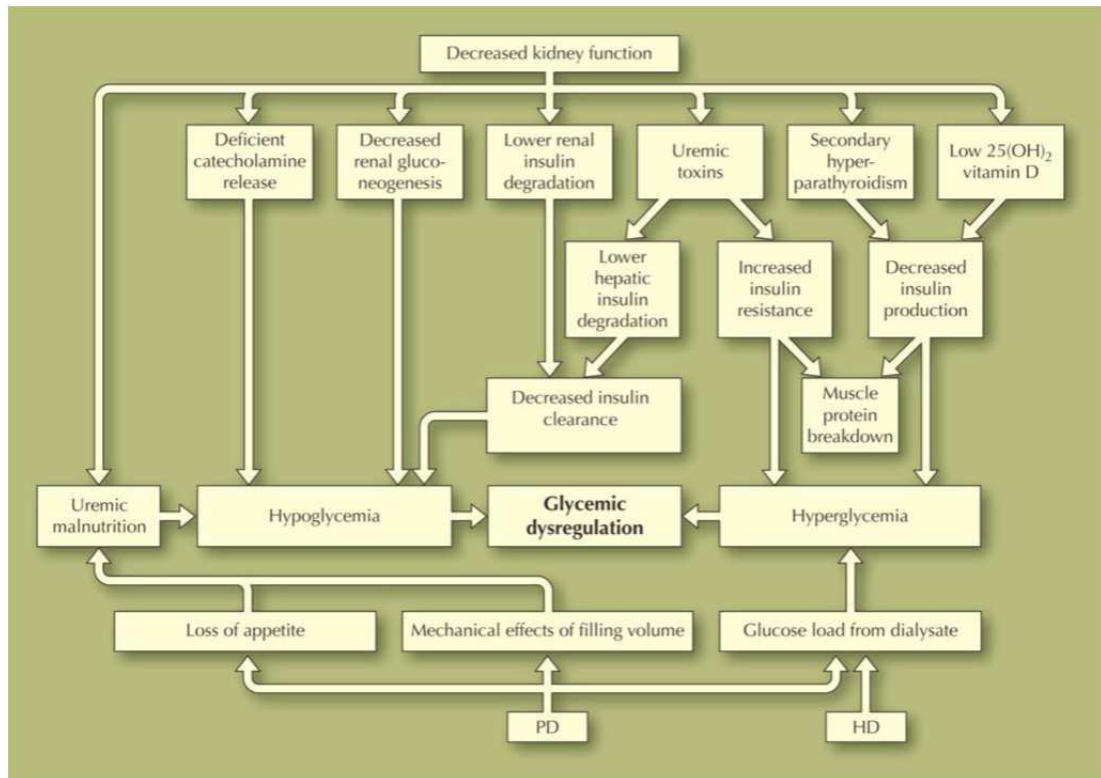
HbA1C reflects averaged glucose whereas in those having intermittent dialysis, marked short-term glycaemic variability that cannot be captured by HbA1c has been well demonstrated in studies using continuous glucose monitoring [76, 77]. Furthermore, glucose variability is a potent inducer of oxidative stress [78]. Though intensive glycaemic control can delay the onset of microvascular complications in newly diagnosed diabetes no trial has shown it can reduce cardiovascular end points or mortality. More recent larger randomised trials in the non-CKD population (ACCORD, ADVANCE, VADT) show that intensified glycaemic control in patients with pre-existing type 2 diabetes and cardiovascular co-morbidity led to either no benefit or significantly increased mortality [79-81]. Recent observational data shows

sustained extremes of glycaemia are variably and weakly associated with decreased survival in ESRD [82].

In summary, glycaemic control is markedly dysregulated in CKD and extrapolation of trial data from the non-CKD population cannot be assumed. There is reverse causality with U-shaped associations of HbA1C to mortality. HbA1C is in itself an imperfect marker of glycaemic control in CKD and ESRD. In the absence of randomised trials, aggressive glycaemic control cannot be routinely recommended for all diabetic HD patients, as there are no proven mortality benefits and the risks of such a strategy are likely increased. Individualized targets and consideration of risks-benefit ratios should be used.

2.1.7. Coronary artery disease

Coronary artery disease (CAD) is both a consequence of cardiovascular disease as well as a risk factor for future cardiovascular events. Clustering of risk factors in ESRD means it is perhaps unsurprising to find clinically silent CAD but there have been few studies to determine the true prevalence in CKD or ESRD. Ohtake et al used coronary angiography to demonstrate >50% coronary artery stenosis in 16 of 30 asymptomatic stage 5 CKD patients, with no history of angina or MI at the initiation of RRT [83]. Hayashi et al used angiography or multi-slice computed tomography to demonstrate significant stenosis in 35 of 60 asymptomatic patients [84]. It should be noted that in the Hayashi study the study population was enriched by a screening step which excluded 20 lower risk patients, so they are likely to have

overestimated true prevalence in an asymptomatic population [84]. Nevertheless, it was notable that scintigraphy had a low sensitivity and specificity in both the latter studies. This is in keeping with the abundance of data demonstrating poor sensitivity and specificity of conventional screening tests such as stress ECG, scintigraphy and echocardiography [85, 86]. In the era prior to the emergence of nephrogenic systemic fibrosis and subsequent contraindication of gadolinium in CKD, Mark et al used gadolinium contrast-enhanced cardiac magnetic resonance imaging in 134 ESRD patients as part of screening for renal transplantation [87]. In 19 patients, they found a pattern of contrast enhancement discrete to a coronary artery territory, consistent with prior and unrecognized MI. Of those 19, 9 had no antecedent history of ischemic heart disease demonstrating a low prevalence (7%) of silent CAD [87]. However as this latter population were candidates for renal transplantation, they might have less co-morbidity with consequently different CAD prevalence than an unselected ESRD population. Andrade et al also conducted a contrast enhanced magnetic resonance study in 72 high-risk but asymptomatic ESRD patients. High-risk was defined similarly to criteria used for CAD screening for renal transplantation; namely type 1 or 2 diabetes, age greater than 50 years and suspected or stable ischemic heart disease. Unrecognized MI was found in 18 patients (25%) [88]. An intriguing recent study examined the heart at autopsy in 120 patients who had been treated by HD for greater than a year [89]. They found a 39% prevalence of significant stenosis (Table 2-3).

Table 2-3- cardiac features at autopsy in 120 prevalent HD patients[89]

Feature	Count n=120	%
Any cardiac calcification	74	62
Coronary artery calcification	74	62
Mitral annular calcification	52	42
Aortic valve calcification	42	35
>75% coronary stenosis	47	39

The initiation of dialysis may play a role in the pattern of acute coronary syndromes. Prior studies have demonstrated that in a cohort of ESRD patients who experience an acute MI, 29% occur in the first year and 52% occur within 2 years [90].

2.1.7.1. Outcomes of coronary interventions in CKD

It is known that patients with ESRD and CKD are routinely excluded from intervention trials in CAD. A recent systematic review estimated 75% and 80% of trials excluded those with CKD or ESRD respectively [91]. Baseline renal function was reported in only 7% of trials [91]. As such there is reliance on either assuming benefits and harms are the same as in the general population or using post-hoc subgroup analyses of those trials. Despite such limitations, data from such post-hoc analyse and large registries consistently demonstrate worse outcomes in CKD from acute coronary syndromes, PCI and CABG. Shroff et al, have recently compared national audit data for acute MI hospitalisations in 31,709 patients with advanced CKD or ESRD to

274, 777 non-CKD patients between 1998 and 2000 [92]. They found that those with CKD were less likely to present with chest pain, less likely to have ST elevation, less likely to receive evidence-based drugs and more likely to be complicated by heart failure or major bleeding [92]. Logistic regression analysis gave adjusted odds ratios denoting 45-55% increase of in-hospital mortality (Table 2-4).

Table 2-4 Adjusted Odds Ratio and 95% CIs of in-hospital clinical events after Acute MI (AMI) from a large registry [92]

	Number	Death	Recurrent AMI	Stroke	Major bleeding
Dialysis	2390	1.55 (1.39-1.74)	1.14 (0.82-1.57)	0.94 (0.66-1.34)	1.41 (1.16-1.73)
Advanced CKD	29319	1.44 (1.39-1.49)	1.30 (1.19-1.42)	0.94 (0.85-1.05)	1.62 (1.53-1.73)
Non-CKD	274777	Reference	Reference	Reference	Reference
P		<.001	<.001	0.52	<.001

Similarly, these worse outcomes are reflected in recent prospective intervention trials of primary PCI for STEMI conducted in the modern era of drug-eluting stents and newer drugs with lower rates of bleeding complications. [93]. Although it is clear that outcomes for PCI and CABG are worse in the presence of CKD, few studies have estimated or compared the alternative of optimal medical management alone. Herzog et al showed that thrombolysis therapy for STEMI was associated with 28% relative-risk reduction in all-cause mortality at 2 years [94]. Hemmelgarn et al used risk-adjusted models to estimate that compared to medical therapy, revascularisation by CABG reduced mortality by a similar degree to the non-CKD population, although crude survival was much lower [95]. PCI showed a benefit in CKD but not ESRD (Table 2-5).

Table 2-5 Unadjusted and Adjusted Survival Rates at 8 Years for CABG and PCI Versus No Revascularization by Category of Kidney Function[95]

	Unadjusted Survival, %		Adjusted* Survival, %		Adjusted* Survival Difference, % (CABG−NR)	Risk-Adjusted Hazard Ratio† (95% CI)	Risk-Adjusted Hazard Ratio† (95% CI) With Propensity Score
	CABG	NR	CABG	NR			
CABG vs NR							
Reference patients	83.4	75.4	85.5	72.3	13.2 (P<0.001)	0.44 (0.40–0.47)	0.58 (0.41–0.82)
Nondialysis kidney disease	36.6	40.0	45.9	29.7	16.2 (P<0.001)	0.59 (0.44–0.79)	0.55 (0.40–0.74)
Dialysis kidney disease	39.1	43.0	44.8	30.4	14.4 (P−0.003)	0.60 (0.43–0.84)	0.43 (0.40–0.47)
PCI vs NR	PCI	NR	PCI	NR	(PCI−NR)		
Reference patients	86.0	75.4	80.4	72.3	8.1 (P<0.001)	0.63 (0.59–0.68)	0.83 (0.70–0.99)
Nondialysis kidney disease	31.6	40.1	32.7	29.7	3.0 (P−0.479)	0.91 (0.69–1.19)	1.00 (0.86–1.15)
Dialysis kidney disease	48.3	43.0	41.2	30.4	10.8 (P−0.027)	0.68 (0.49–0.95)	0.80 (0.77–0.83)

NR indicates no revascularization.

The most definitive observational study to address which strategy to use in the absence of trial data was published recently. Chang et al abstracted data on 21,981 ESRD patients who underwent CABG or PCI for multivessel CAD between 1997 and 2009 [96]. As well as illustrating the remarkable stability in survival rates over time (Figure 2-12), unadjusted analyses showed no differences in 5 year survival of 25% [96]. However using cox-proportional hazards regression as well as a propensity-score matched cohort revealed 13% lower risk of death and 12% lower risk of death or non-fatal MI for CABG compared to PCI.

Figure 2-12 Survival rates at 1, 2, and 5 years after initial multivessel coronary revascularization for 21,981 patients on maintenance dialysis in the USRDS by index year [96].
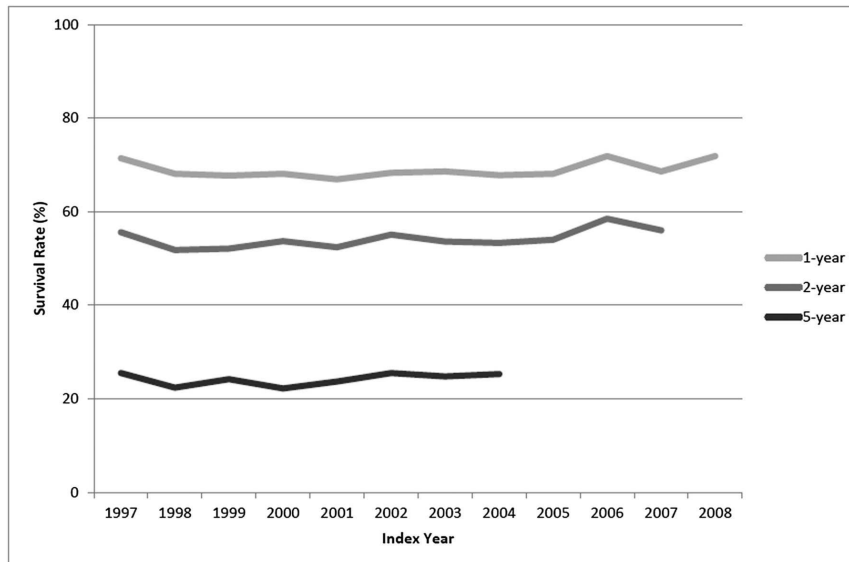
2.1.7.2. Recent insights from non-CKD population studies

There is an abundance of data from non-CKD studies which have clarified indications and benefits of coronary interventions. PCI is recognized to reduce symptoms but not mortality in patients with stable angina. The best recent example of this is the COURAGE trial of 2300 patients demonstrating no benefit of PCI over optimal medical therapy in CAD [97]. This validated uncertainty over whether preventative PCI alters outcomes and clarified that the current first line approach to patients with stable angina is optimal medical management. With the caveats outlined and in the absence of evidence, it underlines uncertainty in the CKD population if stenting 'significant' coronary stenosis will improve outcomes. There had also been uncertainty whether PCI with drug-eluting stents and optimal drug therapy was preferable to CABG in multivessel CAD, particularly in high risk patients,

because of lower procedural risks associated with PCI. The FREDOM trial randomly allocated 1900 patients with diabetes and multivessel CAD to CABG or PCI. Patients were followed for an average of 5 years. The primary outcome of all-cause mortality, nonfatal MI or nonfatal stroke, occurred more frequently in those who underwent PCI vs. CABG (27% vs. 19%, p=0.005) [98]. Stroke, however, occurred more frequently in the CABG group (5.2% vs. 2.4%) [98]. Thus, there appears to be a clear benefit of CABG in diabetics with multivessel CAD, reflecting the outcome of the afore mentioned recent observational data in the ESRD population[96]. Finally, recent data have added to the abundance of existing data refuting the view that coronary angiography should be considered the gold standard for defining CAD. It has long been known that visual or computer based-estimation of coronary stenosis at angiography is a poor guide to functional significance[99]. Confounding factors include vessel tortuosity, overlap of structures, and the effects of lumen shape. The lumen is viewed in a single dimension, and many large constituents of atherosclerotic plaque are radiolucent. Interobserver variability of estimated luminal stenosis is as high as 50% and reported correlations of lumen size by angiography versus coronary ultrasound are as low as r=0.3 after PCI [100]. Coronary ultrasound and serial angiography studies have demonstrated that the majority of acute MIs occur in atherosclerotic plaques with <50% stenosis that would not be considered severe [101, 102]. A recent 60 patient study supports that this pattern is unchanged in CKD [103]. The FAME (Fractional Flow Reserve versus Angiography for Multivessel Evaluation) trial demonstrated that in patients with multivessel CAD, restricting PCI with drug-eluting stents to

functionally significant stenosis, significantly reduced death or MI at 2 years, compared with the conventional practice of PCI to all stenoses >70% [104]. In essence, measuring functional reserve directs the cardiologist as to whether the lesion should have PCI. Patients without functionally significant stenoses do not need PCI, even if the lesions appear severe by angiography.

As I will outline in detail in a later section, it is well recognized that pre-existing LVH, autonomic dysfunction and arterial stiffness are highly prevalent in CKD and they act to reduce coronary flow reserve, such that coronary artery stenosis is not required to produce significant myocardial ischaemia [105]. Thus, the chances of successfully determining whether elective PCI of asymptomatic coronary stenosis will improve outcomes in CKD are likely to be even further reduced.

In summary, in the setting of acute coronary syndromes or symptomatic CAD, the available data clearly suggests that CKD patients still derive significantly improved outcomes from CABG or PCI compared with medical management although those outcomes are worse than the general population. The difficulties arise in detection and management of silent and asymptomatic CAD. This is likely to be common in CKD and ESRD and outcomes from known interventions are worse. Conversely, angiographically significant CAD is not essential to produce ischaemia. Whilst it seems rational to aggressively screen patients for asymptomatic CAD, data from the non-CKD population suggest uncertain benefits of coronary intervention over optimal medical therapy, particularly without measuring fractional flow

reserve. The benefits and harms of such interventions in CKD or ESRD cannot be assumed to be the same.

2.2. Cardiac imaging in CKD

Figure 2-13 The ischaemic cascade
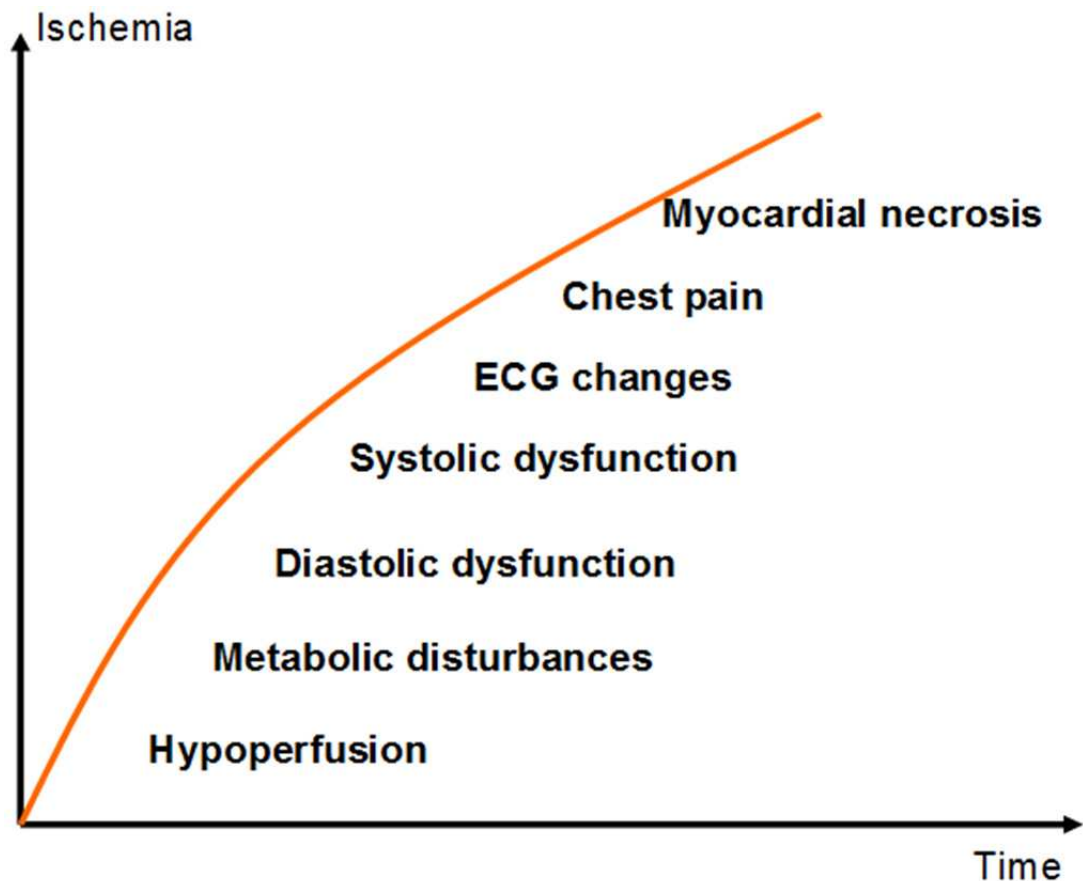
2.2.1. The ischaemic cascade

When coronary artery flow is impaired this leads to an imbalance of oxygen supply and demand, reduced perfusion, metabolic disturbance, regional ventricular dysfunction and electrophysiological change occur in succession. This sequence of events is termed the ischemic cascade. Another way of perceiving this process is that complex changes occur at a microscopic level and cascade to changes detectable at a macroscopic level. In the traditional

'bench-to-beside' approach to research, animal models, basic science and molecular biology are used to elucidate a pathway of a disease at a microscopic level. By resolving this microscopic defect this might translate to alter the course of a disease at a macroscopic level. Similarly at a macroscopic level one can aim to relieve symptoms of myocardial ischaemia by opening up a 'tight' 90% stenosis by angioplasty of a coronary artery to improve microscopic perfusion. Both of these approaches may succeed but often fail to impact on patient-centred outcomes because they might over-simplify the complexity of biological systems. To use a mathematical analogy they treat the macroscopic as classical Euclidean geometry, where shapes have regular edges with integral dimensions which can be reduced by axiomatic formulae to an integer of its smallest essential unit. Thus one, two and three integral dimensions describe a line, area and volume respectively. Despite huge success, Euclidean geometry failed to mathematically describe or model much of the complexity that scientists observed in the world. In the 1960s, the mathematician Benoît Mandelbrot used the adjective "fractal" to indicate objects whose complex geometry can only be characterised by a fractional rather than integral dimension. A fractal is an irregular object composed of self-similar subunits. It was only with the rediscovery and elucidation of fractal geometry and other non-linear dynamics that scientists were better able to model and predict biology [106]. Like fractals, many patterns in biology display detail of microscopic self-similarity superimposed on seemingly random macroscopic variation.

Figure 2-14 Ice crystal formation on a leaf displays a self-similar geometry which can only be mathematically described using non-linear fractal dimensions. Many complex biological processes and patterns may be better described using fractal geometry.

This complexity cannot be predicted using conventional models which rely on predominantly linear statistical modelling and leads to paradoxical findings. Medicine is littered with surrogate markers of disease that have failed, sometimes with the unintended consequences of misguided interventions. Opening a 90% stenosis may not improve perfusion because of the damage the process entails, the complexity of flow dynamics and the fact that the majority of blood is delivered in vessels much smaller than those visible [107]. Cardiac imaging is undergoing a paradigm shift from purely anatomical imaging of anatomy to augmentation by imaging inherent aspects of function. These should perform better as surrogate markers by being more closely tied to disease and hold promise for effecting change in clinical outcomes, the highest standard for a biomarker. An approach based on structural and functional imaging may help in explaining the complexity and the paradoxes

of multiple failed interventional trials to reduce cardiovascular disease In HD patients. It may identify those groups who benefited from an interventional trial but were not identified by the choice of surrogate and composite endpoints. It may also better identify those who require a different approach and produce more focused interventions which focus on treatment environment, timing, mode of delivery and recovery, as much as the treatment itself. In this thesis I will use two main imaging techniques to characterise cardiac abnormalities in HD patients, cardiovascular magnetic resonance and echocardiography.

2.2.2. Two-dimensional transthoracic echocardiography

Cardiac assessment by conventional two-dimensional (2D) transthoracic echocardiography (2DE) is non-invasive, inexpensive to perform, and generates detailed information about gross cardiac anatomy, objective quantification of LVM and the geometry of LV hypertrophy, along with measures of function during systole and diastole. The predictive power of the most commonly used measures of cardiac geometry is underappreciated. Prospective studies have shown left ventricular hypertrophy (LVH) in most (70-80%) patients with end stage renal failure and this confers a poor prognosis [108]. LVM indexed to weight or body surface area (LVMI) confers difficulties in the CKD population with over- or under-estimation of LVMI due to the inherent variations in fluid volume status, body composition and nutritional status. A cohort study of 254 dialysis patients (demonstrated that death and cardiovascular outcomes are better predicted by indexing LVM to height in ESRD patients [109].

The most widely used method for quantifying systolic dysfunction remains LV ejection fraction, derived from one dimensional linear M-mode diameter measurements at end-systole and end-diastole. However M-mode measurements use the Devereux formula to determine LVEF based on a regression model derived from a healthy population. The model performs poorly in populations with asymmetric LV hypertrophy such as those with hypertension or CKD [110]. Major international guidelines now recommend that LVEF be calculated using a bi-plane or tri-plane area length method, that

requires acquisition of 2 and 4 or 2, 3 and 4-chamber image loops capturing end-diastole and systole [111]. Newer software allowing this to be quickly calculated at the time of image acquisition should increase penetration to clinical practice but it is already regarded as standard for clinical research. Various other parameters of systolic dysfunction have been proposed based on fractional shortening (FS) across the entire myocardial wall. These also perform poorly in those with asymmetric LVH such as concentric LVH (present in over one-third of HD patients), due to differential contractility within the endocardium and epicardium. Standard FS has been superseded by mid-wall FS, which increases homogeneity [112]. Zoccali et al demonstrated that midwall FS was more sensitive than LVEF for the identification of asymptomatic dysfunction in HD patients [113]. In the same study, both midwall FS and LVEF had equal prognostic ability for cardiovascular events and death. This study also confirmed that in ESRD the enhanced risk associated with both LVH and systolic dysfunction were additive [113, 114].

2.2.2.1. Left atrial volume

Measures of left atrial (LA) size are useful surrogate markers for left ventricular diastolic dysfunction, and predict cardiovascular events in the non-CKD population [115-117]. A recent cohort study of 249 ESRD patients demonstrated that height-indexed left atrial volume (LAVI) displays predictive power for all-cause mortality over and above that of indexed LV mass and ejection fraction [118]. Furthermore, change in LAVI over one to two years predicts future cardiovascular events independently of LVM and baseline LA

dimensions [119, 120]. Barbareto et al have recently shown in 172 haemodialysis patients that LAVI independently predicts intradialytic hypotension [121]. Chan et al studied a mixed cohort of 200 CKD patients with around half using HD. LA diameter independently predicted long term cardiovascular mortality and was incremental to stress single photon emission computed tomography (SPECT) [122].

2.2.2.2. Limitations of 2D Echocardiography

Notably, echocardiographic measures based on ventricular dimensions are sensitive to the degree of cardiac filling, which is important in dialysis patients where pre-load and after-load change as a function of fluid status. LVM measurements are particularly problematic as they rely on geometric assumptions. LVM calculated by post-dialysis echocardiography may be $26g/m^2$ lower than pre-dialysis because of load dependency. This discrepancy is not seen when utilising cardiac magnetic resonance imaging [123]. Accurate measurements require excellent image quality and good acoustic windows which can be limited in many patients, particularly if obese. Other disadvantages of conventional echocardiography include a greater reliance on subjective interpretation and higher inter-observer variability for LVEF compared to alternative methods [124].

2.2.3. Three-dimensional transthoracic echocardiography

Early approaches to 3D echocardiography (3DE) were based on the principle that a 3D data set could be reconstructed from a series of 2D images. This

method required time consuming acquisition of data as well as off-line image reconstruction and analysis. Improved transducer technology allows faster image acquisition of the heart using ECG-gated images within 4 cardiac cycles, termed real-time 3D echo to distinguish it from the older technologies. From henceforth I shall refer to this as 3D echo (3DE) [125]. Semi-automated LV surface detection technology has reduced off-line processing times. The major advantage of 3DE compared to 2D methods is it makes no assumption of geometry making the accuracy and inter-observer variability comparable to cardiac magnetic resonance which is considered the reference standard [126-128]. The technology has some limitations. To reconstruct the 3D images requires a greater volume of data acquisition and better image registration than 2D echo. This necessitates ECG-gating and multiple breath-holds for the subject to minimise respiration artefact. The breath-hold requirement can be problematic in patients with dyspnoea and arrhythmias and in this respect it is similar to CMR. However, a reduced resolution dataset that still outperforms the 2D technique in many respects can be captured in a single cardiac cycle. The transducer has a limited acquisition angle which may not be large enough to view the LV if it severely dilated. Finally equipment is more expensive, less available and less technical staff are trained to use it. This is particularly relevant for multi-centre research and clinical practice where penetrance is poor. Despite these limitations 3DE is emerging as a promising tool, particularly suited to a CKD population with a high prevalence of abnormal ventricular morphology [129]. As yet there are few studies in this setting [130].

2.2.4. Stress echocardiography

Preoperative screening for coronary artery disease (CAD) is recommended in renal transplant candidates who are at high risk. Nuclear imaging modalities using thallium tracers have conflicting results for the accuracy of detecting (CAD) or predicting future cardiovascular events in the setting of CKD [131-138]. Study comparisons are confounded by significant heterogeneity with cardiac imaging after both exercise and pharmacologic induced stress or a combination of both. Exercise-dependent techniques are limited by poor exercise capability [139, 140], as well as the loss of specificity due to LVH seen in the majority of dialysis patients [141-143]. Therefore patients with CKD are often only considered suitable for pharmacological stress. Conventional 2D dobutamine stress echo (DSE) measures indices of global and regional ventricular dysfunction, and relies on high quality imaging and interpretation by experienced operators. Dobutamine increases heart rate and contractility via sympathetic stimulation, causing both transmural flow redistribution by arteriolar dilatation, and increased oxygen consumption [144]. The propensity for patients with ESRD to develop significant arrhythmias [145] may be a relative contraindication to adrenergic stress testing. Dobutamine-related side effects have been variously reported in about 10% of renal transplant candidates [146, 147]. In contrast, dipyridamole causes transmural flow redistribution by inhibition of adenosine breakdown, leading to arteriolar vasodilatation, subendocardial steal, and ischaemia caused by altering coronary haemodynamics in the presence of critical coronary stenosis.

DSE is sensitive and specific for coronary artery risk screening in renal transplant candidates. Herzog et al studied 50 such patients with both DSE and coronary angiography showing sensitivity of 75% and specificity of 71% for a significant coronary stenosis [147]. Sharma et al have reported a study of 125 renal transplant candidates comparing screening techniques for severe coronary artery disease. DSE was an independent predictor of severe coronary artery disease (CAD), displaying excellent sensitivity of 88% and specificity of 94% for significant CAD [148]. About half of these patients were on dialysis, and made up two-thirds of those found to have severe CAD. Patients with severe CAD had significantly larger LV diameter, and more impaired systolic and diastolic function than those without. Resting ECG was also found to be independently predictive of CAD in this study, although significantly less sensitive (77%) and specific (58%). As expected, patients with diabetes had significantly higher prevalence of severe CAD compared to non-diabetics (44 vs 20%). This raises the possibility of investigating non-diabetic transplant candidates with DSE and resting ECG for risk stratification prior to exposure to the risks of coronary angiography.

However, De Lima et al studied DSE in 126 transplant candidates and showed lower sensitivity of just 44% with specificity 87% to detect CAD on coronary angiography [149]. Doubts about applicability of stress echocardiography in patients with more severe CKD has led to renal disease currently not being categorised in the most recent 'Appropriateness Criteria for Stress Echocardiography' recommendations [150].

A recent observational follow-up study in more than 2000 patients across the spectrum of renal impairment demonstrated that positive DSE for ischaemia

was an independent predictor of both death and hard cardiac events over a mean follow-up period of 8 years at all stages of CKD [151]. Moderate renal impairment and normal baseline DSE conferred the poorest prognosis, with 20% suffering cardiac death or myocardial infarction over 3 years. New wall motion abnormalities also independently predicted survival, although the predictive power of both models was strengthened when index of renal function was added. There have been few direct comparisons of dipyridamole stress echocardiography (DpSE) with DSE in a non-CKD patient group. Comparison in high-risk populations with hypertension or suspected CAD showed conflicting results of prognostic ability [144, 152, 153]. An Italian study aimed to compare DpSE to DSE mainly for adverse effects reporting a slightly lower incidence for dipyridamole [154]. A caveat to many of these studies is that heterogeneity in selection for DSE leads to variable pre-test probability and hence negative predictive value of the test. For example Fragasso et al studied a population that had positive exercise test before DSE which would significantly increase the pre-test probability compared to the other studies of transplant candidates which were less selected [144]. Amongst non-nephrologists CKD is increasingly recognised as an independent risk factor for CV events and it is sobering that the majority of these screening studies have not reported renal excretory function as it alters the pre-test probability [152]. A 2003 meta-analysis confirms the overall prognostic value of stress echocardiography for assessment of CAD in renal transplant candidates [138]. 3DE is emerging as a useful tool in the non-CKD population with the potential to enhance current non-invasive assessment of myocardial perfusion. 2D methods

require the acquisition of multiple views of the heart at peak stress but a 3D dataset can be obtained in a few seconds with the ability to reconstruct infinite views for analysis off-line. 3DE however does not yet have the image resolution of 2D equipment and often requires contrast enhancement. Hence, early published comparisons show similar accuracy of 3D to 2D stress methods to detect CAD in the non-CKD population [155, 156]. In summary, the data on the utility of stress cardiac imaging to screen for CAD in CKD patients have wide heterogeneity and conflicting results.

2.2.5. Myocardial Strain Imaging

Strain is a dimensionless measure of deformation or the relative displacement between two particles caused by an applied force. The terminology of strain was first developed in engineering and physics. Lagrangian strain often denoted as ε_L, represents the fractional or percentage change from the unstressed dimension:

$$\varepsilon_L = (L-L_0)/L = \Delta L/L_0$$

Where L_0 and L are the unstressed and stressed lengths respectively. Therefore strain is usually described as a percentage, decimal or fraction. Mirsky and Palmley were the first to describe strain applied to the myocardium, where L_0 is substituted by end-diastolic length, as the myocytes are never truly under zero stress [157]. Many consider that in biology, Eulerian strain denoted ε_e is a better representation of deformation:

$$\varepsilon_e = L/L_0$$

51

where L_0 is the instantaneous length, that is, the length at the time before, rather than length at time zero. Hence Eulerian strain does not assume zero stress. Lagrangian and Eulerian strain have been shown to be mathematically related. Lagrangian strain is the most commonly reported value. Myocardial strains can be positive (lengthening or expansion) or negative (shortening or compression). Strain rate is the temporal derivative of strain and is a measure of the rate of deformation, with units of 1/s. As strain measures displacement per unit length, then strain rate is also equivalent to change in velocity per unit length. Thus strain, strain rate, displacement (motion) and velocity are both distinct and related. Measuring one of these quantities can be used to derive all four.

Figure 2-15 Relationships of strain and strain rate to velocity and displacement. Figure redrawn with kind permission from Asbjørn Støylen
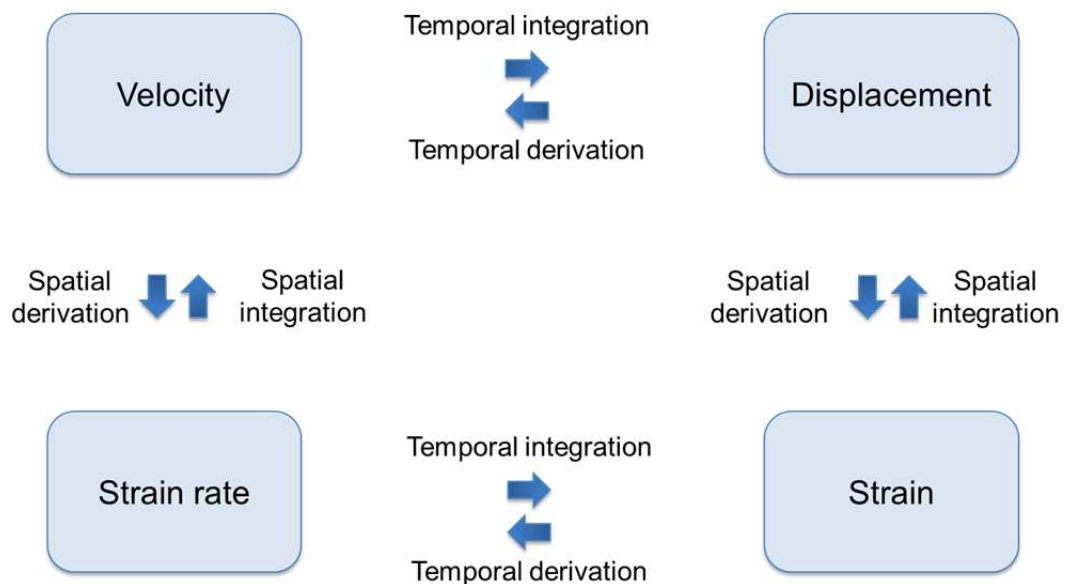
Objects can deform in 3 dimensions. As a further complication there is also displacement in surfaces relative to each other. Therefore strain has three normal and six-shear components (Figure 2-16). In a Cartesian co-ordinate

52

system the components are x, y and z. For simplicity, in the heart, the 3 principle coordinates are used relative to the tissue; longitudinal, circumferential and radial (transmural) as depicted in Figure 2-17.

Figure 2-16 Deformation of a 3D object is described by three normal and six shear strain components. One normal component (a) and three shear components εyx (b), εzx (c) and εxy (d)] are illustrated[158]

(a)

(b)

(c)

(d)
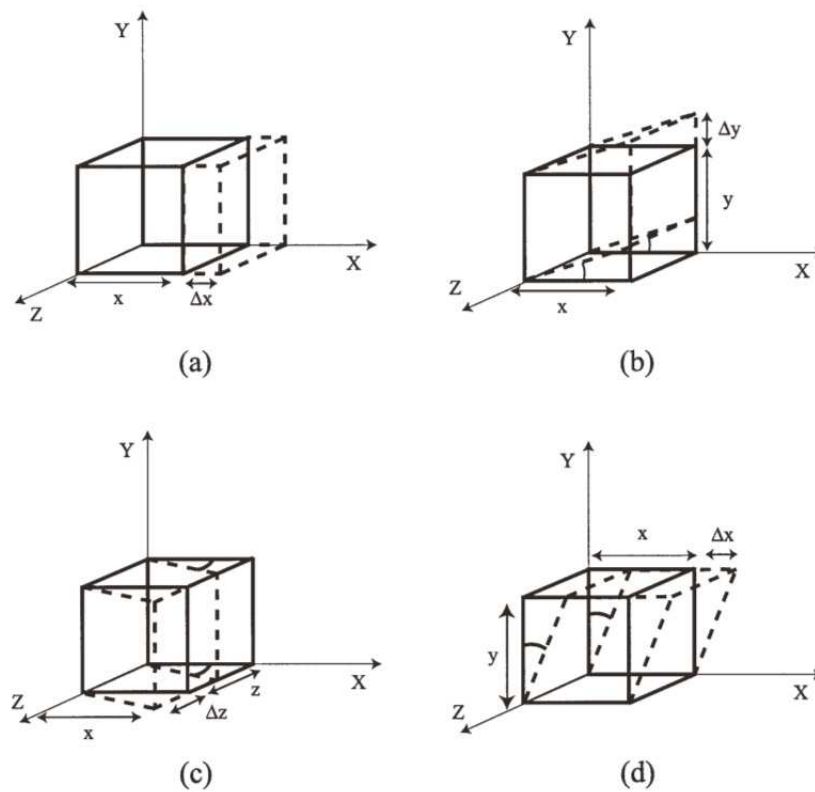
Figure 2-17 Graphic representation of the principal myocardial deformations: longitudinal (A), radial and circumferential (B), and torsion (C). The direction of deformation in systole is shown as solid lines and that in diastole is shown as dashed lines. LONG indicates longitudinal; RAD, radial; and CIRC, circumferential. [159]
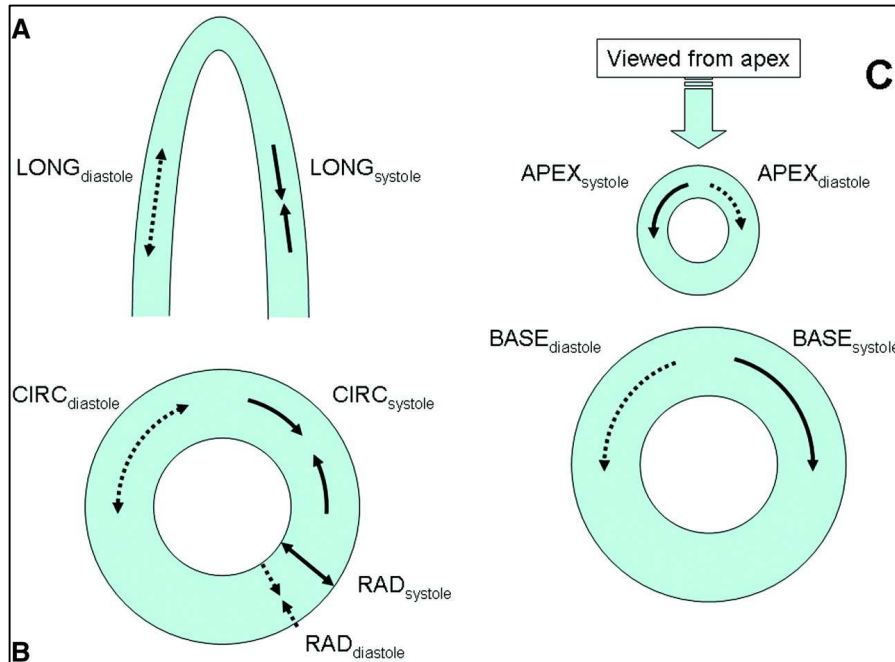
Longitudinal shortening can easily be demonstrated in long axis cardiac imaging. Radial thickening is equivalent to wall thickening, but as the myocardium is almost incompressible it can be shown that much of the wall thickening is a consequence of longitudinal shortening to conserve volume. The value of measuring strain compared to displacement is in being able to distinguish active from passive displacement. An ischemic basal segment may still show normal motion as it is tethered to healthy tissue but will not show deformation. It has been proven that the human eye is not capable of appreciating such subtle changes in deformation [160]. Thus strain and strain rate changes may be more sensitive markers of myocardial function [161, 162] Visual or semi-automated tracking of the endocardial border provide estimates of cardiac volume, which are used to derive ejection fraction, a

quantitative indicator of global ventricular function. This reflects the sum contribution of several regions and does not provide information on regional function. Visual assessment of regional function is subjective and prone to error [163]. The heart has complex deformation which is incapable of being described in a single vector of strain [164]. Much of this complex deformation stems from the orientation of the myocardial fibres (Figure 2-18).

Figure 2-18 Myocardial fibre orientation of the left ventricle from the epicardial to endocardial layer. Left to right epicardial oblique fibres represent a right handed helix, whilst oblique fibres towards the endocardium approximate a left handed helix. Figure adapted from source [165]
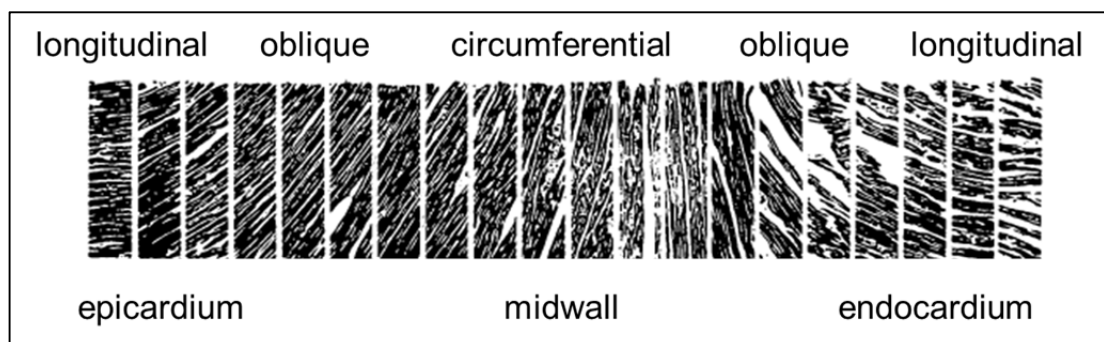
The obliquely orientated fibres form a left and right-handed helical arrangement. This lends the heart a twisting motion which as a strain is represented by the circumferential-longitudinal shear strain. From the base the rotation is clockwise and from the apex counter-clockwise. The twisting motion is an essential part of myocardial function.

Figure 2-19 Schematic representation of rotational motion of the heart during the cardiac cycle during early (A) and mid-systole (B) and viewed from the apex during mid-systole (C). Torsion versus time plot of a healthy adult man at rest (D) with counterclockwise rotation arbitrarily defined as positive and time normalised to percentage duration of systole During early systole (A), both apex (green) and base (red) rotate counterclockwise (blue arrows) whereas later in systole (B), the apex

rotates counterclockwise and the base rotates clockwise (yellow arrow) creating the wringing or torsional motion. Torsion (orange) is derived by subtracting the basal rotation from the apical rotation (D). Caption adapted from Burns et al [166]
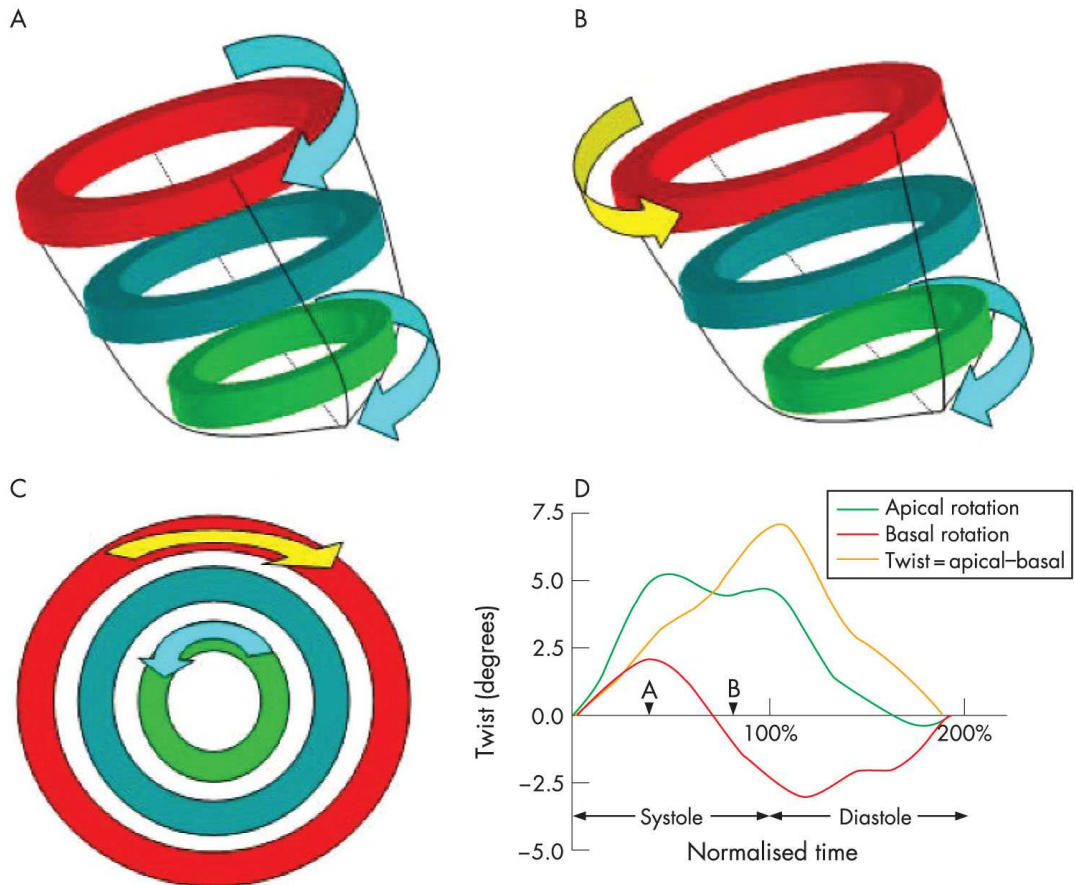
Before the invention of cardiac magnetic resonance tagging study of cardiac motion was restricted to animal or ex-vivo studies using sonomicrometry, implantation of acoustic markers. Advances in cardiac imaging now allow this to be done using several techniques based on cardiac ultrasound and cardiac magnetic resonance. The most commonly used are cardiac magnetic resonance tissue tagging, Tissue Doppler Imaging (TDI) and two-dimensional (2D) speckle tracking echocardiography (STE). Ultrasound based techniques are more widely available.

2.2.6. Tissue Doppler Imaging

Standard Doppler echocardiography imaging uses the Doppler principle which mathematically relates frequency shifts in reflected waves to velocity. Tissue Doppler Imaging (TDI) evolved from standard Doppler imaging by optimising the frequency filter settings of ultrasound to image low-velocity, high-intensity myocardial tissue signal rather than high-velocity, low-intensity signal from blood [167]. TDI is well validated in detecting systolic and diastolic function and regional components of cardiac function such as longitudinal or radial contraction. TDI has been validated against sonomicrometry in whole hearts and tagged CMR [168, 169]. Recent work has focused on longitudinal velocities proving TDI capable of detecting subclinical LV dysfunction. Mogelvang et al has shown that in a community cohort with normal LVEF, TDI detected diastolic dysfunction is an independent predictor of mortality and had incremental prognostic value to conventional echocardiography and biomarkers (Figure 2-20).

Figure 2-20 Kaplan–Meier survival curves by tertiles of the eas index. The eas index includes combined information on systolic and diastolic performance by TDI. Shown are age- and sex-adjusted eas tertiles [170]
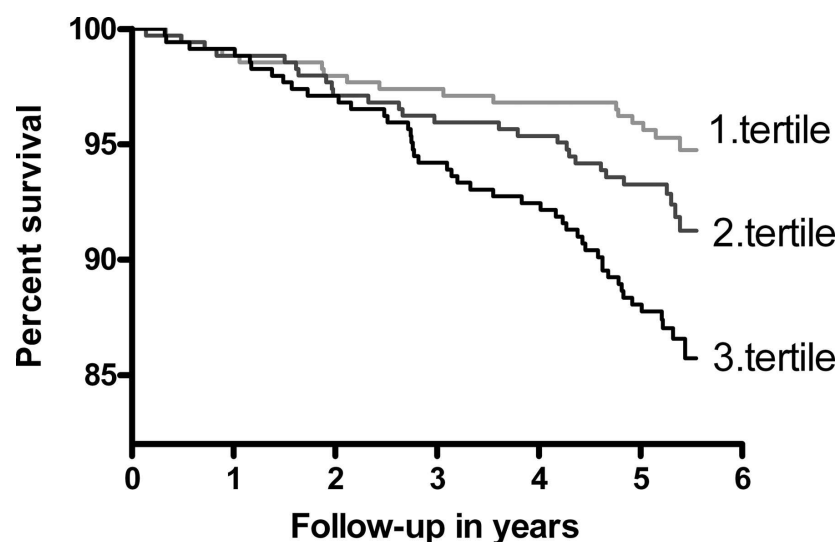
Hayashi et al found that TDI was able to detect systolic and diastolic dysfunction in CKD patients with or without left ventricular hypertrophy [171]. In particular those with LVH had reduced isovolumetric contraction, with reduced peak systolic and early diastolic filling velocities. Galetta et al studied twenty HD patients without overt cardiac disease demonstrated reduced peak systolic and early diastolic velocities, with reduced early to late diastolic velocity (E_m/A_m) ratio post dialysis compared to pre-dialysis. Interestingly, these reductions in systolic and diastolic function negatively correlated with ultrafiltration rate and interdialytic weight gain [172]. Yu et al recently reviewed TDI studies summarising the paramters that had shown prognostic value in studies of heart failure, coronary artery disease and hypertension. Mitral annular or basal segmental (Sm) systolic and early diastolic (Ea or Em) velocities were shown to predict mortality or cardiovascular event [173]. Studies have variously demonstrated early mitral annulus velocity, peak systolic and peak late diastolic velocities to be relatively independent of pre-load in HD [174-176]. The search for pre-load independent echocardiographic measures of cardiac function has led to extensive study of the effect of TDI derived parameters in haemodialysis [172, 174-186]. TDI shares the limitation of all Doppler techniques in being angle dependent.

Figure 2-21 The importance of angle dependency in producing inaccurate velocities by Doppler-based imaging. A jet of known velocity (2.0 m/s) emerges from the aortic valve in systole. Moving 60 degrees from parallel only allows a peak velocity of 1.0 m/s to be recorded. The most accurate velocities are recorded when the transducer is parallel to flow
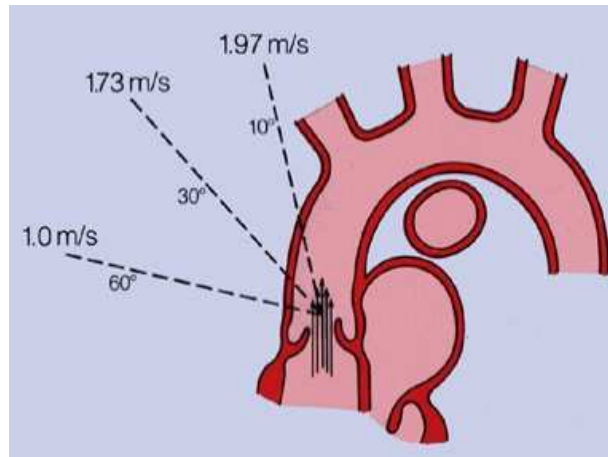
The vector of motion parallel to the ultrasound beam is measured so accuracy relies on an experienced operator to ensure the probe is aligned. This is best achieved in long axis images with higher intra and inter-observer variability of values obtained in the short-axis. TDI also interrogates motion at a single point in the myocardium with reference to the transducer. Thus it is prone to inaccuracies caused by translational motion and tethering effects.

2.2.7. Tissue Velocity Imaging

Whereas TDI measures velocity of myocardial tissue relative to the transducer and remains prone to tethering effects, Tissue Velocity Imaging (TVI) uses TDI at adjacent loci in tissue to measure velocity gradients by regression to generate a Eulerian strain rate curve. The strain rate curve can then be integrated to produce a strain curve. TVI gives accurate quantification of LV filling pressures, myocardial contraction and relaxation.

Systolic myocardial velocities and strain rate quantify systolic function whilst diastolic function is measured with diastolic velocities and isovolumetric relaxation time [168, 187, 188]. Strain rate imaging by TVI has proven capable of detecting locally reduced contractility in small discrete infarcts induced by alcohol septal ablation in ten patients with septal hypertrophy who had normal global function by invasive haemodynamic monitoring [189]. Of particular relevance to the study of dialysis patients, TVI can detect acute changes in LV function [188], and measurements are considered less load dependent than conventional Doppler echocardiography [181]. A study of 13 stable HD patients, without any overt cardiovascular disease, found pre-dialysis peak systolic, early diastolic and late diastolic myocardial velocities were reduced in comparison to age- and sex-matched controls, indicative of systolic and diastolic dysfunction; systolic function improved based on TVI parameters post-dialysis. However, the majority of HD patients had no systolic or diastolic dysfunction detectable by conventional 2D echo, and no difference was discernible between pre-and post-dialysis measures [181]. In non-CKD settings TVI has shown changes in strain precede regional wall-motion or tissue velocity abnormalities under vasodilator stress and can differentiate stunned from ischaemic myocardium [190, 191].

2.2.7.1. Limitations of TDI and TVI

As with TDI, TVI is angle dependent. The angle dependency can be minimised by narrowing the sector width of image acquisition but this compromises spatial coverage and resolution. The velocity-regression technique used to derive strain rate from velocity is exquisitely sensitive to

noise. Altering the temporal resolution to optimise spatial resolution may lead to over or under-estimation of velocities [159]. Also use of the Doppler effect to derive strain rate restricts measurement to one dimension at any one time. Measuring radial strains in short-axis images is extremely limited by the transducer angle, which particularly impairs the reliability of data in the anteroseptal and posterior segments [192]. Even measuring longitudinal strains in long axis images requires care because the myocardium has a curved septum and lateral walls, the same true tissue velocity will produce differential derived velocities that become greater over a larger sampling distance. Hence care is required to place the sampling volumes. This becomes particularly problematic at the apex. The complexity in deriving the measures, the requirement to acquire the TVI image loops separately to the standard B-mode ultrasound loops and the time required for largely off-line analysis reduces the clinical utility of the technique. Distinguishing true pathology from image artefact requires a high skill level [159]. Indeed, published validations of the techniques tend to be from centres with advanced echocardiographic expertise and clinical studies yield lower correlations between ultrasound derived strain and cardiac magnetic resonance tagging than those reported in experimental studies (r values of 0.4-0.5) [192]. This means TDI and TVI are often confined to clinical research studies and have not penetrated into routine clinical practice.

Figure 2-22 Impact of angulation on strain rate imaging by TVI. Interrogation parallel with the wall (mid-septum, shown in blue) identifies long-axis shortening, and at right angles to the wall (apex, shown in red) identifies short-axis thickening. However, an intermediate angle (apical septum, shown in yellow) causes underestimation. A mixture of vectors at 45% produces a net absence of recordable strain. Scan planes are shown as continuous lines, longitudinal and radial contraction vectors as broken lines. Figure and caption from [193]
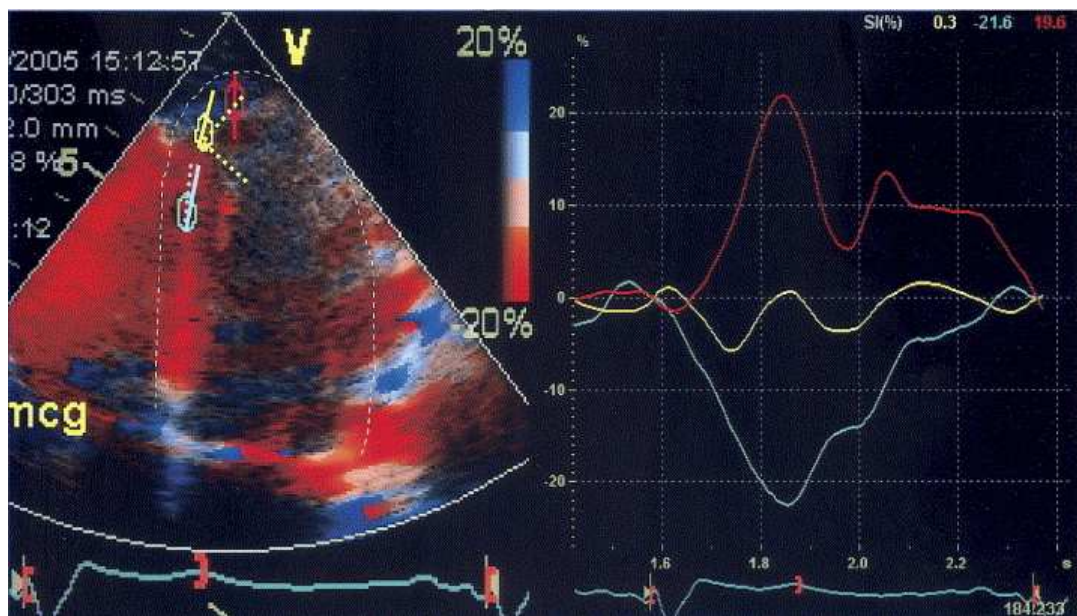
2.2.8. Speckle Tracking Echocardiography

There was a clear need for the development of a Doppler-independent echocardiographic technique for strain and strain rate measurement. Ideally this would be independent of the angle to the transducer, less sensitive to signal noise, able to measure strain in two dimensions and not require additional image acquisition. 2D Speckle Tracking Echocardiography (STE) was first described in 2004 [194]. STE estimates motions by tracking of speckles in the image. The speckles are the result of interference generated when sound waves scatter in tissue. This phenomenon appears when sound waves are reflected by sub-millimetre structures smaller than the wavelength of ultrasound. The resulting interference between waves either destroy or summate their amplitudes (destructive or constructive interference).

Figure 2-23 Schematic of constructive and **destructive interference** which is the source of the unique speckle pattern in biological tissues imaged by ultrasound. **Left, in a regular pattern from just two wave sources and right from multiple scattered sources, approximating the situation in biological tissue. Figures adapted from two sources courtesy of Poon Siew Cheng and Asbjorn Stoylen [195]**
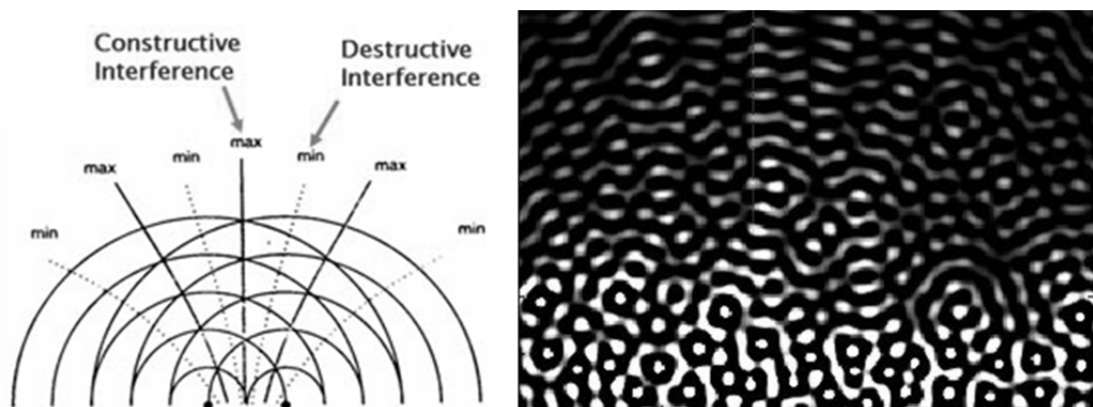
This results in a pattern of bright and dark pixels in a B-mode ultrasound image. When applied to the myocardium, the tissue structures causing interference are stationary within the tissue and randomly distributed. This produces a speckle pattern that is a stable, unique 'fingerprint' of that region that moves with the tissue. The speckle pattern can be tracked using an optical flow method or block-matching algorithm based on finding the smallest sum of absolute differences [196, 197]. The vector (distance and direction) is derived and can be easily combined with time data to determine velocity and strain. Most commercially available software track several regions of interest around 5mm x 5mm and average the vectors to determine average strain, for a sector of the heart using a 16 or 17 segment model. STE has many advantages over Doppler-based methods. Because the end-diastolic length is known, STE inherently measures Lagrangian strain and can derive Eulerian strain. Motion is determined independent of the angle to the ultrasound transducer. Strain is determined as a 2D vector, better approximating true motion for curved regions of myocardium such as at the apex. It can be determined from standard B-mode ultrasound images and does not require additional acquisitions, thus shortening examination time. Junior echocardiographers are more able to acquire images of sufficient quality as it less noise sensitive than Doppler-based strain methods. Strain determination is semi-automated by software, theoretically reducing inter-observer variability. Longitudinal strain can be determined from lateral motion on parasternal long-axis image in addition to longitudinal motion in a long-axis image. Similarly radial strains can be calculated from long-axis as well as short-axis images and should be equivalent. The ability to deal with

curved ROIs mean that it is particularly suited to assessing torsion, rotation, radial and circumferential strains unlike Doppler-based methods which are essentially restricted to long axis images or specific segments in the short-axis. STE has been validated against sonomicrometry and tagged CMR [198]. In summary, the many advantages of strain by STE over strain by Doppler, have led to a more rapid uptake of this technique in research and clinical practice.

Figure 2-24 Two-dimensional (2D) strain is based on comparison of the image texture (i.e., pattern of individual speckle elements) from frame to frame. The distortion of this pattern permits assessment of strain in the axis of movement rather than the axis of the ultrasound transducer[193]
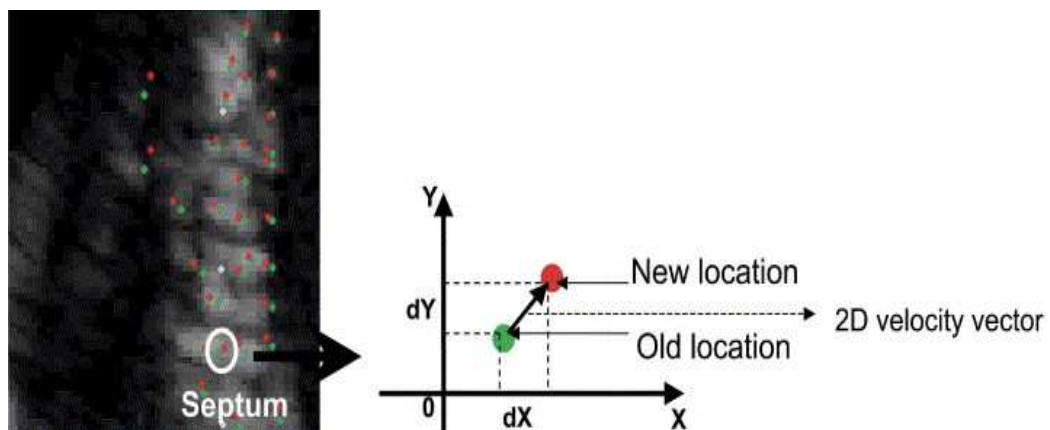
2.2.8.1. Limitations of STE

Frame-rate sensitivity

There are careful considerations to be aware of when acquiring images for analysis by speckle tracking software. Lateral resolution of ultrasound is inherently lower than its vertical resolution and decreases with depth. This means that over short distances (or times) the tracking is better than over

65

larger distances or times, making STE sensitive to the temporal resolution of the image. Low frame rates lead to poor tracking in all directions as too much motion has occurred for the algorithm to reasonably estimate. Too high a frame rate indirectly affects tracking by increasing noise and lowering the lateral resolution of ultrasound resulting in poor lateral tracking relative to vertical. Most published data have shown that the optimal frame rate lies between 40-80 frames/second [193, 199]. This is a much lower frame rate than using Doppler-based methods (>100) and may miss transient and important events in the cardiac cycle such as isovolumetric phases.

Out-of-plane motion

As the myocardium is deforming in 3 dimensions the unique speckle pattern will be degraded by true out-of image plane motion. 3-dimensional STE has recently been developed which may overcome this problem.

Image quality

Most STE studies show a proportion of segments that cannot be analysed due to image quality. In healthy subjects this is about 6% but rises to 15% in studies of disease. Marwick et el showed in a reference range of 250 healthy volunteers that excellent image tracking quality was achieved in only 79% and that there were systematic variations[200]. Tracking was best in the septum and inferior wall and worst in the anterolateral walls, especially at the apex (Figure 2-25).

Figure 2-25 Relationship between tracking quality (TQ) (mean and SD of TQ score, y axis), wall (color coded, see legend), and segment location (x axis) . The TQ scores are best (closest to 1) in the mid-wall and worst (averages >1.5) in the anterior and posterolateral walls. This regional variation emphasizes the role of image quality (especially edge detection) on TQ [200].
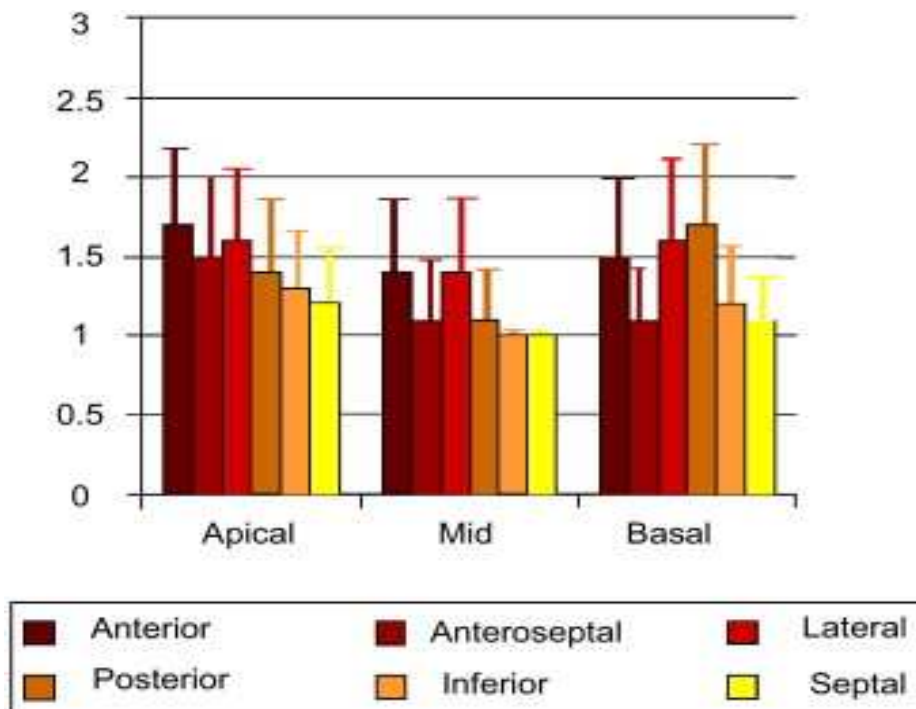
2.2.8.2. Utility of Strain by STE

Normal range, accuracy and precision

Published reference range studies for strain values by STE in healthy volunteers are remarkably consistent with strain by other methodologies such as Doppler-based strain and CMR tagging [200]. Peak longitudinal and circumferential strain ranges from -15% to -20%. Peak radial strain is in the 30-40% range. Values can be reported globally averaged across all 16 or 17 segments of the LV, or segmentally. When reported at a segmental resolution there is significant heterogeneity in values, suggesting that segmental rather than global normal cut-off values could be preferable for clinical use [200]. Marwick et al determined interobserver reproducibility. The mean difference in segmental measurements was 0.24% percentage points, with 95% confidence intervals between −11.4% and +11.8%. Test–retest variability showed no systematic bias, and 95% confidence intervals were between −9.6% and +9.7%. This compares favourably with LVEF by 2D echocardiography which has test–retest variability so that the smallest change of ejection fraction that is detectable with 95% confidence is 11% [201].

Comparisons with Visual Regional Wall Motion Analysis

Echocardiographic assessment of CAD currently relies on visually scored regional wall motion analysis. Guidelines recommend wall motion is scored into 5 categories, but this requires high image quality and a high level of skill and experience in interpretation [202]. However as with TDI, STE has proven

capable of quantifying ischaemia. This was initially proven in animal models [203]. Leitman et al showed in 30 patients with known regional LV dysfunction that there was a graded decrease in longitudinal peak-systolic strain between visually scored normal, hypokinetic and akinetic segments (peak systolic strain 13.4%±4.9 in normal, 10.5%±4.5 if hypokinetic, 6.2%±3.6 if akinetic, P< 0.000001) [204]. Becker et al showed in 62 patients that radial and circumferential systolic strain and strain rate could identify Regional Wall Motion Abnormalities (RWMAs) well compared with RWMAs by CMR [205]. Liel-Cohen et al recently conducted a single centre study in 105 patients, 90 admitted with chest pain and 15 with known dilated cardiomyopathy [206]. The ability of peak-longitudinal strain by STE was compared to the ability of 12 expert echocardiographers to visually determine RWMAs blinded to patient details. Automatic quantification using peak-systolic longitudinal strain with pre-determined cut-offs performed as well as visual analysis by the echocardiographers, with a greater reliability and similar agreement to angiographic findings [206]. This demonstrates the potential to use 2D strain to assist less experienced echocardiographers in identifying regional dysfunction. It should be noted that for the latter study the visual technique does not directly assess the same component of cardiac motion [206]. Wall motion scoring is largely dependent upon radial displacement whereas the automated method was based on longitudinal deformation.

Figure 2-26 Longitudinal strain compares well to expert analysis of regional wall motion in 105 patients with known or suspected heart disease. Mean [SD] values for interobserver and intraobserver reliabilities (A and B, respectively) for binary classification of myocardial segments in normal versus abnormal, hypokinetic versus other, and akinetic versus other segments. An automatic scoring method (ASS) based on cut-offs determined by peak-systolic longitudinal strain by STE are compared to visual scoring (VSS) by 12 expert echocardiographers. Caption adapted from [206].
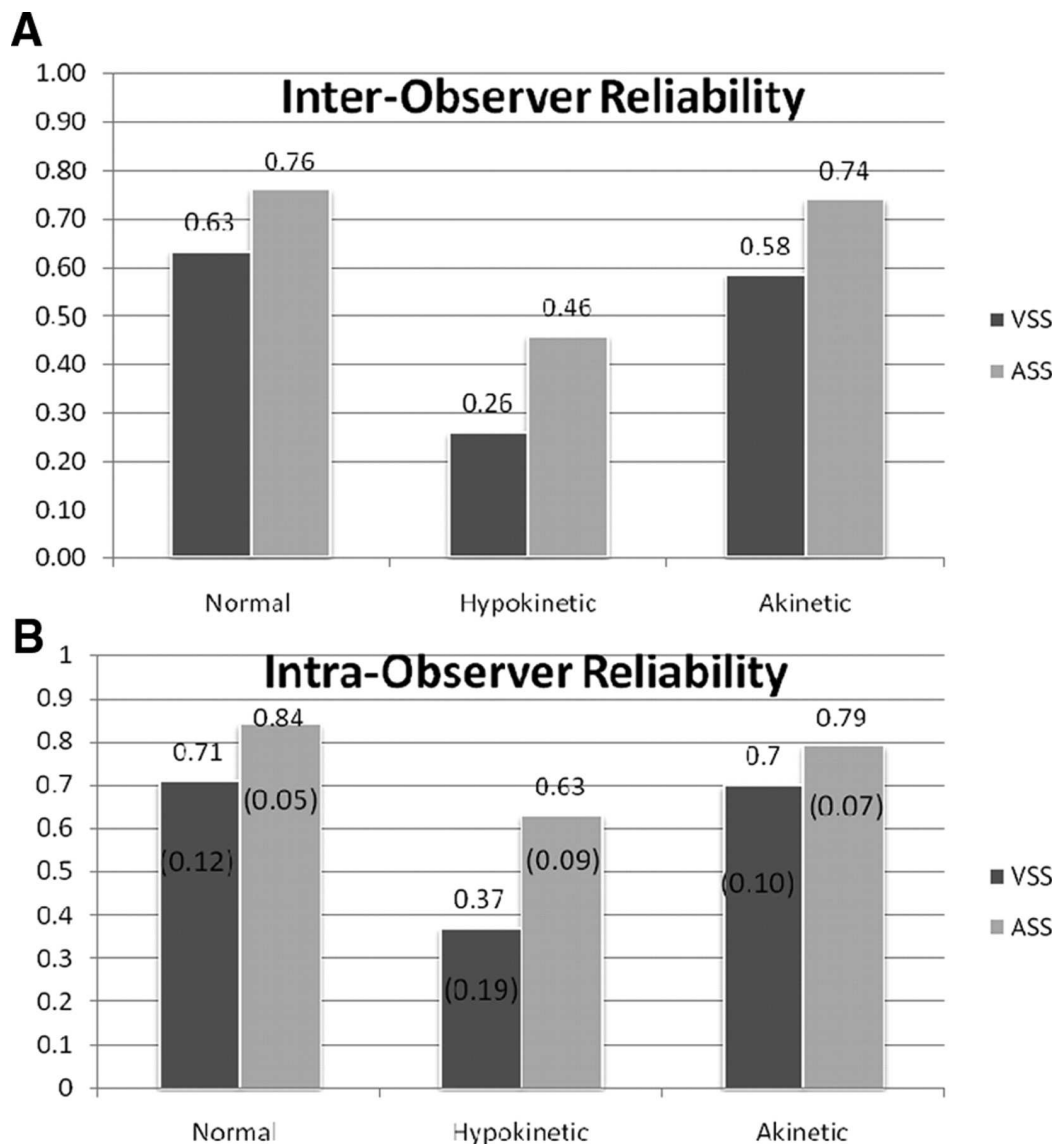
Choi et al showed the utility of strain by STE extended to screening patients with suspected CAD. They studied 108 patients with suspected CAD and no resting RWMAs on conventional echo who underwent resting STE and

70

coronary angiography. They divided into tertiles of risk by severity of CAD at angiography. They then determined the peak-longitudinal systolic strain in each of those tertiles and used receiver operator characteristic curves to show that the groups were best separated by strain with sensitivity and specificity of 79%. The novelty of this study is that strain was able to risk stratify patients without stress testing even when resting wall motion and LV ejection fraction are normal [207]. Therefore, semi-automated determination of longitudinal strain by STE may be a more sensitive marker than wall motion abnormality for severe CAD [207].

2.2.9. Magnetic Resonance Imaging

Magnetic resonance is an imaging technique that evolved from the field of nuclear magnetic resonance and so its origins can be traced back over 100 years with major contributions from several people leading to the imaging technique it is today. Up until the 1970s nuclear magnetic resonance spectroscopy used magnetic fields to determine chemical composition. The signal was one dimensional and could not be localised in space. The shift from spectroscopy to imaging occurred in the 1970s when in a seminal *Nature* paper, Paul Lauterbur proposed a technique of interacting two magnetic fields to create a two-dimensional image in which the image resolution was unconstrained by the wavelength of the imaging field [208]. Unaware of Lauterbur's work Sir Peter Mansfield independently demonstrated using varying interacting fields (gradients) to increase the resolution of the produced image [209, 210]. He also showed how ultra-fast gradient variation could rapidly encode an image [211]. These developments

led to the modern equivalent of encoding an image by frequency and Lauterbur and Mansfield were jointly awarded the 2003 Nobel Prize for Physiology or Medicine. In 1975 Richard Ernst described the first use of Jean Fourier's mathematical methods to decode information from the phase and frequency of the magnetic resonance signal. At present, the Fourier transform remains the basis of image reconstruction.

2.2.9.1. Principles of Magnetic Resonance

Complete confidence in the physics of magnetic resonance is not essential to use the technology but understanding the basic principles will help when trying to optimise image quality and applying more advanced techniques in a clinical research setting. An MRI system consists of a patient table sliding into a fixed magnetic field and several varying magnetic fields. The main field termed B_0, is a large static superconducting electromagnet made by passing electricity through copper tubes supercooled by liquid helium. The B_0 field is in the head-foot direction and is designed to have a completely uniform and homogenous field within its centre. This is usually a sphere of approximately 50cm diameter and this determines the limits of the size of field of view that can be imaged at any one time without moving the patient on the table. Atomic nuclei possess the property of magnetic spin. This refers to a microscopically small rotating local magnetic field called the magnetic moment. MRI can be performed with any nuclei which possess the property of magnetic spin. These nuclei are MR active by virtue of an uneven number of protons and neutrons such as ^{31}P, ^{23}Na, ^{13}C. In clinical practice the most commonly used nucleus for imaging is hydrogen (consisting of a single

proton). This is for two main reasons. Firstly, as the smallest of the MR active nuclei it has the highest spin allowing detection of a larger signal difference for the same strength of external field compared to other nuclei. Secondly, it is abundant in biological tissue as part of water and fat. These intrinsic microscopically small spins are very weak magnetic fields and are normally randomly oriented in the body. When a patient is introduced into the B_0 field of the MR system, the proton spins in the patient have a net alignment of magnetization in the direction of B_0. This net vector of magnetization M in the direction z is termed M_z. Both B_0 and M_z are proportional to the strength of the field measured in units of Tesla.
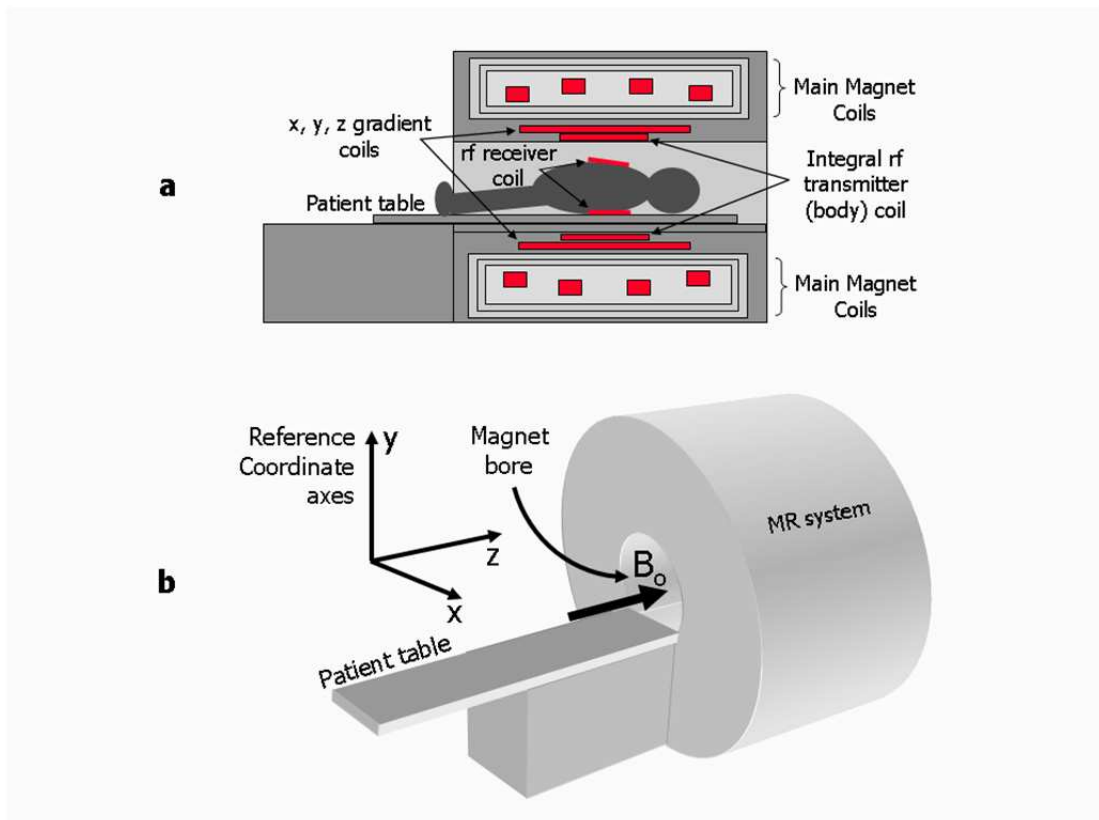
Figure 2-27- MR system components. a) Diagram showing the relative locations of the main magnet coils, x, y, and z gradient coils, integral rf transmitter body coil and rf receiver coils. b) Typical arrangement for a cylindrical bore MR system showing the

magnet bore and the reference coordinate axes with the static Bo field direction along the horizontal z axis

To obtain a signal requires varying magnetic fields to be introduced to the fixed field B_0. These fields can be switched on or off or varied in space on a gradient of field strength. They are called 'gradients' for short and delivered by gradient coils. If a pulse of radiofrequency (RF) waves with the same frequency as the resonant frequency of protons, are introduced perpendicular to B_0 then the protons are excited and this excitation is termed resonance. A simple analogy is a guitar string. It has a note of a certain frequency, which can be made to resonate by introducing a tuning fork with the same harmonic frequency as the string. When the RF pulse stops the protons relax to their resting energy state and radiowaves are emitted and detected by the RF receive coil. The RF pulse tips the direction of the spin from the longitudinal M_z direction into the transverse or xy plane. The angle at which it is tipped is termed the flip angle and the resulting magnetisation is termed transverse magnetisation, M_{xy}. It is the transverse magnetisation that is measured by the receive coil. The received signal has a complex waveform which has no spatial information. To use another musical analogy several voices can be heard from a choir but the signal requires processing to determine location and the pitch of each individual voice. To localize the signal in space a gradient is applied in the head-foot direction at the same time as the RF pulse. This ensures only one part of the patient has protons which will be excited in the centre of the magnet (slice select gradient z). Without applying a simultaneous slice select gradient, protons from the whole patient would be excited and it would be impossible to spatially localize the origin of the signal.

Then a gradient varies frequency of spins along the y direction (frequency encoding). Finally a gradient varies phase of the spins along the x direction. The frequency and phase encoding steps are performed in between excitation and receiving the emitted signal. This only produces a single line in the data-space (termed k-space). The k-space is not a simple cartesian image. Rather, it is a complex image in which each line in k-space contains data from the whole imaging slice. The signal is sampled multiple times and the nature of the signal can be more clearly differentiated with each successive line of k-space. The most essential data is in the centre of k-space with fine and edge detail in the outer k-space.

Figure 2-28- K-space and the corresponding short-axis cardiac image that it produces. K-space is a complex image representing the raw image data which is Fourier transformed (FT) to produce a two-dimensional image.
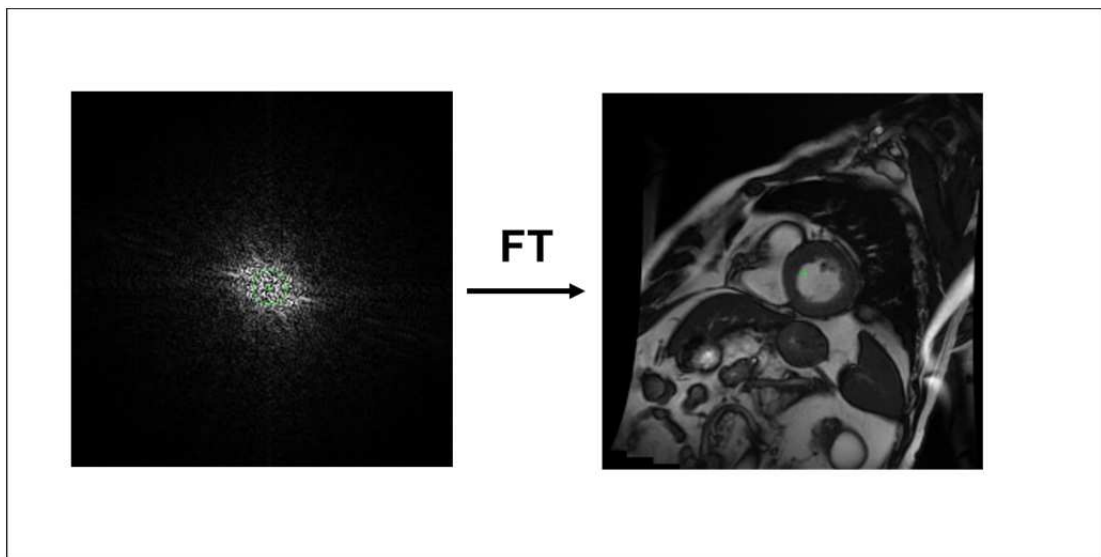
The sequence has to be repeated several times at the desired range of frequencies and phase encoding steps to form a recognizable image. How many times is determined by the spatial image resolution that is sought. Higher image resolution requires more image acquisition time. The final matrix of k-space is then Fourier transformed to produce the final image.

Fourier transform refers to Jean Fourier's set of equations which reduce a complex waveform into a series of sines and cosines enabling description as the set of simple waveforms from which it was derived.

Figure 2-29 A Fourier transform (FT) allows a complex waveform to be simplified into constituent waveforms described by a series of sines and cosines. K-space is Fourier transformed to reproduce the source image. Image adapted with permission of David Higgins[212].
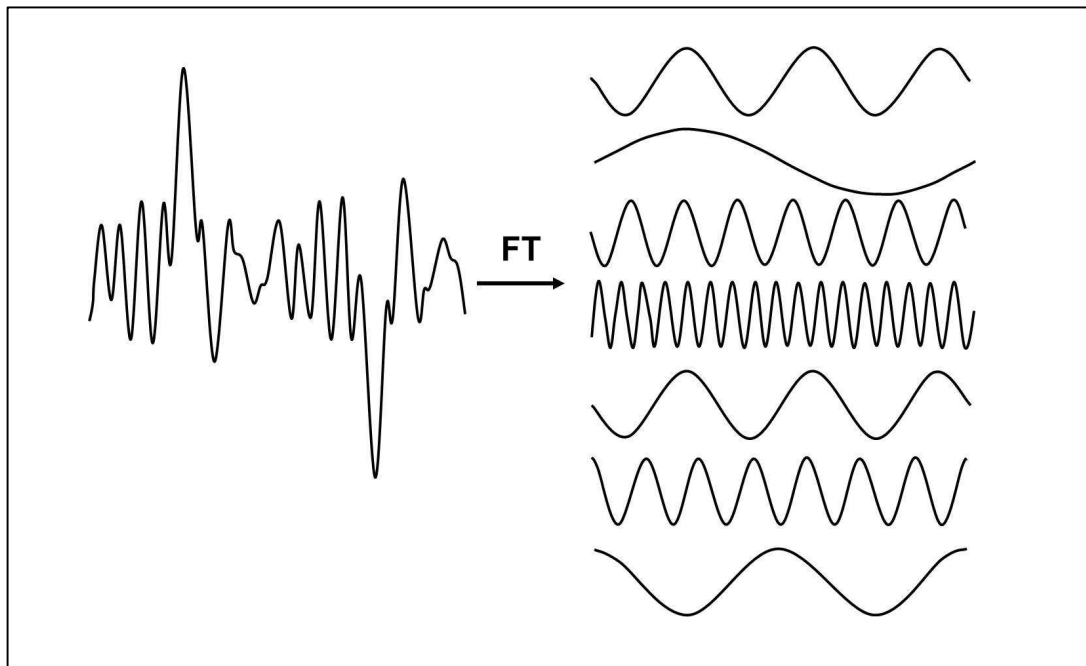
CMR has particular challenges to reduce motion of the heart in the image. This is principally achieved by retrospective ECG-gating of the image and breath-holding to reduce respiratory motion. ECG-gating synchronises the RF pulse to occur after the R-wave of the ECG. The k-space acquisition is segmented into phases of cardiac cycle where each line in k-space is filled from multiple phases. The images are retrospectively phase-ordered to reconstruct a moving cinematographic (cine) image as in Figure 2-30. As such the cine is not a real-time representation of cardiac motion but

constructed from several R-R intervals into a single reconstructed cardiac cycle. How many lines are acquired per R-R interval is the number of k-lines per segment and determines the true temporal resolution of the resulting image and the breath-hold time. The number of k-lines required is determined by the spatial resolution and the size of the field of view. It can be seen that ultimately all images acquired are a trade-off between spatial and temporal resolution, signal-to-noise-ratio and breath-hold time (Figure 2-31).

Figure 2-30- Cine imaging using a segmented k-space acquisition with retrospective ECG-gating. Each line of k-space is acquired from multiple phases of the cardiac cycle, 5 in this example. With prospective gating the R-wave triggers the acquisition. There is a gap before the next R-wave to allow it to be detected. Retrospective gating, acquires data more efficiently and quickly by continuously recording phases and temporal position relative to the R-wave. The data is retrospectively sorted into phase order. Retrospective gating works well with a regular R-R interval but will incorrectly sort and produce a blurred cine if the R-R interval varies or if the MR system mistakes a T-wave for an R wave.
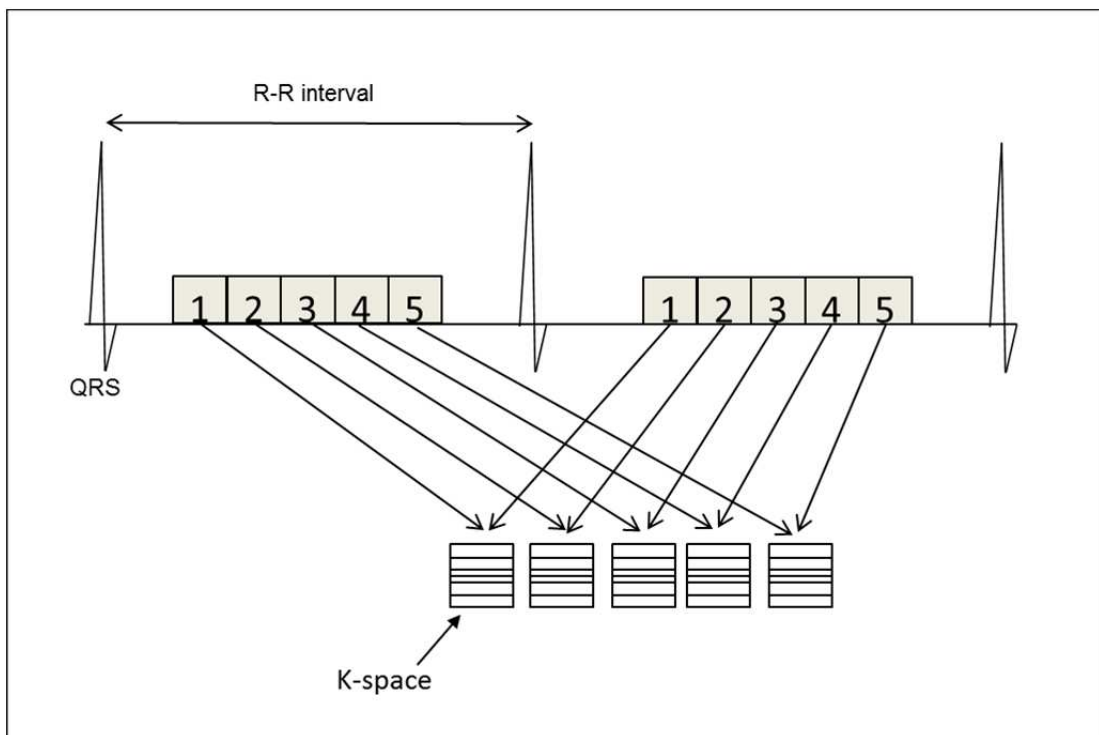
Figure 2-31- Trade-offs in CMR image acquisition. Although several pulse sequence parameters can be user-adjusted, they are all ultimately constrained by acquisition and thus breath-hold time. If patients cannot hold their breath adequately, trade-offs need to be accepted and optimised to achieve diagnostic quality.
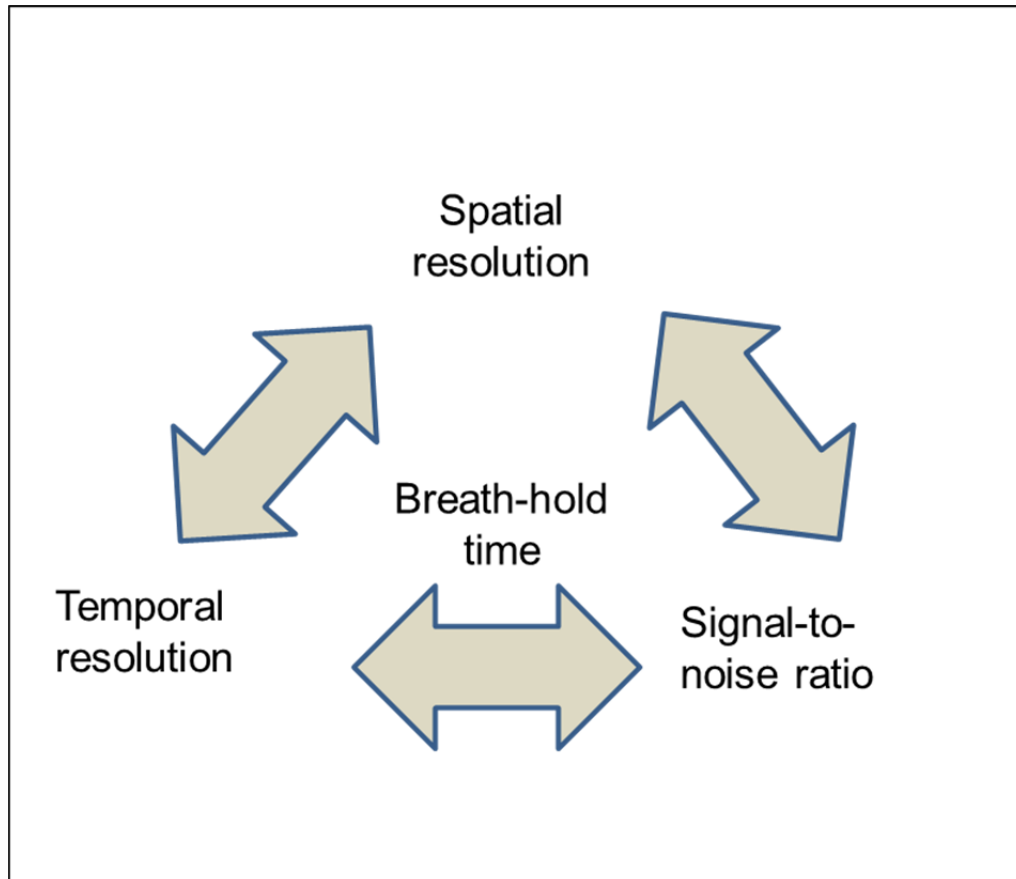
When a proton's spins have been excited, it relaxes to its equilibrium energy state. The length of time over which this energy dissipation occurs are termed T1 and T2 relaxation times. They are essentially inherent properties of the tissue being imaged, varying according to relative water and fat content and the relative freedom of motion that protons have within these molecular structures. T1 is the time after excitation to recover longitudinal magnetisation in equilibrium. T2 relaxation time measures the transverse magnetisation decay. By designing the radiofrequency pulses in a particular way, the image can be weighted to highlight certain characteristics of tissues.

The most commonly used weightings are T1 and T2 weighting. Images can also be T2* and proton-density weighted. The most common sequence used in cardiac imaging is steady-state free precession (SSFP). In terms of weighting SSFP has complex weighting being a mix of T1,T2 and proton-density.

2.2.10.   Cardiac Magnetic Resonance Tagging

Analysis of left ventricular mass and volumes and ejection fraction are the current standard for assessment of global ventricular function and are powerful determinants of cardiovascular mortality. Despite this they are late markers of dysfunction. Assessment of regional deformation within the myocardium may have greater sensitivity and specificity for defining cardiac disease than inferring function from the motion of its boundaries. Strain analysis has been proven to detect early cardiac dysfunction prior to a decline in LVEF in non-uraemic settings [213-216]. Furthermore in heterogenous cardiomyopathy populations with both normal and reduced LVEF, strain was reduced in the subset of populations with normal LVEF and gave additional prognostic information beyond that provided by LVEF and LV mass [217, 218]. Quantifying regional myocardial motion or deformation was first done in animal studies using sonomicrometry, that is surgically implanted acoustic markers [219]. In 1988 Zerhouni et al described for the first time myocardial tissue tagging[220]. It was based upon altering the magnetization to produce visible markers on the myocardium that could be tracked in space and time. The basic principle required slice-selective sinusoidal RF pulses perpendicular to the imaging plane. This saturates the image to produce

areas of dark signal intensity. The sinusoidal nature of the pulse produces a series of lines in the imaging plane. If a second modulated RF pulse is repeated at 90 to the first pulse before image collection then a grid-tag pattern is placed on the heart. Because the magnetization is a property of the tissue the grid follows the shape of the myocardium through the cycle. This allowed visualization of deformation which might otherwise be difficult to visually appreciate. The technique was validated against sonomicrometry in animal and human studies and was termed Spatial Modulation of Magnetisation (SPAMM) [221, 222].

Figure 2-32 SPAMM tagging. (A) SPAMM pulse sequence. The tagging consists of two non-selective 90° RF pulses separated by the tagging gradient (modulation) in the tagging direction, and followed by a crusher gradient to remove residual magnetization. The imaging part is a conventional cartesian k-space acquisition (RO = readout, PE = phase encoding, SS = slice selection). (B)This sequence creates parallel tag lines orthogonal to the x-axis. (C) Example of a SPAMM grid-tagged image showing left ventricle (LV) and right ventricle (RV). Note that this grid pattern needs the application of a second tagging modulation (in the orthogonal direction) next to the first one before imaging takes place. Note also that the dark myocardium between the tag lines is not completely black due to longitudinal relaxation. Figure and caption adapted from [223]
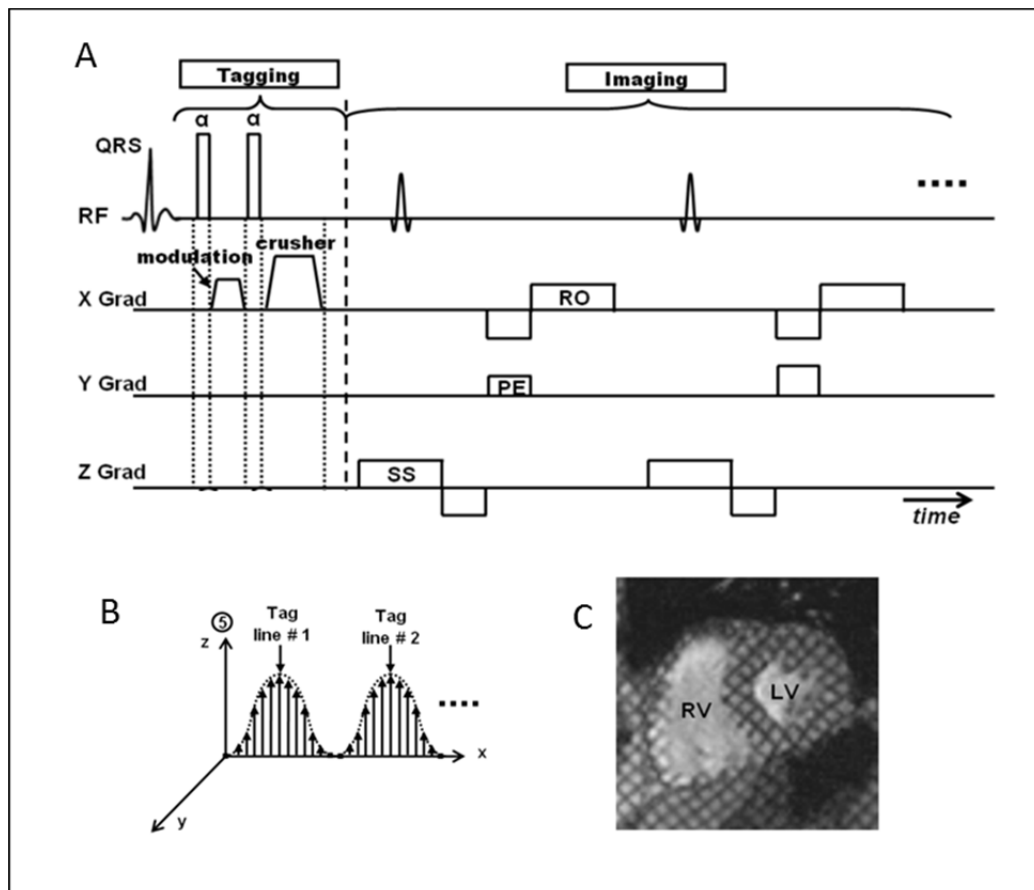
2.2.10.1. Tagging variants

Gradient-recalled echo imaging readout is the commonly used implementation of SPAMM tagging at 1.5T. However at this field strength the tag fades in mid-diastole and is not considered reliable to assess diastolic strain. There have been over 30 variants of tissue tagging since the first description and these have recently been reviewed [223, 224]. The rationale for improvements has been to enhance the utility of tagging by improving several characteristics of the tags including:

i.   Improved temporal and spatial resolution;

ii. increased signal-to-noise ratio;

iii. increased contrast-to-noise ratio;

iv. shorter acquisition time; shorter analysis time

v.   to resolve the issue of through-plane motion in two dimensions.

In 1993 Fischer et al introduced a complementary-SPAMM tagging technique (CSPAMM) [225]. Two consecutive scans are acquired with the same SPAMM tagging parameters except the polarity of one of the tagging RF pulses. This produces a positive tagging grid in one image then a negative tagging grid. Residual magnetization (which limits tagging contrast in subsequent phases) can be removed by subtracting the second from the first image. The subtraction can be done in such a way that the signal is summated (SNR increases 40%) and the noise is 'cancelled'. Therefore at the same signal strength CSPAMM produces sharper tag lines, with less fading and greater access to diastolic phases. The disadvantage is in doubling scan-time compared to SPAMM with implications for the length of

breath-hold required. However, recent modifications to CSPAMM have overcome these problems to enable a tagged image to be acquired in a single breathhold [226].

Gradient-recalled echo imaging readout is the commonly used way of acquiring the imaging readout at 1.5T. More recent developments have been the use of echoplanar imaging (reducing scan time) and steady-state free precession techniques (improving image resolution and contrast) [227]. Other developments have dealt with the issue of through-plane motion by tagging in 3 dimensions [228].

Finally, as tissue tags are saturated magnetization, then greater magnetization by scanning at higher field strengths will also improve SNR and reduce tag-fading by prolonging T1-relaxation time. Comparison of tagging at 1.5T to 3T has shown it has superior diagnostic ability [229].

2.2.10.2. Tagging analysis

Although tagging enabled easier visualization of regional wall motion, its real value lies in highly reproducible and quantitative determination of strain which requires post-processing of the tagged images. Various techniques were historically used including optical flow and active contour tracking methods. These were limited by requiring huge computing power for the era and typically might take 4 hours to analyse a single patient dataset. This confined tagging to the research setting for many years. Interest in tagging has increased since the development of commercially available software that

reduced this time to minutes. HARP analysis was originally developed by Nael Osman and is currently the most widely used method for analysis of tagged images [230]. HARP works by filtering the inverse Fourier transform of the first harmonic of the spectral peaks seen in the k-space (raw data space) of tagged CMR images to yield harmonic magnitude and phase images. Displacement can be calculated from changes in the phase images to determine Lagrangian or Eulerian strain. Strains can be determined locally and spatial resolution is limited to the resolution of the tag (typically 7mm). HARP analysis is now commercially available software (HARP 3.0 Diagnosoft, Palo Alto, California) and has been used in several clinical studies. The accuracy of HARP has been validated in animal and human studies [231, 232].

2.3. MRI of organ perfusion in CKD

2.3.1. Introduction

Blood flow is crucial to ensure normal tissue metabolism. This concept has been confirmed in animal models in several organs, showing that interruption of blood flow leads to impaired oxygenation and metabolism, electrophysiological change, functional impairment and symptoms in quick succession. Appreciation of this continuum has led to the terms 'ischaemic cascade' or 'ischaemic penumbra'(Figure 2-13) [233, 234]. Perfusion is a term used to describe the process of the delivery of blood to the microcirculation of the tissues and microcirculatory impairment marks the start of this cascade. The translation of experimental concepts into efficient treatments for organ ischaemia requires noninvasive methods by which regional blood flow, perfusion, oxygenation and metabolism can be repeatedly interrogated. This allows therapeutic interventions to be directed at the functional significance of disease rather than merely anatomical appearance. An example of such utility is in coronary artery disease. Two - year outcome data from the Fractional Flow Reserve Versus Angiography for Multivessel Evaluation (FAME) trial showed that using an invasive measure of functional reserve rather than degree of arteriographic stenosis to direct the use of drug-eluting stents significantly improved survival [104]. This paradoxical dissociation between the anatomical and functional severity of arterial stenoses is due to the complexity of flow dynamics [235]. This concept can be extended to other organ vascular beds and one can speculate that the lack of knowledge of blood flow or perfusion reserve might

be an explanation for the failure of angioplasty of renal artery stenoses to improve renal functional outcomes in the Angioplasty and Stent for Renal Arterial Lesions (ASTRAL) trial [236].

Perfusion can be measured in animals using radio-labelled microspheres. In humans, quantification can be done by X-ray computed tomography at the expense of a high radiation burden and requirement for use of contrast media. Nuclear scintigraphy is nonquantitative, measuring relative rather than absolute perfusion. Positron emission tomography is quantitative but requires injection of a radioactive tracer and has low spatial and temporal resolution. The noninvasive nature of MRI, its high temporal and spatial resolution and the ability to alter signal characteristics to interrogate physiological change render it ideal to study perfusion. Perfusion measurement by MRI falls broadly into two types: those requiring exogenous contrast media and those that use endogenous tracers by magnetically labelling the blood. Contrast enhanced techniques typically use tracer kinetics of gadolinium chelates, nondiffusible tracers that remain in the vasculature. Delivery of an intravenous bolus of gadolinium shortens the relaxation time of tissue resulting in a large signal difference that can be captured by T1-weighted or T2*-weighted sequences. The nondiffusibility of gadolinium means that it measures local blood volume and using a kinetic model, perfusion can be estimated [237, 238]. This is a well validated technique of high spatial and temporal resolution in several organs. A recent landmark trial including 752 patients showed that it provides greater accuracy than nuclear scintigraphy for the detection of myocardial ischaemia

[239]. However, use of gadolinium is now restricted in chronic kidney disease (CKD) to prevent nephrogenic systemic fibrosis [240]. The clearance times of tracers also render these single-measurement techniques with no ability to repeat the acquisition in the same scan session.

2.3.2. Blood oxygen level-dependent imaging

Measuring tissue function without ionizing radiation, nephrotoxic iodinated contrast or gadolinium is particularly attractive to those managing patients with CKD. Blood oxygen level -dependent (BOLD) imaging uses haemoglobin as an endogenous contrast, exploiting the fact that the transition from diamagnetic oxyhaemoglobin to paramagnetic deoxyhaemoglobin increases microscopic magnetic field inhomogeneity causing more rapid spin dephasing, which decreases the T2*-relaxation time and reduces signal intensity in T2*-weighted sequences. Thus, signal intensity provides an index of tissue oxygenation. BOLD contrast is widely used in functional brain MRI and is the basis of detecting local changes in brain activity with task performance.

In abdominal organs, A multiple gradient-recalled echo (GRE) sequence is most widely used to assess the BOLD signal. This is typically performed under a pharmacological or physiological challenge, such as renal-BOLD contrast following the administration of furosemide and to study water loading [241-243]. Renal-BOLD contrast can also detect the presence of renal hypoxia induced by renal artery stenosis, with an increase in R2* (R2*=1/T2*) in conjunction with a decrease in renal blood flow [244, 245].

Thus it has shown promise in identifying those patients with renal artery stenosis who might benefit from renal angioplasty [245]. BOLD imaging has determined that the angiotensin-receptor blocker olmesartan causes a reduction in R2* indicating improved oxygenation in CKD [246], and has been shown to identify those kidneys with acute rejection from a measured decrease in medulla R2*[247]. However, in the largest human study of abdominal BOLD imaging, Michaely et al, have recently shown that renal-BOLD contrast failed to discriminate between different stages of CKD among 280 patients, questioning its ability to distinguish clinically meaningful differences from single measurements [248].

Some groups have developed novel BOLD schemes using a T2-prepared steady-State free precession (SSFP) signal readout, conferring inherently higher signal-to-noise ratio than GRE sequences with theoretically greater diagnostic accuracy. Arnold et al. studied 60 patients, assessing cardiac-BOLD with T2-prepared SSFP against perfusion by gadolinium contrast-enhanced MRI under adenosine stress [249]. BOLD contrast had an accuracy of 84%, sensitivity of 92% and a specificity of 72% for detecting significant coronary stenosis, compared with 91%, 92%, and 89% respectively for gadolinium contrast-enhanced MRI [249].

It should however be emphasized that using BOLD imaging comes with the caveat that it is an indirect marker of oxygenation, resulting from the complex interplay of perfusion, haematocrit, blood volume, tissue microstructure and oxygen consumption. Further, a number of other factors can alter the T2*-

weighted signal such as magnetic field homogeneity over the organ, vessel geometry and the MRI pulse sequence used. Comparison of myocardial BOLD imaging to perfusion measured by the gold-standard of positron emission tomography with radio-labelled water, showed clear evidence of a dissociation of perfusion and oxygenation as measured by BOLD, with normal oxygenation in 40% of ischaemic segments under adenosine stress [250]. Ultimately, there is no way to convert the BOLD signal intensity alone to a quantitative measure of oxygenation; thus, challenges that modulate the BOLD signal are inherently more meaningful than single baseline measurements. BOLD imaging benefits from improved contrast-to-noise ratio at higher magnetic field strengths; however, inhomogeneity artefacts can become a greater problem [249].

2.3.3. Arterial spin labelling

Arterial spin labelling (ASL) is an MRI technique which provides a non-invasive perfusion measurement. ASL uses the magnetic spins of freely diffusible water in blood as an endogenous tracer. It does so by labelling the magnetization of blood water, typically by inverting the blood water spins before they enter the tissue of interest. The labelled water then exchanges with tissue water, with the magnetization then decaying at a rate limited by the T1-relaxation time of the tissue water. By subtracting the difference of a labelled image from a control image with unlabelled blood water, a *perfusion-weighted* image is obtained for which signal intensity is proportional to perfusion. Direct quantification of perfusion can be calculated from a kinetic model if knowledge of the tissue T1 relaxation time, blood-tissue partition co-efficient and transit time of the blood water to tissue water is known[251]. Common to BOLD imaging, ASL is infinitely repeatable allowing applications that cannot be conceived using contrast media. However, as the signal change is small, ASL imaging relies on the acquisition of multiple label and control image pairs and averaging of the resulting perfusion-weighted images. ASL also has several additional features. The label is short-lived and decays with T1 relaxation time. Although this necessitates rapid image acquisition after labelling, it also ensures the signal is not affected by venous outflow and the kinetics are only related to arterial inflow. Gadolinium based flow measures are inherently volume dependent meaning that the signal depends on bolus timing and the water-tissue exchange slows the disappearance of the signal. ASL is theoretically applicable to any organ

with a well-defined arterial supply. ASL was first used in the brain some 20 years ago and the technique has developed to the extent that it is sufficiently robust for clinical use [252]. However, there is far less published data relating to its use in abdominal or thoracic organs (kidney, liver and heart). In the most advanced brain ASL schemes, the label can be modulated to yield a fast acquisition of perfusion mapped by individual feeding arteries (Figure 2-33). If these advanced ASL schemes can be developed and applied in other organs, examples of utility might include the selective labelling of the left and right coronary arteries.

Figure 2-33 Vessel-encoded ASL allowing three-vessel separation above the Circle of Willis. In the tagging plane shown on the right, the anterior cerebral artery (ACA) is confined to the midline and the corresponding territory is represented in the ASL maps as bright green. The territories supplies by the insula branches of the middle cerebral arteries (MCAs) are well tagged and are bright red and blue, but other smaller branches of the MCAs are not well tagged, leaving the ACA/MCA border unclear. Scan time: 6 min. Adapted with permission from [253]
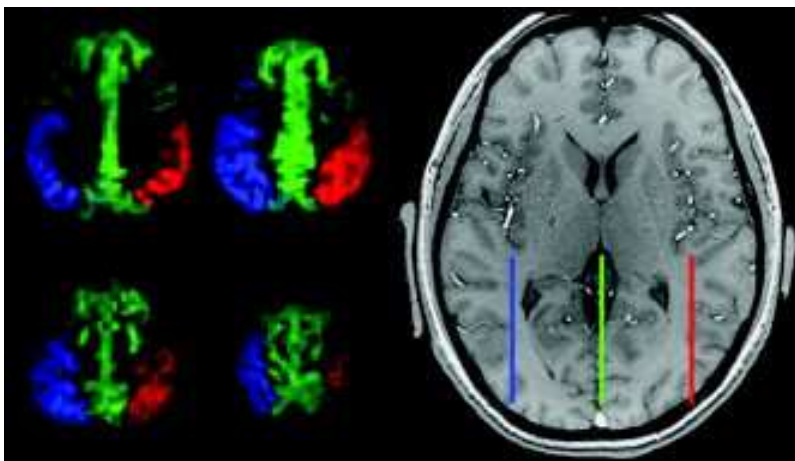
ASL can be broadly divided into two variants, continuous or pseudo-continuous ASL and pulsed ASL. In continuous and pseudocontinuous ASL, the blood is continuously labelled until the magnetization reaches a steady state. Continuous ASL is limited by the requirement of long radiofrequency

pulses causing off-resonance artefacts, loss of the label as it travels to the imaging slice and high specific absorption rates of radiofrequency-induced heating. However, a recent pseudocontinuous ASL method has been introduced which uses a train of rapidly repeating low angle radiofrequency pulses to reduce such effects. In pulsed ASL, a single inversion radiofrequency pulse is used to provide a wide label in a slice of arterial blood and imaging is performed after a few seconds allowing the labelled blood to reach the tissue of interest. One of the most common implementations of ASL in body imaging is the flow-sensitive alternating inversion recovery (FAIR) pulsed ASL scheme, as depicted in Figure 2-34.

Figure 2-34 Principles of arterial spin labelling perfusion measurement by flow-sensitive alternating inversion recovery.

(A) Upper row: An image is collected with renal arterial blood water labelled by magnetic inversion (coronal, axial and sagittal views of a non-selective label slab shown outlined in white to label inflowing blood) which is subtracted from a control image (selective control slab shown outlined in black) to yield a perfusion-weighted image. (B) Lower row: The signal intensity difference between the control and label images generates a perfusion weighted image with signal intensity of ~ 1–4%. Using a kinetic model, this difference image can be converted to a map of absolute regional perfusion values.
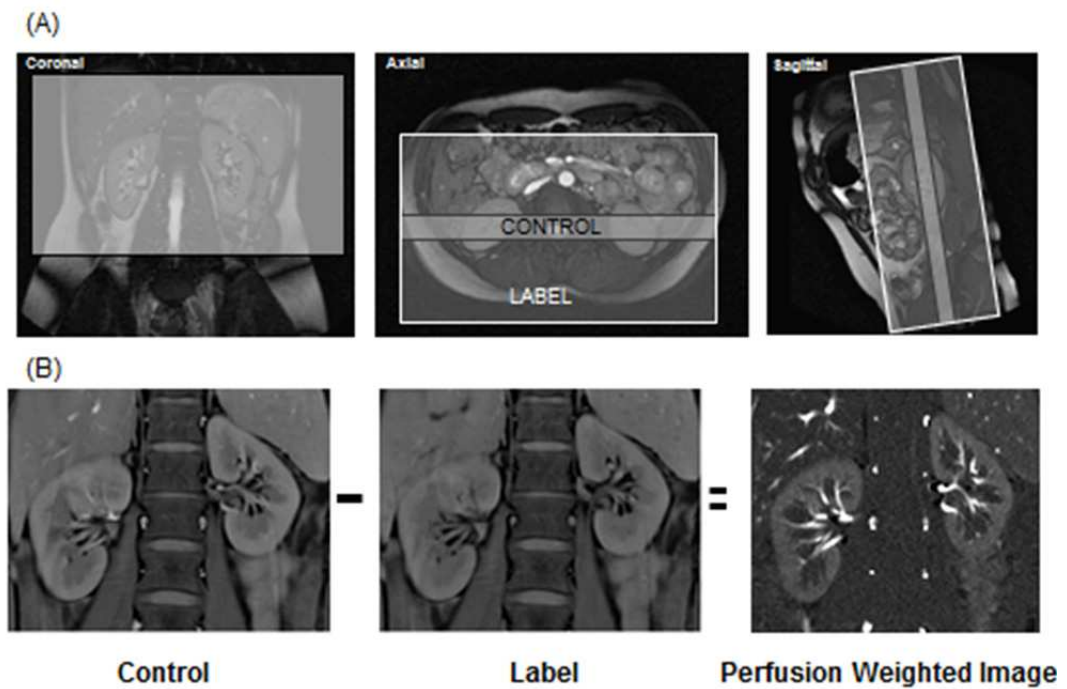
The perfusion weighted signal can be quantified in units of ml/100g/min, when combined with measures of tissue relaxation time and label transit time (Figure 2-35).

Figure 2-35 Estimation of renal perfusion generated by flow-sensitive alternating inversion recovery-arterial spin labelling using a (A) T1-relaxation time map; (B) arterial transit time map and (C) quantitative regional perfusion map in ml/min/100g of tissue.
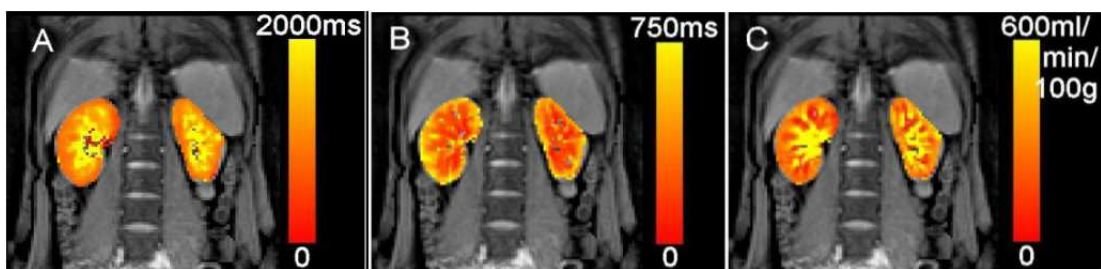
2.3.4. Developments of arterial spin labelling

Cardiac gadolinium contrast-enhanced MRI conveys a signal difference of 40–50% between normal and ischaemic tissue leading to images that are visually diagnostic at the time of acquisition. By comparison, ASL and BOLD images are both limited by low signal intensity differences in the order of 1–4%. This is overcome in ASL by repeating the label-control acquisition to achieve an averaged signal, typically of the order of 40 averages in ASL of the brain. In the kidney, this requires multiple breathholds, and data has typically been acquired in a single 8–10mm slice following the labelling. However, recent advances in parallel imaging exploit multichannel coils to accelerate the time it takes to acquire an image [254]. Gardener and Francis performed the first study combining FAIR-ASL of the kidney with parallel

imaging and a fast imaging readout, allowing whole kidney ASL imaging [255]. ASL is a subtractive technique and is particularly sensitive to tissue motion. In the same study, Gardener and Francis examined strategies to reduce motion artefact, showing that using a respiratory navigator and postacquisition motion correction improved image quality [255].

2.3.5. Renal arterial spin labelling

Glomerular filtration is dependent on renal perfusion. FAIR-ASL -measured perfusion of the kidney has been validated against radio-labelled microspheres in a swine model and para-aminohippurate clearance in humans [256, 257]. It has been shown to clearly differentiate between medullary and cortical perfusion and is capable of being competitive with contrast-enhanced magnetic resonance at 3T [258]. In a recent study including 25 patients, transplanted kidneys showed lower levels of perfusion compared to native kidneys at similar estimated glomerular filtration rate [259]. In a study of 34 hypertensive patients, ASL was used to determine that the renin inhibitor aliskiren causes a temporary increase in renal perfusion, which reversed despite sustained blood pressure reduction [260]. ASL has also recently demonstrated differential effects of 0.9% saline with balanced crystalloids on renal perfusion in 12 healthy volunteers [261]. A recent animal study used renal ASL to demonstrate that contrast-induced nephropathy is mediated at least in part by hypoperfusion [262]. Intravisit reproducibility has also been examined demonstrating excellent intraclass correlation [263, 264].

2.3.6. Cardiac arterial spin labelling

Because of complex three-dimensional motion of the heart, the development of cardiac perfusion imaging using ASL has been challenging, requiring the use of cardiac triggering and breathholding or respiratory triggering. This increases the signal averaging requirements for cardiac ASL, such that a large number of breathholds are required, which can make clinically useful ASL unfeasible without using motion registration techniques to allow free-breathing acquisition. Thus far ASL measurements of myocardial perfusion are proven to be arterial inflow dependent, match the range of published literature values, and are capable of detecting changes with mild induced stress such as handgrip exercise [265]. Zun et al. recently showed that cardiac FAIR-ASL with adenosine stress was able to detect inducible ischaemia in patients with coronary artery disease [266]. The low signal-to-noise ratio of cardiac ASL requires that the signal be averaged over many voxels for quantification. Zun et al. grouped perfusion data for a single short-axis slice to achieve diagnostic accuracy [266], as depicted in Figure 2-36.

Figure 2-36 ASL Perfusion Reserve Maps and X-Ray Angiograms from 2 Patients. (A, B) Patient with total left anterior descending occlusion; (C, D) patient with total right coronary artery occlusion. Myocardial regions with lowered perfusion reserve were consistent with the territories of occluded vessels (arrows). LV left ventricle; RV right ventricle. Reproduced with permission from Zun et al [260]
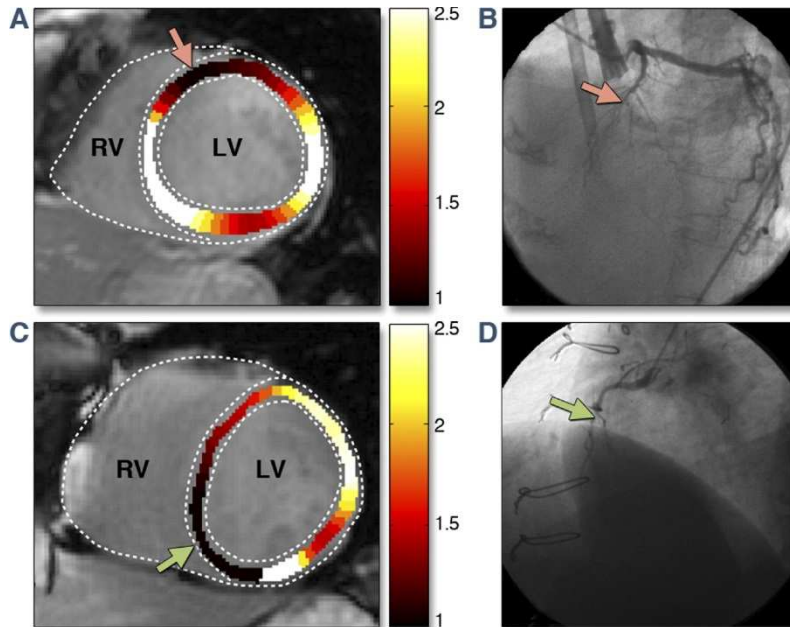
This technique is capable of detecting only large transmural deficits; is far from the currently achievable 1–3mm spatial resolution achievable with gadolinium and would miss subendocardial or diffuse ischaemia. To achieve this, whole heart coverage with acceptable spatial resolution, reduced motion artefacts and increase in signal-to-noise is required. Wang et al. have recently shown that such an approach is feasible using a free-breathing acquisition combined with parallel imaging, motion correction and noise suppression techniques [267]. Higher field strengths prolong the persistence of the label. This would additionally provide improved signal-to-noise ratio, allowing greater spatial and temporal resolution in the same acquisition time or the same spatial and temporal resolution in a shorter time. Another

specific issue to cardiac ASL is that labelling the blood using the commonly implemented pulsed ASL scheme to invert a slab will also label left atrial blood causing a large false signal change in the left ventricle which interferes with the true ASL signal at the endocardial border. This will require strategies such as spatially selective labelling of the left ventricular outflow tract.

2.3.7. Translation of arterial spin labelling into clinical practice

Table 2-6 ASL Variants

	Method	Sequence name
Continuous ASL	Asymmetric	Original CASL
		DAI
	Symmetric	SPDI
	Two coil	Two coil method
Pulsed ASL	Asymmetric	EPISTAR
		PICORE
		TILT
	Symmetric	FAIR
		UNFAIR/EST
		FAIRER
		FAIRER
	Selective	RPI
		PULSAR
		QUASAR
	QUIPSS	QUIPSS I
		QUIPSS II
		Q2TIPS

One can speculate about the barriers of translation of ASL into clinical practice. One may be the sheer flexibility of the technique and its optimization by independent groups. Currently, there are several variants of the methods used to: label the magnetization of inflowing blood, acquire the image, and reduce the effects of motion (such as breathholding, respiratory triggering or navigators), Table 2-6. Finally, there is a lack of large studies to validate or compare the variants in terms of sensitivity, specificity, reproducibility and change with disease state [268]. Table 2-7 suggests a developmental framework for ASL and BOLD imaging and against this

benchmark, clinical use within the kidney and heart remains a few years away.

Table 2-7 Framework of incremental steps required for development of noncontrast MRI to quantify perfusion in thoracic or abdominal organs (adapted with permission from Sado et al. [35]

Each step is harder to fulfil. No current test in development achieves more than 5 of these 15 steps - 7 if abstracts are included—and many whole imaging modalities have never achieved the final step.

1. Technical development and theoretical basis of test.
2. Direct comparison (animal models and then human autopsy material).
3. Detection of changes in established disease compared with normal subjects.
4. Correlation with known markers of impaired perfusion (eg, diastolic function, left ventricular hypertrophy, reduced glomerular filtration).
5. Correlation with known biomarkers of reduced perfusion (eg, cardiac troponins).
6. Demonstration of the test in more than one clinical scenario.
7. Demonstration of test sensitivity (early disease or with age).
8. Demonstration of the ability to track change (with time, after treatment).
9. Demonstration of predictive or prognostic value of the test.
10. Standardisation of the test (reproducibility, different equipment, in non-research settings, quality control, limitations of test).
11. Development of robust age/ethnic normal reference ranges
12. Changes in biomarker remain tied to the disease after treatment.
13. Demonstration of the test as a surrogate trial endpoint.
14. Clinical use and regulatory approval of the test.
15. Proof test use improves clinical outcome.

Preliminary observations support the use of ASL data as an outcome measure in clinical trials [269]. A recent landmark has been the introduction of commercially available BOLD and ASL sequences for use in the brain by MRI manufacturers, with a joint action towards the harmonization of ASL being recently established [268].

Accurate quantification of ASL perfusion also requires knowledge of the tissue T1 equilibrium magnetization, as well as transit time of the label. This is typically measured post-acquisition from additional images. Clinical utility will be increased by automating the post-processing steps (including T1-measurement and kinetic modelling) to allow real-time ASL perfusion maps to guide clinical decisions and the first implementation of this has recently been described [270].

2.3.8. Conclusion

ASL measures perfusion, whereas BOLD imaging provides a marker of tissue oxygenation and these techniques are, therefore, complementary rather than competing measures. ASL is inherently quantitative, whilst BOLD imaging is not. Thus, multiple measurements of BOLD contrast under physiological or pharmacological challenge are more meaningful than single measurements. In body imaging, ASL being a subtraction technique is prone to tissue motion, whereas BOLD imaging is additionally prone to inhomogeneity artefacts and both are relatively low signal techniques compared to contrast-enhanced MRI. However, their non-invasive and infinitely repeatable nature makes them attractive alternatives to using contrast media, particularly in the context of CKD. Given the importance of tissue hypoxia and ischaemia in disease processes, demand for the techniques is likely to be driven by clinical applications such as in CKD, where the greatest incentive to avoid the use of contrast media exists.

2.4. HD induced myocardial ischaemia

2.4.1. Dialysis patients are primed to suffer myocardial ischaemia

Patients with chronic kidney disease requiring either HD or PD are particularly susceptible to myocardial ischaemia. This is due to large vessel and microcirculatory changes resulting in reduced coronary flow reserve (CFR) [271, 272]. This results in reduced ability to increase blood flow to the myocardium during increased demand. This is partly a consequence of left ventricular hypertrophy (LVH), seen in 74% of patients on dialysis [108]. Increased peripheral artery stiffness also reduces the ischaemic threshold [273] whilst a high prevalence of vascular calcification in dialysis populations leads to increased arterial stiffness [274]. The two factors cause a propensity to reduced myocardial blood flow (MBF), and particularly sub-endocardial MBF.

The baroreflex arc is responsible for short-term control of blood pressure (BP) [275]. Abnormalities of the baroreflex arc are well documented in chronic kidney disease (CKD) patients, in both pre-dialysis and dialysis-dependent settings. HD patients characteristically exhibit defective blood pressure (BP) control in the face of ultrafiltration (UF) requirements, in part due to impaired baroreflex sensitivity (BRS). In patients with low BRS values this lack of effective vasoregulation results in a tight association over a dialysis session between change in relative blood volume (RBV) and change in cardiac output. In HD patients with intact BRS the fall in RBV has no

association at all with change in cardiac contractile performance. This lack of a fully intact baroreflex arc leaves cardiac performance excessively dependant on intravascular volume in patients where tissue flow/perfusion has become excessively dependant on pressure [276].

2.4.2. Haemodialysis induced myocardial ischaemia

In the setting of CAD without CKD, transient myocardial ischaemia may lead to left ventricular dysfunction that can persist for several hours after the return of normal perfusion but is eventually followed by functional recovery. This prolonged but reversible dysfunction is known as myocardial stunning [277]. Repetitive episodes of ischaemia are cumulative and eventually lead from myocardial stunning to hibernation to irreversible contractile dysfunction [278].

It has long been suspected that myocardial ischaemia may also be precipitated by HD [279]. Reports of silent ST segment depression during HD were noted some twenty years ago [280]. Although this was noted in 15-40% of HD patients the evidence was inconclusive as the specificity of these changes to detect ischaemia is reduced in the presence of LVH. In addition, several studies confirmed the recognized phenomenon of elevated cardiac troponins in dialysis patients [281]. Short intermittent HD treatments exert significant haemodynamic effects, and 20-30% of treatments are additionally complicated by episodes of significant intradialytic hypotension (IDH) [282, 283]. These studies provided indirect evidence that HD might induce myocardial ischaemia but lacked the techniques to provide definitive proof or elucidate the pathophysiology.

McIntyre et al utilised $H_2{}^{15}O$ positron emission tomography (PET) to measure myocardial blood flow (MBF) during HD. Significant CAD was excluded by angiography. There was a 30% mean reduction in MBF to levels at peak dialytic stress which recovered after dialysis consistent with the development of myocardial stunning [284]. The same study also confirmed that HD-induced segmental left ventricular dysfunction measured by 2D echocardiography correlated with the matched reduction in segmental MBF seen with PET. These findings were confirmed in a study using ^{13}N-NH_3 PET [285].

Figure 2-37 Mean global myocardial blood flow (MBF) reduced significantly during dialysis from baseline with partial restoration in the recovery period
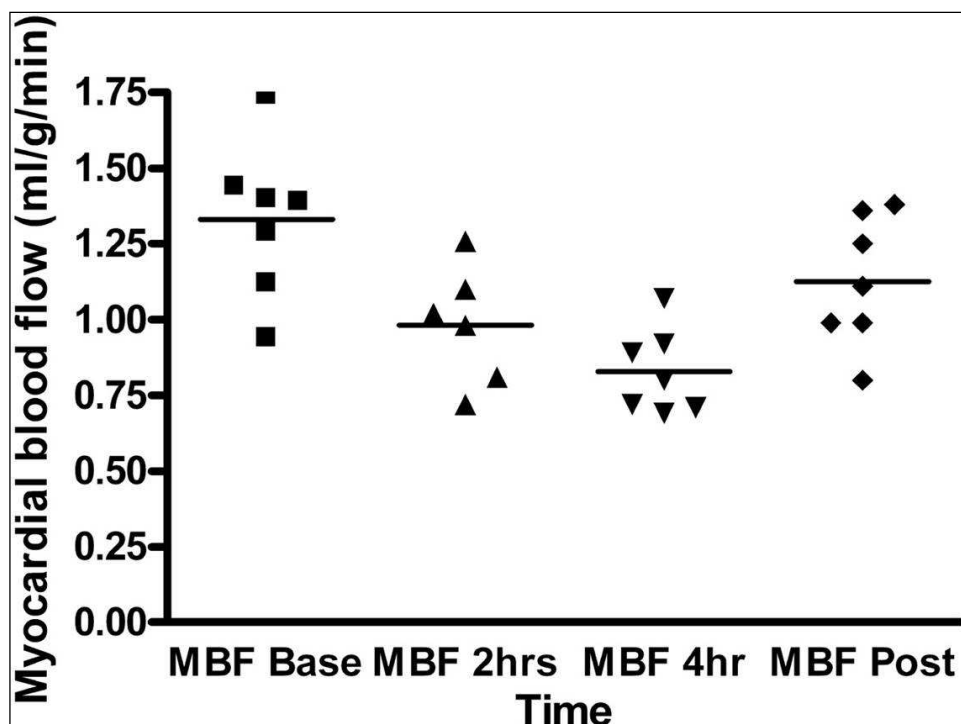
HD is capable of inducing subclinical myocardial ischaemia, and this phenomenon is related to UF and haemodynamic instability. Burton et al studied a cohort of 70 prevalent HD patients. Myocardial stunning was

defined by the development and subsequent recovery of regional wall motion abnormalities (RWMAs) utilising serial intradialytic echocardiography [286]. Myocardial stunning occurred in around two thirds of patients. In multivariate analysis both intradialytic reduction in BP and UF volume independently determined the propensity to suffer HD induced cardiac injury. The only other associated factors of significance from this model were patient age and Troponin T level (pre-dialysis levels being around three times higher in affected patients). These four factors displaced all other standard biochemical, haematological, historical and dialysis treatment based variables. 12 month follow up of this group, revealed significant effects on cardiac structure, function and patient survival. Those patients who did not develop HD induced myocardial stunning experienced only one significant cardiac event, no change in segmental shortening fraction, no reduction in overall LV ejection fraction and 100% survival. This was in contrast to the group characterised by the development of myocardial stunning, where 28% of the patients had died. In those patients that survived to 12 months, shortening fraction had reduced by roughly half with an absolute reduction in LV ejection fraction (at rest and at peak during HD) by around 10% in conjunction with an attendant significant increase in troponin T. At 12 months, intradialytic BP was significantly lower in patients who stunned c.f. their baseline assessment. This was in contrast to patients who did not exhibit dialysis induced myocardial stunning who had identical haemodynamic tolerability of HD at both ends of the study period [286, 287]. Given the underlying vulnerability of hibernating myocardium to increases in demand, coupled with decreased CFR in HD patients, it may be that this

adaptive process actually leads to further segmental injury by exacerbating intradialytic instability. This may be one of the reasons that prevalence of heart failure is so high, and survival so poor in HD patients that start to develop myocardial contractile dysfunction.

Survival may also be determined by the incidence of intradialytic and post-dialytic ventricular arrhythmias. Burton et al studied a cohort of 40 prevalent HD patients with 24 hour Holter recordings started just before a HD session. Patients also had baseline, intra- and post-dialytic echoardiography. The study showed a significantly higher frequency of ventricular arrhythmias in the 27 patients who demonstrated myocardial stunning and in all patients the arrhythmias occurred most frequently during HD [288].

To elucidate the relationship between UF volume or rate and myocardial stunning Jefferies et al performed an observational study in a cohort of stable patients across the spectrum of available quotidian HD regimes. Four patient groups were studied: Conventional in-centre HD 3 times per week (CHD3, n=12), short daily HD 5-6 times per week both in centre (CSD, n=12) and at home (HSD, n=12), and nocturnal home HD (HN, n=10). The groups were matched for age, dialysis vintage and baseline LV ejection fraction. UF volumes and intradialytic systolic BP reduction were both significantly lower in home-based frequent therapies. HD-induced myocardial stunning was ubiquitous in CHD3 patients. The proportion of patients exhibiting dialysis induced RWMAs reduced significantly with increasing dialysis intensity

(CHD3>CSD>HSD>HN). More frequent HD (HSD and HN) was associated with less RWMAs and lower high sensitivity C-reactive protein levels than CHD3. UF rate correlated strongly with the number of RWMAs [289]. This study demonstrated for the first time that more frequent HD regimes are associated with less myocardial stunning compared to conventional HD. It provides a mechanistic subtext to support the findings of large scale observational studies that associate higher UF volumes or rates with worse CV outcomes [26, 290]

2.4.3. Role of epicardial CAD in HD-induced myocardial stunning

There are convincing data that a combination of microcirculatory dysfunction, ischaemic potential of reduced peripheral arterial compliance, in addition to the other non-atheromatous consequences of the uraemic milieau, are capable of allowing dialysis induced injury to occur in the absence of conventional epicardial CAD. Firstly, our initial study of MBF during HD was performed in patients who had first been subjected to coronary angiography. Despite the absence of any significant disease those patients still exhibited a myocardial ischaemic response to HD [284, 285]. Secondly, to acquire a patient group with uraemic cardiovascular disturbances, but in the absence of conventional cardiovascular risk factors, Hothi et al studied a cohort of paediatric HD patients. The dialysis treatments were characterised by particularly large UF requirements and significant relative dialysis induced hypotension. A high proportion of the children (11/12) exhibited evidence of acute dialysis induced myocardial stunning, with some biochemical evidence of cardiac injury [291].

2.4.4. Modifications of HD that abrogate myocardial ischaemia

A variety of therapeutic manoeuvres aimed at improving the haemodynamic tolerability of HD have been demonstrated to reduce dialysis induced myocardial ischaemia.

2.4.4.1. Biofeedback controlled HD

In the first of these studies Selby et al compared standard bicarbonate HD with a biofeedback technique that responded to significant declines in RBV by temporarily reducing UF rate and increasing dialysate conductivity. This was done within defined limits to ensure total fluid and sodium depuration was unaffected [292]. In a separate cohort Selby et al compared standard HD using a dialysate temperature of 37°C to a cooled dialysate of 35°C [293]. In both studies reduced RWMAs and improved mean shortening fraction were demonstrated. It may be that either the higher mean BP or the reduction in IDH was responsible for the reduction in the incidence of RWMAs, although it is also conceivable that the effects of both of these factors were synergistic, with IDH that occurs at a lower mean BP potentially having a greater detrimental effect on myocardial perfusion. In PET based study of intradialytic MBF, use of the biofeedback technique resulted in reduced instability only in the later part of HD and this was associated with a significantly better recovery of MBF post HD, supporting the contention that at least with this technique the beneficial effect on MBF was linked to maintenance of intradialytic BP [284].

2.4.4.2. Individualisation of dialysate sodium

Larger inter-dialytic weight gain (IDWG) or larger ultrafiltration (UF) volumes are associated with increased mortality and myocardial stunning (**Figure 2-38**). These might be removed by more intensified dialysis by treatment length or frequency and daily dialysis is associated with reduced HD induced myocardial stunning [294]. However access to intensified dialysis might be constrained by social and economic factors. Alternative strategies directed at minimising IDWG within the constraints of conventional thrice weekly in-centre HD treatments of around four hours are essential to improve the tolerability of HD and the development of cardiac failure.

Figure 2-38 Larger IDWG is associated with increased all-cause mortality both in registry studies (left Kalantar-Zadeh et al [26] and prospective studies (right, Movilli et al[290]).
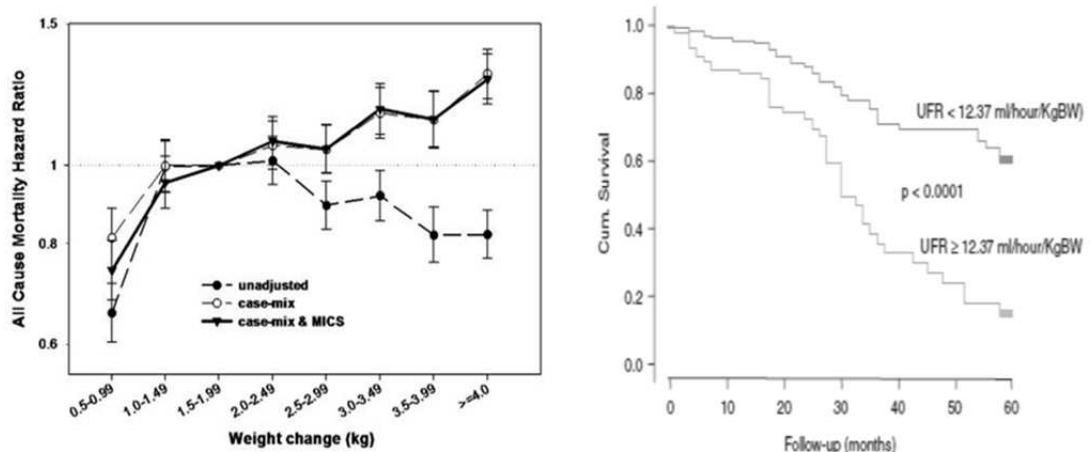
In HD patients without diabetes, larger IDWG is driven entirely by sodium intake. This is largely dietary sodium intake but due to a fixed osmolar set

point, use of one dialysate sodium concentration for a dialysis unit can lead to many patients receiving a net increase in total body sodium during dialysis, so-called 'sodium loading' [295, 296]. This will drive thirst and promote higher IDWG. There have been few attempts to optimise dialysate sodium [297, 298]. We have previously studied use of a fixed two week stepwise reduction in dialysate sodium in this setting but the studies lacked detailed intra-dialytic haemodynamic assessment and the potential of these methods to abrogate myocardial stunning has not been investigated [299, 300]. These studies were further limited by their short duration, failing to capture effects of longer term sodium depuration from myocardium and the resistance vasculature [39, 301]. An important factor in study design is to exclude patients with type 1 or 2 diabetes. HD patients with diabetes have thirst that is equally driven by hyperglycaemia and would require a separate study [43].

2.4.4.3. Remote ischaemic pre-conditioning

Another approach to reduce myocardial stunning may lie in protecting against ischaemia. Several studies have shown cardio-protective benefits of remote-ischemic pre-conditioning but its potential to abrogate HD-induced myocardial stunning remains unexplored. Transient sub-lethal episodes of ischaemia (preconditioning stimulus) before a prolonged ischaemia/reperfusion injury, known as ischemic preconditioning (IPC), induce a state of protection against subsequent prolonged ischaemia. There are 2 phases of protection; the early phase, within minutes of the preconditioning stimulus for up to 4 hours and a 'second window of protection', 24 hours after the preconditioning stimulus, which lasts for up to

72 hours. How this benefit is mediated has not been fully elucidated but involves induction of intracellular kinases and changes in mitochondrial function including activation of the mitochondrial K_{ATP} channel. The realisation that IPC protects tissues that are remote from those undergoing preconditioning (remote ischaemic preconditioning; RIPC) has led to its translation into the clinical setting in multiple studies[302]. RIPC is mechanistically similar to IPC inducing a similar degree of protection. The preconditioning signal is spread systemically by a mechanism that includes activation of the autonomic nervous system and unidentified humoral mediators. RIPC can be applied with a simple blood pressure (BP) cuff applied to a limb for 5 minutes or more at greater than systolic pressure. This has proven to be safe and tolerable in multiple human studies performed to date which have demonstrated cardio-protective benefits in a mixture of clinical and surrogate endpoints in settings including cardiac surgery and coronary angioplasty [303]. The studies are not universally positive, a recent study demonstrated no benefit on surrogate endpoints prior to cardiac surgery [304]. RIPC remains untested in the setting of conventional HD, a model of a repetitive ischaemic injury. There is some evidence suggesting patients with diabetes may have a suboptimal response to IPC [305, 306] hence it is rational to study this group using a pre-specified separation.

2.5. A randomised controlled trial of dialysate cooling

The work presented in this thesis utilises data from the baseline study visit of a current randomised controlled trial of dialysate cooling to prevent left ventricular systolic dysfunction in HD patients. The main hypothesis of this trial is that patients having regular conventional HD will have a smaller decline in cardiac systolic function by using cooler dialysate.

2.5.1. Trial background

Maintenance HD patients represent an extreme phenotype of adverse cardiovascular risk and few interventions have proven efficacy in regressing cardiovascular morbidity. The HD procedure commonly induces cardiac ischaemia, characterised by reversible left ventricular regional wall motion abnormalities on echocardiography. Patients demonstrating such regional abnormalities have later development of cardiac systolic dysfunction and increased mortality [307, 308]. The Frequent Hemodialysis Network (FHN) trials showed regression of left ventricular mass and volumes [309, 310]. Resource availability and patient acceptance of more frequent schedules might be limited in some healthcare systems such that reducing circulatory stress within the constraints of conventional, thrice weekly treatments is of value [311]. Prior studies demonstrated that cooling the dialysate during HD reduces the number of episodes of intra-dialytic hypotension and the prevalence of *de novo* wall motion abnormalities [293, 312]. There are several postulated mechanisms by which cooler dialysate might improve haemodynamic stability, predominately mediated through maintenance of systemic vascular resistance. These include abrogation of thermoregulatory

peripheral vasodilation by reduced extracorporeal heat transfer or reduced nitric oxide release [307, 313].   However, prior studies were either not randomised, applied the intervention for less than one month or report changes in serum biomarkers as the primary outcome. Further, they studied prevalent patients being prone to survivor biases and were underpowered to detect outcomes validated to predict development of heart failure and mortality. The aim of this study is to determine whether individualised cooler dialysate prevents the long-term development of cardiac systolic dysfunction and left ventricular hypertrophy in incident conventional HD patients. Individualised dialysate cooling to $0.5^{o}C$ less than the patient's core temperature is being tested as a pilot study suggested cardioprotective benefit with improved treatment toleration compared to that associated with a fixed temperature reduction strategy [314].

2.5.2. Study design and treatment regimen

The trial is prospectively registered (ISRCTN00206012) and the protocol has previously been published [315]. Trial design is summarised in Figure 2-39. The trial is a multi-center, prospective, open-label, controlled, randomized interventional trial conducted in the dialysis units of four university teaching hospitals in the United Kingdom within a 40 mile radius. The study is performed in accordance with the Declaration of Helsinki. The protocol is approved by Nottingham Ethics Committee prior to study initiation and written informed consent is given by all trial participants.

Figure 2-39 Trial design for a randomised controlled trial of individualised dialysate cooling

Multicentre randomised controlled trial of individualised dialysate cooling

Inclusion criteria:
•On HD at least 3 times/week
•Aged 16 years or over
•Willing and able to give consent

Excluded:
1.Exposure to haemodialysis for >180 days
2.Contraindications for using MRI (eg. patients with pacemakers and metal implants, pregnancy or lactating)
3.Inability to tolerate MRI due to claustrophobia
4.New York Heart Association grade IV heart failure
5.Mental incapacity to consent

n = 72

1:1 Randomisation to individualised cooling or control dialysate temperature

Baseline

•Monitored Dialysis Investigations*
•Cardiac and Brain MRI
•Cognitive assessment

Cool (tympanic temp - 0.5°C)

Control 37°C

12 months. Primary outcome 5% difference in LVEF by Cardiac MRI

•Monitored Dialysis Investigations*
•Cardiac and Brain MRI
•Cognitive assessment

* Monitored Dialysis Investigations comprise:
Non-invasive heart function and peripheral blood vessel monitoring with Finometer and Vicorder, Echocardiography and blood tests

2.5.3. Participants

Enrolment for the trial commenced in September 2009 and closed in January 2012 with the final CMR exams scheduled in January 2013. Inclusion criteria are:

1. Patients aged ≥16 years having HD treatment 3 times per week.
2. Willing and able to provide consent.
3. Exposure to haemodialysis for ≤180 days.

Exclusion criteria are:

1. Contraindications for Magnetic Resonance
2. Inability to tolerate magnetic resonance due to claustrophobia
3. New York Heart Association grade IV heart failure
4. Pregnancy or lactating
5. Mental incapacity to consent

2.5.4. Randomisation and blinding

Randomisation at 1:1 ratio is done in a single block by sealed envelopes generated by an independent statistician. The study is un-blinded as it is not pragmatic to enable appropriate dialysate temperature to be iteratively entered by different dialysis unit nursing staff and technicians. There is however blinding of treatment allocation for centralised analysis of cardiac imaging.

2.5.5. Dialysis Intervention

The control group use a dialysate temperature of 37°C for 12 months. The intervention group use an individualised cooled dialysate temperature for 12 months. The latter is set at 0.5°C less than the patient's own temperature, determined from the mean of 6 prior treatment sessions with a tympanic thermometer, between a minimum of 35°C and a maximum of 36°C, ensuring a minimum temperature separation of 1°C between groups. Adherence to the allocated dialysate temperature is frequently checked by dialysis unit staff with protocol deviations recorded.

2.5.6. Concurrent Treatments

Patients in both trial arms have standard management with dry weight prescribed by the clinical team according to local protocol including three-times weekly HD to achieve an equilibrated Kt/Vurea >1.1, a standardized Kt/Vurea of >2.0 and a treatment time ≥3.5 hours/session (70% of patients ≥4 hours/session). HD treatments use low-flux polysulfone dialyzers, 1.8-2.0 m^{2}, (LOPS 18/20; Braun Medical Ltd, Sheffield, United Kingdom). Dialysate composition is sodium 136-138mmol/l; potassium 2mmol/l; calcium 1.25mmol/l; magnesium 0.5mmol/l; bicarbonate 32-38mmol/l; glucose 5.6mmol/l; and acetate 3mmol/l. Dialysate flow rate is 500 mL/min, blood pump speed 250-450 mL/min. Anticoagulation is by unfractionated heparin.

2.5.7. Data collection

CMR studies for LV volumes, mass and function are conducted on midweek non-dialysis days (avoiding the long break in dialysis after the weekend) at

two centers using identical 1.5T scanners (GE Signa HDxt, GE Healthcare, Milwaukee, US) with retrospective ECG gating and 8-channel phased array coil. Steady-state free precession (SSFP) cine images are acquired in 2, 3 and 4 chamber views to plan a stack of 8mm short-axis slices with a 2mm interslice gap covering the entire LV. Typical parameters are; field of view 38cm, repetition time 3.2 ms, echo time 1.6 ms, matrix 224x224, spatial resolution <2mm, flip angle 60°, 1 signal average, 30 acquired phases per cardiac cycle achieving a heart-rate dependent temporal resolution of 20-40ms. Radiofrequency tagging by a spatial modulation of magnetization (SPAMM) sequence with gradient recalled-echo readout is applied at basal, mid-ventricular and apical levels. Typical parameters are matched to the SSFP cine images except for slice thickness 10mm, matrix 224 x 160, flip angle 12° to achieve temporal resolution of 15-30ms. Brachial artery blood pressure is measured in the non-fistula arm immediately after CMR acquisition in a supine position after 10 minutes rest using an oscillometric device (Datex-Ohmeda, GE Healthcare, USA) and the mean of three readings is recorded.

2.5.8. Data Analysis

All CMR analysis is performed offline blinded to patient details. Volumes and mass are determined using cvi42 software, version 4.0.2 (Circle Cardiovascular Imaging, Calgary, Canada). Epicardial and endocardial LV contours including major papillary muscles and trabeculations are manually traced in end-diastolic and end-systolic frames using a signal-intensity thresholding tool. Left ventricular end-diastolic volume (LVEDV), LV end-

systolic volume (LVESV) and LV ejection fraction (LVEF) are determined. Values are indexed to height and body surface area (BSA) using Mosteller's method [316]. The volume is multiplied by the specific density of the myocardium (1.05 g/cm^3) to determine end-diastolic LV Mass (LVM).

2.5.9. Strain Analysis

Mid-wall circumferential strain is measured in the short-axis tagged LV slices using validated and commercially available software (HARP 3.0, Diagnosoft, Palo Alto, California, USA) [231]. Epicardial and endocardial contours in the frame with optimal myocardial-blood contrast are manually drawn then automatically propagated to create a mesh in each frame. The anterior right ventricular septal insertion point is marked as a reference for segmental analyses. Contour tracking quality is checked and adjusted if required. The software derives lagrangian mid-wall circumferential strain for each time frame and exports to a spreadsheet. Data are regionally mapped to the AHA 16 segment LV model, averaged per short-axis slice and summated across slice values to derive global peak systolic-strain (%), peak-systolic strain-rate (s^{-1}) and peak diastolic strain rate(s^{-1}).

2.5.10.   Statistical Analysis

Descriptive statistics for continuous variables are summarized using mean±SD with independent T test for normal distributions or median(interquartile range) for non-normal distribution. Categorical variables are expressed as counts and percentage. Descriptive summaries of changes in treatment-related variables are provided for the constant cohort with non-missing values at baseline and 12 months after randomization. The effects of

randomized treatment allocation to LVEF, LV volumes and mass are estimated by applying a linear mixed-effects model to baseline and 12-month values using a diagonal covariance matrix with covariate adjustment, including a time interaction for the baseline outcome measures, plus prespecified covariates age, sex and diabetes status. Because outcomes are assessed at a single follow-up time, this model produces essentially identical results to an analysis of covariance adjusted for the baseline value of the outcome and prespecified covariates. The effects of treatment allocation on regional strain and strain-rate are assessed using the American Heart Association 16 segment model of the left ventricle and a linear mixed-effects model with patients modelled as random intercepts and allowing for the within-subjects correlation of segments and adjusted for multiple covariates including age, sex, and baseline left ventricular mass. All analyses use a two-sided significance at $p < 0.05$. Analyses are performed according to an intention-to-treat principle using SPSS for Windows, v20.

2.5.11. Primary Study Outcome

The prespecified primary outcome is the change in resting LVEF by cardiac magnetic resonance (CMR) at 12 months compared to baseline between the intervention and control group.

2.5.12. Secondary Study Outcomes

The main secondary study outcomes are LV mass and LV volumes, adverse LV remodelling assessed by the LV mass/volume ratio and systolic and diastolic function assessed by global peak-systolic strain, global peak-systolic strain rate and global peak-diastolic strain rate.

2.5.13. Rationale for primary and secondary outcomes

Previous observational study showed 13% reduction in LVEF by echocardiography over 12 months in patients with HD induced LV regional wall motion abnormalities [308]. Furthermore, reduced LVEF is a validated predictor of cardiovascular morbidity and mortality with a change greater than 5% approaching the minimum clinically important difference [317]. CMR is the reference standard technique for precise determination of the primary outcome [318]. Strain is the ratio of the maximal change in myocardial length in systole to the original length and large non-CKD population studies show strain detects early cardiac dysfunction prior to a decline in LVEF [213]. Recent data have validated the ability of lower strain to predict all-cause mortality amongst HD patients with preserved LVEF[319].

2.5.14. Sample size estimation

Sample size estimations are performed by a statistician using commercially available software (Nquery Advisor v6) with data from a reference range study with similar CMR acquisition and analytic techniques [320]. Using a two sample t test and assuming a mean LVEF of 67% in the control arm and equal Standard Deviation in each group of 6% [320], we estimated 64 participants would resolve a 5% between-group difference in LVEF from baseline to 12 months, with 90% power at 5%, 2-sided significance level. Allowing for study attrition and death of 10%, target recruitment is set at 72 participants.

2.5.15.   Monitoring for Adverse Events

The number and proportion of participants who reported treatment-emergent adverse events are summarized for each treatment group.

2.5.16.   Trial completion

Commencing in September 2009, trial recruitment of 73 patients was completed by January 2012. Follow-up will be completed in January 2013 with results analysed and reported in mid-late 2013. Based on the final number recruited (73), the study has 90% power to detect a 5% difference in LVEF.

2.6.   Background summary

It is well recognised that HD patients suffer excess cardiac morbidity and mortality that cannot be fully explained by traditional atherosclerotic risk factors such as age, smoking, hypertension, hypercholesterolaemia and hyperglycaemia. There are paradoxical non-linear relationships of many of these risk factors to cardiovascular outcomes compared to the general population and a distinctly different pattern of causes of death. Non-traditional risk factors, specific to CKD such as hypervolaemia, arterial stiffness and advanced glycation end-product deposition are increasingly recognised. A previously demonstrated non-traditional risk factor associated with worse outcomes is the presence of uraemic cardiomyopathy. This pattern of cardiac morphology and function has previously been defined as the presence of left ventricular abnormalities, including left ventricular hypertrophy, dilatation and left ventricular systolic dysfunction. 2D echocardiography relies on geometric assumptions to derive mass, volumes and global systolic function which frequently over or under-estimate abnormalities in HD patients. Cardiac magnetic resonance imaging provides direct measurements of mass and volume with greater precision, sufficient to resolve small differences in longitudinal studies and reduce the numbers required to show between-group differences in clinical trials. Furthermore, by using radiofrequency tagging, multi-directional determination of LV strains allow more sensitive regional and global measures of function without using gadolinium contrast. High spatial resolution magnetic resonance imaging can be extended into the aorta to directly measure aortic stiffness and the interaction with cardiac function. This may be superior to externally measured

aortic stiffness. HD itself is capable of exerting sufficient haemodynamic stress to cause repetitive cardiac ischaemic injury and may promulgate some of the excessive rates of cardiovascular morbidity and mortality. The cardiac tolerability to HD thus represents a HD-associated risk factor. Randomised trials of interventions directed at traditional risk factors have thus far not impacted on cardiovascular mortality and modifications to the process of HD may be the key to improving outcomes. The ischaemic cascade links reduced LV perfusion to reduced motion. Thus identifying HD induced ischemia previously relied on detecting regional radial LV wall motion abnormalities as a surrogate for ischemia by serial 2D echocardiography during dialysis which would be impractical by other modalities. 2D echocardiography can be enhanced by using serial studies tracking cardiac deformation similar to CMR tagging to generate multidimensional measures of regional and global strain in circumferential, radial and longitudinal directions as earlier markers of cardiac dysfunction. Longitudinal strains should be particularly sensitive for subendocardial ischaemia detection due to myocardial fibre orientation and data in non-CKD populations show promise for detection of ischemia.

Aims

3. Aims

For the first time the work in this thesis studies an incident HD population using multi-parametric strain-based imaging. This combines the accuracy of CMR resting cardiac and aortic function augmented with strain by tagging to longitudinal strain changes during HD by speckle-tracking echocardiography. The general aim of this thesis was to characterise the relationship of left ventricular function to HD using strain-based imaging. This might allow characterisation of HD-associated cardiomyopathy which may be distinct from the traditional definition of uraemic cardiomyopathy and may better define those patients who would benefit from modifications to the process of HD.

3.1. Study I

Study I aims to study resting cardiac abnormalities in an unselected incident HD population using strain by CMR tagging as a more sensitive marker of dysfunction compared to an age-matched non-CKD population.

3.2. Study II

Study II aims to investigate the contribution of uraemia to arterial stiffness by directly measuring aortic distensibility using cardiac magnetic resonance in incident HD patients compared to an age-matched non-CKD population.

3.3. Study III

The third study aims to detect dynamic changes in strain during HD by speckle tracking echocardiography and to determine nature and prevalence of HD-induced myocardial stunning to relevant biomarkers in a population new to HD.

4. Materials and methods

4.1. Subjects

The patient flow and study design are summarised separately for HD patients and for non-CKD control participants in Figure 4-1 and Figure 4-2.

4.1.1. Study I

This study compared 54 HD patients to 28 age-matched non-CKD control participants. The original study population comprised of 65 HD patients who completed any part of the study but after withdrawals due to non-tolerance of CMR, 54 HD patients remained. Thirty non-CKD control subjects completed the study and two were excluded from the analysis upon expert advice due to incidental findings of valvular heart disease and probable unrecognized myocardial infarction.

4.1.2. Study II

This study compared 30 HD patients to 19 age and sex-matched controls. The study population was a subgroup of the participants in Study I. Aortic image acquisition was added to the protocol on expert advice after the study commenced and was consecutively available for 30 of the 54 HD patients. This required comparison to 19 of the 28 non-CKD control participants to achieve optimal age and sex-matching.

4.1.3. Study III

This study reports data on 60 patients. The original study population consisted of 65 HD patients. This included 52 of the 54 HD patients from Study I but also describes data for patients who did not tolerate or withdrew

consent for CMR studies but completed echocardiographic studies during

HD. Five subjects were excluded from the analysis due to insufficient quality

of the echocardiographic images.

Figure 4-1 HD patient flow described for all studies in the thesis
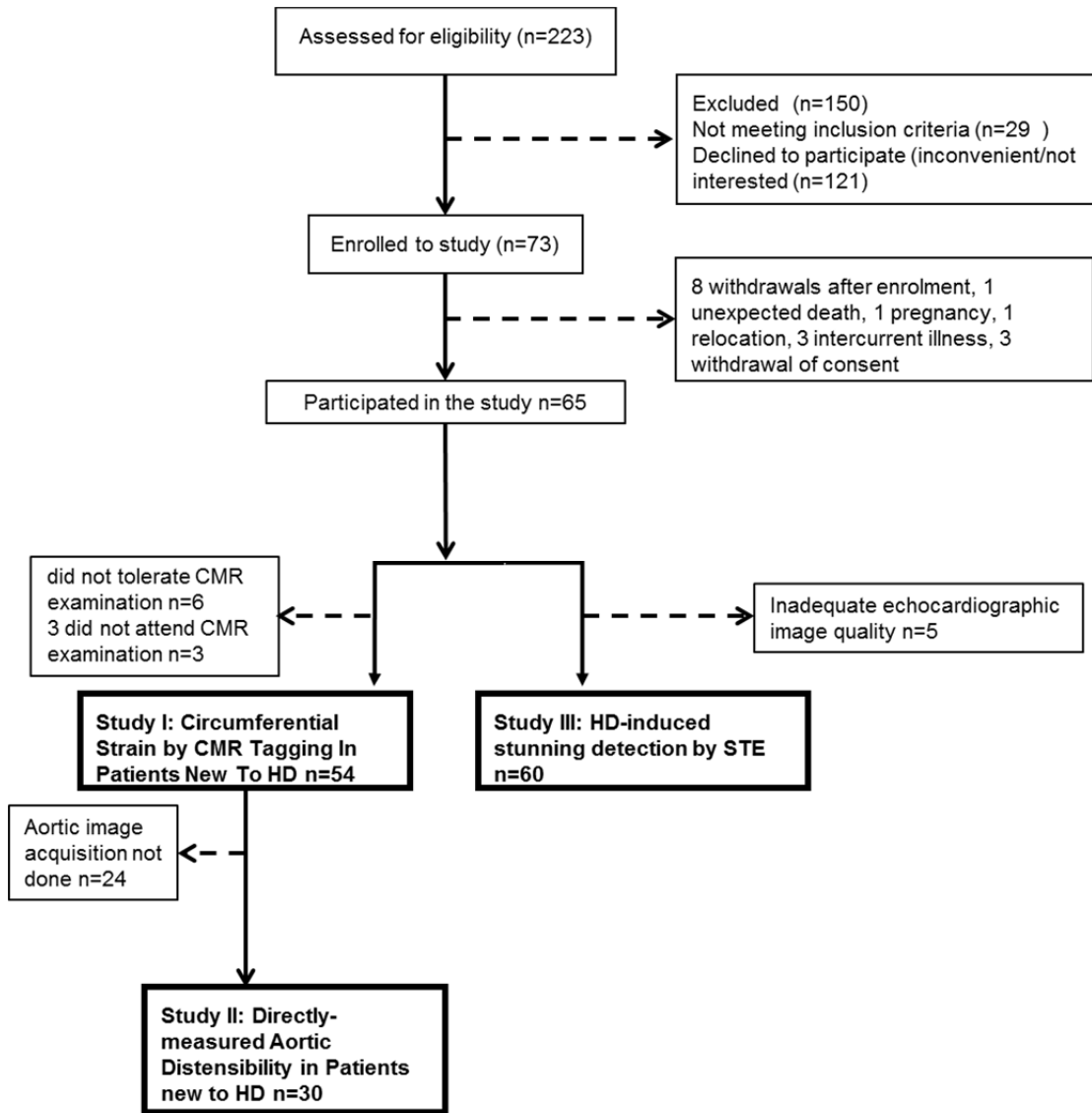
Figure 4-2 Participant flow for non-CKD control subjects described for studies in the thesis
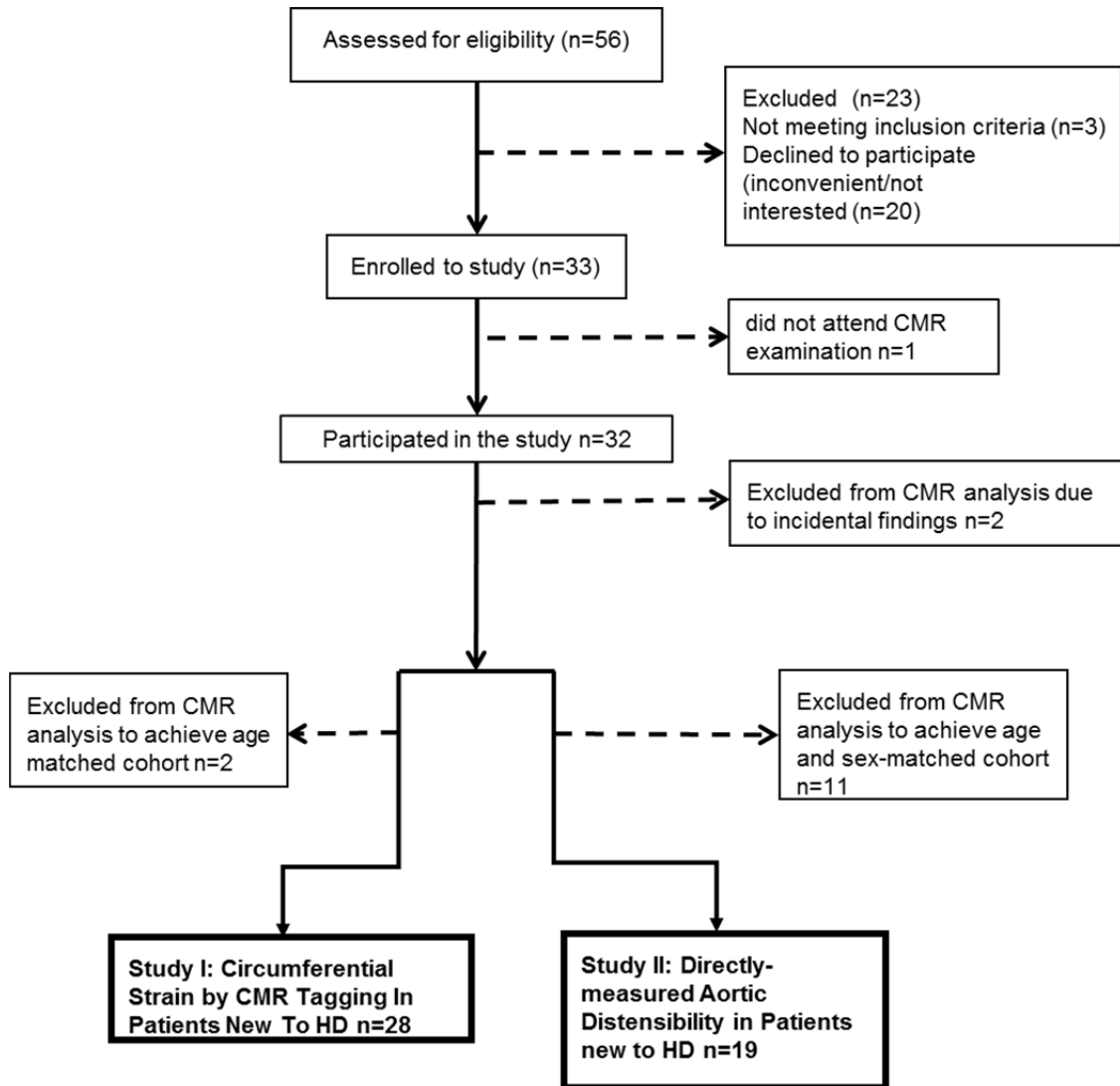
4.2. Ethical approval and eligibility criteria

Ethics approval for the study was obtained from Nottingham Ethics Committee for all participating centres prior to participant enrolment. The studies were performed in accordance with the Research Governance Framework, International Conference on Harmonisation Good Clinical Practice Guideline and the 2000 Scotland Revision of the Declaration of Helsinki. All participants gave written informed consent. The studies compared incident HD patients to age and sex-matched volunteers without CKD. HD patients were recruited within 6 months of commencing in-centre HD at one of 4 UK research sites: Royal Derby Hospital; Stoke Royal Infirmary; Birmingham Heartlands Hospital and Sheffield Teaching Hospitals as part of a randomised trial in dialysate cooling. All patients and non-CKD control volunteers were recruited by myself and Dr Eldehni. Dr Eldehni and I also collected all the data in the study, which involved travelling to all four dialysis centres with the haemodynamic monitoring equipment to study patients on dialysis without changing their dialysis times. Inclusion criteria were: (1) incident HD patients aged over 16 years; (2) within 180 days of commencing in-centre treatment 3 times per week and (3) Mental capacity to consent for the trial. Exclusion criteria were: (1) contraindications for magnetic resonance imaging; (2) inability to tolerate magnetic resonance imaging and (3) New York Heart Association Grade IV heart failure. 30 age and sex-matched healthy volunteers were recruited through a local clinical research healthy volunteer program. Inclusion criteria were: (1) aged over 16 years and (2) mental capacity to consent to the study. Exclusion criteria were: (1) contra-indications for magnetic resonance imaging and (2) history of kidney disease, ischaemic heart disease or cardiomyopathy. Two non-

130

CKD control subjects completed the study but were excluded from the analysis due to incidental findings of valvular heart disease and probable unrecognized myocardial infarction.

4.3. Cardiac Magnetic Resonance Imaging

CMR studies for LV volumes, mass and function were scheduled on midweek non-dialysis days (avoiding the long break in dialysis after the weekend) at two centers using identical 1.5T scanners (GE Signa HDxt, GE Healthcare, Milwaukee, US) with retrospective ECG gating and 8-channel phased array coil. Steady-state free precession (SSFP) cine images were acquired in 2, 3 and 4 chamber views to plan a stack of 8mm short-axis slices with a 2mm interslice gap, covering the entire LV. Typical parameters were; field of view 38cm, repetition time 3.2 ms, echo time 1.6 ms, matrix 224x224, spatial resolution <2mm, flip angle 60°, 1 signal average, 30 acquired phases per cardiac cycle achieving a heart-rate dependent temporal resolution of 20-40ms. Radiofrequency tagging by a spatial modulation of magnetization (SPAMM) sequence with gradient recalled-echo readout was applied at basal, mid-ventricular and apical levels. Typical parameters were matched to the SSFP cine images except for slice thickness 10mm, matrix 224 x 160, flip angle 12° achieving temporal resolution 15-30ms. The LV contours were drawn manually excluding papillary muscles and trabeculations, and left ventricular end-diastolic volume (LVEDV), LV end-systolic volume (LVESV), LV ejection fraction (LVEF) and end-diastolic LV Mass (LVM), mean end-diastolic LV wall thickness (LVWT) were calculated. The interventricular septum was included as part of the LV. The basal slice was included when at

least fifty percent of the blood volume was surrounded by myocardium. The apical slice was defined as the last slice showing intracavity blood pool. Values were indexed by body surface area using Mosteller's method [316], denoted by the suffix 'I,' for example, LVMI. LVM was also indexed to height$^{1.7}$ which has been shown to be the best measure to detect left ventricular hypertrophy in taller and obese subjects [321]. LVWT was calculated by excluding the two most basal and two most apical slices before averaging to reduce the variability of between-subject comparison caused by the basal slice position.

Figure 4-3 Slice positions for short axis cines were planned in end-systolic and checked on end-diastolic images to ensure consistency
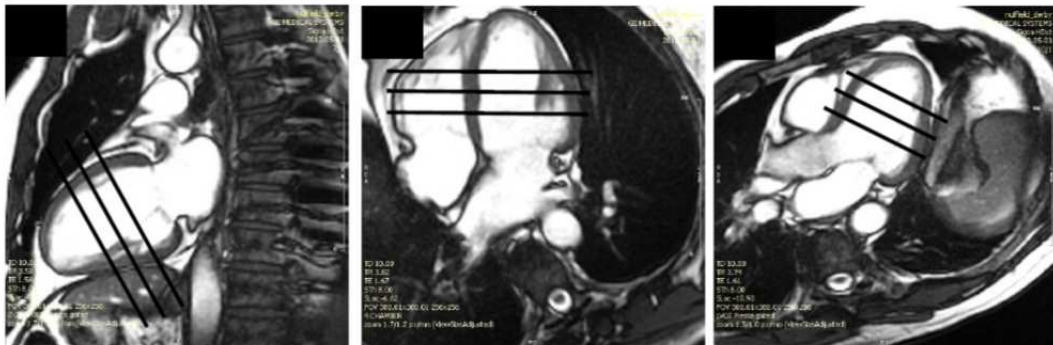
Black lines illustrate SA slice positions for tagging which should be copied from the cines for SA stack . Ensure basal slice is not in LVOT at end-systole.
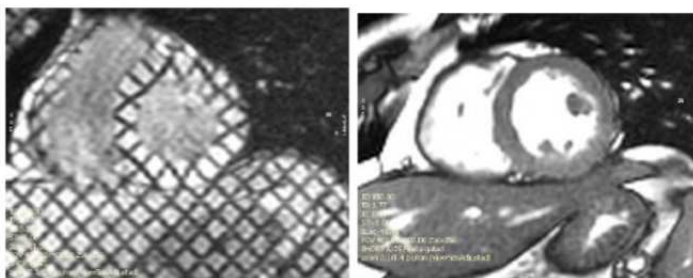
Brachial artery blood pressure was measured in the right arm for non-CKD controls and the non-fistula arm for HD patients immediately after CMR

acquisition in a supine position after 10 minutes rest using an oscillometric device (Datex-Ohmeda, GE Healthcare, USA) and the mean of three readings was recorded.

[322].

All CMR analysis was performed offline blinded to participant details. Volumes and mass were determined using cvi42 software, version 4.0.2 (Circle Cardiovascular Imaging, Calgary, Canada).

4.3.1. Tagging analysis

Strains were measured using dedicated software (HARP 3.0, Diagnosoft, Palo Alto, California, USA) for each of the 3 short axis slices. Data were smoothed using a moving average of 3 points to reduce noise sensitivity and slices were averaged to give global or regional measures.

4.4. Assessing cardiovascular performance during HD

Detailed characterisation of cardiovascular performance will be assessed during HD at baseline and 12 months. This occurs during the patient's usual HD session in their own centre using the same portable data collecting instruments across all centres.

4.4.1. Regional LV functional assessment by 2D echocardiography

2-dimensional echocardiography will be performed using commercially available equipment (1.5-4mhz probe, Vivid-I, GE Healthcare) by one of two

trained technicians in the left lateral position. Sector width, frequency and depth will be optimised to produce optimal border definition and a frame-rate of 50-80 per second. Standard apical 2 and 4-chamber image loops will be recorded pre-dialysis (rest) and 15 minutes before the end of dialysis (stress). Image loops will be anonymised and analysed off-line in random order for regional deformation using dedicated software (EchoPac, GE Vingmed).

4.4.2. Finometer

The finometer utilises a finger-clamp method to detect beat-to-beat changes in digital arterial diameter using an infrared photoplethysmograph. A single brachial artery blood pressure measurement is made for calibration. The time averaged data is subsequently downloaded to the PC based analysis program Beatscope™. Pulse rate, blood pressure, stroke volume, cardiac output, total peripheral resistance and baroreflex sensitivity are derived. The finger-cuff will be placed on an appropriate finger (preferably the middle finger on the non-fistula arm) and on the upper arm of the same arm. For obtaining baseline values, monitoring is commenced 30 minutes before the start of dialysis. All Finometer data will be subsequently downloaded to a PC based analysis program (Beatscope™), allowing averaging of results over defined time periods and display of variables as percentage change from baseline. The finometer has been well validated in several settings including critical care and haemodialysis [274, 323, 324].

Figure 4-4 The Finometer

Finometer Front-End Unit
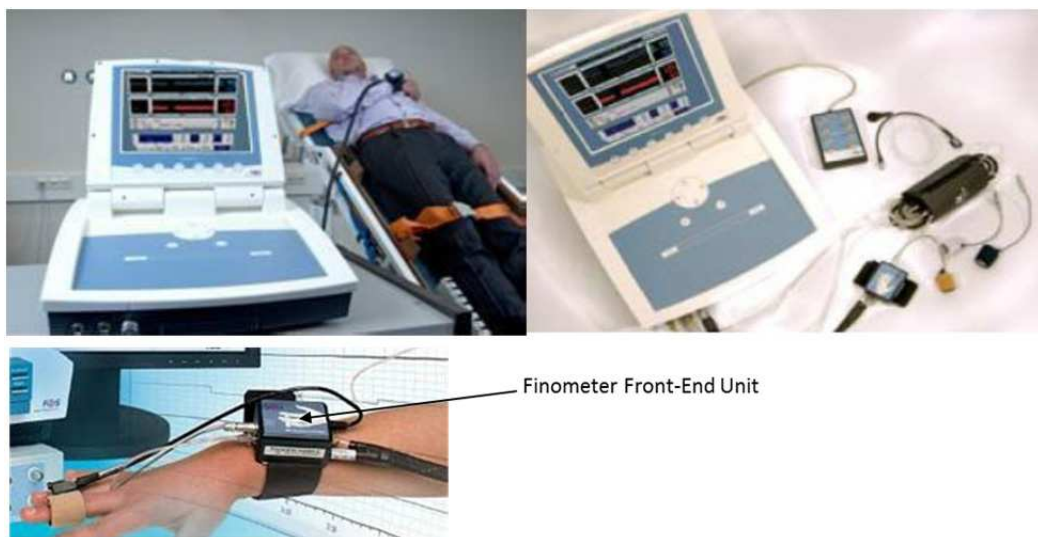
4.4.3. NICOM

Continuous non-invasive cardiac output monitoring will be recorded using a thoracic bioreactance monitor (NICOM™, Cheetah Medical). NICOM™ is based on the appreciation that changes in aortic blood volume induce small changes in the frequency of electrical signals propagating across the thorax. These small changes are highly correlated with blood flow and can thus be used to accurately and consistently report cardiac output. The bioreactance system (NICOM™) consists of applying four pairs of adhesive electrodes to the patient - two on either side of the thorax (marginally below the ribs) and two pairs just below the shoulders (on either side of the mid-axial line) or on the upper back. Each pair of electrodes delivers a low alternating current, sensed for its propagation characteristics along the thorax by the other electrode pairs. This uses phase changes in alternating electrical current to derive cardiac output. The use of phase rather than amplitude, makes the exact location of the electrodes less important and also permits high-notched filtering of electrical interference typically encountered in hospital settings. This endows a greater precision and signal-to-noise ratio than impedance cardiography. This technique has been validated in healthy volunteers, intensive care settings and chronic heart failure [325-327]. A recent study found the monitor comparable to expert DSE to optimise cardiac resynchronisation therapy devices [328].

Figure 4-5 The NICOM™, illustrating the data display and electrode placement

4.4.4. Arterial stiffness by oscillometric PWV

Arterial stiffness measured by pulse wave velocity is independently associated with increased risk of cardiovascular disease in HD patients [329]. Carotid-Femoral pulse wave velocity will be measured by an oscillometric device (Vicorder, Skidmore Medical Ltd, Bristol, UK) as previously described [330]. Briefly, a carotid pressure cuff is applied over the neck to detect the right carotid artery and a pressure cuff is placed around the proximal right upper thigh to detect the right femoral artery. The distance from the suprasternal notch to the middle of the thigh cuff was measured and entered into a PC running the Vicorder software. The cuffs are simultaneously inflated to a low pressure 40-60 mm Hg and signal from each cuff is analysed to derive arterial transit time. PWV is calculated by the software by dividing arterial transit time by measured distance. The mean of 2 measurements was recorded.

Figure 4-6 Oscillometric PWV using the Vicorder

4.4.5. Body composition by bioimpedance

Body composition and assessment of total body water will be done using segmental multifrequency bioimpedance (InBody BS20, Seoul, Korea). Bioelectrical impedance analysis (BIA) is based on the principle of detecting resistance to low-level electrical current flows through intracellular and extracellular fluid [331, 332]. The currents used are imperceptible to the subject. Fat-free mass contains the majority of total body water (TBW) and is a better conductor of electrical current than fat. Therefore BIA is essentially an index of TBW, from which fat-free mass is estimated. Segmental as opposed to whole body BIA is the preferred technique in patients with abnormal fluid states (eg. ascites, chronic kidney disease). It is most useful at tracking intra-patient variability in fluid status changes and is well validated in the setting of haemodialysis [333]. Body composition and assessment of TBW will be taken using a segmental multifrequency BIA analyzer (InBody S20, Biospace Co. Ltd., Seoul, Korea). Measurements will be performed using the standard tetrapolar technique, with electrodes placed on the dorsum of both wrists and anterior aspect of both ankles [334]. After cleaning the skin to ensure good contact, injection electrodes will be attached to the

wrists and ankles over the metacarpophalangeal and metatarsophalangeal joints, with the voltage detector electrodes at the line of the same joints. The analyzer will apply a safe and imperceptible current of 90-4000 µA at a frequency of 1-1000 kHz. The algorithms built into the software of the analyzer will measure resistance and reactance and calculate fat-free mass separately for each limb and the trunk at several frequencies. The extracellular fluid space will be expressed as a proportion of the estimated TBW.

Figure 4-7 InBody S20 Bioimpedance analyser

4.5.   Study of non-CKD healthy volunteers

As is conventional for magnetic resonance studies, healthy volunteer control data is often used to compare data in areas where normal ranges are not clearly established. The non-CKD volunteers underwent identical studies to the non-dialysis day assessment of HD patients comprising of CMR image acquisition, blood pressure and PWV measurement by Vicorder.

Study I Results

5. Study I Results: Circumferential Strain By Cardiac Magnetic Resonance Tagging In Patients New To Haemodialysis

5.1. Abstract

Introduction: HD patients with cardiac abnormalities are vulnerable to HD-induced ischaemia and early identification allows strategies to improve outcomes. 2D-echocardiography uses geometric assumptions which overestimate abnormalities. Cardiac magnetic resonance (CMR) is the gold-standard for analysis of cardiac morphology and strain analysis by tissue tagging detects early dysfunction in non-uraemic settings. Previous CMR studies of renal transplant candidates used prevalent, selected populations and did not investigate strain.

Objectives: We aimed to study cardiac abnormalities in an unselected incident HD population using CMR augmented by strain as a more sensitive marker of dysfunction.

Methods: 84 subjects were studied (54 HD, median vintage 170 days, 30 age and sex-matched controls). Left ventricular (LV) mass and volumes were determined by planimetry. Global and segmental peak systolic circumferential strains (Ecc) were determined from strain curves. Discrete variables are expressed as counts (percentage) and continuous variables as mean ± Standard Deviation or median ± interquartile range (IQR) depending on normality. Comparisons were made by the independent T test or Mann-Whitney test for continuous data and Chi-squared or Fisher's exact test for

categorical data. Linear Regression analysis was applied to identify determinants of Ecc and repeated-measures analysis of variance was used to determine the heterogeneity of Ecc within subjects.

Results: Median values±IQR are presented as HD vs Controls. Global LV function was reduced (LV Ejection Fraction 51.5%±11 vs 58.5%±5.4) with reduced strains (Ecc 15.9%±3.7 vs 19.5%±3.3), all p<0.001. LV mass was increased (63.4g/m^2±24.4 vs 45.9g/m^2±9.3, p<0.001) as was LV remodelling (LV mass/Volume ratio 0.76g/ml±0.22 vs 0.65±0.16g/ml, p=0.003) and LV dilatation (LV end-diastolic volume index 87.6±29.8ml/m^2 vs 71.6±17.7ml/m^2, p=0.03). Subgroup analysis of HD patients and controls with LVEF >50% (n=59) showed reduced strain persisted despite normal LVEF (Ecc 17.5%±3.3 vs 19.9%±3.4 p=0.03). Using 2 Standard Deviations from the mean of the controls, sex-specific cut-offs were determined for abnormal morphology and function in HD patients. 48% (26/54) had abnormal morphology (increased LVH or dilatation) whilst 54% (29/54) had abnormal contractile function (reduced EF or strain) with overlap between categories. Only 19% (10/54) had no abnormalities (chi-squared, p<0.001).

Conclusion: CMR tagging identified reduced circumferential strain in addition to abnormalities in LVEF and LV mass in the majority of incident HD patients. Strain was reduced in the subset of patients with normal LVEF. The independent determinants of strain were LVEF and LV Mass/Volume ratio. Strain shows promise in early identification.

5.2. Introduction

It is well recognised that HD patients suffer excess cardiac morbidity and mortality and this is mainly due to cardiac failure and sudden cardiac death [13, 335]. HD patients are primed by abnormalities in cardiac and structure and function to be vulnerable to HD-induced ischaemia. These changes can occur in the absence of flow-limiting stenosis of the coronary arteries and can be explained by a high prevalence of decreased coronary flow reserve, impaired autonomic function, left ventricular hypertrophy (LVH) and arterial stiffness [336, 337]. Proof-of-concept studies by McIntyre et al showed the process of HD is capable of causing a stress sufficient to reduce myocardial blood flow by 30% [284]. These changes localised to areas of reversible regional wall motion abnormalities on 2D echocardiography. Patients demonstrating such dysfunction had a 30% mortality and mean 13% reduction in left ventricular ejection fraction (LVEF) by 1 year [286]. Whilst it is already recognised that LVH confers an adverse prognosis in HD patients [338], there is increasing evidence that LV remodelling of geometry (measured by the LV mass/volume ratio) determines prognosis [339]. Therefore early identification of cardiac abnormalities might allow strategies to improve outcomes. Conventional 2D-echocardiography is a convenient, inexpensive and widely available imaging modality for determining LV abnormalities. However it is under-recognized that test-retest variability of 2D echocardiography is high, so that the smallest change of LVEF and LV mass that is detectable with 95% confidence is 11% and 59g respectively [201, 340]. Furthermore 2D echocardiography uses geometric assumptions which tend to overestimate LV mass in ESRD [110]. Cardiac magnetic resonance

(CMR) is the gold-standard for analysis of LV mass and volumes with low intra- and inter-observer variability of around 5% [318]. Strain analysis detects early cardiac dysfunction prior to a decline in LVEF in non-uraemic settings [213-216]. Furthermore in heterogenous cardiomyopathy populations with both normal and reduced LVEF, strain was reduced in the subset of populations with normal LVEF and gave additional prognostic information beyond that provided by LVEF and LV mass [217, 218]. CMR assessment of strain by tissue tagging has been validated against sonomicrometry and is considered the gold-standard modality for non-invasive assessment due to high reproducibility [224]. There have been few studies of strain in HD patients using 2D echocardiography with conflicting results [341-343]. Previous CMR studies of ESRD patients being assessed for renal transplant listing used prevalent, selected populations and did not investigate strain [87]. Therefore, we aimed to study cardiac abnormalities in an unselected incident HD population using CMR for accurate mass and volumes augmented with strain by tagging as a more sensitive marker of dysfunction.

5.3. Materials and methods

5.3.1. Subjects

Ethical approval for the study was obtained from Nottingham Ethics Committee for all participating centres prior to study initiation and patient enrolment. The study was performed in accordance with International Conference on Harmonisation Good Clinical Practice Guideline and the 2000 Scotland Revision of the Declaration of Helsinki. All participants provided written informed consent. Patient flow for the study is summarised in Figure 4-1and Figure 4-2. We recruited 54 HD patients within 6 months of

commencing in-centre HD at one of 4 UK research sites as part of a randomised trial in dialysate cooling. Inclusion criteria were incident HD patients aged over 16 years; within 180 days of commencing in-centre treatment 3 times per week and mental capacity to consent for the trial. Exclusion criteria included: contra-indications for magnetic resonance imaging; inability to tolerate magnetic resonance imaging and New York Heart Association Grade IV heart failure. Thirty age and sex-matched healthy volunteers were recruited through a local clinical research healthy volunteer program. Inclusion criteria were aged over 16 years with capacity to consent to the study and. Exclusion criteria were: contra-indications for magnetic resonance imaging; history of kidney disease, ischemic heart disease or cardiomyopathy. Two healthy volunteers completed the study but were excluded from the analysis due to incidental findings of valvular heart disease and probable unrecognized myocardial infarction.

5.3.2. Data collection

CMR studies occurred on non-dialysis days at two centres using identical 1.5T scanners (GE Signa HDxt 1.5T, GE Healthcare, Milwaukee,US) with retrospective ECG gating and 8-channel phased array coil. Steady-state free precession (SSFP) cine images were acquired in 2, 3 and 4 chamber views. A stack of 8mm short-axis slices with a 2mm interslice gap were obtained using cine imaging covering the entire LV from base to apex. Typical parameters were field of view 38cm, repetition time 3.2 ms, echo time 1.6 ms, matrix 224x224, flip angle 60°, 1 signal average, 16 views per segment, 30 reconstructed phases per cardiac cycle to achieve temporal resolution of 20-40ms depending on heart rate. Three short-axis tagged cines were

acquired after planning in mid-systole from the 4 and 3-chamber cine at basal, mid-ventricular and apical levels. A spatial modulation of magnetization (SPAMM) sequence with retrospective ECG gating and gradient recalled-echo readout was obtained. Typical parameters were matched to the SSFP cine images except for slice thickness 10mm, matrix 224 x 160, flip angle 12°, achieving temporal resolution 15-30ms.

Arterial stiffness by pulse wave velocity (PWV) and blood pressure was measured in a supine position after 10 minutes rest.

Brachial artery blood pressure was measured in the non-fistula arm in HD patients and the right arm in NCs using an oscillometric device (Datex-Ohmeda, GE Healthcare, USA).The mean of three readings was recorded. Carotid-to-femoral

PWV was measured using an oscillometric device (Vicorder, Skidmore Medical Ltd, Bristol, UK) as previously described [330]. Briefly, a carotid pressure cuff is applied over the neck to detect the right carotid artery and a pressure cuff is placed around the proximal right upper thigh to detect the right femoral artery. The distance from the suprasternal notch to the middle of the thigh cuff was measured and entered into a PC running the Vicorder software. The cuffs are simultaneously inflated to a low pressure (40-60 mmHg) and signal from each cuff is analysed to derive arterial transit time. PWV is calculated by the software by dividing arterial transit time by measured distance. The mean of 2 measurements was recorded.

In HD patients only, blood samples for determination of high-sensitivity troponin-T and NT-proBNP were taken immediately after insertion of access needles on HD the day before the CMR study. Samples were sent to the laboratory immediately where they were centrifuged and analysed using the Elecsys 2010 system (Roche Diagnostics, Switzerland).). The limits of detection of the troponin-T assay are 0.005µg/L, the 99th percentile 0.014 µg/L and the 10% co-efficient of variation is 0.013 µg/L [344]. The limits of detection of the NT-proBNP assay are 0.6pmol/l and the interassay co-efficient of variation is 3.9%.

5.3.3. Data Analysis

All CMR analysis was performed offline blinded to patient details. Volumes and mass were determined using cvi42 software, version 4.0.2 (Circle Cardiovascular Imaging, Calgary, Canada). The LV contours were drawn manually excluding papillary muscles and trabeculations, and left ventricular end-diastolic volume (LVEDV), LV end-systolic volume (LVESV), LV ejection fraction (LVEF) and end-diastolic LV Mass (LVM), mean end-diastolic LV wall thickness (LVWT) were calculated. The interventricular septum was included as part of the LV. The basal slice was included when at least fifty percent of the blood volume was surrounded by myocardium. The apical slice was defined as the last slice showing intracavity blood pool. Values were indexed by body surface area (BSA) using Mosteller's method [316], denoted by the suffix 'I,' for example, LVMI. LVWT was calculated by excluding the two most basal and two most apical slices before averaging to reduce variability.

5.3.4. Strain Analysis

Peak-systolic mid-wall circumferential strain was measured for each of the 3 short axis slices using dedicated software (HARP 3.0, Diagnosoft, Palo Alto, California, USA) which has been validated in animal and human studies [231, 232]. After confirmation of appropriate k-space setup, epicardial and endocardial contours in the frame with optimal myocardial-blood contrast were drawn then automatically propagated by the software to create a mesh in each frame. The anterior right ventricular septal insertion point was manually marked to enable division of the ventricular slice into segments. Contours were checked for tracking and manually adjusted to ensure the mesh remained within the myocardium. The software subsequently calculated Lagrangian mid-wall circumferential strain for each frame from end-diastole to end-systole allowing export of the data to a spreadsheet. Data were smoothed using a moving average of 3 points to reduce noise sensitivity and the peak systolic-strain value was extracted (**Error! Reference source not found.**). Data was analysed for the AHA 16 segment LV model, averaged per short-axis slice and across all segments to give a global measure (Peak Ecc) expressed as a percentage.

Figure 5-1 Representative mid-ventricular circumferential strain curve from a single patient. Peak Ecc represents peak-systolic circumferential strain.

5.3.5. Statistical Analysis

Normality was assessed using the Kolmogorov-Smirnov test, histograms and normal Q-Q plot. Continuous data were expressed as mean (±standard deviation (SD)) if normally distributed and median (±interquartile range (IQR)) if not. Categorical data were expressed as counts and percentage. Unadjusted data were analysed using independent sample t-tests for normally distributed variables; Mann-Whitney U for non-parametric variables and Chi-Squared or Fisher's exact test for categorical variables. Pearson's test was used to assess univariate correlations with Peak Ecc for normally distributed variables and Spearman's test if not. Variables with right-skewed distribution were log transformed for the correlations. Multivariable linear regression analysis, using the forward stepwise method, was used to identify independent determinants of Peak Ecc. A threshold of $p<0.05$ was used for a variable to enter the model which was built using a hierarchical approach that introduced one-by-one variables on the basis of biological plausibility determined by literature review and the strength of association in univariate

analyses. A scatter plot of regression residuals versus predicted values and Cook's Distance plot were used for testing the assumptions of linear regression and identifying outliers. The adjusted R-squared value is reported as a measure of goodness-of-fit, with the regression coefficients (95% Confidence Intervals) and standardised coefficients. SPSS version 20.0 was used for all analyses and graphs. All analyses were 2 sided, and significance was judged at $p < 0.05$.

5.4. Results

Table 5-1 Subject characteristics, CMR and Oscillometric findings. Continuous variables are mean±SD or median(IQR) depending on normality and comparisons use Independent t test or Mann-Whitney Test as appropriate. Categorical data are counts[percentage] and comparisons use Fisher's exact test. Cut-offs for abnormalities by CMR: LVH; LVMI >77.7g/m2 males >56.g/m2 females, Low Peak Ecc <15.6%. LVEF <47% males, <53% females

	HD (n=54)	Controls (28)	P val
Age (years)	60 ±24	60±23	0.83
Female	15[28]	14[46]	0.03
BMI (kg/m^2)	27±8	27±3	0.79
BSA (m^2)	2.0±0.2	2.0±0.2	0.89
Medical history			
HD vintage (days)	149 (150)	-	-
Diabetes mellitus	15 [28]	2[7]	0.045*
Ischaemic heart disease	13[24]	1[3]	0.029*
Current/Ex-smoker	25[46]	8[29]	0.23
Medication			
Treated hypertension	42[78]	2[7]	<0.001
RAAS antagonist	14[26]	1[3]	0.029*
Beta blocker	19[35]	0[0]	<0.001**
Other antihypertensive	37[69]	2[7]	<0.001
Statin use	23[43]	4[14]	0.02*
Laboratory results			
High-sensitivity troponin-T	32(58)	-	-
NT-ProBNP (pg/ml)	177(476)	-	-
CMR and oscillometric findings			
Peak Ecc (%)	15.9(3.7)	19.5(3.3)	<0.001**
Basal Ecc (%)	14.8(4.9)	17.9 (4.9)	<0.001**
Mid Ecc (%)	16.6(5.8)	19.1(5.5)	0.001**
Apical Ecc (%)	16.4(5.5)	19.4(4.6)	0.003**
HR	72(19)	63(11)	0.014*
SBP (mmHg)	141±28	141±26	0.89
DBP (mmHg)	76(19)	82(14)	0.07
PP (mmHg)	61(30)	59(20)	0.29
PWV (m/s)	7.3(2.6)	8.9(2.5)	0.026*
LVEDVI (ml/m^2)	87.6(29.8)	71.6(17.7)	0.03*
LVEF	51.5(11.0)	58.5(5.4)	<0.001**
CI (l/min/m^2)	3.1(0.7)	2.7(0.5)	0.006**
LVMI (g/m^2)	63.4(24.4)	45.9(9.3)	<0.001**
LV Mass/Volume ratio (g/ml)	0.76(0.22)	0.65 (0.16)	0.003**
Mean ED wall thickness (mm)	7.8(2.2)	6.5(1.0)	<0.001**
Abnormalities by CMR			
LVH	20 [37]	1[4]	0.02
LV dilatation	15 [28]	0[0]	<0.001
Ecc	26 [48]	3[11]	0.03
LVEF	19 [35]	1[4]	<0.001
Normal CMR	10[19]	21[75]	<0.001

Subject characteristics and the main CMR and oscillometric findings are presented in Table 5-1 as HD vs NCs. The groups were well matched for age, BMI, BSA and smoking status but not sex. Most HD patients were treated for hypertension (78%) and 26% were treated with a renin angiotensin aldosterone system (RAAS) antagonist.

Global function

Global LV function was reduced in HD patients (LVEF 51.5%±11.0 vs 58.5%±5.4). Peak Ecc was reduced in HD compared to NCs. (Peak Ecc 15.9%±3.7 vs 19.5%±3.3, $p<0.001$).

Mass

All measures of LV mass were increased in HD patients, with greater hypertrophy, LV remodelling and wall thickness ($p<0.05$, Table 5-1).

Regional function

Ecc was significantly reduced in each short axis slice in HD patients compared to NCs ($p<0.003$, Table 5-1). Regional reductions in Ecc in HD extended to all 16 LV segments, being statistically significant in 9 (**Table 5-2**).

Table 5-2 Between-group comparisons of Peak Ecc using the AHA 16 segment model of the Left Ventricle. Ecc values are median % ±IQR P values are by Mann-Whitney test

	Basal			Mid			Apical			
Segment	HD	NC	P val	HD	NC	P val	**Segment**	HD	NC	P val
Anterior	10.0±5.9	12.8±7.6	0.021*	14.6±7.0	15.8±6.3	0.076	**Anterior**	14.0±6.3	16.4±9.0	0.014*
Antero-septal	7.9±6.5	11.2±6.9	0.011*	12.2±7.0	14.3±6.5	0.002**	**Septal**	13.9±7.3	16.0±8.8	0.042*
Infero-septal	7.8±7.9	12.1±9.3	0.105	12.6±8.4	14.3±6.8	0.087	**Inferior**	14.0±6.2	15.3±8.2	0.189
Inferior	9.5±9.9	15.0±8.3	0.047*	14.0±9.0	18.9±5.6	0.008**	**Lateral**	14.9±5.4	17.2±5.9	0.021*
Postero-Lateral	13.7±5.6	17.3±8.4	0.007**	15.8±7.2	17.9±7.2	0.141				
Antero-Lateral	12.7±6.6	15.3±4.3	0.070	14.4±6.9	16.1±3.7	0.040*				

153

Subgroup comparisons

Strain was also significantly lower in HD patients with diabetes (Peak Ecc 16.6±3.3 vs 14.1±4.0, p=0.027) but there was no relationship to age (r=-0.1,p=0.37), sex ((HD, p=0.22, NC p=0.33) history of ischaemic heart disease (p=0.23) or smoking status (p=0.16).

Using 2 Standard Deviations from the mean of the control group, sex-specific cut-offs were determined for abnormal morphology and function in HD patients. 48% (26/54) had abnormal morphology (increased LVH or dilatation) whilst 54% (29/54) had abnormal contractile function (reduced LVEF or strain) with overlap between categories (Table 5-1).

Univariate and Multivariable analyses

Strain showed significant univariate correlations to LVEF, troponin-T, measures of cardiac hypertrophy and PWV (Table 5-3). Multiple stepwise linear regression analysis showed that LVEF and LV mass/volume ratio were independent determinants of strain (R^2=0.44, Table 5-4).

Table 5-3 Significant Univariate Correlations to Peak Ecc. P values use Pearson's correlation for normally distribution or Spearman rank correlation for non-normally distributed data. *Troponin-T was only measured in HD patients.

	Total Cohort (unadjusted)	
	r	P-value
LVEF	0.519	<0.001
LVWT	-0.389	<0.001
Post HD High-sensitivity troponin-T*	-0.376	0.017
Pre HD High-sensitivity troponin-T*	-0.354	0.015
LV Mass/Volume ratio	-0.334	0.002
LVMI	-0.308	0.006
PWV	-0.209	0.04

Table 5-4 Independent Determinants of Ecc by Multiple Stepwise Linear Regression analysis B = un-standardised coefficient (95% confidence intervals), β= standardized coefficient. Independent variables that did not enter the model were: LVWT, troponin-T, LVMI and PWV

	Total Cohort Adjusted R^2= 0.44		
	B (95% CI)	β	p value
LVEF (per 1%r)	1.41(1.25-1.52)	0.57	<0.001
LV mass/vol ratio (per 1g/ml)	1.12(0.83-1.28)	-0.36	<0.001

Within-subjects analysis for heterogeneity of strain

One way repeated-measures analysis of variance was conducted to determine the within-subject heterogeneity in strain between short-axis slices in each study group. Data were normally distributed after logarithmic transformation and the Greenhouse-Geisser correction was applied due to violation of sphericity. Mean Peak Ecc differed statistically significantly between the 16 LV segments in both HD and NCs (F statistic 16.62 (7.65, 382.28), P <0.001). Post-hoc tests using the Bonferroni correction revealed that Ecc increased from the base to the apex in both HD and NCs.

Finally, to determine if Peak Ecc could stratify HD patients with normal LVEF, we divided the HD patients into 2 groups by LVEF (group 2, LVEF≥50%, Group 3, LVEF<50%) and compared them to NCs (group 1, LVEF>50%). Ecc was significantly reduced in HD compared to NCs (p=0.03) despite non-significant differences to NCs for LVEF (p=0.09) (Figure 5-2**Error! Reference source not found.**).

Figure 5-2 Boxplots of median±IQR for A) LVEF and B) Peak Ecc by study groups stratified by LVEF. Blue: normal controls with LVEF>50%; Green, HD patients with LVEF≥50%; Pink, HD patients with LVEF<50%. Ecc was able to stratify significant differences between all 3 groups whilst LVEF was not.
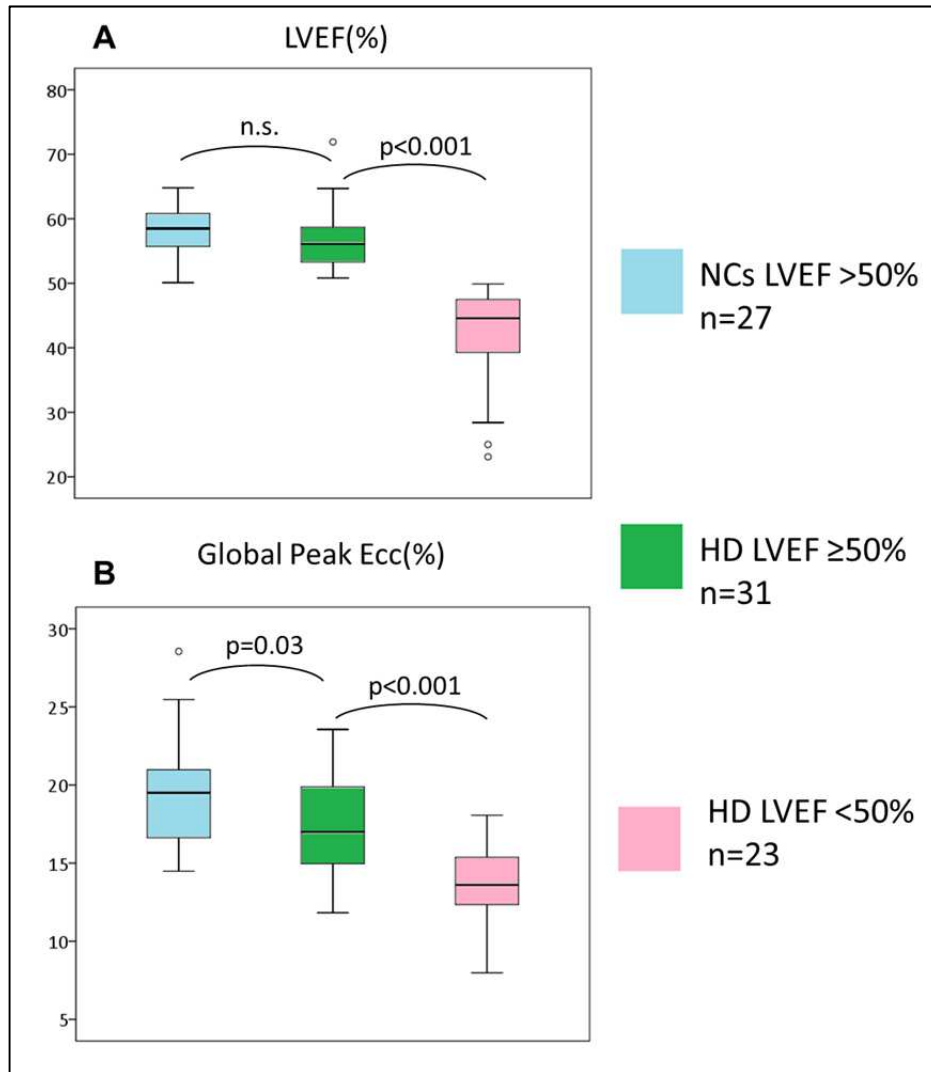
5.5.   Discussion

In this study we used CMR augmented by myocardial tissue tagging to characterise abnormalities in cardiac mass, volumes and circumferential strain in a population of unselected patients new to HD, compared to age-matched controls. To our knowledge this is the first report of strain by CMR tagging in HD patients. The principle findings of the study are that unselected incident HD patients have significantly reduced circumferential strain and LVEF compared to age-matched controls. In those with normal LVEF, strain was still significantly reduced. The reduced strain was seen at a global, slice and segmental level with an increase from the base to the apex. Secondly, Ecc was significantly correlated to LVEF, troponin-T, measures of cardiac hypertrophy and arterial stiffness. It was also higher in patients with diabetes. LVEF and LV mass/volume ratio were independent determinants of strain but accounted for only 44% of observed biological variability. Finally, only 19% of HD patients had a normal CMR.

Our results support and augment previously published data in prevalent HD patients using CMR without strain as well as data reporting strain by other imaging modalities. Mark et al studied 134 patients with end-stage renal disease (ESRD) using gadolinium contrast-enhanced CMR as part of assessment for renal transplant listing [87]. The study was conducted prior to knowledge of the association of gadolinium with nephrogenic systemic fibrosis and did not investigate strain or relationships to troponin-T. Using cut-offs derived from published reference range studies, they showed a prevalence of 72% for LVH, 11.2% for LV dilatation and 8.2% for reduced

LVEF. This compares to 37%, 28% and 35% respectively in the present study. Stewart et al used CMR to compare 44 prevalent HD patients to 11 age-matched controls. They also did not determine strain. Their findings were concordant to our study demonstrating lower LVEF and greater LV mass in HD patients but with significantly different absolute values [345]. The differences between these prior studies and the present are likely to be explained by the different ESRD populations studied, different cut-offs used to determine abnormalities and different decisions with regards to manual contouring of the LV contours to determine the mass and volumes. Mark et al studied a mixed ESRD population using both HD and peritoneal dialysis who were candidates for renal transplantation and so would tend to have less co-morbidity than an unselected population [87]. Also the population was prevalent with a median exposure to dialysis of 365±1308 compared to 149±150 days in our study. Study of selected prevalent populations can lead to survivor bias [346]. Furthermore their study used cut-offs derived from published studies whereas we used cut-offs derived from our own control subjects. Finally we chose to exclude papillary muscles and trabeculations from the mass and include in the volume. This was because such an approach was shown in the largest CMR-based longitudinal study of 5093 subjects to have higher test-retest reliability and lower inter-and intra-observer variability [339]. This is particularly important as follow-up studies are planned but such an approach will lead to slightly lower LV mass and LVEF than alternative contouring methods [347]. There are few studies that reported normal ranges for circumferential strain by CMR tagging in healthy volunteers [348]. These report mean peak strains in the region of 16-19%

which is reassuringly in keeping with the values for the healthy volunteers in our study (19.5%±3.3). There are no previous studies that measured strain by CMR tagging in HD patients. A limited number of studies have reported data in HD patients on strain by Tissue Doppler or Speckle Tracking Echocardiography. Direct comparisons of our strain values to those studies carry the caveat that there is little data that directly compared strain values by CMR tagging to echocardiographic techniques [169, 349, 350]. Absolute differences of 1-3% have commonly been reported (relative difference 10-20%), with r values of 0.5 in one study [194]. Gulel et al used Tissue Doppler echocardiography to determine strain in 31 HD patients matched to 23 normal controls [351]. Importantly, patients with LVEF<50% were excluded and the length of exposure to HD was not reported. Peak strain was reduced in HD patients compared to controls to a similar extent as in the present study (15.0%±7.4 vs 18.8%±4.2, p=0.02). Tissue Doppler is limited due to dependency on angle of insonation, tethering artefacts and requiring advanced echocardiographic expertise to acquire and interpret. More recently, 2D speckle tracking echocardiography (STE) has emerged as a robust angle-independent method of estimating strain in a shorter time [194]. Yan et al compared 36 HD patients to 17 non-dialysis CKD patients and 18 healthy controls [343]. They could not demonstrate statistically different strains in HD patients to CKD patients or controls. However, in keeping with our study, they did demonstrate increased strains from the LV base to apex.

Another important finding in our study were the modest univariate correlations of strain to LVEF, measures of cardiac hypertrophy (LVMI and

LVWT); LV remodelling (LV mass/volume ratio) and arterial stiffness (PWV). Furthermore in HD patients there was a modest inverse correlation of strain to high sensitivity troponin-T(-0.354,P=0.015). The link to LVH is well established in HD patients. LVH is thought to be a maladaptive response that allows for normal LVEF despite abnormal pressure or volume load. This maladaptation is associated with increased risk of coronary events, heart failure, arrhythmia and stroke. In addition to traditional atherosclerotic risk factors, multiple factors are thought to be contributory in CKD including aortic stiffness, volume and pressure overload, hyperphosphataemia and neurohormonal activation [51]. Recent work has extended this picture with the implication of endogenous digitalis glycosides and fibroblast growth factor 23, both known to have higher concentrations in ESRD [52, 53]. In particular, sodium has been shown to induce adrenal gland secretion of endogenous digitalis glycosides and in vitro studies have shown they directly induce myocyte hypertrophy, thus providing a novel mechanism linking high dietary salt intake and impaired sodium excretion to hypertension and LVH in HD patients [54]. LV geometric changes, termed remodelling, have mainly been investigated by echocardiography in relationship to cardiovascular events. Concentric remodelling is defined as the presence of LVH and a high ratio of LV wall thickness relative to LV diameter from 1 dimensional M-mode echocardiography [352]. The presence and type of ventricular remodelling has been noted to prognosticate cardiovascular risk beyond that by LVH in some but not all studies in the HD and general population [353]. Studies in HD using echocardiography must be cautiously interpreted with respect to the timing of the study because the definition is limited by volume changes

such that calculated mass changes by 26g/m^2 over a HD treatment session [354]. As CMR determines mass and volumes without geometric assumptions, concentric remodelling is more simply determined by LV mass/volume ratio. The Multi-Ethnic Study of Atherosclerosis (MESA) used CMR in over 5000 healthy subjects followed for 5 years, showing LV mass/volume ratio was associated with a greater risk of cardiovascular events [355]. In our data HD patients had higher LV mass/vol ratio and this remained an independent determinant of strain after multiple regression.

We also demonstrated a modest correlation of strain to troponin-T that was not independent of LV mass. This is concordant with recent data. Elevated troponin is frequently associated with LV hypertrophy in the HD population [356]. A recent study using strain by 2D echocardiography showed that longitudinal but not circumferential strain was reduced in asymptomatic HD patients with elevated cardiac troponin-T and preserved LVEF [357].

We saw a lower strain in patients with diabetes. This is in keeping with some data supporting that reduced systolic and diastolic strains by tissue Doppler echocardiography are the earliest signs of diabetic cardiomyopathy in the absence of LVH, CKD or overt heart disease [358]. Impaired lipid metabolism causing reduced adenosine triphosphatase activity and consequent decreased contractility is a postulated mechanism. However data in this area are conflicting.

5.6.   Strengths and limitations

This is a cross-sectional observational study so causal relationships cannot be proven. A limitation of this study is the wide heterogeneity of global

systolic function in the HD group limited our ability to explore the utility of strain to detect subclinical cardiomyopathy. However we were able to demonstrate reduced strain in the subgroup with normal LVEF. We have also not examined diastolic function as the SPAMM technique used for tissue tagging fades during the cardiac cycle and is known to produce less reliable strain data in the diastolic phase. Future studies using tagging techniques optimised for diastole or performed at higher magnetic fields would be useful. Furthermore we did not have a CKD or treated hypertension control group and thus cannot determine the extent of their relative contributions to the observed between group differences.

The strengths of the study are the unselected population increases the generalisability of the findings. This study provides the first data on systolic strain by CMR, arterial stiffness and high sensitivity-troponin-T in incident HD revealing a greater degree of cardiac dysfunction in patients new to HD than previously recognized.

5.7.   Conclusion

In summary, in an unselected cohort, CMR tagging identified reduced circumferential strain in addition to abnormalities in LVEF and LV mass in the majority of patients new to HD. Strain was reduced in the subset of patients with normal LVEF. The independent determinants of strain were LVEF and LV Mass/Volume ratio. Strain shows promise in aiding early identification of cardiac disease in HD patients.

Study II Results

6. Study II Results: Directly-measured Aortic Distensibility in Patients new to Haemodialysis

6.1. Abstract

Aim: To investigate the contribution of uraemia to arterial stiffness

Methods: We used Cardiac Magnetic Resonance Imaging (CMR) to directly measure aortic distensibility (AD) in the ascending aorta of haemodialysis (HD, n=30) and age and sex-matched control (NC, n=19) subjects. These results were compared with concurrently measured left ventricular mass, volumes and strain by CMR and carotid-femoral pulse wave velocity (PWV) using an oscillometric device.

Results: Univariate analysis across both groups showed significant inverse correlations of AD to age (r=−0.668, P<0.001), PWV (r=-0.407 p=0.005) and left ventricular mass(r=−0.34, p=0.016). AD was positively correlated to ejection fraction (r=0.429, p=0.002) and peak-circumferential strain (r=0.327, p=0.023). In HD patients, AD was also inversely correlated to high sensitivity troponin-T(r=−0.46, p=0.014). There were no significant relations to body mass index, body surface area or NT-Pro-BNP. AD was reduced in HD patients compared to NCs, despite similar blood pressure and PWV ($2.0\pm1.8\text{mmHg}^{-1}\times10^{-3}$ vs $4.0\pm4.8\text{mmHg}^{-1}\times10^{-3}$, p<0.001). Multivariable regression analysis identified age, HD status and diabetes as the strongest independent determinants of lower AD (adjusted R^2=0.65). PWV did not enter the final model.

Conclusion: In a cohort of incident HD patients, age and diabetes were independent determinants of AD. Long-term follow-up will investigate AD as an independent risk factor for adverse LV remodelling in HD patients.

6.2. Introduction

Measurement of blood pressure is the most frequently method used to assess peripheral vascular function but pressure is not the only component. The association of stiffening of arteries with age and disease was first described in Ebers papyrus in 1550 BC. As early as 150 years ago, physiologists developed sphygmographs to investigate characteristics of arterial pressure waves [359]. Today, there is strong evidence that central arterial stiffening is associated with adverse cardiovascular outcomes in the general populations and populations at high baseline cardiovascular risk [360, 361]. Patients with end-stage renal disease (ESRD) have a greatly increased risk of premature cardiovascular morbidity and mortality. Although there is clustering of traditional cardiovascular risk factors for atherosclerosis, the relationship of those risk factors to outcome is not always clear and can only partly explain the increased risk [16, 362]. Epidemiological and clinical studies have frequently shown that increased arterial stiffness, most commonly assessed by measurement of pulse wave velocity (PWV) or augmentation index, is independently associated with cardiovascular morbidity and mortality in HD patients [36]. Although these studies are robust, applanation tonometry as an indirect measure of central arterial stiffness has limitations. The length of arterial path has to be estimated and there are problems in patients with obesity [363, 364]. The studies also did

not determine the relationship of these measures to cardiac structure or function.

Due to high spatial and temporal resolution, cardiovascular magnetic resonance imaging (CMR) is the gold standard for measuring left ventricular volumes and mass as it uses no geometric assumptions [318, 365]. CMR can be extended to cine imaging of the aorta allowing direct measurements of aortic distensibility (AD) and flow [366]. A previous study used CMR to determine AD in ESRD patients [367]. This study used a prevalent population using both haemodialysis (HD) and peritoneal dialysis, who were candidates for renal transplantation [367]. The study did not determine the relationship of AD to PWV, cardiac biomarkers or cardiac strain, an early marker of cardiac dysfunction [213]. We aimed to study AD in an incident HD population and relate to PWV, cardiac structure, cardiac function including strain and biomarkers. Furthermore we wished to compare the ability of AD to PWV to discriminate between study groups.

6.3.   Materials and methods
6.3.1. Patients

Ethical approval for the study was obtained from Nottingham Ethics Committee for all participating centres prior to study initiation and patient enrolment. The study was performed in accordance with International Conference on Harmonisation Good Clinical Practice Guideline and the 2000 Scotland Revision of the Declaration of Helsinki. All participants provided written informed consent. HD patients were recruited within 6 months of commencing in-centre HD at one of 4 UK research sites as part of a

randomised trial in dialysate cooling. Inclusion criteria were incident HD patients aged over 16 years within 180 days of commencing in-centre treatment 3 times per week with capacity to consent for the trial and without contra-indications for magnetic resonance imaging. Exclusion criteria included not meeting inclusion criteria, inability to tolerate magnetic resonance imaging and New York Heart Association Grade IV heart failure. 19 age and sex-matched healthy volunteers were recruited through a local clinical research healthy volunteer program. Inclusion criteria were aged over 16 years with capacity to consent to the study and without contra-indications for magnetic resonance imaging. Exclusion criteria were history of kidney disease, ischemic heart disease or cardiomyopathy.

6.3.2. Data collection

6.3.2.1. CMR acquisition

CMR studies occurred on non-dialysis days at two centres using the same model of 1.5T scanner (GE Signa HDxt 1.5T, GE Healthcare, Milwaukee,US) with retrospective ECG triggering and 8-channel phased array cardiac coil. Steady-state free precession (SSFP) cine images were acquired in 2, 3 and 4 chamber views. A stack of 8mm short-axis slices with a 2mm interslice gap were obtained using cine imaging covering the entire left ventricle (LV) from base to apex. Typical parameters were FOV 38, matrix 224x224, TR 3.2ms, TE 1.6ms, FA 60, Phase FOV 80%, Nex 1, views per segment 16, 30 reconstructed phases, temporal resolution 20-40ms depending on heart rate, spatial resolution 1.7mm x 1.7mm, ASSET disabled. Myocardial tissue tagging with a spatial modulation of magnetization (SPAMM) sequence with retrospective ECG gating and gradient recalled-echo readout was obtained.

Typical parameters were FOV 38, slice thickness 10mm, matrix 224 x 160, TR 3.2ms, TE 1.6ms, FA 12, Phase FOV 80%, Nex 1, ASSET disabled, views per segment 10, 30 phases/cardiac cycle, temporal resolution 15-30ms depending on heart rate, spatial resolution 1.7mm x 1.7mm. Three short-axis tagged images were planned in mid-systole from the 4 and 3-chamber cine at base, mid-ventricular and apical levels. Three plane localizer images were obtained to identify the ascending and descending aorta through to the pulmonary artery bifurcation. SSFP cines were acquired in an oblique sagittal orientation to demonstrate the full length of the aorta. This was used to acquire a 5 mm thick axial cine planned at the level of the pulmonary artery bifurcation with FOV 28 and the remaining parameters identical to the short-axis stack.

6.3.2.2. Blood pressure

PWV and blood pressure were measured in a supine position after 10 minutes rest. Brachial artery blood pressure was measured in the non-fistula arm in HD patients and the right arm in NCs using an oscillometric device (Datex-Ohmeda, GE Healthcare, USA).The mean of three readings was recorded.

6.3.2.3. Aortic PWV by external device

Carotid-to-femoral arterial PWV was measured using an oscillometric device (Vicorder, Skidmore Medical Ltd, Bristol, UK) as previously described [330]. Briefly, a carotid pressure cuff is applied over the neck to detect the right carotid artery and a pressure cuff is placed around the proximal right upper thigh to detect the right femoral artery. The distance from the suprasternal

notch to the middle of the thigh cuff was measured and entered into a PC running the Vicorder software. The cuffs were simultaneously inflated to a low pressure 40-60 mm Hg and signal from each cuff was analysed to derive arterial transit time. PWV was calculated by the software by dividing arterial transit time by measured distance. The mean of two measurements was recorded. In HD patients only, blood samples for determination of high-sensitivity troponin-T and BNP were taken immediately after insertion of access needles on HD the day before the CMR study. Samples were sent to the laboratory immediately for centrifugation then analysis using the Elecsys 2010 system (Roche Diagnostics, Switzerland). The limits of detection of the troponin-T assay were 0.005 µg/L, the 99th percentile 0.014 µg/L and the 10% co-efficient of variation was 0.013 µg/L [344].

6.3.3. Analysis

6.3.3.1. CMR analysis

All CMR analysis was performed offline blinded to patient details. Volumes and mass were determined using cvi42 software, version 4.0.2 (Circle Cardiovascular Imaging, Calgary, Canada). The LV contours were drawn manually excluding papillary muscles and trabeculations, and left ventricular end-diastolic volume (LVEDV), LV end-systolic volume (LVESV), LV ejection fraction (LVEF), end-diastolic LV Mass (LVM) and mean end-diastolic LV wall thickness (LVWT) were calculated. The interventricular septum was included as part of the LV. The basal slice was included when at least fifty percent of the blood volume was surrounded by myocardium. The apical slice was defined as the last slice showing intracavity blood pool. Values were indexed

by body surface area using Mosteller's method [316], denoted by the suffix 'I,' for example, LVMI. LVWT was calculated by excluding the two most basal and two most apical slices before averaging to reduce variability.

6.3.3.2. AD analysis

The scout images were used to plan a sagittal oblique view of the aortic arch and from this an axial cine and phase contrast acquisition at the middle of the pulmonary artery bifurcation to view both the ascending and proximal descending aorta (Figure 6-1). The aortic areas in all 30 phases of the axial aortic cines were traced using cvi42 software (Figure 6-1). The areas were exported into a spreadsheet and an area-time graph was drawn (Figure 6-2). AD was calculated using the Bramwell-Hill formula (Max area-Min area)/(Min area x delta P), where delta P is pulse pressure [368].

Figure 6-1 Aortic image acquisition. A: Sagittal oblique view of the aortic arch used to plan acquisition of axial cine and phase-contrast imaging. The dotted line represents the middle of the pulmonary artery bifurcation and the solid white line represents the path of the aortic pulse wave used to determine PWV B: axial cine manually traced in 30 phases at the middle of the pulmonary artery bifurcation used to determine aortic distensibility
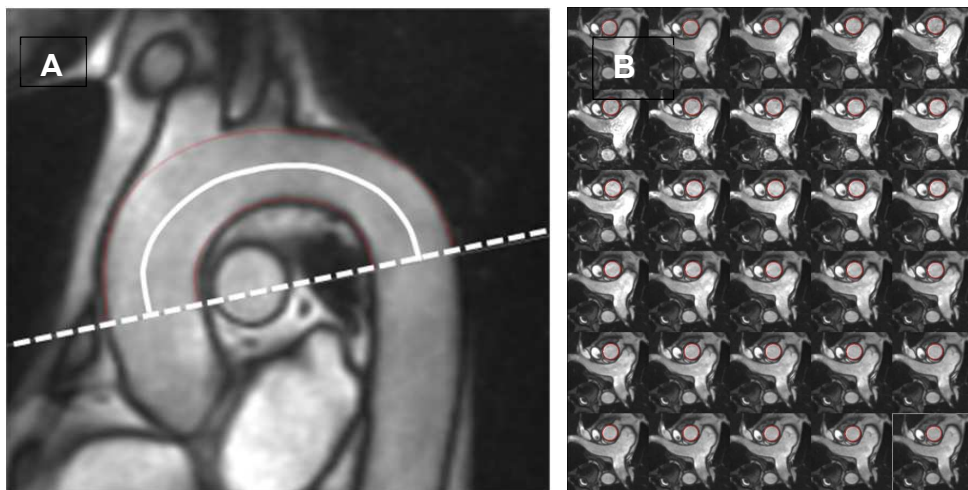
Figure 6-2 Aortic area (red line, left y axis) and aortic blood flow (blue line, right y axis) against time in a typical study subject. Maximal flow occurs early in systole.
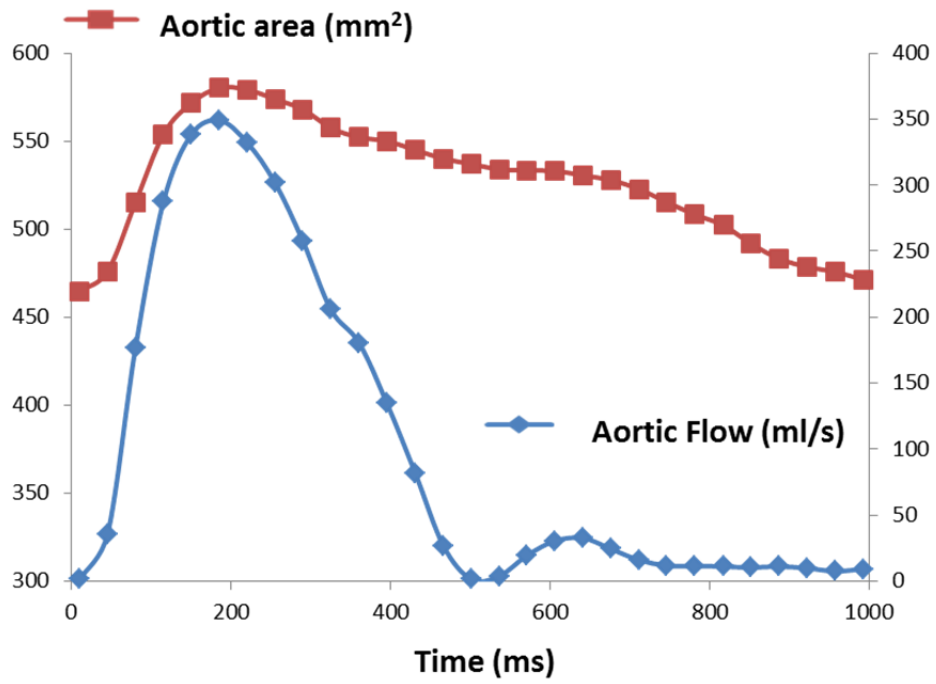
6.3.3.3. Aortic PWV by CMR

Aortic arch PWV was derived from the axial phase-contrast images using through-plane velocity encoded flow vs time traces processed by a bespoke algorithm written in Javascript for Jim software (Jim version 6. Xinapse software, UK). It can be shown that the maximum correlation between the curves corresponds to the delay between the upslope of the ascending and descending aortic pulse waves. The cross-correlation approach has been shown to be superior to time-to-foot of the pulse wave methods for calculating the transit delay[369].
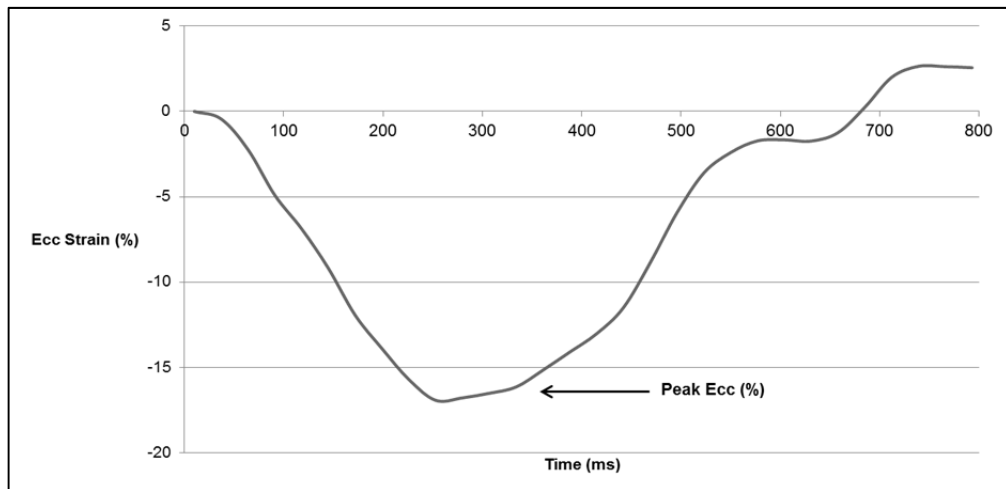
Figure 6-3 Principles of PWV determination using cross-correlation of aortic flow vs time curves
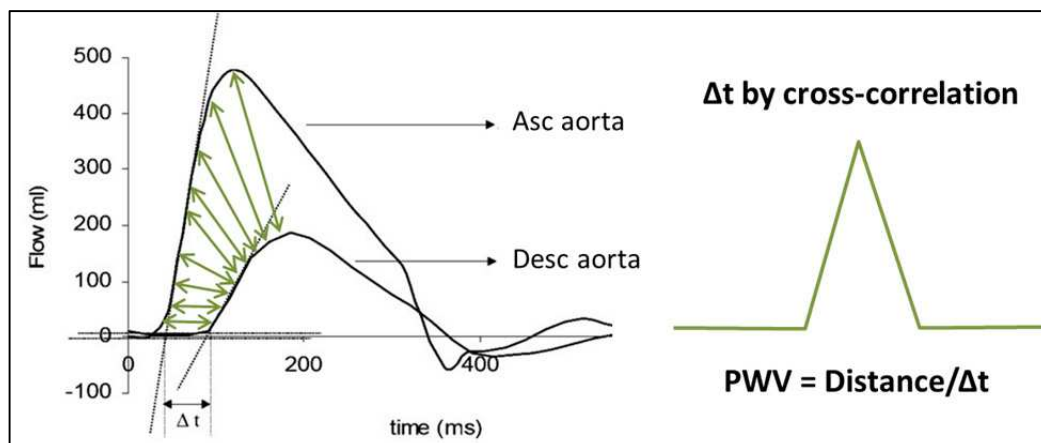
6.3.3.4. Tagging analysis

Peak-systolic mid-wall circumferential strain (Ecc) was measured using dedicated software (HARP 3.0, Diagnosoft, Palo Alto, California, USA) for each of the 3 short axis slices. Data were smoothed using a moving average of 3 points to reduce noise sensitivity and slices were averaged to give a global measure (Peak Ecc).

Figure 6-4 Representative mid-ventricular circumferential strain curve from a single patient. Peak Ecc refers to peak-systolic strain.

6.3.4. Statistical Analysis

Normality was assessed using the Kolmogorov-Smirnov test, histograms and normal Q-Q plot. Continuous data were expressed as mean (±standard deviation (SD)) if normally distributed and median (±interquartile range (IQR)) if not. Categorical data were expressed as counts and percentage. Unadjusted data were analysed using independent sample t-tests for normally distributed variables; Mann-Whitney U for non-parametric variables and Chi-Squared or Fisher's exact test for categorical variables. Pearson's test was used to assess univariate correlations with AD for variables with normal distribution or Spearman's test if the distribution was not normal. Variables with skewed distribution (exponential) were log transformed for the correlations. Multivariable linear regression analysis, using the forward stepwise method, was used to identify independent determinants of AD. $p < 0.05$ was used for a variable to enter the model. The model was built using a hierarchical approach that introduced one-by-one variables on the basis of a literature review, biological plausibility, and the strength of association in

univariate analyses adjusted for age. Blood pressure was excluded from the analysis as it is not independent of AD. A scatter plot of regression residuals versus predicted values and Cook's Distance plot were used for testing the assumptions of linear regression and identifying any outliers. The adjusted R-squared value is reported as a measure of goodness-of-fit. The regression coefficients (95% Confidence Intervals) and standardised coefficients are presented from the final multivariable model. Receiver operator characteristic (ROC) curve analysis under the non-parametric assumption was used to compare the discriminatory ability of AD and PWV for the study groups. SPSS version 20.0 was used for all analyses. All p values are based on two-sided tests and <0.05 was considered statistically significant. Graphs were drawn in SPSS or GraphPad Prism version 6.01 for Windows (GraphPad Software, California, USA).

6.4.   Results

Baseline characteristics:

Detailed characteristics of the study population are in Table 6-1 and CMR findings are summarized in Table 6-2. The control group was well matched for age, sex, blood pressure, body mass index and body surface area. AD was right-skewed in distribution and was log-transformed for correlations and regression analyses.

Table 6-1 Participant characteristics. Continuous variables are mean±SD or median(IQR) depending on normality and use Independent t test or Mann-Whitney Test as appropriate. Categorical data are counts[percentage] and comparisons use Fisher's exact test.

	HD	NC	P val
	(n=30)	(n=19)	
Age (years)	55(27)	55 (26)	0.98
Female	7 (23)	8 (42)	0.17
HD vintage (days)	161(146)	-	-
Diabetes	7 [23]	1 [5]	0.13
IHD	6 [20]	0 [0]	0.07
Treated hypertension	21 [70]	2 [11]	<0.001
Smoking status (never/current/ex/)	14/8/8	15/1/3	0.11
PVD	4 [13]	0 [0]	0.15
Statin use	12 [40]	1 [5]	0.01
RAAS antagonist	5 [17]	1 [5]	0.39
BSA (m^2)	1.9 ±0.3	1.9 ±0.2	0.55
Body Mass Index (kg/m^2)	27.6 ±8.0	26.8 ±4.6	0.97
Troponin-T (µg/L)	41 (56)	-	-
BNP (pg/ml)	234 (531)	-	-

Table 6-2 CMR and oscillometric findings Values are mean±SD or median(IQR) depending on normality. P values use Independent t test or Mann-Whitney Test as appropriate.

	HD	NC	P val
AD (mmHg)-1x 10-3	2.0 (1.8)	4.1 (4.8)	0.001
MR-PWV (m/s)	7.9 (3.5)	5.3(1.9)	0.014
Ex-PWV (m/s)	8.4(3.0)	8.4(1.5)	1.0
LVEF (%)	50.3 ±11.1	58.7 ±5.1	<0.001
LVMI (g/m2)	64.1 (35.0)	45.8 (11.3)	<0.001
Peak Ecc (%)	15.5 ±4.2	19.8 ±4.6	0.001
LVEDVI (ml/m2)	89.8 (40.2)	72.7 (12.7)	0.043
CI (ml/m2)	3.4 (0.9)	2.7 (0.6)	0.07
HR	73 (19)	64 (11)	0.08
SBP (mmHg)	140 ±32	138 ±30	0.4
DBP (mmHg)	77 (16)	83 (16)	0.44
PP (mmHg)	57 (26)	51 (18)	0.12
PWV (m/s)	7.9 (2.9)	8.8 (2.3)	0.2
LVSVI (ml/m2)	38.8 (23.9)	41.5 (7.5)	0.58

Figure 6-5 Spearman's rank correlation of Age to AD in the entire study cohort of Study II. AD was log-transformed prior to the correlation as it was right-skewed. It shows AD decreases with advancing age.
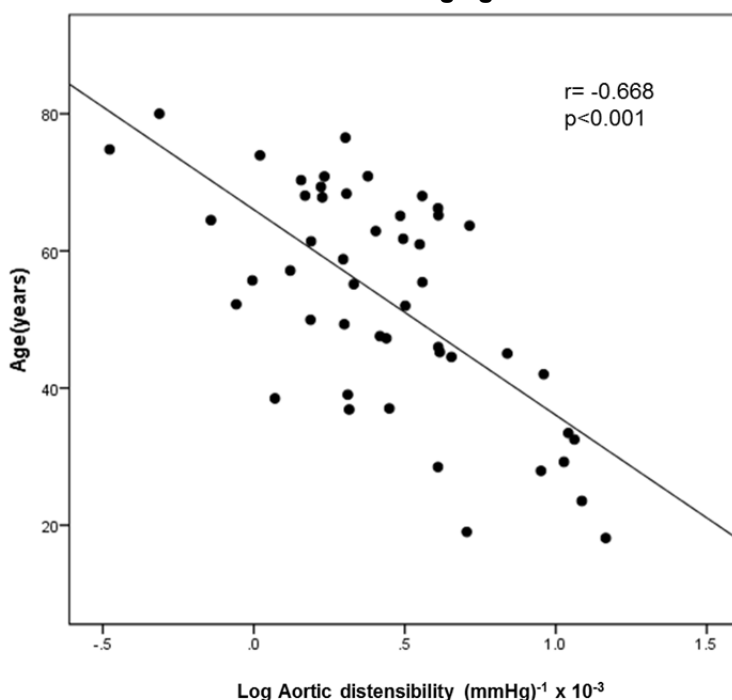
Table 6-3 Significant Univariate Correlations to AD. P values use Pearson's correlation for normally distribution or Spearman rank correlation for non-normally distributed data. *Troponin-T was only measured in HD patients.

	Total Cohort (unadjusted)	
	r	P-value
MR-PWV	-0.72	<0.001
Age (years)	-0.67	<0.001
Skin autofluorescence	-0.57	0.013
LVEF	0.43	0.002
LV wall thickness	-0.44	0.009
External-PWV	-0.41	0.005
High-sensitivity troponin-T*	-0.53	0.014
LV Mass Index	-0.34	0.016

Aortic distensibility

Univariate correlations to AD are summarized in Table 6-3. AD was significantly inversely correlated to age, MR-PWV Ex-PWV and LVMI. AD was positively correlated to global measures of cardiac systolic function including LVEF and Peak Ecc. In HD patients, AD was also inversely correlated to high sensitivity troponin-T(r=−0.46, p=0.014). There were no significant relations to body mass index, body surface area or NT-Pro-BNP. Table 6-2 and Figure 6-6 shows AD was reduced in HD patients compared to NCs, despite similar age and blood pressure. AD was also significantly reduced in diabetic versus non-diabetic subjects (Figure 6-7). AD was reduced in males compared to females but this did not reach statistical significance (2.5 ± 2.4 vs 3.1 ± 3.5 mmHg$^{-1}\times10^{-3}$, p=0.47). The ROC curve to discriminate between study groups showed that AD had a greater sensitivity and specificity to determine study groups than PWV (Figure 6-8). Forward stepwise multiple linear regression identified age, presence or absence of HD and presence or absence of diabetes as independent determinants of AD (Table 6-4).

Figure 6-6 Median and IQR of AD in HD patients vs controls (NCs). P values uses Mann-Whitney test.
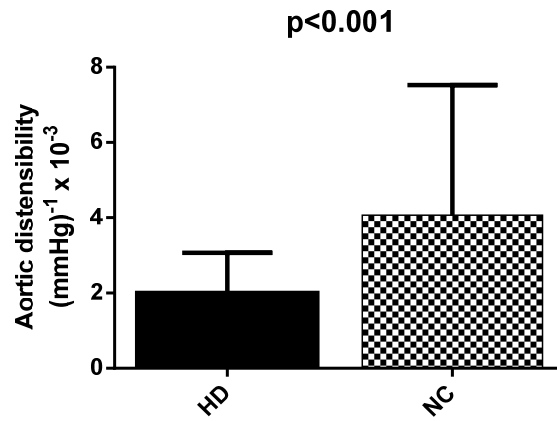
Figure 6-7 Median and IQR of AD in diabetic vs non-diabetic subjects. P values uses Mann-Whitney test.
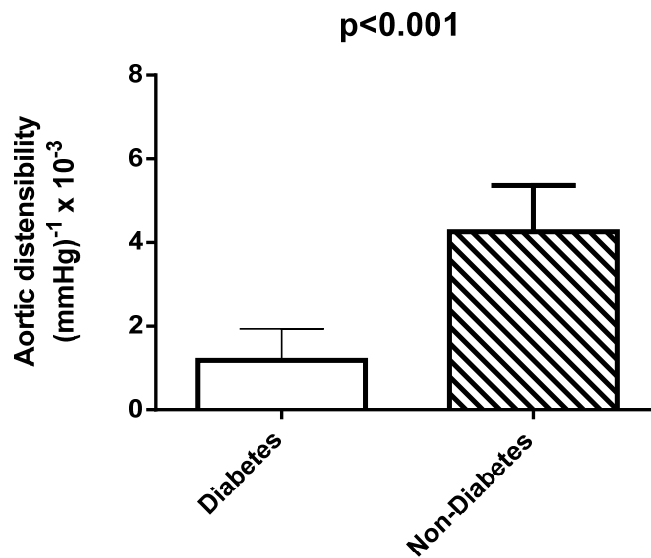
Figure 6-8 Receiver Operator Characteristic curves to compare diagnostic accuracy of AD or PWV to discriminate between HD and NC study groups. This demonstrates AD has greater sensitivity and specificity than externally measured PWV distinguishes between groups
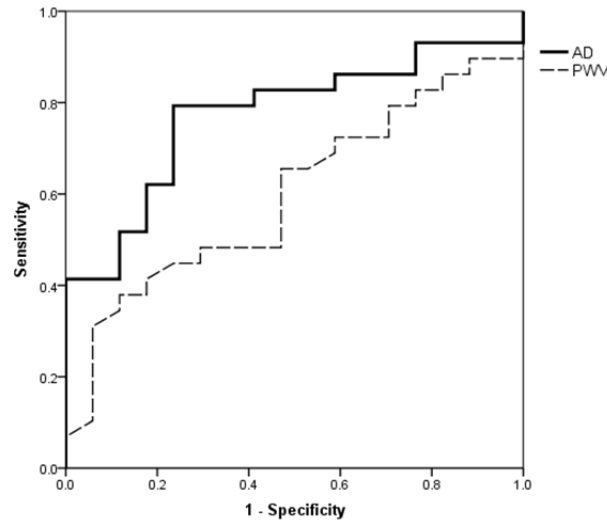
	AUC	95%CI	P val
AD	0.77	0.64-0.91	0.002
PWV	0.60	0.43-0.77	0.270

Table 6-4 Independent Determinants of AD by multiple linear regression. B = un-standardised coefficient (95% confidence intervals), β = standardized coefficient. Independent variables that did not enter the model were: PWV, smoking status, history of IHD, log high sensitivity Troponin T, LVMI, LVEF, Peak Ecc and LV wall thickness.

	Total Cohort Adjusted R^2= 0.65		
	B (95% CI)	β	p value
Age (per 1year)	0.99 (0.98-0.99)	-0.62	<0.001
HD (yes vs no)	1.29 (1.13-1.46)	0.34	<0.001
Diabetes (yes vs no)	0.78 (0.65 to 0.92)	-0.26	0.005

Vicorder measured Pulse wave velocity

PWV by Vicorder (Ex-PWV) was significantly correlated to age (r=0.52, p<0.001) systolic blood pressure(r=0.308, p<0.037), and pulse pressure (r=0.299, p=0.043). In contrast to AD there were no significant correlations to measures of LV function, LV mass or troponin T.

6.4.1. Discussion

This study showed that AD is higher in HD patients, after adjusting for age and diabetes status. Although unintended, the groups were well matched for BP further strengthening the independence of the findings. AD was also lower in diabetic versus non-diabetic subjects. In addition, AD had significant univariate correlations to high sensitivity troponin-T and multiple measures of LV function and mass that were not seen for PWV. This suggested that AD had a greater diagnostic accuracy than PWV to discriminate between groups and this was confirmed by the ROC analysis. Multivariable regression analysis identified age, HD status and diabetes as the strongest independent determinants of lower AD (adjusted R^2=0.65). PWV did not enter the final model.

The data are concordant with the findings of previous research but also contain novel findings. Zimmerli et al compared CMR determined AD and PWV in 35 prevalent ESRD patients to 24 controls and 24 patients with multivessel CAD [367] The study design was different to the present in that AD was calculated from volumes precluding comparison of absolute values.

Furthermore the 24 ESRD patients were subdivided into patients with or without CAD. Despite the design differences a number of comparisons can be drawn. We found a similarly strong correlation of AD to age that remained an independent determinant in the regression analysis. Intergroup comparisons were also similar to the present study, with a significantly lower AD and higher LV mass in ESRD vs controls and no significant difference in PWV. The strong relationship of age to AD is remarkably consistent across multiple methodologies and multiple disease groups [370-372]. The mechanisms proposed for reduced AD with age include disruption of the elastic component of the vessel wall, fibrosis and increase in collagen at the expense of medial vascular smooth muscle cells [373-375]. It may also be related to a deficiency of nitric oxide bioavailability and fatigue fracture of elastin fibres [376, 377]. This would partly explain the tendency for the age related increase in AD to occur mostly in the proximal aorta where elastin is most prominent. Such mechanisms are difficult to separate from the overlapping and additional changes known to be induced by CKD. Increased deposition of advance glycation end-products (AGEs) are known to increase collagen cross-linking and provide a direct mechanism of reduced AD [378]. AGE levels are markedly increased in HD patients and predictive of mortality [38]. McIntyre et al previously demonstrated that increased AGE levels occur in early stage CKD [379]. Other mechanisms to reduce AD which are more prevalent in HD patients include vascular calcification. This can be medial and intimal but is particularly medial in HD patients. In vitro studies show vascular smooth muscle cells undergo transformation to osteochondroblasts promoting calcification when cultured in phosphate at concentrations similar

to those seen in HD patients [380]. Another relationship seen in our study that is concordant with prior studies was reduced AD in subjects with diabetes. Van de Meer et al used CMR to determine AD was lower in 13 patients with diabetes compared to 15 healthy subjects (4.5±2.2 vs. 7.4±3.3mmHg^{-1}×10^{-3} p<0.05) [381]. The multiple regression analysis of Zimmerli et al showed that the independent determinants of AD were age, presence or absence of ESRD and presence or absence of CAD [367]. In the present study, the determinants were age, presence or absence of ESRD (HD) and diabetes. Given that we examined an incident population which had been exposed to HD for a median 170 days, it is likely that the changes we saw in HD patients occurred at least in part, prior to commencing HD. Edwards et al compared CMR-determined AD in patients with CKD stage 3 to normal controls [382]. They derived similar values to the present study (2.2±1.8 vs 4.1±1.3mmHg^{-1}×10^{-3}, p<0.01 in Edwards et al compared with 2.0±1.8 vs 4.0±4.8mmHg^{-1}×10^{-3}, p<0.001 in the present study) [382]. However AD was not the focus of their study preventing further comparisons.

The novel findings in our study include a relationship of AD to high sensitivity troponin-T and Peak Ecc. A direct mechanism linking AD to both raised troponin-T and increased LV mass is subendocardial perfusion due to increased afterload. Afterload is LV end-systolic wall stress. Increased aortic stiffness leads to increased afterload and reduces aortic pressure throughout diastole. Animal studies show this leads to an increased myocardial oxygen demand, hypertrophy and compromised coronary perfusion [383, 384]. Such a reduction in coronary flow reserve is well described in HD patients [337].

McIntyre et al previously used intra-dialytic myocardial perfusion imaging by positron emission tomography with radio-labelled water during HD to demonstrate that the HD process itself exerted sufficient stress to precipitate myocardial ischaemia [385]. This raises the intriguing possibility that the combination of patients primed by aortic stiffness and repetitively stressed by HD might cause higher troponin-T levels. Such ischaemia would be independent of flow-limiting coronary artery disease in its absence and additive to coronary artery disease in its presence. The relationship of AD to HD-induced myocardial ischaemia will require further studies that separate the contributions of LV hypertrophy and coronary artery disease.

6.4.2. Limitations

This is a cross-sectional observational study so causal relationships cannot be proven. A limitation of this study is that invasive local assessment of aortic pulse pressure was not performed, which would have defined AD more accurately than the use of brachial pulse pressure. Furthermore we did not have a CKD or treated hypertension control group and thus cannot determine the extent of their relative contributions to the observed between group differences. The strengths of the study are achieved matching for age, sex, body mass index and surface area and measured blood pressure used for the AD calculation. To our knowledge we are the first to have shown associations of AD to raised troponin-T, LV mass and LV function by strain in HD patients.

6.4.3. Conclusions

Our study documents for the first time the strong association of CMR-determined AD to measures of LV systolic function and high sensitivity troponin-T. Age, diabetes and HD status were independent determinants of AD. Long-term follow-up will investigate AD as an independent risk factor for adverse LV remodelling in HD patients.

Study III Results

7. Study III Results: Haemodialysis-induced stunning detection using Strain by Speckle Tracking Echocardiography

7.1. Abstract

Introduction: Haemodialysis can induce recurrent myocardial ischemia (myocardial stunning) and early identification allows strategies to improve outcomes. This was previously assessed by lateral wall motion analysis of echocardiographic images in prevalent populations. Recently, myocardial tissue deformation using 2D strain by speckle tracking echocardiography (STE) has proven to be a powerful tool for detecting ischemia in the non-CKD setting but has not been applied to detect stunning during HD. Furthermore, the prevalence of HD-induced stunning in incident patients is not known.

Objectives: The aims of the study were i) To detect HD-induced stunning using reversible abnormalities by STE ii) Study determinants of stunning with structural and functional biomarkers and iii) Determine prevalence of stunning in an incident HD population.

Methods: 60 subjects were studied (median vintage 170 days). STE was performed immediately before HD (Pre) and 15 minutes before the end of HD (Peak). Segmental and global peak-systolic longitudinal strain (GLS) and strain rate (GLSR) were determined using commercially available software. HD-induced stunning was defined as any reduction in GLSR at Peak-HD compared to Pre-HD. Aortic stiffness was measured by carotid-femoral pulse wave velocity and advanced glycation end-products were estimated by skin autofluorescence. The severity of intradialytic hypotension (IDH) was

determined by tertiles of frequency of 15% reduction from baseline using continuously recorded blood pressure data.

Results: Data are presented as Median±IQR and Pre-HD vs Peak-HD. 70% (42/60) had reduced GLSR at Peak-HD and were defined as stunning. Stunning was associated with higher NT-proBNP values (323±839 vs 81±120 pmol/ml, p<0.001) and greater troponin-T concentrations (46±51 vs 14±35ng/ml, p=0.011).   In logistic regression analyses, NT-proBNP concentration was the only independent predictor of myocardial stunning (Odds ratio for 100pmol/l increase 1.766, 95% CI 1.099-2.839, p=0.019).and Troponin-T concentration was the only significant independent predictor of frequency of IDH (Odds ratio for 10μg/l increase 1.138, 95% CI 1.013-1.276, p=0.038).

Conclusion: Strain-based imaging by speckle tracking echocardiography shows promise for detection of HD induced stunning. A decreased change in strain rate across HD was associated with higher BNP and troponin-T, arterial stiffness and hypervolemia by bioimpedance. Further studies are required to determine if a strain-based definition of HD-induced myocardial stunning can replace current methods.

7.2.   Introduction

HD patients represent an extreme phenotype of cardiovascular risk with a pattern of disease distinct from that in the general population [1, 2]. A high prevalence of impaired autonomic function, left ventricular hypertrophy (LVH) and arterial stiffness result in a decrease in coronary flow reserve enabling demand myocardial ischemia to occur without flow-limiting stenosis of the coronary arteries. We previously used perfusion imaging during HD to show the process of HD is capable of causing a stress sufficient to reduce myocardial blood flow by 30% in the majority of prevalent patients [284]. The ischemia was localised to areas of reversible left ventricular (LV) regional wall motion abnormalities on 2D echocardiography. Patients demonstrating such dysfunction had 30% mortality at 1 year [284]. These findings were confirmed by another group using LV wall-motion score index (WMSI) by expert observer [386]. These studies are robust and the motion indexes were predictive of higher mortality. However as the human vision has a relatively poor temporal resolution the WMSI requires a high-level of clinical expertise and remains subjective with high inter-observer variability [163]. In addition, such approaches cannot distinguish between active myocardial motion and that due to passive tethering of dysfunctional segments by adjacent healthy tissue, potentially reducing specificity [189].

Assessment of regional deformation (strain) within the myocardium may have greater sensitivity and specificity than measuring function by the motion of its boundaries. Speckle Tracking Echocardiography (STE) estimates motion by tracking of speckles in a greyscale 2D ultrasound images. The speckles are the result of interference generated by microscopic intramyocardial structures

189

and represent tissue markers that can be tracked during the cardiac cycle with a block-matching algorithm. Recently 2D myocardial strain imaging by STE has proven to be a powerful tool for detecting ischemia in the non-CKD setting [194]. Furthermore, prior studies of HD-induced stunning used prevalent populations and so the true incidence in patients new to HD is not known.

Objectives: We aimed to detect HD-induced myocardial stunning using reversible abnormalities in longitudinal strain and strain rate by STE in an unselected population new to HD and study associations with cardiac biomarkers, arterial stiffness and haemodynamic changes. We hypothesised that we could identify stunning by two modes of response to the stress of HD: A normal stress response, with an increase in strain and strain rate or an abnormal stress response with a reduction.

7.3.   Materials and methods
7.3.1. Patients

Ethical approval for the study was obtained from Nottingham Ethics Committee for all participating centres prior to study initiation and patient enrolment. The study was performed in accordance with Good Clinical Practice Guideline and the Declaration of Helsinki. All participants provided written informed consent.. HD patients from 4 UK research sites were screened for enrolment and 73 consented to this study as part of a randomised trial in dialysate cooling (ISRCTN00206012). Patient flow is summarised in . Inclusion criteria were HD patients aged over 16 years within 180 days of commencing in-centre treatment 3 times per week with capacity to consent for the trial and without contra-indications for magnetic resonance

imaging. Exclusion criteria included not meeting inclusion criteria, inability to tolerate magnetic resonance imaging and New York Heart Association Grade IV heart failure. The data presented here is from screening data prior to the application of any intervention.

Figure 7-1 Patient flow in the study
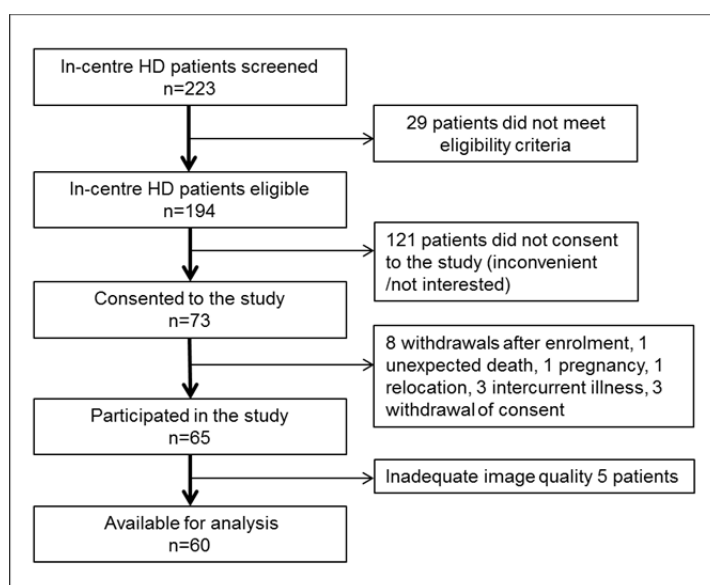
7.3.2. HD Details

Dialysis was performed using low-flux polysulfone dialyzers, either 1.8 m^2 or 2.0 m^2, per individual patients' usual prescriptions (LOPS 18/20; Braun Medical Ltd, Sheffield, United Kingdom). Dialysate composition was sodium 136-138mmol/l; potassium 2mmol/l; calcium 1.25mmol/l; magnesium 0.5mmol/l; bicarbonate 32-38mmol/l; glucose, 5.6mmol/l; and acetate 3mmol/l. 40 of 65 patient treatments were of 4 hours duration with the remainder at 3.5 hours. Anticoagulation was by unfractionated heparin. The dialysate flow rate was 500 mL/min and dialysate temperature was set at 36-37°C. For each session, net fluid removal was set on an individual basis

according to ideal dry weight. Blood pump speed varied between 250 and 450 mL/min, depending on the patient's vascular access.

7.3.3. Echocardiography

Conventional 2D grayscale echocardiography with second harmonic imaging was performed using commercially available equipment (1.5-4mhz probe, Vivid-I, GE Healthcare, Horten, Norway) by one of two trained technicians in the left lateral position. Sector width, frequency and depth were optimised to produce optimal border definition and a frame-rate of 50-80 per second. Loops of 3 consecutive cardiac cycles in standard apical 2 and 4-chamber views were recorded pre-dialysis (rest) and 15 minutes before the end of dialysis (stress).

7.3.4. Strain Analyses

Longitudinal strain was measured by STE in 12 segments (2 and 4 chamber views) of an 18-segment LV model. The regions of interest (ROIs) were manually adjusted to include the entire LV myocardium and exclude the pericardium. Segments with poor tracking were automatically identified by the software and excluded manually if necessary. Peak negative systolic strain, representing the maximum systolic longitudinal shortening before aortic valve closure was noted for each segment. Peak negative systolic longitudinal strain rate represents the slope of the strain curve. Values of all segments were averaged to obtain global longitudinal strain (GLS) and global longitudinal strain rate (GLSR). All echocardiographic and strain analyses were performed separately and blinded to other patient data in random order.

7.3.5. Intradialytic Hypotension

Continuous systemic blood pressure was monitored during HD using digital infra-red plethysmography in the non-fistula arm. (Finometer, Finapres Medical Systems, Arnhem, The Netherlands). This utilises pulse-wave analysis to reconstruct a central aortic waveform by a validated transfer function allowing a beat-to-beat tracking of blood pressure throughout the treatment [387]. The raw data was exported into mathematical analysis software (MATLAB R2012a, Mathworks Inc.) and severity of intradialytic hypotension (IDH) was determined by tertiles of frequency using systolic blood pressure data with a bespoke algorithm which compared 5 minute averaged samples to a baseline reference of stable readings and defined an episode as 15% reduction.

7.3.6. Body Composition by Bioimpedance

Bioimpedance analysis (BIA) measurements of resistance and reactance were taken in the recumbent position after 5 min of rest using a multifrequency, multisegmental, BIA device (InBody S20; Biospace, Seoul, Korea). This device has previously been validated in HD patients [388]. Total body water (TBW) and extracellular water (ECW) were derived on the basis of the manufacturer's impedance algorithm, which sums estimates for each of the limbs and the trunk. ECW/TBW ratio as a marker of hypervolemia is reported.

7.3.7. Aortic Stiffness

Aortic stiffness by carotid-to-femoral pulse wave velocity (PWV) was measured with the patient lying at 30 degrees after 5 minutes rest using an oscillometric device (Vicorder, Skidmore Medical Ltd, Bristol, UK) as previously described [330]. The mean of 2 measurements was recorded.

7.3.8. Skin autofluorescence

Advanced Glycation End product (AGE) deposition has been implicated as a risk factor for arterial stiffness. AGE deposition determined by skin autofluorescence (AF) reflects the systemic burden and has shown to be predictive of cardiovascular mortality [389]. AF was measured on the non-fistula arm using an AGE Reader device (DiagnOptics, Groningen, Netherlands). The mean of three readings was recorded. Readings are known to be unreliable on dark skin and were not done in this event. Values are expressed in arbitrary units (AU) [379].

7.3.9. Haematological and Biochemical Variables

Predialysis blood samples were drawn immediately after insertion of access needles and collected into lithium heparin and EDTA tubes. Haematological samples were immediately sent to the laboratory at each research site. Biochemical samples were centrifuged and frozen at -80°C before batch analysis in the laboratory of the lead site for determination of high-sensitivity troponin-T (hsTnT) and NT-proBNP (BNP) using a multichannel autoanalyser (Elecsys 2010 system, Roche Diagnostics, Switzerland). The limits of detection of the hsTnT assay are 0.005µg/L, the 99th percentile 0.014 µg/L

and the 10% co-efficient of variation is 0.013 µg/L [344]. The limits of detection of the NT-proBNP assay are 0.6pmol/l and the interassay co-efficient of variation is 3.9%.

7.3.10. Definitions

HD-induced stunning was defined as any reduction in GLSR or GLS at Peak-HD compared to Pre-HD. The rationale was that a normal response to a haemodynamic stress should be to improve contractility and GLSR is a less load-dependent marker of contractility than GLS [193, 390].

7.3.11. Outcomes

The primary variables of interest were changes in GLSR and GLS, frequency of IDH and Troponin-T.

7.3.12. Statistical Analysis

Normality was assessed using the Kolmogorov-Smirnov test, histograms and normal Q-Q plot. Continuous data were expressed as mean±standard deviation if normally distributed and median(interquartile range) if not. Categorical data were expressed as counts[percentage]. Comparisons between resting and stress STE at peak HD were made by the paired T test or Wilcoxon signed ranks test. Univariate correlations to changes in GLS and GLSR and biomarkers were analysed by Pearson's or Spearman's Rank correlation coefficient as appropriate. Variables with right-skewed distribution were logarithmically transformed for the correlations. Binary logistic regression analysis was applied to identify independent determinants of changes in GLS and GSLR. Univariate correlations then ordinal logistic regression were applied to identify determinants of the number of IDH

episodes. A threshold of p<0.1 was used for a variable to enter regression models. Models used a hierarchical approach ranking variables by the strength of the univariate association as well as biological plausibility. Only one cardiac measurement was entered at a time to satisfy the requirements of collinearity. The adjusted R-squared value (Nagalkarke) is reported as a measure of goodness-of-fit. SPSS version 20.0 was used for all analyses. All analyses were 2 sided, and significance was judged at p <0.05.

7.4. Results

Table 7-1 Patient characteristics Continuous variables are mean±SD or median(IQR) depending on normality and comparisons use Independent t test or Mann-Whitney Test as appropriate. Categorical data are counts[percentage] and comparisons use Fisher's exact test.

	Control	Intervention	P val
Age (years)	60(24)	62(22)	0.57
Female	8[36]	7[33]	0.84
BMI (kg/m^2)	28.8±6.0	28.2±6.0	0.70
BSA (m^2)	1.9±0.2[]	1.9±0.2[]	0.90
Medical history			
HD vintage (days)	165(168)	122(159)	0.47
Tunnelled catheter	8[35]	3[14]	0.05
Diabetes mellitus	6[27]	6[28]	1.0
Ischaemic heart disease	2[9]	2[10]	1.0
Current/Ex-smoker	7[37]	11[58]	0.3
Peripheral vascular disease	2[9]	5[24]	0.2
Primary renal disease			
Diabetes Mellitus	6[27]	6[28]	1.0
Glomerulonephritis	4[18]	3[14]	0.9
Interstitial nephritis	2[9]	2[10]	1.0
Vasculitis	2[9]	1[5]	0.7
Polycystic Kidney Disease	0[0]	1[5]	0.7
Renovascular disease/malignant hypertension	3[14]	3[14]	1.0
Plasma cell dyscrasias	0[0]	2[10]	0.9
Unknown/Others	5[23]	3[14]	0.6
Medication			
Treated hypertension	17[74]	18[86]	0.5
RAAS antagonist	5[22]	6[29]	0.7
Beta blocker	8[35]	7[33]	1.0
Statin use	10[44]	10[48]	1.0
Phosphate binder			
Calcium-based	9[39]	4[19]	0.2
Non-calcium	7[30]	5[23]	0.7
Erythropoeisis Stimulating Agent	16[70]	15[71]	1.0
Vitamin D analogue	13[57]	11[53]	1.0

Table 7-2 Laboratory results and clinical parameters. Values for continuous variables are given as mean±SD with independent T test if normally distributed or median(interquartile range) with Mann-Whitney test if non-normal.

	All (n=60)	'Stun' Reduced GLSR (n=42)	'Non-Stun' Preserved GLSR (n=18)	P val
Laboratory results				
High-sensitivity troponin-T (ng/ml)	37(56)	46(51)	14(35)	0.011
NT-Pro-BNP (pmol/ml)	163(427)	323(839)	81(120)	0.001*
Total Cholesterol	3.4±0.9	3.7±1.0	3.3±0.1	0.59
HDL Cholesterol	1.0±0.3	1.1±0.4	1.0±0.0	0.70
Total/HDL Ratio	3.4±0.6	3.4±0.6	3.3±0.2	0.73
PTH	169(211)	186(225)	147(94)	0.55
Calcium	2.33±0.14	2.34±0.15	2.33±0.10	0.91
Albumin	36.0±3.4	35.7±3.6	36.5±3.7	0.51
Phosphate	1.56±0.46	1.53±0.48	1.64±0.48	0.48
CRP	4.0(8.0)	5.5(8.8)	4.0(12.5)	1.0
Clinical parameters				
PWV (m/s)	7.3(2.7)	7.7(2.7)	6.8(2.3)	0.11
Skin Autofluorescence (AU)	3.5±1.0	3.5±1.0	2.8±0.6	0.05
Ultrafiltration volume (l)	1.9(0.9)	1.6(1.3)	2.0(0.7)	0.17
Ultrafiltration volume/Post HD	25±16	25±13	25±7	0.99
ECW/TBW by bioimpedance	0.40(0.02)	0.40(0.02)	0.39(0.02)	0.04
Left ventricular mass indexed to BSA	67.5±18.1	70.2±18.3	62.0±12.4	0.09

198

Patient characteristics are presented in Table 7-1 with clinical parameters in Table 7-2 for the whole group and categorised by the contractile response at Peak-HD. It should be noted that GLS and GLSR are conventionally expressed as negative numbers with more negative strain or strain rate denoting improved contractile function.

Prevalence of HD-induced stunning

60% (42/60) had reduced GLSR at Peak-HD compared to Pre-HD. This group had greater NT-Pro BNP levels, greater Troponin-T concentrations, higher skin autofluorescence levels. There was also greater usage of calcium based phosphate binders and erythropoeisis stimulating agents. There were trends towards higher PWV and higher LV mass.

Pre-HD Resting Global Longitudinal Strain and Strain Rate

Pre-HD GLS had positive correlations (denoting worse strain) to age, markers of ischemia, endotoxin, hypervolemia, central arterial stiffness (PWV) and advanced end-glycation product deposition (Skin AF). Pre-HD GLSR had similar correlations but had a weaker non-significant correlation to age and was more strongly tied to hypervolemia with positive correlations to NT-proBNP and LVEDV. Both Pre-HD GLS and GLSR showed negative correlations (improved strain) to LVEF as denoted in Table 7-3.

Table 7-3 Significant Univariate Correlations to Pre-HD GLS and GLSR. P values use Spearman rank correlation.

	Pre-HD GLS		Pre-HD GLSR	
	r	P-value	r	P-value
Skin AF	-0.604	0.002	0.608	0.002
LVMI	-0.206	ns	0.536	<0.001
Pre-HD LVEF	0.485	0.001	-0.489	0.001
Post-HD Endotoxin	-0.324	0.036	0.419	0.006
NT-ProBNP	-0.139	ns	0.406	0.003
LVEDV	0.158	ns	0.393	0.012
Troponin-T	-0.401	0.003	0.358	0.009
PWV	-0.365	0.012	0.327	0.025
ECW/TBW	-0.399	0.007	0.310	0.04
Age	-0.299	0.03	0.124	ns

Changes in Global Longitudinal Strain and Strain Rate

GLSR decreased from pre- to peak HD in 70% (42/60) and increased in 30% (18/60). The group who decreased strain rate indicating impaired stress response and lack of contractile reserve were defined as demonstrating HD-induced stunning. The group who increased strain rate would be characterized as a normal stress response demonstrating contractile reserve and were defined as not stunning. Stunning prevalence was not increased by age, diabetes, male sex, or history of ischaemic heart disease. Stunning was correlated to markers of ischemia, hypervolemia or cardiac stress including hsTnT, ECW/TBW by bioimpedance and NT-proBNP. Stunning was also correlated to lower level of strain and strain rate at baseline (Table 7-5). The stunning group with negative ΔGLSR also had a decrease in GLS during HD that did not reach statistical significance (-16.2±3.8% to -14.5±2.1%, p=0.17). Conversely the positive ΔGLSR in the non-stunning group (improved strain rate) was accompanied by an increase in GLS that did not reach statistical significance.

Table 7-4 Changes in Strain, Strain rate and LVEF during HD P values use paired T test or Wilcoxon signed rank test as appropriate

	'Stun' Reduced GLSR (n=42)			'Non-Stun' Preserved GLSR (n=18)		
	Pre-HD	Peak-HD	Pval	Pre-HD	Peak-HD	Pval
GLS (%)	-16.2±3.8	-14.5±2.1	0.165	-14.0±4.4	-14.4±4.0	0.227
GLSR (1/s)	-1.27±0.25	-1.14±0.28	0.004	-1.06±0.3	-1.33±0.3	<0.001
LVEF (%)	54.9±11.3	48.0±14.7	0.032	52.4±13.1	52.8±14.8	0.875
SBP	139(24.0)	135(34)	0.02	131(23.5)	129(9.0)	0.14
DBP	76(20)	79(19)	0.14	80(20)	71(21)	0.7

Changes in ejection fraction

In the stunning group there was a significant mean reduction in LVEF whilst

LVEF was maintained in the non-stunning group (Table 7-4).

Table 7-5 Significant Univariate Correlations to ΔGLSR. P values use Pearson's correlation coefficient for normally distributed variables or Spearman rank correlation for non-normally distributed variables.

	r	P-value
NT-ProBNP	-0.53	<0.001
Troponin-T*	-0.338	0.011
ECW/TBW	-0.305	0.042
Pre-HD GLSR	-0.317	0.021
Pre-HD GLS	-0.288	0.038

Troponin-T

hsTnT was highly correlated to several markers of cardiovascular stress or

factors implicated in accelerated cardiovascular disease (Table 7-6). There

was a strong correlation to hypervolemia as measured by ECW/TBW (r=0.71,

p<0.001) as well as to NT-proBNP (r=0.53, p<0.001). Left ventricular

hypertrophy (LVMI r=0.464, p<0.001) and arterial stiffness by PWV (r=0.379, p=0.006). Skin AF, a measure of advanced glycation end-products implicated in causing arterial stiffness was also well correlated (r=0.502, p<0.008). Interestingly, hsTnt was not only significantly related to baseline strain and strain rate but also the change in strain during HD (Table 7-6). Hence, hsTnT was higher in the stunning group (46±51 vs 14±35ng/ml, p=0.011, Figure 7-2).

Table 7-6 Significant Univariate Correlations to Troponin-T. P values use Pearson's correlation for normally distributed variables or Spearman rank correlation for non-normally distributed data.

	r	P-value
ECW/TBW	0.714	<0.001
NT-ProBNP	0.53	<0.001
Skin AF	0.502	0.008
LVEF	-0.473	0.001
LVMI	0.464	0.001
Pre-HD GLS	0.401	0.003
PWV	0.379	0.006
Pre-HD GLSR	0.358	0.009
Age	0.334	0.012

Figure 7-2 Troponin-T between study groups where HD-induced stunning was defined as a reduction in global longitudinal strain rate (GLSR). Median±IQR shown. P values use Mann-Whitney test
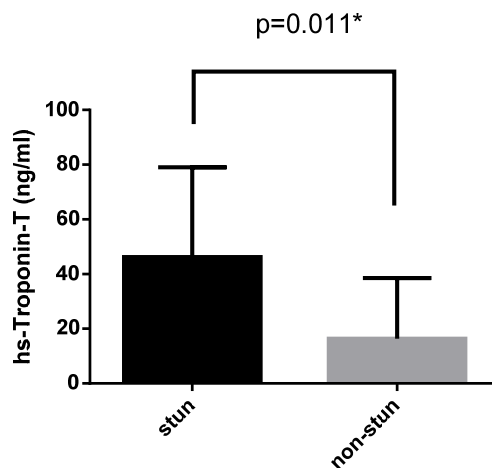
NT-proBNP

BNP was highly correlated to both baseline (GLSR) and HD-induced changes in strain rate (ΔGLSR) as seen in Table 7-7 . There were also good correlations to bioimpedance markers of hypervolemia and LVEDVI. BNP was also higher with lower LVEF or ΔGLS but the correlation did not reach statistical significance. BNP was significantly higher in the stunning group (324±751 vs 74±135 pmol/ml, p<0.001) as depicted in Figure 7-3. In binary logistic regression analysis BNP remained the only independent determinant of myocardial stunning (Nagelkerke adjusted R^2=0.342, p<0.0001; Odds ratio for 100pmol/l increase 1.766, 95% CI 1.099-2.839, p=0.019).

Table 7-7 Significant Univariate Correlations to NT-ProBNP. P values use Spearman rank correlation coefficient.

	r	P-value
ECW/TBW	0.472	0.001
LVEDVI	0.48	0.001
Pre-HD GLSR	0.369	0.007
ΔGLSR	0.48	<0.001

Figure 7-3 Median±IQR of NT-proBNP between stunning and non-stunning groups defined by reductions in global longitudinal strain rate. P values use Mann-Whitney test
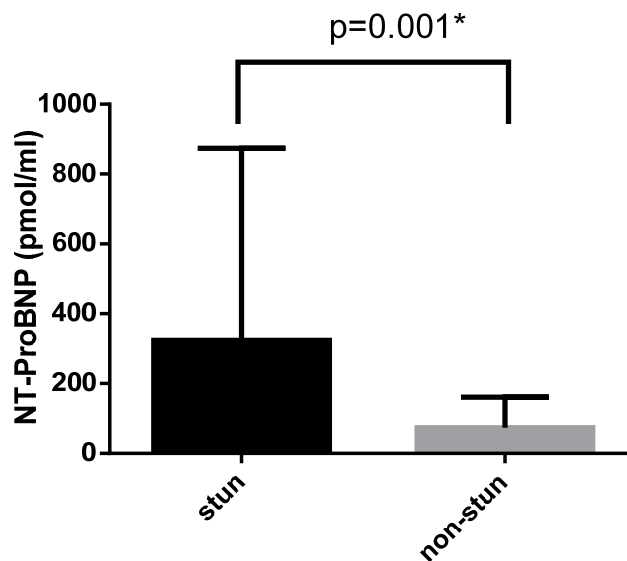
Intradialytic hypotension

At least 1 episode of IDH was detected in 31% (18/58) of patients. The number of IDH episodes correlated with higher levels of hsTnT (r=0.487, p<0.005). IDH was categorised for severity by tertiles of the number of episodes; stage 1, ≤ 5; stage 2, 6-15; stage 3, >15. Ordinal regression analysis was performed to examine predictors of IDH. Factors assessed one-by-one were age, sex, history of ischaemic heart disease, smoking status, diabetes status, ultrafiltration volume, body composition by bioimpedance, NT-proBNP and endotoxin. hsTnT concentration was the only significant predictor of stage of IDH (Nagelkerke adjusted R^2=0.132, p=0.029; Odds ratio for 10μg/l increase 1.138, 95% CI 1.013-1.276, p=0.038).

Figure 7-4 **Segmental strain curves for a typical patient Upper row are Pre-HD and Peak-HD longitudinal strain, lower row is pre-HDand peak-HD longitudinal strain rate. The 2 and 4 chamber views are divided into 6 segments to determine 12 segments of an 18 segment model of the left ventricle. In this example note that both the magnitude od the peak strain as well as the degree of LV dyssynchrony worsen at peak-HD compared to pre-HD. NOte laso that the peak strain rate is relatively unchaged in magnitude but worsens in the degree of dyssynchrony at peak-HD. In both curves the apical and mid-lateral walls (dark blue and pink lines) are particularly affected.**
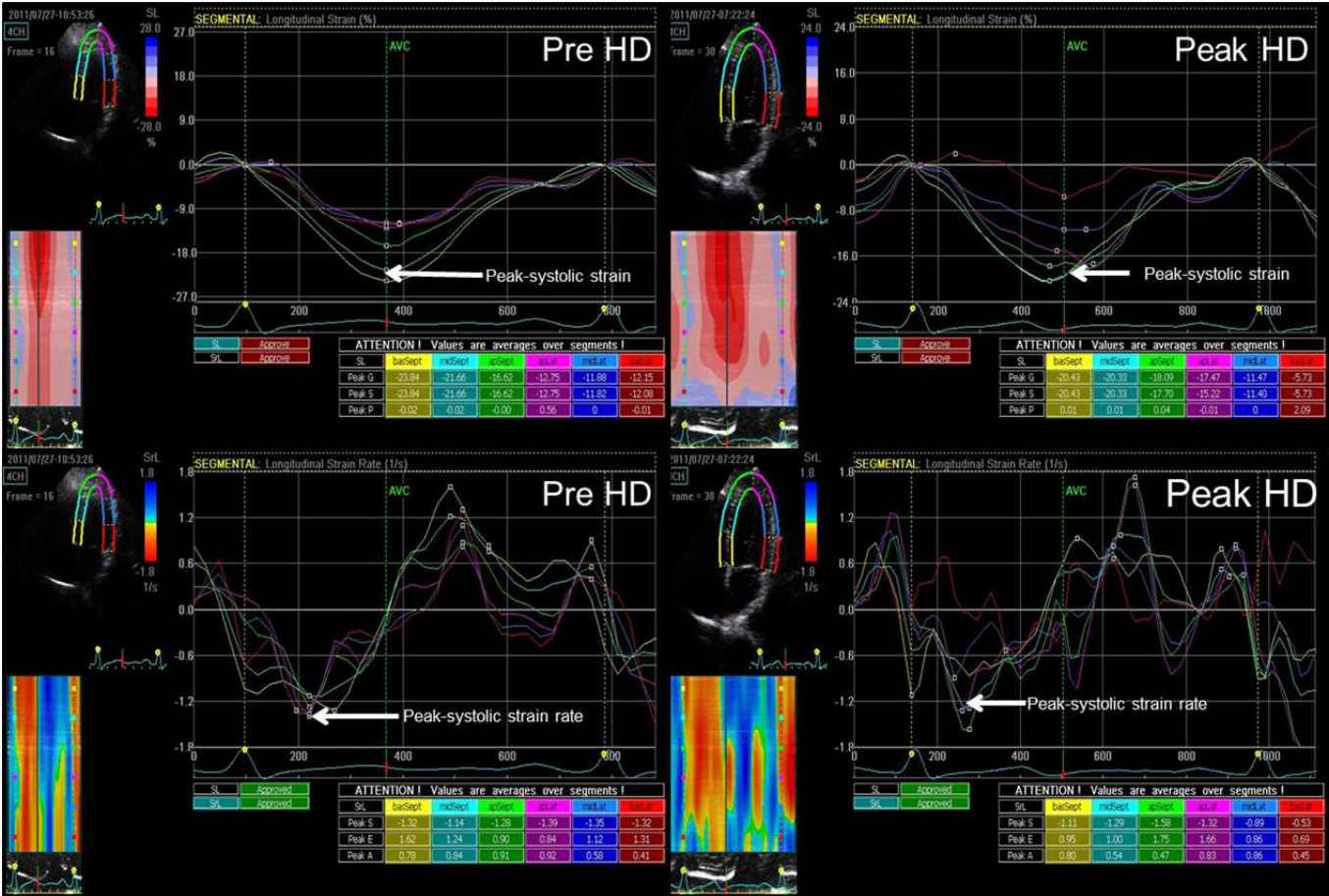
7.5. Discussion

In this study we examined the ability of strain-based imaging using STE to detect HD-induced myocardial stunning and the associations of strain and strain rate changes during HD to cardiac biomarkers and haemodynamic changes associated with ischemia. We also wished to determine prevalence of HD-induced stunning in an incident population. The main findings of the study were:

1) We were able to dichotomise patients by a strain-based response to HD, 70% of patients decreased strain rate during HD and 30% increase strain rate during HD.

2) The size of the response appeared to be well correlated with other markers of ventricular distress and hypervolemia, supporting a relation to contractile reserve.

3) The response was also well correlated to known risk factors for myocardial ischemia.

4) The proportion of patients with HD-induced stunning in this incident population was within the range of previously reported prevalent HD patients.

This study supports and augments previous data on HD-induced stunning and also extends data on the utility of strain-based imaging in HD patients.

Rationale for a strain-based definition of HD-induced myocardial ischemia

The rationale that a strain-based definition is at least non-inferior to wall motion analysis for detection of HD-induced myocardial ischemia is well supported by recently published data in non-dialysis settings. In a cohort of 30 patients with suspected IHD, Leitman et al demonstrated a graded

decrease in GLS between visually scored normal, hypokinetic and akinetic segments (GLS -13.4%±4.9 in normal, -10.5%±4.5 if hypokinetic, -6.2%±3.6 if akinetic, P<0.000001) [204]. Becker et al showed in 62 patients that radial and circumferential systolic strain and strain rate by 2D echocardiography could identify RWMAs well compared with RWMAs by cardiac magnetic resonance [205]. Liel-Cohen et al recently conducted a single centre study in 105 patients, 90 admitted with chest pain and 15 with known dilated cardiomyopathy [206]. The ability of an automated score determined using GLS by STE was compared to the ability of 12 expert echocardiographers to visually determine RWMAs blinded to patient details. Automatic quantification using GLS with pre-determined cut-offs performed as well as visual analysis by the echocardiographers, with a greater reliability and similar agreement to angiographic findings [206]. This demonstrated the potential to use 2D strain to assist less experienced echocardiographers in identifying regional dysfunction. Yu et al performed dobutamine stress echocardiography (DSE) in 34 patients with angiographically-proven multivessel CAD and compared to 42 non-CAD controls with preserved LVEF and previously negative DSE [391]. The control group had a relative increase of around 10% in GLS (-17.6±3.1% to -19.4±3.2%) compared to less than 1% in the CAD group (-15.28±2.4% to -15.41±3.5%, p<0.001). There was a 25% increase in peak strain rate under stress in controls (-0.95±0.19s^{-1} to -1.19±0.24^{s-1}) compared to a 9% increase in CAD patients (-0.83s^{-1} to -0.91s^{-1}, p<0.001). No significant changes were demonstrated for circumferential strains. Multivariate analysis showed that ΔGLSR (odds ratio (OR), 1.63; 95 % CI, 1.12–2.82) was an independent predictor for the detection of multivessel

CAD [391]. This independence remained significant after adjustments for age, sex, heart rate, blood pressure, LVEF and WMSI. By crude comparison, our study showed 11% decrease in strain rate and 12% decrease in strain amongst the stunning group with a 25% increase in strain rate and 3% increase in strain in the non-stunning group (). Strain by STE under dobutamine stress has also been used to differentiate subendocardial from transmural ischemia to determine viability and contractile reserve. Chan et al demonstrated reduced contractile reserve by strain rate with dobutamine infusion localised to segments with transmural scars by contrast-enhanced CMR, outperforming RWMA analysis [392]. Delgado et al used strain by STE to study 222 consecutive patients with IHD (including 99 with acute ST-segment elevation MI,STEMI) and 123 patients with ischaemic cardiomyopathy and 20 age-matched controls [393]. Average values for the entire group were 11.1±4.8% for GLS and 37±14% for LVEF. For the overall study population GLS was highly correlated to LVEF (r = 0.83; P <001) but the correlation was less strong in patients with STEMI or heart failure (r=0.42 and r=0.62, both P<001). This compares to our correlation of GLS to LVEF (r=0.48, p=0.001). These data support that STE derived strain reflects different aspects of systolic left ventricular function, performing as well if not better than visual wall motion analysis.

There are obviously significant differences between our study and these. The studies were not in the setting of HD, coronary artery status of subjects was known and there was pre-selection of candidates altering diagnostic accuracy. Therefore the data and derived cut-offs cannot be directly

translated in the HD setting. However it serves as proof-of-principle to emphasise that patients with myocardial ischemia have both lower baseline strain and strain rate as well as a blunted or absent increase in strain and strain rate when myocardial oxygen demand is increased. Indeed, there are case reports suggesting the magnitude of perfusion-imaging proven ischemia induced by the stress of HD is greater than that induced by pharmacological stress [85].

Relations of strain to ischemia and hypervolemia in the present study

There were strong correlations of both resting GLS and GLSR and ΔGLSR across dialysis to risk factors for and markers of ventricular distress and hypervolemia. Previous data supports that increased arterial stiffness lowers coronary flow reserve by causing pulse waves to arrive in diastole [105]. Data also supports that in addition to vascular calcification, several uraemic factors such as increase endogenous inhibitors of nitric oxide production and increased AGE deposition, promote arterial stiffness. To that end these data reflect the literature in showing a correlation of greater arterial stiffness by PWV (r=0.37) and higher AGE deposition by skin autofluorescence (r=0.6) to both lower baseline strain and strain rate () [213]. Breidthardt et al showed recently that Troponin-T reflected the presence and severity of HD-induced stunning [394]. We also demonstrated a good correlation to ΔGLSR and demonstrated a significant difference between patients with or without myocardial stunning using a newer high-sensitivity assay.

Prior data on strain-based changes in HD patients

There have recently been a number of studies using STE in a HD setting [342, 395-397]. However they are mostly distinct from the present in that they have compared HD patients on inter-dialytic days to normal or CKD controls, broadly showing lower levels of baseline strain or strain rate in the HD patients. Of note these studies do reflect our data in showing correlations of lower strain to higher LV mass or arterial stiffness [396]. Few studies have performed strain-based imaging during HD. Hayashi et al used a Doppler based tissue velocity imaging before and after HD in 13 stable HD patients [181]. They showed increased peak systolic tissue velocities and strain rate after HD compared to before with no change in LVEF or shortening fractions. They concluded that systolic function improved during HD but diastolic function did not and explained their results in terms of load dependency or removal of uraemic factors enhancing contractility. Although methodologies are different their finding that strain rate increases reflects that seen in 25% (18/60) of patients in the present study. We propose that an increased strain rate across dialysis more likely reflects normal contractile reserve and not enhanced contractile function. The decreased strain rate seen in the majority of our patients supports that HD induces ischemia in those with limited contractile reserve and that factors such as increased arterial stiffness, higher left ventricular mass and hypervolemia are pre-disposing factors.

Prevalence of HD-induced stunning

We estimated that proportion of HD induced stunning was 60% which is within the range of the reported prevalence of 27-91% in prior studies of

prevalent HD populations [287, 311, 386, 398]. Assa et el recently reported HD induced stunning detected by WMSI in a population with median dialysis vintage of 21 months [386]. 105 patients completed the study. 27% of patients showed stunning during HD using a definition of an increase in wall motion score at any of three time points during and after HD compared to baseline in more than 2 of 16 LV segments. Stunning was higher in those with higher baseline WMSI and 1 year follow up showed a graded increase in mortality by the number of stunned segments. This is reflected in our study where lower resting GLS was associated with reduction in strain rate. In addition, we demonstrated significant univariate correlations to pre-dialysis Troponin T, BNP, PWV and hypervolemia. These biomarkers independently predict high mortality and development of heart failure. It is noteworthy that Assa et al also demonstrated that stunning was higher with higher LV mass. We demonstrated a trend towards stunning with higher LV mass and found that baseline strain rate was well correlated to LV mass (r=0.536, p<0.001). LV mass was also well correlated to Troponin-T supporting that myocyte-capillary mismatch induced by LVH increases the risk of HD-induced ischemia as shown in experimental studies [399]. Burton et al reported prevalence of HD-induced stunning of 66% in 70 patients with median vintage of 45 months using a similar definition of increased LV radial wall motion score in more than 2 of 10 segments using semi-automated software [286]. The most pertinent difference between these prior studies is that our population was incident with a median vintage of 6 months. This may have a substantial effect as prevalent studies may lead to a survivor bias. The definition of stunning is also significantly different. We used mean change in

longitudinal deformation averaged over 12 segments as opposed to a segmental scoring index. The differences in definition, along with the different HD vintage and burden of co-morbidity may account for the reported differences.

7.6.   Strengths and Limitations

There are a number of limitations to this study. Firstly, we did not know the coronary artery disease status of our population and cannot correlate HD induced strain abnormalities to angiographic findings. However we would propose that a reduction in strain or strain-rate in response to HD-induced stress suggests impaired contractile reserve which can occur in the presence or absence of functionally significant coronary artery stenoses. Future studies should address the proportion of contribution of coronary artery disease. Secondly, we used an arbitrary definition of HD-induced stunning which has not been validated by perfusion imaging. It is possible that the cut-offs will alter diagnostic accuracy for stunning and the data requires validation. Further it is a cross-sectional study and although we have inferred relationships, neither causality nor direction of cause can be determined. Finally we did not assess diastolic dysfunction. The lower frame rate of STE compared to Doppler-base imaging makes diastolic indices less reliable and there is a lack of consensus on the most robust diastolic indices. However diastolic indices are by their nature load-independent and may provide valuable insights into characterising the haemodynamic response to HD.

The strengths of the study are in the comprehensive nature of the assessment being the first study to report HD-related echocardiographic

changes with independently measured biomarkers, arterial stiffness, skin autofluorescence and volume status by bioimpedance. We are the first to determine HD-induced stunning by strain rate or report STE data at two time points in incident HD patients. We are also the first to relate contractile reserve by strain rate change to be limited by arterial stiffness, higher LV mass and to be associated with higher BNP and troponin T.

7.7. Conclusion

In summary we were able to dichotomise patients by a strain-based response to HD, 70% (42/60) of patients decreased strain rate during HD and 30% (18/60) increased strain rate. A decreased change in strain rate across HD was associated with higher BNP, troponin-T, arterial stiffness and hypervolemia. Further studies are required to determine if a strain-based definition of HD-induced myocardial stunning can replace current methods.

Discussion

8. Discussion

8.1. Main findings

In Study I we aimed to study cardiac abnormalities in an unselected incident HD population using strain by CMR tagging as a more sensitive marker of dysfunction. We identified reduced circumferential strain in addition to abnormalities in ejection fraction and mass in the majority of incident HD patients. Strain remained reduced in the subset of patients with normal ejection fraction. The independent determinants of strain were ejection fraction and left ventricular geometry.

In Study II we aimed to investigate the contribution of uraemia to arterial stiffness by directly measuring aortic distensibility using cardiac magnetic resonance. There was a clear increase in directly-measured aortic stiffness between HD patients and age-matched controls despite similar blood pressure. Aortic stiffness increased with age and with greater degrees of ventricular hypertrophy, lower ejection fraction and lower circumferential strain. Aortic stiffness also was also inversely correlated to biomarkers of myocardial ischaemia. Age, dialysis status and diabetes were the independent determinants.

In the final study we used strain by speckle tracking echocardiography to detect HD-induced myocardial ischemia in a population new to HD. 70% of patients decreased strain rate during HD whilst 30% had increased strain rate. A decreased strain rate across HD was associated with markers of

hypervolaemia, ischaemia, stiffness and ventricular stress, suggesting that ischemia was the cause of observed reductions in strain. Further studies are required to determine if a strain-based definition of HD-induced myocardial ischemia can replace current methods.

8.2.   Main limitations

The study limitations were outlined in the chapters but the main overall limitation is the lack of a CKD-control group. As the HD population was relatively new to HD (median 6 months) many of the observed structural and functional abnormalities will have occurred in early or late stage CKD and an age-matched CKD control group might have allowed more insights into natural history. However it is planned to follow this cohort with CMR at 1 year as part of the dialysate cooling trial and this will allow greater insights without the problems of achieving adequate matching. Another limitation was the heterogeneity in the HD patients. For example ejection fraction ranged from 20-80%. This sometimes limited the ability to see subclinical abnormalities. We performed subgroup analyses where possible to overcome this. It is an important principle to conduct studies which do not preselect the population but there are inherent problems. Both the speckle tracking and CMR tagging analyses were limited by not examining diastole.   The CMR tagging technique used is prone to fading in diastole and this also led to noise in the strain curves. This reduces data resolution and the ability to determine between group differences.

8.3. Future work

This thesis contributes to our understanding of haemodialysis-associated cardiomyopathy. The most pertinent future work is longitudinal follow-up of the present cohort to give a rare insight into the development of cardiomyopathy and whether cooler dialysate prevents the expected decline in left ventricular function. Future work should focus on novel interventions to reduce cardiovascular disease and studies with higher resolution to determine difference.

A huge number of interventions remain untested. Many are being pursued by Prof McIntyre's group and collaborators worldwide. An incomplete list would include remote-preconditioning to protect against HD-induced ischemia. Pre-conditioning mimetics may be able to pharmacologically produce the same effect. Interventional studies to lower dialysate sodium or improve glycaemic control to reduce hypervolaemia have commenced. Arrhythmogenic risk due to ionic fluxes both during and between HD are a 'black box' that remains to be fully elucidated. 3D echocardiography and speckle-tracking allows bedside echocardiography without geometric assumptions. Less known are improvements in automated function imaging allowing on-line and more accurate measurements by echocardiography. Advances in harmonic imaging allow better image resolution, essential for strain-based studies. Most exciting are the developments in non-contrast magnetic resonance. MRI is truly capable of going beyond imaging anatomy to interrogate aspects of function. Most importantly for the setting of kidney disease, these techniques do not require contrast media. CMR tagging at higher fields or using novel sequences to allow better spatial and temporal resolution would

be of great benefit. Studies combining renal and cardiac arterial spin-labelling to determine the heart and kidney interaction are an obvious target. This could be extended to study the effects of several drugs on cardiac and renal perfusion, particularly renin-aldosterone-angiotensin-system antagonists. These drugs which have proven cardiac benefits but are underused in CKD and ESRD because of perceived risks to glomerular filtration, require detailed studies which would have wide clinical impact. CMR angiography is developing rapidly and will allow studies to unselectively determine coronary artery status and combine it with perfusion and oxygenation data from a single examination. There are cautions. Healthcare costs are rising and healthcare payers are wary of 'test layering'. Patients rarely have one test. A developmental framework must be followed to show that newer but more expensive techniques have real utility and can be used to improve outcomes. Used judiciously, cardiac imaging remains one of the key tools we have to improve outcomes most quickly in our patients by enabling clinical trials to be conducted in fewer people with faster results and mechanisms elucidated.

Conclusion

9. Conclusion

In summary the work presented in this thesis has identified abnormalities in cardiac structure, motion and deformation in haemodialysis patients using strain-based imaging. The remaining challenge is to evolve the interpretation of the results particularly with respect to time on dialysis that will allow better use of the data in the amelioration of cardiac disease in haemodialysis patients.

References

10.   References

1.   **Chronic Kidney Disease: Early identification and management of chronic kidney disease in adults in primary and secondary care**. In. Edited by Health Do; 2008.

2.   Evans PD, Taal MW: **Epidemiology and causes of chronic kidney disease**. *Medicine* 2011, **39**(7):402-406.

3.   Stevens PE, O'Donoghue DJ, de Lusignan S, Van Vlymen J, Klebe B, Middleton R, Hague N, New J, Farmer CK: **Chronic kidney disease management in the United Kingdom: NEOERICA project results**. *Kidney Int* 2007, **72**(1):92-99.

4.   de Lusignan S, Chan T, Stevens P, O'Donoghue D, Hague N, Dzregah B, Van Vlymen J, Walker M, Hilton S: **Identifying patients with chronic kidney disease from general practice computer records**. *Fam Pract* 2005, **22**(3):234-241.

5.   Gonzalez ELM, Johansson S, Wallander MA, Rodriguez LAG: **Trends in the prevalence and incidence of diabetes in the UK: 1996-2005**. *J Epidemiol Community Health* 2009, **63**(4):332-336.

6.   Coresh J, Selvin E, Stevens LA, Manzi J, Kusek JW, Eggers P, Van Lente F, Levey AS: **Prevalence of chronic kidney disease in the United States**. *Jama* 2007, **298**(17):2038-2047.

7.   Ansell D, Feehally, J., Tomson, C., Williams, A.J., Warwick, G.: **11th UK Renal Registry Report** In. Bristol, UK; 2009.

8.   Keith DS, Nichols GA, Gullion CM, Brown JB, Smith DH: **Longitudinal follow-up and outcomes among a population with chronic kidney**

disease in a large managed care organization. *Arch Intern Med* 2004, **164**(6):659-663.

9.   Menon V, Gul A, Sarnak MJ: **Cardiovascular risk factors in chronic kidney disease**. *Kidney Int* 2005, **68**(4):1413-1418.

10.   Castledine C, Casula A, Fogarty D: **Chapter 2 UK RRT Prevalence in 2010: National and Centre-Specific Analyses**. *Nephron Clin Pract* 2012, **120 Suppl 1**:c29-54.

11.   Foley RN, Parfrey PS, Sarnak MJ: **Epidemiology of cardiovascular disease in chronic renal disease**. *J Am Soc Nephrol* 1998, **9**(12 Suppl):S16-23.

12.   Villar E, Remontet L, Labeeuw M, Ecochard R, Rhone-Alpes obotARdNd, Epidemiology tFR, Information Network Registry: **Effect of Age, Gender, and Diabetes on Excess Death in End-Stage Renal Failure**. *J Am Soc Nephrol* 2007, **18**(7):2125-2134.

13.   Kalantar-Zadeh K, Block G, Humphreys MH, Kopple JD: **Reverse epidemiology of cardiovascular risk factors in maintenance dialysis patients**. *Kidney Int* 2003, **63**(3):793-808.

14.   (USRDS) URDS: **Annual Data Report: Atlas of Chronic Kidney Disease and End-Stage Renal Disease in the United States**. In. Bethesda, MD: National Institute of Diabetes and Digestive and Kidney Diseases; 2011.

15.   Matsushita K, van der Velde M, Astor BC, Woodward M, Levey AS, de Jong PE, Coresh J, Gansevoort RT: **Association of estimated glomerular filtration rate and albuminuria with all-cause and cardiovascular mortality in general population cohorts: a collaborative meta-analysis**. *Lancet* 2010, **375**(9731):2073-2081.

16.	Shah DS, Polkinghorne KR, Pellicano R, Kerr PG: **Are traditional risk factors valid for assessing cardiovascular risk in end-stage renal failure patients?** *Nephrology* 2008, **13**(8):667-671.

17.	**Prospective Studies Collaboration. Age-specific relevance of usual blood pressure to vascular mortality: a meta-analysis of individual data for one million adults in 61 prospective studies**. *The Lancet* 2002, **360**(9349):1903-1913.

18.	Foley RN, Parfrey PS, Harnett JD, Kent GM, Murray DC, Barre PE: **Impact of hypertension on cardiomyopathy, morbidity and mortality in end-stage renal disease**. *Kidney Int* 1996, **49**(5):1379-1385.

19.	Lucas MF, Quereda C, Teruel JL, Orte L, Marcen R, Ortuno J: **Effect of hypertension before beginning dialysis on survival of hemodialysis patients**. *Am J Kidney Dis* 2003, **41**(4):814-821.

20.	Kalantar-Zadeh K, Kilpatrick RD, McAllister CJ, Greenland S, Kopple JD: **Reverse epidemiology of hypertension and cardiovascular death in the hemodialysis population: the 58th annual fall conference and scientific sessions**. *Hypertension* 2005, **45**(4):811-817.

21.	Chien CC, Yen CS, Wang JJ, Chen HA, Chou MT, Chu CC, Chio CC, Hwang JC, Wang HY, Lu YH *et al*: **Reverse epidemiology of hypertension-mortality associations in hemodialysis patients: A long-term population-based study**. *American Journal of Hypertension* 2012, **25**(8):900-906.

22.	Agarwal R, Sinha AD: **Cardiovascular Protection With Antihypertensive Drugs in Dialysis Patients**. *Hypertension* 2009, **53**(5):860-866.

23.   Goldsmith D, Covic A: **Blood pressure control in CKD stage 5D patients—are we more or less certain what to do in 2009?** *Nephrology Dialysis Transplantation* 2009, **24**(12):3597-3601.

24.   Messerli FH, Panjrath GS: **The J-Curve Between Blood Pressure and Coronary Artery Disease or Essential HypertensionExactly How Essential?** *Journal of the American College of Cardiology* 2009, **54**(20):1827-1834.

25.   Konings C, Kooman J, Schonck M, Dammers R, Cheriex E, Palmans Meulemans A, Hoeks A, van Kreel B, Gladziwa U, van der Sande F *et al*: **Fluid status, blood pressure, and cardiovascular abnormalities in patients on peritoneal dialysis**. *Peritoneal Dialysis International* 2002, **22**(4):477-487.

26.   Kalantar-Zadeh K, Regidor DL, Kovesdy CP, Van Wyck D, Bunnapradist S, Horwich TB, Fonarow GC: **Fluid Retention Is Associated With Cardiovascular Mortality in Patients Undergoing Long-Term Hemodialysis**. *Circulation* 2009, **119**:671-679.

27.   Sinha AD, Light RP, Agarwal R: **Relative Plasma Volume Monitoring During Hemodialysis Aids the Assessment of Dry Weight**. *Hypertension* 2010, **55**(2):305-311.

28.   Agarwal R, Weir MR: **Dry-weight: a concept revisited in an effort to avoid medication-directed approaches for blood pressure control in hemodialysis patients**. *Clin J Am Soc Nephrol* 2010, **5**(7):1255-1260.

29.   Chan C, McIntyre C, Smith D, Spanel P, Davies SJ: **Combining Near-Subject Absolute and Relative Measures of Longitudinal Hydration in**

Hemodialysis. *Clinical Journal of the American Society of Nephrology* 2009, **4**(11):1791-1798.

30.   Chamney PW, Wabel P, Moissl UM, Muller MJ, Bosy-Westphal A, Korth O, Fuller NJ: **A whole-body model to distinguish excess fluid from the hydration of major body tissues**. *The American journal of clinical nutrition* 2007, **85**(1):80-89.

31.   Wizemann V, Wabel P, Chamney P, Zaluska W, Moissl U, Rode C, Malecka-Masalska T, Marcelli D: **The mortality risk of overhydration in haemodialysis patients**. *Nephrology Dialysis Transplantation* 2009, **24**(5):1574-1579.

32.   Machek P, Jirka T, Moissl U, Chamney P, Wabel P: **Guided optimization of fluid status in haemodialysis patients**. *Nephrology Dialysis Transplantation* 2010, **25**(2):538-544.

33.   Wabel P, Moissl U, Chamney P, Jirka T, Machek P, Ponce P, Taborsky P, Tetta C, Velasco N, Vlasak J *et al*: **Towards improved cardiovascular management: the necessity of combining blood pressure and fluid overload**. *Nephrology Dialysis Transplantation* 2008, **23**(9):2965-2971.

34.   Van Biesen W, Williams JD, Covic AC, Fan S, Claes K, Lichodziejewska-Niemierko M, Verger C, Steiger J, Schoder V, Wabel P *et al*: **Fluid Status in Peritoneal Dialysis Patients: The European Body Composition Monitoring (EuroBCM) Study Cohort**. *PloS one* 2011, **6**(2).

35.   Doulton TW, MacGregor GA: **Review: Blood pressure in haemodialysis patients: The importance of the relationship between the**

renin-angiotensin-aldosterone system, salt intake and extracellular volume. *Journal of Renin-Angiotensin-Aldosterone System* 2004, **5**(1):14-22.

36.   Blacher J, Guerin AP, Pannier B, Marchais SJ, Safar ME, London GM: **Impact of aortic stiffness on survival in end-stage renal disease**. *Circulation* 1999, **99**(18):2434-2439.

37.   Sigrist MK, Taal MW, Bungay P, McIntyre CW: **Progressive vascular calcification over 2 years is associated with arterial stiffening and increased mortality in patients with stages 4 and 5 chronic kidney disease**. *Clin J Am Soc Nephrol* 2007, **2**(6):1241-1248.

38.   Meerwaldt R, Hartog JWL, Graaff R, Huisman RJ, Links TP, den Hollander NC, Thorpe SR, Baynes JW, Navis G, Gans ROB *et al*: **Skin Autofluorescence, a Measure of Cumulative Metabolic Stress and Advanced Glycation End Products, Predicts Mortality in Hemodialysis Patients**. *Journal of the American Society of Nephrology* 2005, **16**(12):3687-3693.

39.   Charra B, Bergstrom J, Scribner BH: **Blood pressure control in dialysis patients: importance of the lag phenomenon**. *Am J Kidney Dis* 1998, **32**(5):720-724.

40.   Titze J: **Water-Free Na+ Retention: Interaction with Hypertension and Tissue Hydration**. *Blood purification* 2008, **26**(1):95-99.

41.   Oberleithner H, Kusche-Vihrog K, Schillers H: **Endothelial cells as vascular salt sensors**. *Kidney Int* 2010, **77**(6):490-494.

42.   Shaldon S, Vienken J: **The long forgotten salt factor and the benefits of using a 5-g-salt-restricted diet in all ESRD patients**. *Nephrology Dialysis Transplantation* 2008, **23**(7):2118-2120.

43.   Ramdeen G, Tzamaloukas AH, Malhotra D, Leger A, Murata GH: **Estimates of interdialytic sodium and water intake based on the balance principle: differences between nondiabetic and diabetic subjects on hemodialysis**. *ASAIO J* 1998, **44**(6):812-817.

44.   Muniyappa R, Montagnani M, Koh KK, Quon MJ: **Cardiovascular actions of insulin**. *Endocr Rev* 2007, **28**(5):463-491.

45.   Selby NM, Fialova J, Burton JO, McIntyre CW: **The haemodynamic and metabolic effects of hypertonic-glucose and amino-acid-based peritoneal dialysis fluids**. *Nephrol Dial Transplant* 2007, **22**(3):870-879.

46.   Günal AI, Duman S, Özkahya M, Töz H, Asçi G, Akçiçek F, Basçi A: **Strict volume control normalizes hypertension in peritoneal dialysis patients**. *Am J Kidney Dis* 2001, **37**(3):588-593.

47.   Charalambous BM, Stephens RC, Feavers IM, Montgomery HE: **Role of bacterial endotoxin in chronic heart failure: the gut of the matter**. *Shock* 2007, **28**(1):15-23.

48.   McIntyre CW, Harrison LE, Eldehni MT, Jefferies HJ, Szeto CC, John SG, Sigrist MK, Burton JO, Hothi D, Korsheed S *et al*: **Circulating endotoxemia: a novel factor in systemic inflammation and cardiovascular disease in chronic kidney disease**. *Clin J Am Soc Nephrol* 2011, **6**(1):133-141.

49.   Eldehni MT, McIntyre CW: **Does haemodialysis result in brain injury?** *Seminars in Dialysis* 2011, **In press**.

50.   Parfrey PS, Foley RN, Harnett JD, Kent GM, Murray D, Barre PE: **Outcome and risk factors of ischemic heart disease in chronic uremia**. *Kidney Int* 1996, **49**(5):1428-1434.

51.   Glassock RJ, Pecoits-Filho R, Barberato SH: **Left Ventricular Mass in Chronic Kidney Disease and ESRD**. *Clinical Journal of the American Society of Nephrology* 2009, **4**(Supplement 1):S79-S91.

52.   Stella P, Manunta P, Mallamaci F, Melandri M, Spotti D, Tripepi G, Hamlyn JM, Malatino LS, Bianchi G, Zoccali C: **Endogenous ouabain and cardiomyopathy in dialysis patients**. *Journal of Internal Medicine* 2008, **263**(3):274-280.

53.   Gutierrez OM, Januzzi JL, Isakova T, Laliberte K, Smith K, Collerone G, Sarwar A, Hoffmann U, Coglianese E, Christenson R *et al*: **Fibroblast growth factor 23 and left ventricular hypertrophy in chronic kidney disease**. *Circulation* 2009, **119**(19):2545-2552.

54.   Bagrov AY, Fedorova OV: **Cardenolide and bufadienolide ligands of the sodium pump. How they work together in NaCl sensitive hypertension**. *Frontiers in bioscience : a journal and virtual library* 2005, **10**:2250-2256.

55.   Lewington S, Whitlock G, Clarke R, Sherliker P, Emberson J, Halsey J, Qizilbash N, Peto R, Collins R: **Blood cholesterol and vascular mortality by age, sex, and blood pressure: a meta-analysis of individual data from 61 prospective studies with 55,000 vascular deaths**. *Lancet* 2007, **370**(9602):1829-1839.

56.   Cholesterol Treatment Trialists C: **The effects of lowering LDL cholesterol with statin therapy in people at low risk of vascular disease: meta-analysis of individual data from 27 randomised trials**. *The Lancet*, **380**(9841):581-590.

57.   Ritz E, Wanner C: **Lipid Abnormalities and Cardiovascular Risk in Renal Disease**. *Journal of the American Society of Nephrology* 2008, **19**(6):1065-1070.

58.   Liu Y CJEJA, et al.: **Association between cholesterol level and mortality in dialysis patients: Role of inflammation and malnutrition**. *JAMA: The Journal of the American Medical Association* 2004, **291**(4):451-459.

59.   Wanner C, Krane V, März W, Olschewski M, Mann JFE, Ruf G, Ritz E: **Atorvastatin in Patients with Type 2 Diabetes Mellitus Undergoing Hemodialysis**. *New England Journal of Medicine* 2005, **353**(3):238-248.

60.   Fellstrom BC, Jardine AG, Schmieder RE, Holdaas H, Bannister K, Beutler J, Chae DW, Chevaile A, Cobbe SM, Gronhagen-Riska C *et al*: **Rosuvastatin and cardiovascular events in patients undergoing hemodialysis**. *N Engl J Med* 2009, **360**(14):1395-1407.

61.   Baigent C, Landray MJ, Reith C, Emberson J, Wheeler DC, Tomson C, Wanner C, Krane V, Cass A, Craig J *et al*: **The effects of lowering LDL cholesterol with simvastatin plus ezetimibe in patients with chronic kidney disease (Study of Heart and Renal Protection): a randomised placebo-controlled trial**. *Lancet* 2011, **377**(9784):2181-2192.

62.   Halimi JM, Giraudeau B, Vol S, Caces E, Nivet H, Lebranchu Y, Tichet J: **Effects of current smoking and smoking discontinuation on renal function and proteinuria in the general population**. *Kidney Int* 2000, **58**(3):1285-1292.

63.   LONGENECKER JC, CORESH J, KLAG MJ, LEVEY AS, MARTIN AA, FINK NE, POWE NR, Study FTC: **Validation of Comorbid Conditions**

on the End-Stage Renal Disease Medical Evidence Report. *Journal of the American Society of Nephrology* 2000, **11**(3):520-529.

64. Liebman SE, Lamontagne SP, Huang L-S, Messing S, Bushinsky DA: **Smoking in Dialysis Patients: A Systematic Review and Meta-analysis of Mortality and Cardiovascular Morbidity**. *American Journal of Kidney Diseases* 2011, **58**(2):257-265.

65. Coresh J, Selvin E, Stevens LA, Manzi J, Kusek JW, Eggers P, Van Lente F, Levey AS: **Prevalence of Chronic Kidney Disease in the United States**. *JAMA* 2007, **298**(17):2038-2047.

66. Huang Y, Bi YF, Wang WQ, Xu M, Xu Y, Li MA, Wang TG, Chen YH, Li XY, Ning G: **Glycated Hemoglobin A1c, Fasting Plasma Glucose, and Two-Hour Postchallenge Plasma Glucose Levels in Relation to Carotid Intima-Media Thickness in Chinese with Normal Glucose Tolerance**. *Journal of Clinical Endocrinology & Metabolism* 2011, **96**(9):E1461-E1465.

67. Selvin E CJGSHBFLFARSMW: **Glycemic control and coronary heart disease risk in persons with and without diabetes: The atherosclerosis risk in communities study**. *Archives of Internal Medicine* 2005, **165**(16):1910-1916.

68. Menon V, Greene T, Pereira AA, Wang X, Beck GJ, Kusek JW, Collins AJ, Levey AS, Sarnak MJ: **Glycosylated Hemoglobin and Mortality in Patients with Nondiabetic Chronic Kidney Disease**. *Journal of the American Society of Nephrology* 2005, **16**(11):3411-3417.

69. **U.S. Renal Data System, USRDS 2009 Annual Data Report: Atlas of Chronic Kidney Disease and End-Stage Renal Disease in the United**

States, National Institutes of Health, National Institute of Diabetes and Digestive and Kidney Diseases, Bethesda, MD, 2009.** In.; 2009.

70.   Schroijen M, Dekkers O, Grootendorst D, Noordzij M, Romijn J, Krediet R, Boeschoten E, Dekker F: **Survival in dialysis patients is not different between patients with diabetes as primary renal disease and patients with diabetes as a co-morbid condition**. *BMC Nephrol* 2011, **12**(1):1-7.

71.   Ricks J, Molnar MZ, Kovesdy CP, Shah A, Nissenson AR, Williams M, Kalantar-Zadeh K: **Glycemic Control and Cardiovascular Mortality in Hemodialysis Patients With Diabetes: A 6-Year Cohort Study**. *Diabetes* 2012, **61**(3):708-715.

72.   **The Effect of Intensive Treatment of Diabetes on the Development and Progression of Long-Term Complications in Insulin-Dependent Diabetes Mellitus**. *New England Journal of Medicine* 1993, **329**(14):977-986.

73.   **Intensive blood-glucose control with sulphonylureas or insulin compared with conventional treatment and risk of complications in patients with type 2 diabetes (UKPDS 33)**. *The Lancet* 1998, **352**(9131):837-853.

74.   Inaba M, Okuno S, Kumeda Y, Yamada S, Imanishi Y, Tabata T, Okamura M, Okada S, Yamakawa T, Ishimura E *et al*: **Glycated Albumin Is a Better Glycemic Indicator than Glycated Hemoglobin Values in Hemodialysis Patients with Diabetes: Effect of Anemia and Erythropoietin Injection**. *J Am Soc Nephrol* 2007, **18**(3):896-903.

75.   Kovesdy CP, Sharma K, Kalantar-Zadeh K: **Glycemic control in diabetic CKD patients: Where do we stand?** *American Journal of Kidney Diseases* 2008, **52**(4):766-777.

76.   Kazempour-Ardebili S, Lecamwasam VL, Dassanyake T, Frankel AH, Tam FW, Dornhorst A, Frost G, Turner JJ: **Assessing Glycaemic Control in Maintenance Haemodialysis Patients with Type 2 Diabetes**. *Diabetes Care* 2009.

77.   Riveline JP, Teynie J, Belmouaz S, Franc S, Dardari D, Bauwens M, Caudwell V, Ragot S, Bridoux F, Charpentier G *et al*: **Glycaemic control in type 2 diabetic patients on chronic haemodialysis: use of a continuous glucose monitoring system**. *Nephrology Dialysis Transplantation* 2009, **24**(9):2866-2871.

78.   Monnier L, Mas E, Ginet C, Michel F, Villon L, Cristol J-P, Colette C: **Activation of Oxidative Stress by Acute Glucose Fluctuations Compared With Sustained Chronic Hyperglycemia in Patients With Type 2 Diabetes**. *JAMA* 2006, **295**(14):1681-1687.

79.   Action to Control Cardiovascular Risk in Diabetes Study G, Gerstein HC, Miller ME, Byington RP, Goff DC, Jr., Bigger JT, Buse JB, Cushman WC, Genuth S, Ismail-Beigi F *et al*: **Effects of intensive glucose lowering in type 2 diabetes**. *N Engl J Med* 2008, **358**(24):2545-2559.

80.   Group TAC: **Intensive Blood Glucose Control and Vascular Outcomes in Patients with Type 2 Diabetes**. *New England Journal of Medicine* 2008, **358**(24):2560-2572.

81.   Reaven PD, Moritz TE, Schwenke DC, Anderson RJ, Criqui M, Detrano R, Emanuele N, Kayshap M, Marks J, Mudaliar S *et al*: **Intensive**

glucose-lowering therapy reduces cardiovascular disease events in veterans affairs diabetes trial participants with lower calcified coronary atherosclerosis. *Diabetes* 2009, **58**(11):2642-2648.

82.   Williams ME, Lacson E, Wang W, Lazarus JM, Hakim R: **Glycemic Control and Extended Hemodialysis Survival in Patients with Diabetes Mellitus: Comparative Results of Traditional and Time-Dependent Cox Model Analyses**. *Clinical Journal of the American Society of Nephrology* 2010, **5**(9):1595-1601.

83.   Ohtake T, Kobayashi S, Moriya H, Negishi K, Okamoto K, Maesato K, Saito S: **High prevalence of occult coronary artery stenosis in patients with chronic kidney disease at the initiation of renal replacement therapy: an angiographic examination**. *J Am Soc Nephrol* 2005, **16**(4):1141-1148.

84.   Hayashi T, Obi Y, Kimura T, Iio K-i, Sumitsuji S, Takeda Y, Nagai Y, Imai E: **Cardiac troponin T predicts occult coronary artery stenosis in patients with chronic kidney disease at the start of renal replacement therapy**. *Nephrology Dialysis Transplantation* 2008, **23**(9):2936-2942.

85.   Assa S, Dasselaar JJ, Slart RHJA, de Jong PE, Voors AA, Tio RA, Franssen CFM: **Comparison of Cardiac Positron Emission Tomography Perfusion Defects During Stress Induced by Hemodialysis Versus Adenosine**. *American Journal of Kidney Diseases* 2012, **59**(6):862-864.

86.   Venkataraman R, Hage FG, Dorfman TA, Heo J, Aqel RA, de Mattos AM, Iskandrian AE: **Relation Between Heart Rate Response to Adenosine and Mortality in Patients With End-Stage Renal Disease**. *The American Journal of Cardiology* 2009, **103**(8):1159-1164.

87. Mark PB, Johnston N, Groenning BA, Foster JE, Blyth KG, Martin TN, Steedman T, Dargie HJ, Jardine AG: **Redefinition of uremic cardiomyopathy by contrast-enhanced cardiac magnetic resonance imaging**. *Kidney Int* 2006, **69**(10):1839-1845.

88. Andrade JM, Gowdak LH, Giorgi MC, de Paula FJ, Kalil-Filho R, de Lima JJ, Rochitte CE: **Cardiac MRI for detection of unrecognized myocardial infarction in patients with end-stage renal disease: comparison with ECG and scintigraphy**. *AJR Am J Roentgenol* 2009, **193**(1):W25-32.

89. Roberts WC, Taylor MA, Shirani J: **Cardiac findings at necropsy in patients with chronic kidney disease maintained on chronic hemodialysis**. *Medicine (Baltimore)* 2012, **91**(3):165-178.

90. Herzog CA, Ma JZ, Collins AJ: **Poor Long-Term Survival after Acute Myocardial Infarction among Patients on Long-Term Dialysis**. *New England Journal of Medicine* 1998, **339**(12):799-805.

91. Charytan D, Kuntz RE: **The exclusion of patients with chronic kidney disease from clinical trials in coronary artery disease**. *Kidney Int* 2006, **70**(11):2021-2030.

92. Shroff GR, Frederick PD, Herzog CA: **Renal failure and acute myocardial infarction: clinical characteristics in patients with advanced chronic kidney disease, on dialysis, and without chronic kidney disease. A collaborative project of the United States Renal Data System/National Institutes of Health and the National Registry of Myocardial Infarction**. *Am Heart J* 2012, **163**(3):399-406.

93.   Saltzman AJ, Stone GW, Claessen BE, Narula A, Leon-Reyes S, Weisz G, Brodie B, Witzenbichler B, Guagliumi G, Kornowski R *et al*: **Long-Term Impact of Chronic Kidney Disease in Patients With ST-Segment Elevation Myocardial Infarction Treated With Primary Percutaneous Coronary Intervention: The HORIZONS-AMI (Harmonizing Outcomes With Revascularization and Stents in Acute Myocardial Infarction) Trial**. *JACC: Cardiovascular Interventions* 2011, **4**(9):1011-1019.

94.   Herzog CA, Ma JZ, Collins AJ: **Long-term outcome of dialysis patients in the United States with coronary revascularization procedures**. *Kidney Int* 1999, **56**(1):324-332.

95.   Hemmelgarn BR, Southern D, Culleton BF, Mitchell LB, Knudtson ML, Ghali WA, Investigators ftAPPfOAiCHD: **Survival After Coronary Revascularization Among Patients With Kidney Disease**. *Circulation* 2004, **110**(14):1890-1895.

96.   Chang TI, Shilane D, Kazi DS, Montez-Rath ME, Hlatky MA, Winkelmayer WC: **Multivessel Coronary Artery Bypass Grafting Versus Percutaneous Coronary Intervention in ESRD**. *Journal of the American Society of Nephrology* 2012, **23**(12):2042-2049.

97.   Boden WE, O'Rourke RA, Teo KK, Hartigan PM, Maron DJ, Kostuk WJ, Knudtson M, Dada M, Casperson P, Harris CL *et al*: **Optimal Medical Therapy with or without PCI for Stable Coronary Disease**. *New England Journal of Medicine* 2007, **356**(15):1503-1516.

98.   Farkouh ME, Domanski M, Sleeper LA, Siami FS, Dangas G, Mack M, Yang M, Cohen DJ, Rosenberg Y, Solomon SD *et al*: **Strategies for**

Multivessel Revascularization in Patients with Diabetes. *New England Journal of Medicine* 2012, **367**(25):2375-2384.

99.   Topol EJ, Nissen SE: **Our Preoccupation With Coronary Luminology: The Dissociation Between Clinical and Angiographic Findings in Ischemic Heart Disease**. *Circulation* 1995, **92**(8):2333-2342.

100.   Tobis JM, Mallery J, Mahon D, Lehmann K, Zalesky P, Griffith J, Gessert J, Moriuchi M, McRae M, Dwyer ML: **Intravascular ultrasound imaging of human coronary arteries in vivo. Analysis of tissue characterizations with comparison to in vitro histological specimens**. *Circulation* 1991, **83**(3):913-926.

101.   HACKETT D, DAVIES G, MASERI A: **Pre-existing coronary stenoses in patients with first myocardial infarction are not necessarily severe**. *European Heart Journal* 1988, **9**(12):1317-1323.

102.   Little WC, Constantinescu M, Applegate RJ, Kutcher MA, Burrows MT, Kahl FR, Santamore WP: **Can coronary angiography predict the site of a subsequent myocardial infarction in patients with mild-to-moderate coronary artery disease?** *Circulation* 1988, **78**(5):1157-1166.

103.   Charytan D, Garg P, Varma M, Garshick M, Jeon C, Mauri L: **Angiographic characteristics of coronary arterial segments progressing to myocardial infarction in patients with and without chronic kidney disease**. *Clin Exp Nephrol* 2012:1-8.

104.   Pijls NH, Fearon WF, Tonino PA, Siebert U, Ikeno F, Bornschein B, van't Veer M, Klauss V, Manoharan G, Engstrom T *et al*: **Fractional flow reserve versus angiography for guiding percutaneous coronary intervention in patients with multivessel coronary artery disease: 2-year**

follow-up of the FAME (Fractional Flow Reserve Versus Angiography for Multivessel Evaluation) study. *J Am Coll Cardiol* 2010, **56**(3):177-184.

105.   Kingwell BA, Waddell TK, Medley TL, Cameron JD, Dart AM: **Large artery stiffness predicts ischemic threshold in patients with coronary artery disease**. *J Am Coll Cardiol* 2002, **40**(4):773-779.

106.   Kaandorp JA: **Fractal modelling : growth and form in biology**. Berlin ; London: Springer-Verlag; 1994.

107.   Amann K, Ritz E: **Microvascular disease--the Cinderella of uraemic heart disease**. *Nephrol Dial Transplant* 2000, **15**(10):1493-1503.

108.   Foley RN, Parfrey PS, Harnett JD, Kent GM, Martin CJ, Murray DC, Barre PE: **Clinical and echocardiographic disease in patients starting end-stage renal disease therapy**. *Kidney Int* 1995, **47**(1):186-192.

109.   Zoccali C, Benedetto FA, Mallamaci F, Tripepi G, Giacone G, Cataliotti A, Seminara G, Stancanelli B, Malatino LS: **Prognostic impact of the indexation of left ventricular mass in patients undergoing dialysis**. *J Am Soc Nephrol* 2001, **12**(12):2768-2774.

110.   Mark PB, Patel RK, Jardine AG: **Are we overestimating left ventricular abnormalities in end-stage renal disease?** *Nephrol Dial Transplant* 2007, **22**(7):1815-1819.

111.   Lang RM, Bierig M, Devereux RB, Flachskampf FA, Foster E, Pellikka PA, Picard MH, Roman MJ, Seward J, Shanewise JS *et al*: **Recommendations for chamber quantification: a report from the American Society of Echocardiography's Guidelines and Standards Committee and the Chamber Quantification Writing Group, developed in conjunction with the European Association of Echocardiography, a**

branch of the European Society of Cardiology. *J Am Soc Echocardiogr* 2005, **18**(12):1440-1463.

112.   Shimizu G, Hirota Y, Kita Y, Kawamura K, Saito T, Gaasch WH: **Left ventricular midwall mechanics in systemic arterial hypertension. Myocardial function is depressed in pressure-overload hypertrophy**. *Circulation* 1991, **83**(5):1676-1684.

113.   Zoccali C, Benedetto FA, Mallamaci F, Tripepi G, Giacone G, Cataliotti A, Seminara G, Stancanelli B, Malatino LS: **Prognostic value of echocardiographic indicators of left ventricular systolic function in asymptomatic dialysis patients**. *J Am Soc Nephrol* 2004, **15**(4):1029-1037.

114.   Zoccali C, Benedetto FA, Tripepi G, Mallamaci F, Rapisarda F, Seminara G, Bonanno G, Malatino LS: **Left ventricular systolic function monitoring in asymptomatic dialysis patients: a prospective cohort study**. *J Am Soc Nephrol* 2006, **17**(5):1460-1465.

115.   Tsang TS, Barnes ME, Gersh BJ, Bailey KR, Seward JB: **Left atrial volume as a morphophysiologic expression of left ventricular diastolic dysfunction and relation to cardiovascular risk burden**. *Am J Cardiol* 2002, **90**(12):1284-1289.

116.   Tsang TS, Barnes ME, Gersh BJ, Takemoto Y, Rosales AG, Bailey KR, Seward JB: **Prediction of risk for first age-related cardiovascular events in an elderly population: the incremental value of echocardiography**. *J Am Coll Cardiol* 2003, **42**(7):1199-1205.

117.   Kizer JR, Bella JN, Palmieri V, Liu JE, Best LG, Lee ET, Roman MJ, Devereux RB: **Left atrial diameter as an independent predictor of first**

clinical cardiovascular events in middle-aged and elderly adults: the Strong Heart Study (SHS). *Am Heart J* 2006, **151**(2):412-418.

118.   Tripepi G, Benedetto FA, Mallamaci F, Tripepi R, Malatino L, Zoccali C: **Left atrial volume in end-stage renal disease: a prospective cohort study**. *J Hypertens* 2006, **24**(6):1173-1180.

119.   Tripepi G, Benedetto FA, Mallamaci F, Tripepi R, Malatino L, Zoccali C: **Left atrial volume monitoring and cardiovascular risk in patients with end-stage renal disease: a prospective cohort study**. *J Am Soc Nephrol* 2007, **18**(4):1316-1322.

120.   Barberato SH, Pecoits-Filho R: **Usefulness of left atrial volume for the differentiation of normal from pseudonormal diastolic function pattern in patients on hemodialysis**. *J Am Soc Echocardiogr* 2007, **20**(4):359-365.

121.   Barberato SH, Misocami M, Pecoits-Filho R: **Association between Left Atrium Enlargement and Intradialytic Hypotension: Role of Diastolic Dysfunction in the Hemodynamic Complications during Hemodialysis**. *Echocardiography* 2009.

122.   Chan MY, Wong H-B, Ong H-Y, Yeo T-C: **Prognostic value of left atrial size in chronic kidney disease**. *Eur J Echocardiogr* 2008, **9**(6):736-740.

123.   Hunold P, Vogt FM, Heemann UW, Zimmermann U, Barkhausen J: **Myocardial mass and volume measurement of hypertrophic left ventricles by MRI--study in dialysis patients examined before and after dialysis**. *J Cardiovasc Magn Reson* 2003, **5**(4):553-561.

124.   Picano E, Lattanzi F, Orlandini A, Marini C, L'Abbate A: **Stress echocardiography and the human factor: the importance of being expert**. *J Am Coll Cardiol* 1991, **17**(3):666-669.

125.   Hung J, Lang R, Flachskampf F, Shernan SK, McCulloch ML, Adams DB, Thomas J, Vannan M, Ryan T: **3D echocardiography: a review of the current status and future directions**. *J Am Soc Echocardiogr* 2007, **20**(3):213-233.

126.   Jacobs LD, Salgo IS, Goonewardena S, Weinert L, Coon P, Bardo D, Gerard O, Allain P, Zamorano JL, de Isla LP *et al*: **Rapid online quantification of left ventricular volume from real-time three-dimensional echocardiographic data**. *Eur Heart J* 2006, **27**(4):460-468.

127.   Caiani EG, Corsi C, Sugeng L, MacEneaney P, Weinert L, Mor-Avi V, Lang RM: **Improved quantification of left ventricular mass based on endocardial and epicardial surface detection with real time three dimensional echocardiography**. *Heart* 2006, **92**(2):213-219.

128.   Jenkins C, Bricknell K, Hanekom L, Marwick TH: **Reproducibility and accuracy of echocardiographic measurements of left ventricular parameters using real-time three-dimensional echocardiography**. *J Am Coll Cardiol* 2004, **44**(4):878-886.

129.   Yap S-C, van Geuns R-JM, Nemes A, Meijboom FJ, McGhie JS, Geleijnse ML, Simoons ML, Roos-Hesselink JW: **Rapid and accurate measurement of LV mass by biplane real-time 3D echocardiography in patients with concentric LV hypertrophy: comparison to CMR**. *Eur J Echocardiogr* 2008, **9**(2):255-260.

130. Krenning BJ, Voormolen MM, Geleijnse ML, van der Steen AFW, ten Cate FJ, Ie EHY, Roelandt JRTC: **Three-Dimensional Echocardiographic Analysis of Left Ventricular Function during Hemodialysis**. *Nephron Clinical Practice* 2007, **107**(2):c43-c49.

131. Koistinen MJ, Huikuri HV, Pirttiaho H, Linnaluoto MK, Takkunen JT: **Evaluation of exercise electrocardiography and thallium tomographic imaging in detecting asymptomatic coronary artery disease in diabetic patients**. *Br Heart J* 1990, **63**(1):7-11.

132. Holley JL, Fenton RA, Arthur RS: **Thallium stress testing does not predict cardiovascular risk in diabetic patients with end-stage renal disease undergoing cadaveric renal transplantation**. *Am J Med* 1991, **90**(5):563-570.

133. Marwick TH, Steinmuller DR, Underwood DA, Hobbs RE, Go RT, Swift C, Braun WE: **Ineffectiveness of dipyridamole SPECT thallium imaging as a screening technique for coronary artery disease in patients with end-stage renal failure**. *Transplantation* 1990, **49**(1):100-103.

134. Brown JH, Vites NP, Testa HJ, Prescott MC, Hunt LP, Gokal R, Mallick NP: **Value of thallium myocardial imaging in the prediction of future cardiovascular events in patients with end-stage renal failure**. *Nephrol Dial Transplant* 1993, **8**(5):433-437.

135. Brown KA, Rimmer J, Haisch C: **Noninvasive cardiac risk stratification of diabetic and nondiabetic uremic renal allograft candidates using dipyridamole-thallium-201 imaging and radionuclide ventriculography**. *Am J Cardiol* 1989, **64**(16):1017-1021.

136.   Camp AD, Garvin PJ, Hoff J, Marsh J, Byers SL, Chaitman BR: **Prognostic value of intravenous dipyridamole thallium imaging in patients with diabetes mellitus considered for renal transplantation**. *Am J Cardiol* 1990, **65**(22):1459-1463.

137.   Dahan M, Viron BM, Faraggi M, Himbert DL, Legallicier BJJ, Kolta AM, Pessione F, Le Guludec D, Gourgon R, Mignon FE: **Diagnostic accuracy and prognostic value of combined dipyridamole-exercise thallium imaging in hemodialysis patients**. *Kidney Int* 1998, **54**(1):255-262.

138.   Rabbat CG, Treleaven DJ, Russell JD, Ludwin D, Cook DJ: **Prognostic Value of Myocardial Perfusion Studies in Patients with End-Stage Renal Disease Assessed for Kidney or Kidney-Pancreas Transplantation: A Meta-Analysis**. *J Am Soc Nephrol* 2003, **14**(2):431-439.

139.   Morrow CE, Schwartz JS, Sutherland DE, Simmons RL, Ferguson RM, Kjellstrand CM, Najarian JS: **Predictive value of thallium stress testing for coronary and cardiovascular events in uremic diabetic patients before renal transplantation**. *Am J Surg* 1983, **146**(3):331-335.

140.   Philipson JD, Carpenter BJ, Itzkoff J, Hakala TR, Rosenthal JT, Taylor RJ, Puschett JB: **Evaluation of cardiovascular risk for renal transplantation in diabetic patients**. *Am J Med* 1986, **81**(4):630-634.

141.   DePuey EG, Guertler-Krawczynska E, Perkins JV, Robbins WL, Whelchel JD, Clements SD: **Alterations in myocardial thallium-201 distribution in patients with chronic systemic hypertension undergoing single-photon emission computed tomography**. *Am J Cardiol* 1988, **62**(4):234-238.

142.   Houghton JL, Frank MJ, Carr AA, von Dohlen TW, Prisant LM: **Relations among impaired coronary flow reserve, left ventricular hypertrophy and thallium perfusion defects in hypertensive patients without obstructive coronary artery disease**. *J Am Coll Cardiol* 1990, **15**(1):43-51.

143.   Schulman DS, Francis CK, Black HR, Wackers FJ: **Thallium-201 stress imaging in hypertensive patients**. *Hypertension* 1987, **10**(1):16-21.

144.   Fragasso G, Lu C, Dabrowski P, Pagnotta P, Sheiban I, Chierchia SL: **Comparison of stress/rest myocardial perfusion tomography, dipyridamole and dobutamine stress echocardiography for the detection of coronary disease in hypertensive patients with chest pain and positive exercise test**. *J Am Coll Cardiol* 1999, **34**(2):441-447.

145.   Kimura K, Tabei K, Asano Y, Hosoda S: **Cardiac arrhythmias in hemodialysis patients. A study of incidence and contributory factors**. *Nephron* 1989, **53**(3):201-207.

146.   Bates JR, Sawada SG, Segar DS, Spaedy AJ, Petrovic O, Fineberg NS, Feigenbaum H, Ryan T: **Evaluation using dobutamine stress echocardiography in patients with insulin-dependent diabetes mellitus before kidney and/or pancreas transplantation**. *Am J Cardiol* 1996, **77**(2):175-179.

147.   Herzog CA, Marwick TH, Pheley AM, White CW, Rao VK, Dick CD: **Dobutamine stress echocardiography for the detection of significant coronary artery disease in renal transplant candidates**. *Am J Kidney Dis* 1999, **33**(6):1080-1090.

148.   Sharma R, Pellerin D, Gaze DC, Gregson H, Streather CP, Collinson PO, Brecker SJ: **Dobutamine stress echocardiography and the resting but not exercise electrocardiograph predict severe coronary artery disease in renal transplant candidates**. *Nephrol Dial Transplant* 2005, **20**(10):2207-2214.

149.   De Lima JJG, Sabbaga E, Vieira MLC, de Paula FJ, Ianhez LE, Krieger EM, Ramires JAF: **Coronary Angiography Is the Best Predictor of Events in Renal Transplant Candidates Compared With Noninvasive Testing**. *Hypertension* 2003, **42**(3):263-268.

150.   Douglas PS, Khandheria B, Stainback RF, Weissman NJ, Peterson ED, Hendel RC, Stainback RF, Blaivas M, Des Prez RD, Gillam LD *et al*: **ACCF/ASE/ACEP/AHA/ASNC/SCAI/SCCT/SCMR 2008 appropriateness criteria for stress echocardiography: a report of the American College of Cardiology Foundation Appropriateness Criteria Task Force, American Society of Echocardiography, American College of Emergency Physicians, American Heart Association, American Society of Nuclear Cardiology, Society for Cardiovascular Angiography and Interventions, Society of Cardiovascular Computed Tomography, and Society for Cardiovascular Magnetic Resonance: endorsed by the Heart Rhythm Society and the Society of Critical Care Medicine**. *Circulation* 2008, **117**(11):1478-1497.

151.   Karagiannis SE, Feringa HH, Elhendy A, van Domburg R, Chonchol M, Vidakovic R, Bax JJ, Karatasakis G, Athanasopoulos G, Cokkinos DV *et al*: **Prognostic significance of renal function in patients undergoing**

dobutamine stress echocardiography. *Nephrol Dial Transplant* 2008, **23**(2):601-607.

152.   Dagianti A, Penco M, Agati L, Sciomer S, Dagianti A, Rosanio S, Fedele F: **Stress echocardiography: comparison of exercise, dipyridamole and dobutamine in detecting and predicting the extent of coronary artery disease**. *J Am Coll Cardiol* 1995, **26**(1):18-25.

153.   Pingitore A, Picano E, Varga A, Gigli G, Cortigiani L, Previtali M, Minardi G, Colosso MQ, Lowenstein J, Mathias W, Jr. *et al*: **Prognostic value of pharmacological stress echocardiography in patients with known or suspected coronary artery disease: a prospective, large-scale, multicenter, head-to-head comparison between dipyridamole and dobutamine test. Echo-Persantine International Cooperative (EPIC) and Echo-Dobutamine International Cooperative (EDIC) Study Groups**. *J Am Coll Cardiol* 1999, **34**(6):1769-1777.

154.   Cortigiani L, Zanetti L, Bigi R, Desideri A, Fiorentini C, Nannini E: **Safety and feasibility of dobutamine and dipyridamole stress echocardiography in hypertensive patients**. *J Hypertens* 2002, **20**(7):1423-1429.

155.   Matsumura Y, Hozumi T, Arai K, Sugioka K, Ujino K, Takemoto Y, Yamagishi H, Yoshiyama M, Yoshikawa J: **Non-invasive assessment of myocardial ischaemia using new real-time three-dimensional dobutamine stress echocardiography: comparison with conventional two-dimensional methods**. *Eur Heart J* 2005, **26**(16):1625-1632.

156.   Eroglu E, D'Hooge J, Herbots L, Thijs D, Dubois C, Sinnaeve P, Dens J, Vanhaecke J, Rademakers F: **Comparison of real-time tri-plane and**

conventional 2D dobutamine stress echocardiography for the assessment of coronary artery disease. *Eur Heart J* 2006, **27**(14):1719-1724.

157.	MIRSKY I, PARMLEY WW: **Assessment of Passive Elastic Stiffness for Isolated Heart Muscle and the Intact Heart**. *Circulation Research* 1973, **33**(2):233-243.

158.	D'Hooge J, Heimdal A, Jamal F, Kukulski T, Bijnens B, Rademakers F, Hatle L, Suetens P, Sutherland GR: **Regional strain and strain rate measurements by cardiac ultrasound: principles, implementation and limitations**. *Eur J Echocardiogr* 2000, **1**(3):154-170.

159.	Abraham TP, Dimaano VL, Liang HY: **Role of tissue Doppler and strain echocardiography in current clinical practice**. *Circulation* 2007, **116**(22):2597-2609.

160.	Choi JO, Cho SW, Song YB, Cho SJ, Song BG, Lee SC, Park SW: **Longitudinal 2D strain at rest predicts the presence of left main and three vessel coronary artery disease in patients without regional wall motion abnormality**. *Eur J Echocardiogr* 2009, **10**(5):695-701.

161.	Hashimoto I, Li X, Hejmadi Bhat A, Jones M, Zetts A, Sahn D: **Myocardial strain rate is a superior method for evaluation of left ventricular subendocardial function compared with tissue Doppler imaging.** *J Am Coll Cardiol* 2003, **42**(9):1574-1583.

162.	Blessberger H, Binder T: **NON-invasive imaging: Two dimensional speckle tracking echocardiography: basic principles**. *Heart* 2010, **96**(9):716-722.

163.   Blondheim DS, Beeri R, Feinberg MS, Vaturi M, Shimoni S, Fehske W, Sagie A, Rosenmann D, Lysyansky P, Deutsch L *et al*: **Reliability of visual assessment of global and segmental left ventricular function: a multicenter study by the Israeli Echocardiography Research Group**. *J Am Soc Echocardiogr* 2010, **23**(3):258-264.

164.   Pavlopoulos H, Nihoyannopoulos P: **Strain and strain rate deformation parameters: from tissue Doppler to 2D speckle tracking.** *Int J Cardiovasc Imaging* 2008, **24**(5):479-491.

165.   STREETER DD, Jr., SPOTNITZ HM, PATEL DP, ROSS J, Jr., SONNENBLICK EH: **Fiber Orientation in the Canine Left Ventricle during Diastole and Systole**. *Circ Res* 1969, **24**(3):339-347.

166.   Burns AT, McDonald IG, Thomas JD, MacIsaac A, Prior D: **Doin' the twist: new tools for an old concept of myocardial function**. *Heart* 2008, **94**(8):978-983.

167.   Van de Veire NR, De Sutter J, Bax JJ, Roelandt JRTC: **Technological advances in tissue Doppler imaging echocardiography**. *Heart* 2008, **94**(8):1065-1074.

168.   Urheim S, Edvardsen T, Torp H, Angelsen B, Smiseth OA: **Myocardial strain by Doppler echocardiography. Validation of a new method to quantify regional myocardial function**. *Circulation* 2000, **102**(10):1158-1164.

169.   Edvardsen T, Gerber BL, Garot J, Bluemke DA, Lima JA, Smiseth OA: **Quantitative assessment of intrinsic regional myocardial deformation by Doppler strain rate echocardiography in humans: validation against**

three-dimensional tagged magnetic resonance imaging. *Circulation* 2002, **106**(1):50-56.

170.   Mogelvang R, Sogaard P, Pedersen SA, Olsen NT, Marott JL, Schnohr P, Goetze JP, Jensen JS: **Cardiac Dysfunction Assessed by Echocardiographic Tissue Doppler Imaging Is an Independent Predictor of Mortality in the General Population**. *Circulation* 2009, **119**(20):2679-2685.

171.   Hayashi SY, Rohani M, Lindholm B, Brodin LA, Lind B, Barany P, Alvestrand A, Seeberger A: **Left ventricular function in patients with chronic kidney disease evaluated by colour tissue Doppler velocity imaging**. *Nephrol Dial Transplant* 2006, **21**(1):125-132.

172.   Galetta F, Cupisti A, Franzoni F, Carpi A, Barsotti G, Santoro G: **Acute effects of hemodialysis on left ventricular function evaluated by tissue Doppler imaging**. *Biomed Pharmacother* 2006, **60**(2):66-70.

173.   Yu C-M, Sanderson JE, Marwick TH, Oh JK: **Tissue Doppler Imaging: A New Prognosticator for Cardiovascular Diseases**. *Journal of the American College of Cardiology* 2007, **49**(19):1903-1914.

174.   Lee TY, Kang PL, Hsiao SH, Lin SK, Mar GY, Chiou CW, Liu CP: **Tissue Doppler velocity is not totally preload-independent: a study in a uremic population after hemodialysis**. *Cardiology* 2007, **107**(4):415-421.

175.   Fijalkowski M, Koprowski A, Gruchala M, Galaska R, Debska-Slizien A, Rogowski J, Rutkowski B, Rynkiewicz A: **Effect of preload reduction by hemodialysis on myocardial ultrasonic characterization, left atrial volume, and Doppler tissue imaging in patients with end-stage renal disease**. *J Am Soc Echocardiogr* 2006, **19**(11):1359-1364.

176.   Graham RJ, Gelman JS, Donelan L, Mottram PM, Peverill RE: **Effect of preload reduction by haemodialysis on new indices of diastolic function**. *Clin Sci (Lond)* 2003, **105**(4):499-506.

177.   Chakko S, Girgis I, Contreras G, Perez G, Kessler KM, Myerburg RJ: **Effects of hemodialysis on left ventricular diastolic filling**. *Am J Cardiol* 1997, **79**(1):106-108.

178.   Dincer I, Kumbasar D, Nergisoglu G, Atmaca Y, Kutlay S, Akyurek O, Sayin T, Erol C, Oral D: **Assessment of left ventricular diastolic function with Doppler tissue imaging: effects of preload and place of measurements**. *Int J Cardiovasc Imaging* 2002, **18**(3):155-160.

179.   Drighil A, Madias JE, Mathewson JW, El Mosalami H, El Badaoui N, Ramdani B, Bennis A: **Haemodialysis: effects of acute decrease in preload on tissue Doppler imaging indices of systolic and diastolic function of the left and right ventricles**. *Eur J Echocardiogr* 2008, **9**(4):530-535.

180.   Drighil A, Perron JM, Lafitte S, Rakotoarison P, Bader H, Zabsonre P, Chraibi N, Roudaut R: **[Study of variations in preload on the new echocardiography parameters of diastolic function in health subjects]**. *Arch Mal Coeur Vaiss* 2002, **95**(6):573-580.

181.   Hayashi SY, Brodin LA, Alvestrand A, Lind B, Stenvinkel P, Mazza do Nascimento M, Qureshi AR, Saha S, Lindholm B, Seeberger A: **Improvement of cardiac function after haemodialysis. Quantitative evaluation by colour tissue velocity imaging**. *Nephrol Dial Transplant* 2004, **19**(6):1497-1506.

182.   Rozich JD, Smith B, Thomas JD, Zile MR, Kaiser J, Mann DL: **Dialysis-induced alterations in left ventricular filling: mechanisms and clinical significance**. *Am J Kidney Dis* 1991, **17**(3):277-285.

183.   Sztajzel J, Ruedin P, Stoermann C, Monin C, Schifferli J, Leski M, Rutishauser W, Lerch R: **Effects of dialysate composition during hemodialysis on left ventricular function**. *Kidney Int Suppl* 1993, **41**:S60-66.

184.   Barberato SH, Mantilla DE, Misocami MA, Goncalves SM, Bignelli AT, Riella MC, Pecoits-Filho R: **Effect of preload reduction by hemodialysis on left atrial volume and echocardiographic Doppler parameters in patients with end-stage renal disease**. *Am J Cardiol* 2004, **94**(9):1208-1210.

185.   Agmon Y, Oh JK, McCarthy JT, Khandheria BK, Bailey KR, Seward JB: **Effect of volume reduction on mitral annular diastolic velocities in hemodialysis patients**. *Am J Cardiol* 2000, **85**(5):665-668, A611.

186.   Palecek T, Skalicka L, Lachmanova J, Tesar V, Linhart A: **Effect of preload reduction by hemodialysis on conventional and novel echocardiographic parameters of left ventricular structure and function**. *Echocardiography* 2008, **25**(2):162-168.

187.   Oki T, Tabata T, Yamada H, Wakatsuki T, Shinohara H, Nishikado A, Iuchi A, Fukuda N, Ito S: **Clinical application of pulsed Doppler tissue imaging for assessing abnormal left ventricular relaxation**. *Am J Cardiol* 1997, **79**(7):921-928.

188.   Gorcsan J, 3rd, Strum DP, Mandarino WA, Gulati VK, Pinsky MR: **Quantitative assessment of alterations in regional left ventricular**

contractility with color-coded tissue Doppler echocardiography. Comparison with sonomicrometry and pressure-volume relations. *Circulation* 1997, **95**(10):2423-2433.

189.	Abraham TP, Nishimura RA, Holmes Jr DR, Belohlavek M, Seward JB: **Strain rate imaging for assessment of regional myocardial function: Results from a clinical model of septal ablation**. *Circulation* 2002, **105**(12):1403-1406.

190.	Armstrong G, Pasquet A, Fukamachi K, Cardon L, Olstad B, Marwick T: **Use of Peak Systolic Strain as an Index of Regional Left Ventricular Function: Comparison with Tissue Doppler Velocity During Dobutamine Stress and Myocardial Ischemia**. *Journal of the American Society of Echocardiography* 2000, **13**(8):731-737.

191.	Derumeaux G, Ovize M, Loufoua J, Pontier G, André-Fouet X, Cribier A: **Assessment of Nonuniformity of Transmural Myocardial Velocities by Color-Coded Tissue Doppler Imaging: Characterization of Normal, Ischemic, and Stunned Myocardium**. *Circulation* 2000, **101**(12):1390-1395.

192.	Sutherland GR, Di Salvo G, Claus P, D'Hooge J, Bijnens B: **Strain and strain rate imaging: a new clinical approach to quantifying regional myocardial function**. *J Am Soc Echocardiogr* 2004, **17**(7):788-802.

193.	Marwick TH: **Measurement of strain and strain rate by echocardiography: ready for prime time?** *J Am Coll Cardiol* 2006, **47**(7):1313-1327.

194.	Leitman M, Lysyansky P, Sidenko S, Shir V, Peleg E, Binenbaum M, Kaluski E, Krakover R, Vered Z: **Two-dimensional strain-a novel software**

for real-time quantitative echocardiographic assessment of myocardial function. *J Am Soc Echocardiogr* 2004, **17**(10):1021-1029.

195.   [http://h2physics.org]

196.   Wei S-g, Yang L, Chen Z, Liu Z-f: **Motion Detection Based on Optical Flow and Self-adaptive Threshold Segmentation**. *Procedia Engineering* 2011, **15**(0):3471-3476.

197.   Yeung F, Levinson SF, Parker KJ: **Multilevel and Motion Model-Based Ultrasonic Speckle Tracking Algorithms**. *Ultrasound in Medicine & Biology* 1998, **24**(3):427-441.

198.   Amundsen BH, Helle-Valle T, Edvardsen T, Torp H, Crosby J, Lyseggen E, Stoylen A, Ihlen H, Lima JAC, Smiseth OA *et al*: **Noninvasive myocardial strain measurement by speckle tracking echocardiography: validation against sonomicrometry and tagged magnetic resonance imaging**. *Journal of the American College of Cardiology* 2006, **47**(4):789-793.

199.   Reisner SA, Lysyansky P, Agmon Y, Mutlak D, Lessick J, Friedman Z: **Global longitudinal strain: a novel index of left ventricular systolic function**. *J Am Soc Echocardiogr* 2004, **17**(6):630-633.

200.   Marwick TH, Leano RL, Brown J, Sun JP, Hoffmann R, Lysyansky P, Becker M, Thomas JD: **Myocardial strain measurement with 2-dimensional speckle-tracking echocardiography: definition of normal range**. *JACC Cardiovasc Imaging* 2009, **2**(1):80-84.

201.   Otterstad JE, Froeland G, St. John Sutton M, Holme I: **Accuracy and reproducibility of biplane two-dimensional echocardiographic**

measurements of left ventricular dimensions and function. *European Heart Journal* 1997, **18**(3):507-513.

202.   Gillam LD: **Automated Versus Visual Segmental Scoring**. *Circulation: Cardiovascular Imaging* 2010, **3**(1):5-7.

203.   Sun JP, Niu J, Chou D, Chuang HH, Wang K, Drinko J, Borowski A, Stewart WJ, Thomas JD: **Alterations of regional myocardial function in a swine model of myocardial infarction assessed by echocardiographic 2-dimensional strain imaging**. *J Am Soc Echocardiogr* 2007, **20**(5):498-504.

204.   Leitman M, Lysyansky P, Gurevich J, Friedman Z, Sucher E, Rosenblatt S, Kaluski E, Krakover R, Fuchs T, Vered Z: **Real-time quantitative automatic assessment of left ventricular ejection fraction and regional wall motion by speckle imaging**. *The Israel Medical Association journal : IMAJ* 2007, **9**(4):281-285.

205.   Becker M, Bilke E, Kühl H, Katoh M, Kramann R, Franke A, Bücker A, Hanrath P, Hoffmann R: **Analysis of myocardial deformation based on pixel tracking in two dimensional echocardiographic images enables quantitative assessment of regional left ventricular function**. *Heart* 2006, **92**(8):1102-1108.

206.   Liel-Cohen N, Tsadok Y, Beeri R, Lysyansky P, Agmon Y, Feinberg MS, Fehske W, Gilon D, Hay I, Kuperstein R *et al*: **A New Tool for Automatic Assessment of Segmental Wall Motion Based on Longitudinal 2D Strain A Multicenter Study by the Israeli Echocardiography Research Group**. *Circulation-Cardiovascular Imaging* 2010, **3**(1):47-53.

207.	Choi J-O, Cho SW, Song YB, Cho SJ, Song BG, Lee S-C, Park SW: **Longitudinal 2D strain at rest predicts the presence of left main and three vessel coronary artery disease in patients without regional wall motion abnormality**. *European Journal of Echocardiography* 2009, **10**(5):695-701.

208.	Lauterbur PC: **Image Formation by Induced Local Interactions - Examples Employing Nuclear Magnetic-Resonance**. *Nature* 1973, **242**(5394):190-191.

209.	Mansfield P, Grannell PK: **NMR 'diffraction' in solids?** *Journal of Physics C: Solid State Physics* 1973, **6**(22):L422.

210.	Garroway AN, Grannell PK, Mansfield P: **Image formation in NMR by a selective irradiative process**. *Journal of Physics C: Solid State Physics* 1974, **7**(24):L457.

211.	Mansfield P: **Multi-planar image formation using NMR spin echoes**. *Journal of Physics C: Solid State Physics* 1977, **10**(3):L55.

212.	**how k-space works** [www.revisemri.com]

213.	Fernandes VRS, Polak JF, Edvardsen T, Carvalho B, Gomes A, Bluemke DA, Nasir K, O'Leary DH, Lima JAC: **Subclinical Atherosclerosis and Incipient Regional Myocardial Dysfunction in Asymptomatic IndividualsThe Multi-Ethnic Study of Atherosclerosis (MESA)**. *Journal of the American College of Cardiology* 2006, **47**(12):2420-2428.

214.	Edwards NC, Hirth A, Ferro CJ, Townend JN, Steeds RP: **Subclinical abnormalities of left ventricular myocardial deformation in early-stage chronic kidney disease: the precursor of uremic cardiomyopathy?** *J Am Soc Echocardiogr* 2008, **21**(12):1293-1298.

215.   Dandel M, Lehmkuhl H, Knosalla C, Suramelashvili N, Hetzer R: **Strain and strain rate imaging by echocardiography - basic concepts and clinical applicability**. *Curr Cardiol Rev* 2009, **5**(2):133-148.

216.   Young AA, Kramer CM, Ferrari VA, Axel L, Reichek N: **Three-dimensional left ventricular deformation in hypertrophic cardiomyopathy**. *Circulation* 1994, **90**(2):854-867.

217.   Hor KN, Wansapura J, Markham LW, Mazur W, Cripe LH, Fleck R, Benson DW, Gottliebson WM: **Circumferential Strain Analysis Identifies Strata of Cardiomyopathy in Duchenne Muscular Dystrophy: A Cardiac Magnetic Resonance Tagging Study**. *Journal of the American College of Cardiology* 2009, **53**(14):1204-1210.

218.   Cho GY, Marwick TH, Kim HS, Kim MK, Hong KS, Oh DJ: **Global 2-Dimensional Strain as a New Prognosticator in Patients With Heart Failure**. *Journal of the American College of Cardiology* 2009, **54**(7):618-624.

219.   Arts T, Hunter WC, Douglas A, Muijtjens AMM, Reneman RS: **Description of the deformation of the left ventricle by a kinematic model**. *Journal of Biomechanics* 1992, **25**(10):1119-1127.

220.   Zerhouni EA, Parish DM, Rogers WJ, Yang A, Shapiro EP: **Human heart: tagging with MR imaging--a method for noninvasive assessment of myocardial motion**. *Radiology* 1988, **169**(1):59-63.

221.   Lima JA, Jeremy R, Guier W, Bouton S, Zerhouni EA, McVeigh E, Buchalter MB, Weisfeldt ML, Shapiro EP, Weiss JL: **Accurate systolic wall thickening by nuclear magnetic resonance imaging with tissue tagging: correlation with sonomicrometers in normal and ischemic myocardium**. *J Am Coll Cardiol* 1993, **21**(7):1741-1751.

222.   Yeon SB, Reichek N, Tallant BA, Lima JAC, Calhoun LP, Clark NR, Hoffman EA, Ho KKL, Axel L: **Validation of in vivo myocardial strain measurement by magnetic resonance tagging with sonomicrometry**. *Journal of the American College of Cardiology* 2001, **38**(2):555-561.

223.   Ibrahim el SH: **Myocardial tagging by cardiovascular magnetic resonance: evolution of techniques--pulse sequences, analysis algorithms, and applications**. *J Cardiovasc Magn Reson* 2011, **13**:36.

224.   Shehata ML, Cheng S, Osman NF, Bluemke DA, Lima JA: **Myocardial tissue tagging with cardiovascular magnetic resonance**. *J Cardiovasc Magn Reson* 2009, **11**(1):55.

225.   Fischer SE, McKinnon GC, Maier SE, Boesiger P: **Improved myocardial tagging contrast**. *Magn Reson Med* 1993, **30**(2):191-200.

226.   Zwanenburg JJM, Kuijer JPA, Marcus JT, Heethaar RM: **Steady-state free precession with myocardial tagging: CSPAMM in a single breathhold**. *Magnetic Resonance in Medicine* 2003, **49**(4):722-730.

227.   Markl M, Reeder SB, Chan FP, Alley MT, Herfkens RJ, Pelc NJ: **Steady-State Free Precession MR Imaging: Improved Myocardial Tag Persistence and Signal-to-Noise Ratio for Analysis of Myocardial Motion1**. *Radiology* 2004, **230**(3):852-861.

228.   Hess AT, Zhong X, Spottiswoode BS, Epstein FH, Meintjes EM: **Myocardial 3D strain calculation by combining cine displacement encoding with stimulated echoes (DENSE) and cine strain encoding (SENC) imaging**. *Magn Reson Med* 2009, **62**(1):77-84.

229.   Markl M, Scherer S, Frydrychowicz A, Burger D, Geibel A, Hennig J: **Balanced left ventricular myocardial SSFP-tagging at 1.5T and 3T**. *Magnetic Resonance in Medicine* 2008, **60**(3):631-639.

230.   Osman NF, Kerwin WS, McVeigh ER, Prince JL: **Cardiac motion tracking using CINE harmonic phase (HARP) magnetic resonance imaging**. *Magnetic Resonance in Medicine* 1999, **42**(6):1048-1060.

231.   Garot J, Bluemke DA, Osman NF, Rochitte CE, McVeigh ER, Zerhouni EA, Prince JL, Lima JAC: **Fast Determination of Regional Myocardial Strain Fields From Tagged Cardiac Images Using Harmonic Phase MRI**. *Circulation* 2000, **101**(9):981-988.

232.   Liu W, Chen J, Ji S, Allen JS, Bayly PV, Wickline SA, Yu X: **Harmonic phase MR tagging for direct quantification of Lagrangian strain in rat hearts after myocardial infarction**. *Magn Reson Med* 2004, **52**(6):1282-1290.

233.   Kwong RY: **Imaging the Physiology of the Ischemic Cascade**. *Circulation: Cardiovascular Imaging* 2008, **1**(2):92-93.

234.   Heiss WD: **The ischemic penumbra: correlates in imaging and implications for treatment of ischemic stroke. The Johann Jacob Wepfer award 2011**. *Cerebrovasc Dis* 2011, **32**(4):307-320.

235.   Gould KL: **Does Coronary Flow Trump Coronary Anatomy?** *JACC: Cardiovascular Imaging* 2009, **2**(8):1009-1023.

236.   Wheatley K, Ives N, Gray R, Kalra PA, Moss JG, Baigent C, Carr S, Chalmers N, Eadington D, Hamilton G *et al*: **Revascularization versus medical therapy for renal-artery stenosis**. *N Engl J Med* 2009, **361**(20):1953-1962.

237.   Tofts PS, Brix G, Buckley DL, Evelhoch JL, Henderson E, Knopp MV, Larsson HB, Lee TY, Mayr NA, Parker GJ *et al*: **Estimating kinetic parameters from dynamic contrast-enhanced T(1)-weighted MRI of a diffusable tracer: standardized quantities and symbols**. *J Magn Reson Imaging* 1999, **10**(3):223-232.

238.   Nagel E, Klein C, Paetsch I, Hettwer S, Schnackenburg B, Wegscheider K, Fleck E: **Magnetic Resonance Perfusion Measurements for the Noninvasive Detection of Coronary Artery Disease**. *Circulation* 2003, **108**(4):432-437.

239.   Greenwood JP, Maredia N, Younger JF, Brown JM, Nixon J, Everett CC, Bijsterveld P, Ridgway JP, Radjenovic A, Dickinson CJ *et al*: **Cardiovascular magnetic resonance and single-photon emission computed tomography for diagnosis of coronary heart disease (CE-MARC): a prospective trial**. *Lancet* 2012, **379**(9814):453-460.

240.   Kaewlai R, Abujudeh H: **Nephrogenic Systemic Fibrosis**. *American Journal of Roentgenology* 2012, **199**(1):W17-W23.

241.   Tumkur SM, Vu AT, Li LP, Pierchala L, Prasad PV: **Evaluation of intra-renal oxygenation during water diuresis: a time-resolved study using BOLD MRI**. *Kidney Int* 2006, **70**(1):139-143.

242.   Li LP, Storey P, Pierchala L, Li W, Polzin J, Prasad P: **Evaluation of the reproducibility of intrarenal R2* and DeltaR2* measurements following administration of furosemide and during waterload**. *J Magn Reson Imaging* 2004, **19**(5):610-616.

243.   Warner L, Glockner JF, Woollard J, Textor SC, Romero JC, Lerman LO: **Determinations of renal cortical and medullary oxygenation using**

blood oxygen level-dependent magnetic resonance imaging and selective diuretics. *Invest Radiol* 2011, **46**(1):41-47.

244.   Juillard L, Lerman LO, Kruger DG, Haas JA, Rucker BC, Polzin JA, Riederer SJ, Romero JC: **Blood oxygen level-dependent measurement of acute intra-renal ischemia**. *Kidney Int* 2004, **65**(3):944-950.

245.   Chrysochou C, Mendichovszky IA, Buckley DL, Cheung CM, Jackson A, Kalra PA: **BOLD imaging: a potential predictive biomarker of renal functional outcome following revascularization in atheromatous renovascular disease**. *Nephrol Dial Transplant* 2012, **27**(3):1013-1019.

246.   Manotham K, Ongvilawan B, Urusopone P, Chetsurakarn S, Tanamai J, Limkuansuwan P, Tungsanga K, Eiam-Ong S: **Angiotensin II receptor blocker partially ameliorated intrarenal hypoxia in chronic kidney disease patients: a pre-/post-study**. *Intern Med J* 2012, **42**(4):e33-37.

247.   Xiao WB, Xu JJ, Wang QD, Xu Y, Zhang MM: **Functional evaluation of transplanted kidneys in normal function and acute rejection using BOLD MR imaging**. *European journal of radiology* 2012, **81**(5):838-845.

248.   Herment A, Lefort M, Kachenoura N, De Cesare A, Taviani V, Graves MJ, Pellot-Barakat C, Frouin F, Mousseaux E: **Automated estimation of aortic strain from steady-state free-precession and phase contrast MR images**. *Magnetic Resonance in Medicine* 2011, **65**(4):986-993.

249.   Arnold JR, Karamitsos TD, Bhamra-Ariza P, Francis JM, Searle N, Robson MD, Howells RK, Choudhury RP, Rimoldi OE, Camici PG *et al*: **Myocardial Oxygenation in Coronary Artery Disease: Insights From Blood Oxygen Level–Dependent Magnetic Resonance Imaging at 3**

Tesla. *Journal of the American College of Cardiology* 2012, **59**(22):1954-1964.

250.   Karamitsos TD, Leccisotti L, Arnold JR, Recio-Mayoral A, Bhamra-Ariza P, Howells RK, Searle N, Robson MD, Rimoldi OE, Camici PG *et al*: **Relationship between regional myocardial oxygenation and perfusion in patients with coronary artery disease: insights from cardiovascular magnetic resonance and positron emission tomography**. *Circ Cardiovasc Imaging* 2010, **3**(1):32-40.

251.   Buxton RB, Frank LR, Wong EC, Siewert B, Warach S, Edelman RR: **A general kinetic model for quantitative perfusion imaging with arterial spin labeling**. *Magn Reson Med* 1998, **40**(3):383-396.

252.   Detre JA, Rao H, Wang DJ, Chen YF, Wang Z: **Applications of arterial spin labeled MRI in the brain**. *J Magn Reson Imaging* 2012, **35**(5):1026-1037.

253.   Wong EC: **Vessel-encoded arterial spin-labeling using pseudocontinuous tagging**. *Magnetic Resonance in Medicine* 2007, **58**(6):1086-1091.

254.   Ferre JC, Petr J, Bannier E, Barillot C, Gauvrit JY: **Improving quality of arterial spin labeling MR imaging at 3 Tesla with a 32-channel coil and parallel imaging**. *J Magn Reson Imaging* 2012, **35**(5):1233-1239.

255.   Gardener AG, Francis ST: **Multislice perfusion of the kidneys using parallel imaging: Image acquisition and analysis strategies**. *Magnetic Resonance in Medicine* 2010, **63**(6):1627-1636.

256.   Ritt M, Janka R, Schneider MP, Martirosian P, Hornegger J, Bautz W, Uder M, Schmieder RE: **Measurement of kidney perfusion by magnetic**

resonance imaging: comparison of MRI with arterial spin labeling to para-aminohippuric acid plasma clearance in male subjects with metabolic syndrome. *Nephrology Dialysis Transplantation* 2010, **25**(4):1126-1133.

257.   Artz NS, Wentland AL, Sadowski EA, Djamali A, Grist TM, Seo S, Fain SB: **Comparing Kidney Perfusion Using Noncontrast Arterial Spin Labeling MRI and Microsphere Methods in an Interventional Swine Model**. *Investigative Radiology* 2011, **46**(2):124-131.

258.   Wu W-C, Su M-Y, Chang C-C, Tseng W-YI, Liu K-L: **Renal Perfusion 3-T MR Imaging: A Comparative Study of Arterial Spin Labeling and Dynamic Contrast-enhanced Techniques**. *Radiology* 2011, **261**(3):845-853.

259.   Artz NS, Sadowski EA, Wentland AL, Grist TM, Seo S, Djamali A, Fain SB: **Arterial spin labeling MRI for assessment of perfusion in native and transplanted kidneys**. *Magn Reson Imaging* 2011, **29**(1):74-82.

260.   Schneider MP, Janka R, Ziegler T, Raff U, Ritt M, Ott C, Veelken R, Uder M, Schmieder RE: **Reversibility of the effects of aliskiren in the renal versus systemic circulation**. *Clin J Am Soc Nephrol* 2012, **7**(2):258-264.

261.   Chowdhury AH, Cox EF, Francis ST, Lobo DN: **A randomized, controlled, double-blind crossover study on the effects of 2-L infusions of 0.9% saline and plasma-lyte(R) 148 on renal blood flow velocity and renal cortical tissue perfusion in healthy volunteers**. *Annals of surgery* 2012, **256**(1):18-24.

262.   Liu Y, Song R, Liang CH, Chen X, Liu B: **Arterial spin labeling blood flow magnetic resonance imaging for evaluation of renal injury**. *American journal of physiology Renal physiology* 2012.

263.   Artz NS, Sadowski EA, Wentland AL, Djamali A, Grist TM, Seo S, Fain SB: **Reproducibility of renal perfusion MR imaging in native and transplanted kidneys using non-contrast arterial spin labeling**. *J Magn Reson Imaging* 2011, **33**(6):1414-1421.

264.   Cutajar M, Thomas D, Banks T, Clark C, Golay X, Gordon I: **Repeatability of renal arterial spin labelling MRI in healthy subjects**. *Magnetic Resonance Materials in Physics, Biology and Medicine* 2012, **25**(2):145-153.

265.   Zun Z, Wong EC, Nayak KS: **Assessment of myocardial blood flow (MBF) in humans using arterial spin labeling (ASL): feasibility and noise analysis**. *Magn Reson Med* 2009, **62**(4):975-983.

266.   Zun Z, Varadarajan P, Pai RG, Wong EC, Nayak KS: **Arterial Spin Labeled CMR Detects Clinically Relevant Increase in Myocardial Blood Flow With Vasodilation**. *JACC: Cardiovascular Imaging* 2011, **4**(12):1253-1261.

267.   Wang DJ, Bi X, Avants BB, Meng T, Zuehlsdorff S, Detre JA: **Estimation of perfusion and arterial transit time in myocardium using free-breathing myocardial arterial spin labeling with navigator-echo**. *Magn Reson Med* 2010, **64**(5):1289-1295.

268.   Golay X, Guenther M: **Arterial spin labelling: final steps to make it a clinical reality**. *Magnetic Resonance Materials in Physics, Biology and Medicine* 2012, **25**(2):79-82.

269.   Murphy K, Harris AD, Diukova A, Evans CJ, Lythgoe DJ, Zelaya F, Wise RG: **Pulsed arterial spin labeling perfusion imaging at 3 T: estimating the number of subjects required in common designs of clinical trials**. *Magn Reson Imaging* 2011, **29**(10):1382-1389.

270.   Alsop D: **Arterial spin labeling: its time is now**. *Magnetic Resonance Materials in Physics, Biology and Medicine* 2012, **25**(2):75-77.

271.   Niizuma S, Takiuchi S, Okada S, Horio T, Kamide K, Nakata H, Yoshihara F, Nakamura S, Kawano Y, Nakahama H *et al*: **Decreased coronary flow reserve in haemodialysis patients**. *Nephrol Dial Transplant* 2008, **23**(7):2324-2328.

272.   Ragosta M, Samady H, Isaacs RB, Gimple LW, Sarembock IJ, Powers ER: **Coronary flow reserve abnormalities in patients with diabetes mellitus who have end-stage renal disease and normal epicardial coronary arteries**. *Am Heart J* 2004, **147**(6):1017-1023.

273.   Kingwell BA, Waddell TK, Medley TL, Cameron JD, Dart AM: **Large artery stiffness predicts ischemic threshold in patients with coronary artery disease**. *Journal of the American College of Cardiology* 2002, **40**(4):773-779.

274.   Sigrist M, Bungay P, Taal MW, McIntyre CW: **Vascular calcification and cardiovascular function in chronic kidney disease**. *Nephrol Dial Transplant* 2006, **21**(3):707-714.

275.   Malpas SC: **Neural influences on cardiovascular variability: possibilities and pitfalls**. *Am J Physiol Heart Circ Physiol* 2002, **282**(1):H6-20.

276.   Chesterton LJ, Selby NM, Burton JO, Fialova J, Chan C, McIntyre CW: **Categorization of the hemodynamic response to hemodialysis: The importance of baroreflex sensitivity**. *Hemodialysis international International Symposium on Home Hemodialysis* 2009.

277.   Braunwald E, Kloner RA: **The stunned myocardium: prolonged, postischemic ventricular dysfunction**. *Circulation* 1982, **66**(6):1146-1149.

278.   Camici PG, Prasad SK, Rimoldi OE: **Stunning, Hibernation, and Assessment of Myocardial Viability**. *Circulation* 2008, **117**(1):103-114.

279.   Selby NM, McIntyre CW: **The acute cardiac effects of dialysis**. *Semin Dial* 2007, **20**(3):220-228.

280.   Zuber M, Steinmann E, Huser B, Ritz R, Thiel G, Brunner F: **Incidence of arrhythmias and myocardial ischaemia during haemodialysis and haemofiltration**. *Nephrol Dial Transplant* 1989, **4**(7):632-634.

281.   Khan NA, Hemmelgarn BR, Tonelli M, Thompson CR, Levin A: **Prognostic value of troponin T and I among asymptomatic patients with end-stage renal disease: a meta-analysis**. *Circulation* 2005, **112**(20):3088-3096.

282.   Bos WJ, Bruin S, van Olden RW, Keur I, Wesseling KH, Westerhof N, Krediet RT, Arisz LA: **Cardiac and hemodynamic effects of hemodialysis and ultrafiltration**. *Am J Kidney Dis* 2000, **35**(5):819-826.

283.   Boon D, van Montfrans GA, Koopman MG, Krediet RT, Bos WJ: **Blood pressure response to uncomplicated hemodialysis: the importance of changes in stroke volume**. *Nephron Clin Pract* 2004, **96**(3):c82-87.

284.   McIntyre CW, Burton JO, Selby NM, Leccisotti L, Korsheed S, Baker CSR, Camici PG: **Hemodialysis-Induced Cardiac Dysfunction Is Associated with an Acute Reduction in Global and Segmental Myocardial Blood Flow**. *Clin J Am Soc Nephrol* 2008, **3**(1):19-26.

285.   Dasselaar JJ, Slart RHJA, Knip M, Pruim J, Tio RA, McIntyre CW, de Jong PE, Franssen CFM: **Haemodialysis is associated with a pronounced fall in myocardial perfusion**. *Nephrol Dial Transplant* 2009, **24**(2):604-610.

286.   Burton JO, Jefferies HJ, Selby NM, McIntyre CW: **Hemodialysis-induced cardiac injury: determinants and associated outcomes**. *Clin J Am Soc Nephrol* 2009, **4**(5):914-920.

287.   Burton JO, Jefferies HJ, Selby NM, McIntyre CW: **Hemodialysis-Induced Repetitive Myocardial Injury Results in Global and Segmental Reduction in Systolic Cardiac Function**. *Clin J Am Soc Nephrol* 2009.

288.   Burton JO, Korsheed S, Grundy BJ, McIntyre CW: **Hemodialysis-induced left ventricular dysfunction is associated with an increase in ventricular arrhythmias**. *Ren Fail* 2008, **30**(7):701-709.

289.   Jefferies HJ, Virk B, Doss S, Sun S, John S, Moran J, Schiller B, McIntyre C: **Frequent Haemodialysis Regimens Are Associated with Reduction in Dialysis-Induced Myocardial Stunning and Systemic Inflammation** In: *American Society of Nephrology.* San Diego; 2009.

290.   Movilli E, Gaggia P, Zubani R, Camerini C, Vizzardi V, Parrinello G, Savoldi S, Fischer MS, Londrino F, Cancarini G: **Association between high ultrafiltration rates and mortality in uraemic patients on regular haemodialysis. A 5-year prospective observational multicentre study**. *Nephrol Dial Transplant* 2007, **22**(12):3547-3552.

291.   Hothi DK, Rees L, Marek J, Burton J, McIntyre CW: **Pediatric myocardial stunning underscores the cardiac toxicity of conventional hemodialysis treatments**. *Clin J Am Soc Nephrol* 2009, **4**(4):790-797.

292.   Selby NM, Lambie SH, Camici PG, Baker CS, McIntyre CW: **Occurrence of regional left ventricular dysfunction in patients undergoing standard and biofeedback dialysis**. *Am J Kidney Dis* 2006, **47**(5):830-841.

293.   Selby NM, Burton JO, Chesterton LJ, McIntyre CW: **Dialysis-induced regional left ventricular dysfunction is ameliorated by cooling the dialysate**. *Clin J Am Soc Nephrol* 2006, **1**(6):1216-1225.

294.   Jefferies HJ, Virk B, Doss S, Sun S, Moran J, Schiller B, C M: **Frequent Haemodialysis Regimens are associated with Reduction in Dialysis-Induced Myocardial Stunning**. *Abstract O22, Renal Association Meeting 2009, available at http://wwwrenalorg 2009*.

295.   Flanigan M: **How Should Dialysis Fluid Be Individualized for the Chronic Hemodialysis Patient?** *Seminars in Dialysis* 2008, **21**(3):226-229.

296.   Keen ML, Gotch FA: **The association of the sodium "setpoint" to interdialytic weight gain and blood pressure in hemodialysis patients**. *Int J Artif Organs* 2007, **30**(11):971-979.

297.   de Paula FM, Peixoto AJ, Pinto LV, Dorigo D, Patricio PJ, Santos SF: **Clinical consequences of an individualized dialysate sodium prescription in hemodialysis patients**. *Kidney Int* 2004, **66**(3):1232-1238.

298.   Pozzoni P, S DIF, Pontoriero G, Locatelli F: **Effectiveness of sodium and conductivity kinetic models in predicting end-dialysis plasma water**

sodium concentration: preliminary results of a single-center experience. *Hemodial Int* 2007, **11**(2):169-177.

299.   Lambie SH, Taal MW, Fluck RJ, McIntyre CW: **Online conductivity monitoring: validation and usefulness in a clinical trial of reduced dialysate conductivity**. *ASAIO J* 2005, **51**(1):70-76.

300.   Selby NM, Taal MW, McIntyre CW: **Comparison of progressive conductivity reduction with diacontrol and standard dialysis**. *ASAIO J* 2007, **53**(2):194-200.

301.   Titze J: **Water-Free Na + Retention: Interaction with Hypertension and Tissue Hydration**. *Blood Purification* 2008, **26**(1):95-99.

302.   Hausenloy DJ, Yellon DM: **Remote ischaemic preconditioning: underlying mechanisms and clinical application**. *Cardiovasc Res* 2008, **79**(3):377-386.

303.   Kharbanda RK, Nielsen TT, Redington AN: **Translation of remote ischaemic preconditioning into clinical practice**. *Lancet* 2009, **374**(9700):1557-1565.

304.   Rahman IA, Mascaro JG, Steeds RP, Frenneaux MP, Nightingale P, Gosling P, Townsend P, Townend JN, Green D, Bonser RS: **Remote Ischemic Preconditioning in Human Coronary Artery Bypass Surgery: From Promise to Disappointment?** *Circulation* 2010, **122**(11_suppl_1):S53-59.

305.   Ishihara M, Inoue I, Kawagoe T, Shimatani Y, Kurisu S, Nishioka K, Kouno Y, Umemura T, Nakamura S, Sato H: **Diabetes mellitus prevents ischemic preconditioning in patients with a first acute anterior wall myocardial infarction**. *J Am Coll Cardiol* 2001, **38**(4):1007-1011.

306.   Hassouna A, Loubani M, Matata BM, Fowler A, Standen NB, Galinanes M: **Mitochondrial dysfunction as the cause of the failure to precondition the diabetic human myocardium**. *Cardiovasc Res* 2006, **69**(2):450-458.

307.   Passlick-Deetjen J, Bedenbender-Stoll E: **Why thermosensing? A primer on thermoregulation**. *Nephrol Dial Transplant* 2005, **20**(9):1784-1789.

308.   Burton JO, Jefferies HJ, McIntyre CW: **Haemodialysis induced repetitive myocardial stunning results in segmental and global reduction in systolic cardiac function.** *submitted JACC* 2008.

309.   Chan CT, Greene T, Chertow GM, Kliger AS, Stokes JB, Beck GJ, Daugirdas JT, Kotanko P, Larive B, Levin NW *et al*: **Effects of Frequent Hemodialysis on Ventricular Volumes and Left Ventricular Remodeling**. *Clinical Journal of the American Society of Nephrology* 2013.

310.   Rocco MV, Lockridge RS, Jr., Beck GJ, Eggers PW, Gassman JJ, Greene T, Larive B, Chan CT, Chertow GM, Copland M *et al*: **The effects of frequent nocturnal home hemodialysis: the Frequent Hemodialysis Network Nocturnal Trial**. *Kidney Int* 2011, **80**(10):1080-1091.

311.   Jefferies HJ, Virk B, Schiller B, Moran J, McIntyre CW: **Frequent hemodialysis schedules are associated with reduced levels of dialysis-induced cardiac injury (myocardial stunning)**. *Clin J Am Soc Nephrol* 2011, **6**(6):1326-1332.

312.   Selby NM, McIntyre CW: **A systematic review of the clinical effects of reducing dialysate fluid temperature**. *Nephrol Dial Transplant* 2006, **21**(7):1883-1898.

313.   van der Sande FM, Wystrychowski G, Kooman JP, Rosales L, Raimann J, Kotanko P, Carter M, Chan CT, Leunissen KML, Levin NW: **Control of Core Temperature and Blood Pressure Stability during Hemodialysis**. *Clin J Am Soc Nephrol* 2009, **4**(1):93-98.

314.   Jefferies HJ, Burton JO, McIntyre CW: **Individualised dialysate temperature improves intradialytic haemodynamics and abrogates haemodialysis-induced myocardial stunning, without compromising tolerability**. *Blood purification* 2011, **32**(1):63-68.

315.   Odudu A, Eldehni MT, Fakis A, McIntyre CW: **Rationale and design of a multi-centre randomised controlled trial of individualised cooled dialysate to prevent left ventricular systolic dysfunction in haemodialysis patients**. *BMC Nephrol* 2012, **13**:45.

316.   Mosteller RD: **Simplified calculation of body-surface area**. *N Engl J Med* 1987, **317**(17):1098.

317.   Komajda M, Carson PE, Hetzel S, McKelvie R, McMurray J, Ptaszynska A, Zile MR, DeMets D, Massie BM: **Factors Associated With Outcome in Heart Failure With Preserved Ejection Fraction Findings From the Irbesartan in Heart Failure With Preserved Ejection Fraction Study (I-PRESERVE)**. *Circ-Heart Fail* 2011, **4**(1):27-U73.

318.   Bellenger NG, Davies LC, Francis JM, Coats AJ, Pennell DJ: **Reduction in sample size for studies of remodeling in heart failure by the use of cardiovascular magnetic resonance**. *J Cardiovasc Magn Reson* 2000, **2**(4):271-278.

319.   Liu Y-W, Su C-T, Sung J-M, Wang SPH, Su Y-R, Yang C-S, Tsai L-M, Chen J-H, Tsai W-C: **Association of Left Ventricular Longitudinal Strain**

with Mortality among Stable Hemodialysis Patients with Preserved Left
Ventricular Ejection Fraction. *Clinical Journal of the American Society of
Nephrology* 2013, **8**(9):1564-1574.

320.   Hudsmith LE, Petersen SE, Francis JM, Robson MD, Neubauer S:
**Normal human left and right ventricular and left atrial dimensions using
steady state free precession magnetic resonance imaging**. *J Cardiovasc
Magn Reson* 2005, **7**(5):775-782.

321.   Chirinos JA, Segers P, De Buyzere ML, Kronmal RA, Raja MW, De
Bacquer D, Claessens T, Gillebert TC, St John-Sutton M, Rietzschel ER: **Left
ventricular mass: allometric scaling, normative values, effect of obesity,
and prognostic performance**. *Hypertension* 2010, **56**(1):91-98.

322.   Maceira AM, Prasad SK, Khan M, Pennell DJ: **Normalized left
ventricular systolic and diastolic function by steady state free
precession cardiovascular magnetic resonance**. *J Cardiovasc Magn
Reson* 2006, **8**(3):417-426.

323.   Hirschl MM, Binder M, Herkner H, Bur A, Brunner M, Seidler D,
Stuhlinger HG, Laggner AN: **Accuracy and reliability of noninvasive
continuous finger blood pressure measurement in critically ill patients**.
Crit Care Med 1996, **24**(10):1684-1689.

324.   Imholz BP, Wieling W, van Montfrans GA, Wesseling KH: **Fifteen
years experience with finger arterial pressure monitoring: assessment
of the technology**. *Cardiovasc Res* 1998, **38**(3):605-616.

325.   Myers J, Gujja P, Neelagaru S, Burkhoff D: **Cardiac Output and
Cardiopulmonary Responses to Exercise in Heart Failure: Application**

of a New Bio-Reactance Device. *Journal of Cardiac Failure* 2007, **13**(8):629-636.

326.   Raval N, Squara P, Cleman M, Yalamanchili K, Winklmaier M, Burkhoff D: **Multicenter Evaluation of Noninvasive Cardiac Output Measurement by Bioreactance Technique**. *Journal of Clinical Monitoring and Computing* 2008, **22**(2):113-119.

327.   Squara P, Denjean D, Estagnasie P, Brusset A, Dib J, Dubois C: **Noninvasive cardiac output monitoring (NICOM): a clinical validation**. *Intensive Care Medicine* 2007, **33**(7):1191-1194.

328.   Khan FZ, Virdee MS, Pugh PJ, Read PA, Fynn SP, Dutka DP: **Non-invasive cardiac output measurements based on bioreactance for optimization of atrio- and interventricular delays**. *Europace* 2009, **11**(12):1666-1674.

329.   Guérin AP, Pannier B, Métivier F, Marchais SJ, London GM: **Assessment and significance of arterial stiffness in patients with chronic kidney disease**. *Current opinion in nephrology and hypertension* 2008, **17**(6):635-641 610.1097/MNH.1090b1013e32830dcd32835c.

330.   Pucci G, Cheriyan J, Hubsch A, Hickson SS, Gajendragadkar PR, Watson T, O'Sullivan M, Woodcock-Smith J, Schillaci G, Wilkinson IB *et al*: **Evaluation of the Vicorder, a novel cuff-based device for the noninvasive estimation of central blood pressure**. *J Hypertens* 2012.

331.   Kyle UG, Bosaeus I, De Lorenzo AD, Deurenberg P, Elia M, Gomez JM, Heitmann BL, Kent-Smith L, Melchior JC, Pirlich M *et al*: **Bioelectrical impedance analysis--part I: review of principles and methods**. *Clin Nutr* 2004, **23**(5):1226-1243.

332.	Kyle UG, Bosaeus I, De Lorenzo AD, Deurenberg P, Elia M, Manuel Gomez J, Lilienthal Heitmann B, Kent-Smith L, Melchior JC, Pirlich M *et al*: **Bioelectrical impedance analysis-part II: utilization in clinical practice**. *Clin Nutr* 2004, **23**(6):1430-1453.

333.	Cooper BA, Aslani A, Ryan M, Zhu FYP, Ibels LS, Allen BJ, Pollock CA: **Comparing different methods of assessing body composition in end-stage renal failure**. *Kidney Int* 2000, **58**(1):408-416.

334.	Cornish BH, Jacobs A, Thomas BJ, Ward LC: **Optimizing electrode sites for segmental bioimpedance measurements**. *Physiol Meas* 1999, **20**(3):241-250.

335.	Bleyer AJ, Russell GB, Satko SG: **Sudden and cardiac death rates in hemodialysis patients**. *Kidney Int* 1999, **55**(4):1553-1559.

336.	McIntyre CW: **Recurrent circulatory stress: the dark side of dialysis**. *Semin Dial* 2010, **23**(5):449-451.

337.	Niizuma S, Takiuchi S, Okada S, Horio T, Kamide K, Nakata H, Yoshihara F, Nakamura S, Kawano Y, Nakahama H *et al*: **Decreased coronary flow reserve in haemodialysis patients**. *Nephrology Dialysis Transplantation* 2008, **23**(7):2324.

338.	Foley RN, Parfrey PS, Kent GM, Harnett JD, Murray DC, Barre PE: **Long-term evolution of cardiomyopathy in dialysis patients**. *Kidney Int* 1998, **54**(5):1720-1725.

339.	Bluemke DA, Kronmal RA, Lima JAC, Liu K, Olson J, Burke GL, Folsom AR: **The Relationship of Left Ventricular Mass and Geometry to Incident Cardiovascular Events**. *Journal of the American College of Cardiology* 2008, **52**(25):2148-2155.

340.   Gottdiener JS, Livengood SV, Meyer PS, Chase GA: **Should echocardiography be performed to assess effects of antihypertensive therapy? Test-retest reliability of echocardiography for measurement of left ventricular mass and function**. *Journal of the American College of Cardiology* 1995, **25**(2):424-430.

341.   Chan CT, Arab S, Carasso S, Moravsky G, Li GH, Liu PP, Rakowski H: **Impact of Frequent Nocturnal Hemodialysis on Myocardial Mechanics and Cardiomyocyte Gene Expression / Clinical Perspective**. *Circulation: Cardiovascular Imaging* 2012, **5**(4):474-480.

342.   Liu YW, Su CT, Huang YY, Yang CS, Huang JW, Yang MT, Chen JH, Tsai WC: **Left ventricular systolic strain in chronic kidney disease and hemodialysis patients**. *Am J Nephrol* 2011, **33**(1):84-90.

343.   Yan P, Li H, Hao C, Shi H, Gu Y, Huang G, Chen J: **2D-Speckle Tracking Echocardiography Contributes to Early Identification of Impaired Left Ventricular Myocardial Function in Patients with Chronic Kidney Disease**. *Nephron Clinical Practice* 2011, **118**(3):232-240.

344.   Giannitsis E, Kurz K, Hallermayer K, Jarausch J, Jaffe AS, Katus HA: **Analytical Validation of a High-Sensitivity Cardiac Troponin T Assay**. *Clin Chem* 2010, **56**(2):254-261.

345.   Stewart GA, Mark PB, Johnston N, Foster JE, Cowan M, Rodger RS, Dargie HJ, Jardine AG: **Determinants of hypertension and left ventricular function in end stage renal failure: a pilot study using cardiovascular magnetic resonance imaging**. *Clin Physiol Funct Imaging* 2004, **24**(6):387-393.

346.	Hernan MA, Hernandez-Diaz S, Robins JM: **A structural approach to selection bias**. *Epidemiology (Cambridge, Mass)* 2004, **15**(5):615-625.

347.	Papavassiliu T, Kuhl HP, Schroder M, Suselbeck T, Bondarenko O, Bohm CK, Beek A, Hofman MM, van Rossum AC: **Effect of endocardial trabeculae on left ventricular measurements and measurement reproducibility at cardiovascular MR imaging**. *Radiology* 2005, **236**(1):57-64.

348.	Moore CC, Lugo-Olivieri CH, McVeigh ER, Zerhouni EA: **Three-dimensional systolic strain patterns in the normal human left ventricle: characterization with tagged MR imaging**. *Radiology* 2000, **214**(2):453-466.

349.	Bansal M, Cho GY, Chan J, Leano R, Haluska BA, Marwick TH: **Feasibility and Accuracy of Different Techniques of Two-Dimensional Speckle Based Strain and Validation With Harmonic Phase Magnetic Resonance Imaging**. *Journal of the American Society of Echocardiography* 2008, **21**(12):1318-1325.

350.	Cho GY, Chan J, Leano R, Strudwick M, Marwick TH: **Comparison of two-dimensional speckle and tissue velocity based strain and validation with harmonic phase magnetic resonance imaging**. *Am J Cardiol* 2006, **97**(11):1661-1666.

351.	Gulel O, Soylu K, Yuksel S, Karaoglanoglu M, Cengiz K, Dilek M, Hamiseyev C, Kale A, Arik N: **Evidence of left ventricular systolic and diastolic dysfunction by color tissue Doppler imaging despite normal ejection fraction in patients on chronic hemodialysis program**. *Echocardiography* 2008, **25**(6):569-574.

352.   Koren MJ, Devereux RB, Casale PN, Savage DD, Laragh JH: **Relation of left ventricular mass and geometry to morbidity and mortality in uncomplicated essential hypertension**. *Annals of internal medicine* 1991, **114**(5):345-352.

353.   Zoccali C, Benedetto FA, Mallamaci F, Tripepi G, Giacone G, Stancanelli B, Cataliotti A, Malatino LS: **Left ventricular mass monitoring in the follow-up of dialysis patients: prognostic value of left ventricular hypertrophy progression**. *Kidney Int* 2004, **65**(4):1492-1498.

354.   Harnett JD, Murphy B, Collingwood P, Purchase L, Kent G, Parfrey PS: **The reliability and validity of echocardiographic measurement of left ventricular mass index in hemodialysis patients**. *Nephron* 1993, **65**(2):212-214.

355.   Cheng S, Fernandes VRS, Bluemke DA, McClelland RL, Kronmal RA, Lima JAC: **Age-Related Left Ventricular Remodeling and Associated Risk for Cardiovascular Outcomes / CLINICAL PERSPECTIVE**. *Circulation: Cardiovascular Imaging* 2009, **2**(3):191-198.

356.   Mallamaci F, Zoccali C, Parlongo S, Tripepi G, Benedetto FA, Cutrupi S, Bonanno G, Fatuzzo P, Rapisarda F, Seminara G *et al*: **Diagnostic value of troponin T for alterations in left ventricular mass and function in dialysis patients**. *Kidney Int* 2002, **62**(5):1884-1890.

357.   Liu Y-W, Su C-T, Chou C-C, Wang SPH, Yang C-S, Huang Y-Y, Tsai L-M, Chen J-H, Tsai W-C: **Association of Subtle Left Ventricular Systolic Dysfunction with Elevated Cardiac Troponin T in Asymptomatic Hemodialysis Patients with Preserved Left Ventricular Ejection Fraction**. *Acta Cardiol Sin* 2012, **28**:95-102.

358.   Desai AS, Mitchell GF, Fang JC, Creager MA: **Central Aortic Stiffness is Increased in Patients With Heart Failure and Preserved Ejection Fraction**. *Journal of Cardiac Failure* 2009, **15**(8):658-664.

359.   Laurent S, Cockcroft J, Van Bortel L, Boutouyrie P, Giannattasio C, Hayoz D, Pannier B, Vlachopoulos C, Wilkinson I, Struijker-Boudier H: **Expert consensus document on arterial stiffness: methodological issues and clinical applications**. *Eur Heart J* 2006, **27**(21):2588-2605.

360.   Townsend RR, Wimmer NJ, Chirinos JA, Parsa A, Weir M, Perumal K, Lash JP, Chen J, Steigerwalt SP, Flack J *et al*: **Aortic PWV in chronic kidney disease: a CRIC ancillary study**. *Am J Hypertens* 2010, **23**(3):282-289.

361.   Vlachopoulos C, Aznaouridis K, Stefanadis C: **Prediction of Cardiovascular Events and All-Cause Mortality With Arterial Stiffness A Systematic Review and Meta-Analysis**. *Journal of the American College of Cardiology* 2010, **55**(13):1318-1327.

362.   Kalantar-Zadeh K, Abbott KC, Salahudeen AK, Kilpatrick RD, Horwich TB: **Survival advantages of obesity in dialysis patients**. *The American Journal of Clinical Nutrition* 2005, **81**(3):543-554.

363.   Segers P, Kips J, Trachet B, Swillens A, Vermeersch S, Mahieu D, Rietzschel E, De Buyzere M, Van Bortel L: **Limitations and pitfalls of non-invasive measurement of arterial pressure wave reflections and pulse wave velocity**. *Artery Research* 2009, **3**(2):79-88.

364.   Kracht D, Shroff R, Baig S, Doyon A, Jacobi C, Zeller R, Querfeld U, Schaefer F, Wuhl E, Schmidt BM *et al*: **Validating a new oscillometric**

device for aortic pulse wave velocity measurements in children and adolescents. *Am J Hypertens* 2011, **24**(12):1294-1299.

365.   Bottini PB, Carr AA, Prisant LM, Flickinger FW, Allison JD, Gottdiener JS: **Magnetic resonance imaging compared to echocardiography to assess left ventricular mass in the hypertensive patient**. *Am J Hypertens* 1995, **8**(3):221-228.

366.   Honda T, Yano K, Matsuoka H, Hamada M, Hiwada K: **Evaluation of aortic distensibility in patients with essential hypertension by using cine magnetic resonance imaging**. *Angiology* 1994, **45**(3):207-212.

367.   Zimmerli LU, Mark PB, Steedman T, Foster JE, Berg GA, Dargie HJ, Jardine AG, Delles C, Dominiczak AF: **Vascular function in patients with end-stage renal disease and/or coronary artery disease: a cardiac magnetic resonance imaging study**. *Kidney Int* 2007, **71**(1):68-73.

368.   Bramwell JC, Hill AV: **Velocity of transmission of the pulse-wave: And elasticity of arteries**. *The Lancet* 1922, **199**(5149):891-892.

369.   Fielden SW, Fornwalt BK, Jerosch-Herold M, Eisner RL, Stillman AE, Oshinski JN: **A new method for the determination of aortic pulse wave velocity using cross-correlation on 2D PCMR velocity data**. *J Magn Reson Imaging* 2008, **27**(6):1382-1387.

370.   Mohiaddin RH, Firmin DN, Longmore DB: **Age-related changes of human aortic flow wave velocity measured noninvasively by magnetic resonance imaging**. *Journal of Applied Physiology* 1993, **74**(1):492-497.

371.   Redheuil A, Yu WC, Wu CO, Mousseaux E, de Cesare A, Yan R, Kachenoura N, Bluemke D, Lima JA: **Reduced ascending aortic strain and**

distensibility: earliest manifestations of vascular aging in humans. *Hypertension* 2010, **55**(2):319-326.

372.   Nelson AJ, Worthley SG, Cameron JD, Willoughby SR, Piantadosi C, Carbone A, Dundon BK, Leung MC, Hope SA, Meredith IT *et al*: **Cardiovascular magnetic resonance-derived aortic distensibility: validation and observed regional differences in the elderly**. *J Hypertens* 2009, **27**(3):535-542.

373.   Schlatmann TJ, Becker AE: **Histologic changes in the normal aging aorta: implications for dissecting aortic aneurysm**. *Am J Cardiol* 1977, **39**(1):13-20.

374.   Virmani R, Avolio AP, Mergner WJ, Robinowitz M, Herderick EE, Cornhill JF, Guo SY, Liu TH, Ou DY, O'Rourke M: **Effect of aging on aortic morphology in populations with high and low prevalence of hypertension and atherosclerosis. Comparison between occidental and Chinese communities**. *The American journal of pathology* 1991, **139**(5):1119-1129.

375.   Åstrand H, Stålhand J, Karlsson J, Karlsson M, Sonesson B, Länne T: **In vivo estimation of the contribution of elastin and collagen to the mechanical properties in the human abdominal aorta: effect of age and sex**. *Journal of Applied Physiology* 2011, **110**(1):176-187.

376.   Goh KL, Holmes DF, Lu Y, Purslow PP, Kadler KE, Bechet D, Wess TJ: **Bimodal collagen fibril diameter distributions direct age-related variations in tendon resilience and resistance to rupture**. *Journal of Applied Physiology* 2012, **113**(6):878-888.

377.   Wang JC, Bennett M: **Aging and Atherosclerosis: Mechanisms, Functional Consequences, and Potential Therapeutics for Cellular Senescence**. *Circulation Research* 2012, **111**(2):245-259.

378.   Zieman S, Kass D: **Advanced glycation end product cross-linking: pathophysiologic role and therapeutic target in cardiovascular disease**. *Congestive heart failure* 2004, **10**(3):144-149; quiz 150-141.

379.   McIntyre NJ, Fluck RJ, McIntyre CW, Taal MW: **Skin Autofluorescence and the Association with Renal and Cardiovascular Risk Factors in Chronic Kidney Disease Stage 3**. *Clin J Am Soc Nephrol* 2011.

380.   Jono S, McKee MD, Murry CE, Shioi A, Nishizawa Y, Mori K, Morii H, Giachelli CM: **Phosphate Regulation of Vascular Smooth Muscle Cell Calcification**. *Circulation Research* 2000, **87**(7):e10-e17.

381.   van der Meer RW, Diamant M, Westenberg JJ, Doornbos J, Bax JJ, de Roos A, Lamb HJ: **Magnetic resonance assessment of aortic pulse wave velocity, aortic distensibility, and cardiac function in uncomplicated type 2 diabetes mellitus**. *J Cardiovasc Magn Reson* 2007, **9**(4):645-651.

382.   Edwards NC, Ferro CJ, Townend JN, Steeds RP: **Aortic distensibility and arterial-ventricular coupling in early chronic kidney disease: a pattern resembling heart failure with preserved ejection fraction**. *Heart* 2008, **94**(8):1038-1043.

383.   Watanabe H, Ohtsuka S, Kakihana M, Sugishita Y: **Coronary circulation in dogs with an experimental decrease in aortic compliance**. *J Am Coll Cardiol* 1993, **21**(6):1497-1506.

384.   Bouthier JD, De Luca N, Safar ME, Simon AC: **Cardiac hypertrophy and arterial distensibility in essential hypertension**. *American Heart Journal* 1985, **109**(6):1345-1352.

385.   McIntyre CW, Burton JO, Selby NM, Leccisotti L, Korsheed S, Baker CS, Camici PG: **Hemodialysis-induced cardiac dysfunction is associated with an acute reduction in global and segmental myocardial blood flow**. *Clin J Am Soc Nephrol* 2008, **3**(1):19-26.

386.   Assa S, Hummel YM, Voors AA, Kuipers J, Westerhuis R, de Jong PE, Franssen CF: **Hemodialysis-induced regional left ventricular systolic dysfunction: prevalence, patient and dialysis treatment-related factors, and prognostic significance**. *Clin J Am Soc Nephrol* 2012, **7**(10):1615-1623.

387.   Wesseling KH, Jansen JR, Settels JJ, Schreuder JJ: **Computation of aortic flow from pressure in humans using a nonlinear, three-element model**. *J Appl Physiol* 1993, **74**(5):2566-2573.

388.   Chan C, McIntyre C, Smith D, Spanel P, Davies SJ: **Combining near-subject absolute and relative measures of longitudinal hydration in hemodialysis**. *Clinical journal of the American Society of Nephrology : CJASN* 2009, **4**(11):1791-1798.

389.   Meerwaldt R, Lutgers HL, Links TP, Graaff R, Baynes JW, Gans RO, Smit AJ: **Skin autofluorescence is a strong predictor of cardiac mortality in diabetes**. *Diabetes Care* 2007, **30**(1):107-112.

390.   Hanekom L, Cho GY, Leano R, Jeffriess L, Marwick TH: **Comparison of two-dimensional speckle and tissue Doppler strain measurement**

during dobutamine stress echocardiography: an angiographic correlation. *Eur Heart J* 2007, **28**(14):1765-1772.

391.   Yu Y, Villarraga HR, Saleh HK, Cha SS, Pellikka PA: **Can ischemia and dyssynchrony be detected during early stages of dobutamine stress echocardiography by 2-dimensional speckle tracking echocardiography?** *Int J Cardiovasc Imaging* 2012.

392.   Chan J, Hanekom L, Wong C, Leano R, Cho GY, Marwick TH: **Differentiation of subendocardial and transmural infarction using two-dimensional strain rate imaging to assess short-axis and long-axis myocardial function**. *J Am Coll Cardiol* 2006, **48**(10):2026-2033.

393.   Delgado V, Mollema SA, Ypenburg C, Tops LF, van der Wall EE, Schalij MJ, Bax JJ: **Relation between global left ventricular longitudinal strain assessed with novel automated function imaging and biplane left ventricular ejection fraction in patients with coronary artery disease**. *J Am Soc Echocardiogr* 2008, **21**(11):1244-1250.

394.   Breidthardt T, Burton JO, Odudu A, Eldehni MT, Jefferies HJ, McIntyre CW: **Troponin T for the detection of dialysis-induced myocardial stunning in hemodialysis patients**. *Clin J Am Soc Nephrol* 2012, **7**(8):1285-1292.

395.   Liu YW, Su CT, Wang SP, Yang CS, Huang JW, Hung KY, Chen JH, Tsai WC: **Application of speckle-tracking echocardiography in detecting coronary artery disease in patients with maintenance hemodialysis**. *Blood purification* 2011, **32**(1):38-42.

396.   de Bie MK, Ajmone Marsan N, Gaasbeek A, Bax JJ, Groeneveld M, Gabreels BA, Delgado V, Rabelink TJ, Schalij MJ, Jukema JW: **Left

ventricular diastolic dysfunction in dialysis patients assessed by novel speckle tracking strain rate analysis: prevalence and determinants. *International journal of nephrology* 2012, **2012**:963504.

397.   Wang H, Liu J, Yao XD, Li J, Yang Y, Cao TS, Yang B: **Multidirectional myocardial systolic function in hemodialysis patients with preserved left ventricular ejection fraction and different left ventricular geometry**. *Nephrol Dial Transplant* 2012, **27**(12):4422-4429.

398.   Hothi DK, Rees L, Marek J, Burton J, McIntyre CW: **Pediatric myocardial stunning underscores the cardiac toxicity of conventional hemodialysis treatments**. *Clinical Journal of The American Society of Nephrology: CJASN* 2009, **4**(4):790-797.

399.   Amann K, Breitbach M, Ritz E, Mall G: **Myocyte/capillary mismatch in the heart of uremic patients**. *Journal of the American Society of Nephrology : JASN* 1998, **9**(6):1018-1022.

11. Appendices

11.1. Abbreviations

AD   Aortic distensibility

AGE   Advanced Glycation End-Products

BIA Bioelectrical impedance analysis

BMI   Body Mass Index

BNP   Brain Natriuretic Peptide

BP   Blood Pressure

BSA   Body Surface Area

CABG coronary artery bypass graft

CI   Cardiac Index

CKD   Chronic Kidney Disease

DBP   Diastolic blood pressure

ESRD End-stage renal disease

GFR   Glomerular filtration rate

GLS   Global longitudinal strain

GLSR Global longitudinal strain rate

HD haemodialysis

HLA   Horizontal long-axis (4 chamber view)

IDH   Intra-dialytic hypotension

IHD   Ischaemic Heart Disease

LVEDVI   Left ventricular end-diastolic volume index

LVH   Left ventricular hypertrophy

LVMI Left ventricular mass index

LVSVI Left ventricular stroke volume index

MI   Acute myocardial infarction

MRI   magnetic resonance imaging

NSTEMI Non-ST elevation myocardial infarction

PD Peritoneal dialysis

PP   Pulse pressure

PWV   Pulse wave velocity

RF Radiofrequency

RRT   Renal replacement therapy

RWMA Regional Wall Motion Abnormality

SBP   Systolic blood pressure

SPAMM   Spatial modulation of magnetization

SSFP Steady-state free precesssion

STE Speckle tracking echocardiography

TBW   Total body water

TVI Tissue Velocity Imaging

TDI Tissue Doppler Imaging

VLA   Vertical long-axis (2 chamber view)

11.3. Standard Operating Procedure (SOP) for Bioimpedance analysis with InBody S20

SOP Number: SOP-DHRD/2009/031-05		Title: Standard Operating Procedure (SOP) for Bioimpedance analysis with InBody S20	
Effective Date:	10/09/09	Revision Date:	
Supersedes:	Nil		
Prepared by:	Aghogho Odudu		Date: 10/09/09
Checked by:			Date: 10/09/09
Approved by:	Dr Chris McIntyre – Chief Investigator		Date: 10/09/09

Bioelectrical impedance analysis (BIA) is based on the principle of detecting resistance to low-level electrical current flows through intracellular and extracellular fluid. The analyzer will apply a safe current of 90-4000 µA at a frequency of 1-1000 kHz for 3 minutes. The currents used are imperceptible to the subject but it is **contraindicated if the patient has a pacemaker, or intracardiac defibrillator.** The algorithms built into the software of the analyzer will measure resistance and reactance and calculate fat-free mass separately for each limb and the trunk at several frequencies. The extracellular fluid space will be expressed as a proportion of the estimated TBW. **Measurements are taken at least 5 minutes pre-dialysis and at-least 5 minutes post-dialysis.**

Equipment required

- InBody S20 analyser

- Electrodes

- Biospace Electrolyte tissue

- Power supply

- Biospace printer

Instructions for the BIA analyser

Safety notes:

a. InBody S20 should not be touched with wet hands, nor should it be used to measure a wet body. If water soaks into the equipment, it may cause an electrical shock or corrosions on equipment.

b. This product should always be grounded. Always use a three-pole socket that has ground electrode.

c. Do not operate this equipment if it has a damaged power cord or plug, if it is not working properly, or if it has been damaged.

d. Do not immerse power cord in water or use the equipment near water.

e. Do not touch signal parts for external communication such as the parallel port, a serial port, etc. and a human body at the same time.
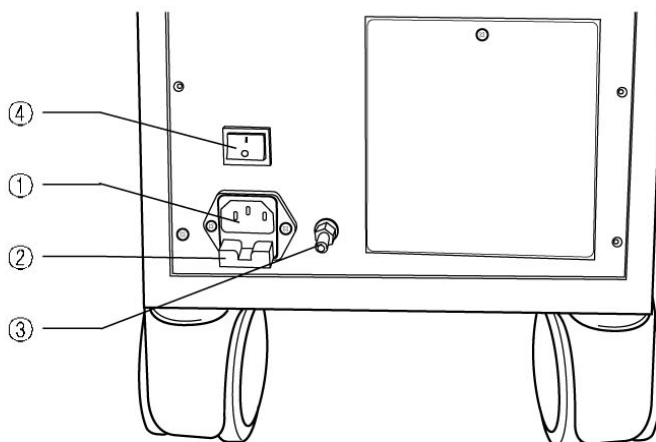
f. Connect ③ in the above picture- the equipotential terminal of InBody S20 to an equipotential line of the medical room. This

protects a patient against an undesirable current that may occur when several devices use the same power source.

g. Individuals with any kind of contagious disease or any kind of injury to the palm or sole must not use or come in contact with this product.

Test procedure

1. Plug the power cable to the mains. If battery is charged it will run without mains. See troubleshooting section for info on battery power display.

2. Turn on at the back. There are 2 switches. The one nearest the floor is for the battery only. The power switch for the analyser itself is at the top. When main power and system switch are turned on, InBody S20 starts **system boot up; this takes 10 minutes, so start before patient arrives or on arrival.**
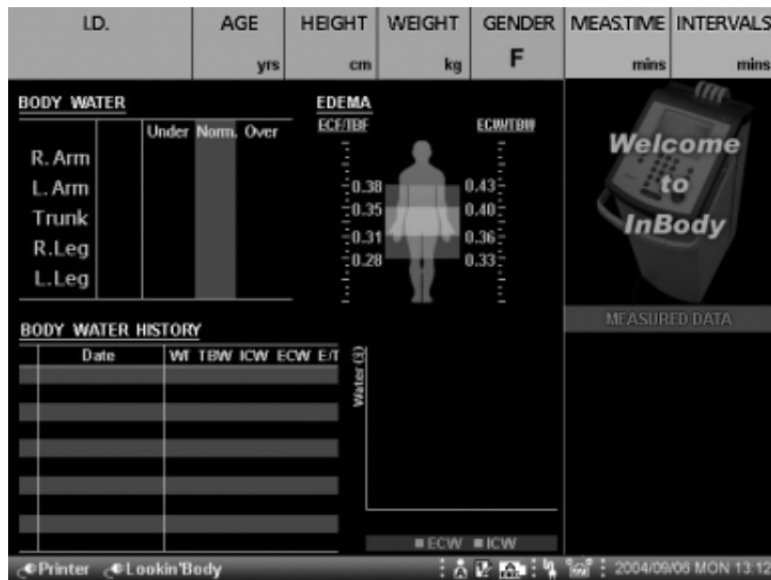
3. When the system boots up, the startup window comes up, allowing you enter data. **If patient is non-caucasian this must be changed in the set-up menu**. Press 'SET-UP' button and choose from asian-african-hispanic-others and be sure to change back after taking post-HD values. Otherwise, the mistake will only be apparent after the analysis is completed on your next patient .

4. **Remove watches/metal/gold chains** from the subject prior to measurement.

5. Clean palms and soles with electrolyte tissue.

6. Attach electrodes (see 'detailed notes on testing methodology' below for position if you are unsure)

7. **Enter patient ID in the form study ID_visit no_pre/post** eg AOBS001v1a for pre-HD and AOBS001v1b for post-HD measure. This is to ensure you don't overwrite your pre-HD value with your post HD-value. Enter ID, Age, Height Weight, and Gender (Female is selected as a default. Use male/female button on panel). **Enter weight and height (cm) and weight (kg)to one decimal place**

8. **Ensure measure time is set at 3 minutes.** 'Intervals' refer to time between test and is 60 mins by default but you will disattach electrodes during dialysis and save post-dialysis values as a new file so this is not relevant.

9. After finishing the data entry, press the 'Enter' button and see the information window prompting the patient to get ready for a test.

10. Check patient position and ask them to relax, maintain posture and avoid flexing muscles for 3 minutes then press ENTER again and testing will commence. **Problems at this stage are usually due to inadequate electrode contacts. Use the electrolyte tissue/alcowipes. Check your contacts.**

11. When testing is complete this is displayed on screen. Results are automatically saved under patient ID.

12. **Check data.** Look at the cole-cole plot at the bottom of the screen to make sure it is a good curve before taking the electrodes off. Also look at the electrical data- ALL the limbs measurement should be in POSITIVE values but you can expect to have SMALLER and occasionally NEGATIVE values for the TRUNK segment. If there is some suspicious data, repeat the measurement.

13. For post-HD values ensure you save under a new file, especially as you will now input the **post-HD weight.**

14. The machine is then switched off at the back.

Data transfer

1. For download of data use USB lead or stick. **The download is of the entire database** of up to 7000 unique IDs**.** Results export as an unlabelled Excel spreadsheet. This can be 'decoded' with our labelled template 'BIA template.xls' on the secure drive S:/cooling study/data/BIA. We have written a macro to link this to our study database for ease of analysis.

2. However **it is imperative to print a results sheet after the test** on the Inbody S20 specific results paper using the biospace printer. The printer cannot be used near the patient and can only be attached when the analyser is off. For this reason printout is best done after the whole study procedure is complete or even the next day. **File the results sheet in the CRF**.

Detailed notes on testing methodology for best results

1. **Data entry**. After entering two digits for age and three digits for height, move on to the next text field. If you want to use the decimal digits for age and height, use the direction buttons (◄) to return to previous fields and enter the values for decimal digits using the 'point' button to the left of '0'. Use backspace key (←) to delete incorrect data. **It is impossible to re-enter data whilst analysis is in progress**. In this case press 'stop'. Re-enter data and start again. Press ENTER when data input is complete.

2. **Position**. Lie subject as close to flat as possible, 30 degrees at the most, with arms and legs stretched out comfortably. Do not leave the arms by the side but form an angle of 15 degree between the arms and the side. Also ask subject to adduct lower limbs by the same angle.

3. **Electrodes** To improve electrical contact, use the biospace branded electrolyte tissue to wet the palms and soles. Don't excessively wet the skin and avoid wetting the leads as this might cause corrosion of the metal.

4. **Use the A type electrode position as illustrated.** The leads are labelled for the

Palm

A type

Red

Black

Red
(Back on third toe of the top of the foot)

Black(The center of the heel)
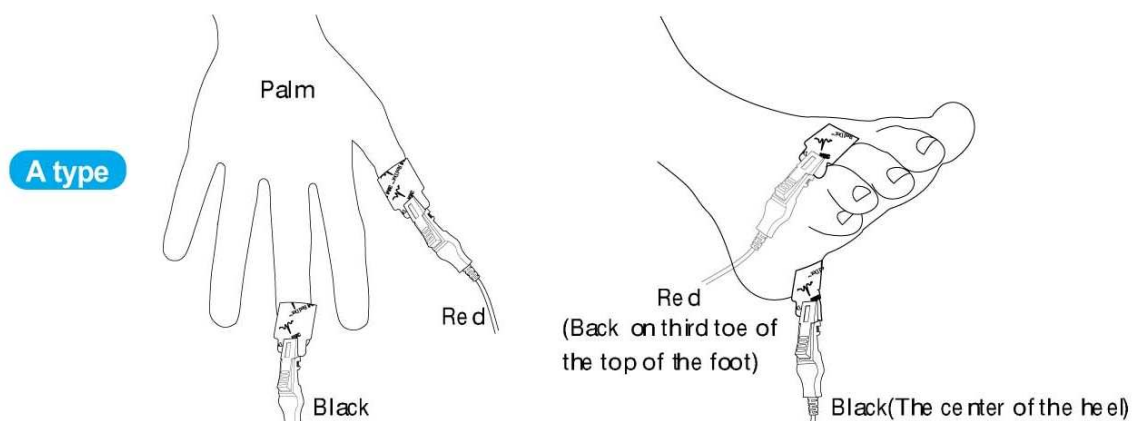
appropriate limb- eg RA=right arm. **Black electrode is placed medial, red lateral in the anatomical position.**

5. **Alternatively use tactile electrodes- this first requires you to change to tactile mode in set-up menu by pressing 'SET-UP' button:**

a. **Hand electrode**. Affix tactile electrode onto the hand as illustrated below, so that metal part of the electrode touches the bottom (palmar surface) of fingers. Put **red electrode (I) to the thumb and black electrode (V) to the middle finger.** Check the mark on the electrode module and use the correct one (RA-Thumb: right thumb, RA-Middle: right middle finger, LA Thumb:left thumb, LA-Middle: left middle finger).
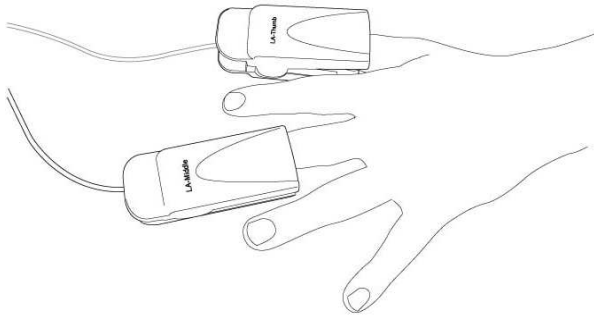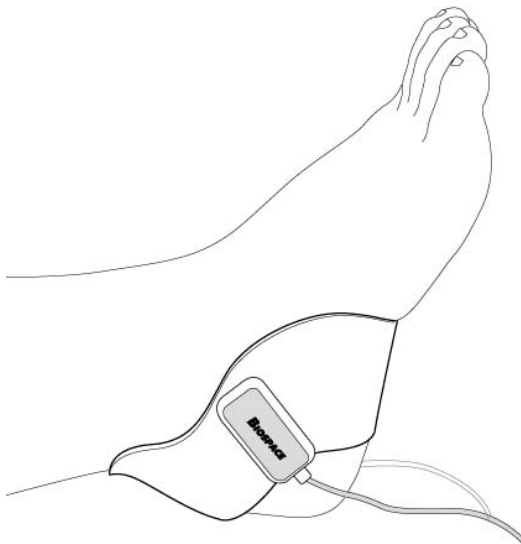
b. **Foot electrode** Affix foot electrode onto the foot like the illustration, in such a way that marked side of the electrode touches the sole of the foot. **Put red electrode (I) to the inner part of foot and black electrode (V) to the outer part.**

6. **Other tips for accurate testing:**

a. Enter the exact height and weight. This can be entered to one decimal place.

b. Keep the room temperature between 20-25 deg C. Subject should warm up for 20 minutes before a test in winter.

c. Wait 2 hours post-meal before testing.

d. Subject should pass water/open bowels before testing.

e. Do not exercise or have a bath before a test.

f. Lie on the back for 5 minutes before a test.

g. Do not have a test while taking diuretic.

h. Avoid having a test during menstruation.

Troubleshooting
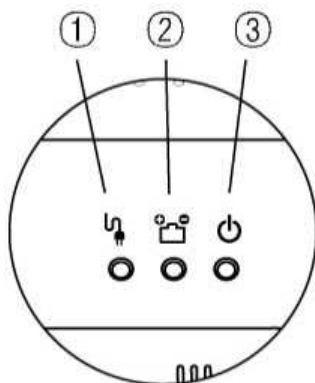
Power indication lamps

The lamp displays the battery conditions of InBody S20, as well as whether the main power and system power are 'On' or 'Off' status.

① Mains- red is on and charging starts.

② Charging indication lamp: shows the charged conditions of InBody S20.

- When it blinks: it indicates that InBody S20 is at low voltage. In this case, the system power will go out automatically if not attached to mains.

- Yellow light: signals that the battery is half charged.

-Green light: signals that the battery is fully charged.

③ Green lamp lights on if system power is turned on.

References

Inbody s20 User's manual.

Company website: www.biospace.kr

Chan C, McIntyre C, Smith D, Spanel P, Davies SJ: Combining near-subject absolute and relative measures of longitudinal hydration in hemodialysis. Clin J Am Soc Nephrol 2009;4:1791-1798.

Contact details for servicing and consumables:

Phillip Middleton

Derwent Healthcare Ltd

Widdrington House

35 South Side

Stamfordham

Newcastle upon Tyne

NE18 0PD

Tel: 01661 886169 - Mobile 07970 384130

11.4. Standard Operating Procedure (SOP) for Finometer measurements

SOP Number: SOP-DHRD/2009/031-04	Title: Standard Operating Procedure (SOP) for Finometer measurements	
Effective Date:	10/09/09	Revision Date:	
Supersedes:	Nil	
Prepared by:	Aghogho Odudu	Date: 10/09/09
Checked by:		Date: 10/09/09
Approved by:	Dr Chris McIntyre – Chief Investigator	Date: 10/09/09

The improved Finapres apparatus, known as the Finometer, measures finger blood pressure noninvasively on a beat-to-beat basis and gives waveform

measurements similar to intra-arterial recordings. The Finometer measures brachial pressure and corrects for finger pressure accordingly. It also corrects for the hydrostatic height of the finger with respect to the heart level. Do take care not to damage the delicate finger cuffs which cost over £300 each to replace.

Instructions for setting up the finometer

2. Ensure switched on at the mains

3. Press rocker switch at the back to On

4. On the front panel, press finometer "research" button twice

5. Press "mark" to confirm and go

6. Insert gender, age, height and weight using direction arrows so that the

7. correct values are highlighted in orange.

8. Press "describe subject" to confirm changes

9. Place BP cuff on arm as accurately as possible with arterial marker over brachial artery.

10. Attach Finometer unit to wrist with the Velcro straps.

Finometer Front-End Unit

11. The main components of the finger cuff are an inflatable air bladder, and a plethysmograph consisting of a light source (infrared light light-emitting diode) and a light detector (infrared photodiode). These appear as two circular dots on

the inside of the cuff. The air bladder is connected to the front-end unit via an air hose and both components of the infrared plethysmograph via a cuff cable. The front-end unit is connected to the main unit and pump unit in the Finometer. Place appropriately sized finger cuff on middle finger ideally but any finger will do. Ensure the laser "spots" are parallel with each other, that the attachments emerge from the proximal end of the cuff and that the cuff is snug but not too tight.

12. Attach connections from finger cuff to the front-end unit

13. Press the two height sensors together and press mark to calibrate the

14. sensors and ensure the "hite" is reading 0 or below

15. Attach the rectangular sensor to the finger cuff and the round sensor to the arm BP cuff

16. Warn the patient they will be aware of the finger cuff inflating and deflating

17. Press "start"

18. After approximately 2 minutes, perform a return-to-flow "RTF" calibration:

a. Move highlighted orange box across the screen to highlight the RTF box

b. Using direction arrows highlight "ramp" in orange

c. Press "RTF" button, arm BP cuff should inflate and you will be informed that the RTF calibration has been successful. This gives more accurate values of the Fimoneters outputs.

19. Ask nurse/technician to insert the needles into AV fistula or attach lines to commence dialysis and press "mark" to mark the trace after a period of pre-dialysis monitoring. You should also mark the trace at the start of the 225 min intra-dialytic and the 15 min post-dialytic echocardiography recording.

20. Once you have finished recording, press stop.

Instructions for downloading the finometer outputs

The Finometer traces are analysed through the Beatscope software, this can be installed on any laptop with admin rights. It is also installed on the laptop in the research office known as the "brick".

1. Ensure the computer and Finometer are attached to the mains and switched on

2. Open Beatscope software

3. Select "finometer" with the mouse

4. Select "download"

5. Ensure correct directory for storage of the information has been selected in the left hand column.

6. Highlight files in right hand column that you wish to download

7. Click on "<" button to start downloading

8. Once downloading has finished:

9. Click on "x" in the top right corner to close the screen

10. Click "yes" to confirm closing the download

11. Close Beatscope

12. Rename file in the format studyID_fino_visitnumber, eg AOBS006_fino_v1

13. Transfer file to Derby Hospitals NHS FT secure drive folder path:

The Effects of Cooling The Dialysate on Systolic Dysfunction in Haemodialysis Patients/Data/Finometer Data

References

Schutte, A. E., H. W. Huisman, et al. Validation of the Finometer device for measurement of blood pressure in black women *J Hum Hypertens* 2004 **18**(2): 79-84

11.5. Standard Operating Procedure (SOP) for Pulse Wave Velocity (PWV) Measurements using the Vicorder®

SOP Number: SOP-DHRD/2009/031-04	**Title: Standard Operating Procedure (SOP) for Pulse Wave Velocity (PWV) Measurements using the Vicorder®**

Effective Date:	10/09/09	**Revision Date:**	
Supersedes:	**Nil**		
Prepared by:	**Aghogho Odudu**		**Date: 10/09/09**
Checked by:			**Date: 10/09/09**
Approved by:	**Dr Chris McIntyre – Chief Investigator**		**Date: 10/09/09**

Aim: The purpose of this test is to determine a measurement of arterial stiffness by calculating Carotid-femoral pulse wave velocity (PWV).

Equipment needed:

- Vicorder
- Neck cuff
- Thigh cuff
- Laptop with 2 USB ports or a USB hub
- Red and Blue Inflation tubing
- Measuring tape (preferably metal so as not to stretch over time)

- Vicorder software installed on a password protected NHS trust notebook computer

Intialisation

1. Plug in the 2 USB leads from the Vicorder into the laptop

2. Turn on the laptop after the USB leads are plugged in.

3. Open and minimise Vicorder software (version 3.2.3483.15471)

4. From the Quick Launch window on the right of the screen select PWV with the mouse

Aortic pulse wave velocity measurement using the neckpad

The Patient should be in a semi-prone position with the head and shoulders raised by approximately 30 degrees, this should prevent Venous contamination of the Arterial signal. 30°

The Neckpad is placed around the Patients neck with the pressure pad over the right Carotid area.

…...and secured with the Velcro fixing, do not over-tighten. Remind the patient this will inflate so may be uncomfortable but to a very low pressure (less than 30mm Hg).

A cuff is placed around the Patients upper right thigh.

Both Neckpad and thigh cuff are connected to the Vicorder (Red cuff- carotid (proximal),

Blue cuff- femoral.
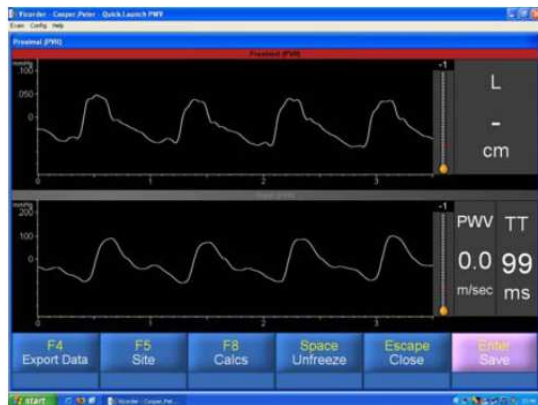
1. Measure the distance between Supra-Sterna Notch and thigh cuff in centimetres and enter via the Calcs button (F8).

2. Warn the subject about the inflation again, then inflate the cuffs, by pressing the space bar, adjust the displayed waveforms for amplitude if required (let run for at least 4 runs).

3. Acquire several steady pulses of data and freeze.

4. Pulse Wave Velocity and Transit Time are displayed (but not stored).

5. Record the PWV onto the case report form.

6. Press Enter to save the data, you will be prompted for a filename and it will export as a comma separated file which can be uploaded into Microsoft acces, excel or SPSS. The filename should be saved in the format study ID_PWV_Visit No eg AOBS009_PWV_v1.csv

7. After the study procedures are completed the file should then be transferred onto the Derby Hospitals NHSFT secure server in the appropriate vicorder data folder and removed from the operators laptop.

Troubleshooting

.

Note : If the Jugular Vein is particularly active (example on the upper trace) make sure the Patient is at 30°, if so ask the Patient to take a deep breath, exhale and hold. Take the measurement during the held breath.

References:

Davis,B. Aortic Pulse Wave Velocity measurement using the Vicorder (January, 2008). Skidmore Medical Ltd, Bristol, UK.

11.6. Standard Operating Procedure (SOP) for Magnetic Resonance Imaging

SOP Number: SOP-DHRD/2009/031-07	Title: Standard Operating Procedure (SOP) for Magnetic Resonance Imaging	
Effective Date: 15/03/2011	Revision Date:	
Supersedes:	Version 4, 1/02/2011	
Prepared by:	Aghogho Odudu, Tarek Eldehni, Rachel Hall and Kathryn Appleyard, Gerry McCann	Date: 15/03/11
Checked by:	Aghogho Odudu	Date: 15/03/2011
Approved by:	Dr Chris McIntyre – Chief Investigator	Date: 15/03/2011

Aim: The purpose of this test is:

(1) To record magnetic resonance images that allow geometric and strain measurements of the heart, using standard cine imaging and myocardial tagging

(2) To allow assessment of ventricular-arterial coupling by measuring aortic distensibility and aortic-pulse wave velocity

Prerequisites:

Studies will occur on standardised post-midweek haemodialysis day at a single centre (Nuffield Hospital Derby) using a 1.5T scanner (GE Signa HDxt 1.5T, GE Healthcare, Milwaukee,US)

Participant arrives:

309

MRI safety questionnaire (see appendix) is completed only by trained personnel.

Cardiac geometric imaging protocol:

1. Serial contiguous short axis cines will be piloted from vertical or horizontal long axis of the LV and RV, LVOT and RVOT.

2. Using ECG-gated, FIESTA 2D CINE sequence; TR 45ms, TE 1.7 ms, -FA60°.

3. Short axis images acquired at slice thickness 8mm, with no spacing from apex to base of LV (below level of mitral valve) using validated methodologies (Maceira 2006).

4. Matrix 256 x 160, Smallest FOV possible , typically 320mm x 320mm, Nex 1.

Myocardial tagging protocol:

1. Using Prospective ECG-gated, FastCARD Gradient-Recalled Echo sequence

2. Asset enabled

3. 8-mm slice thickness.

4. 3 tagged short-axis images parallel to the cine sequence, equally spaced from LV base (full disc in all phases) to mid-papillary level to apex (full blood pool visible in all phases), hence spacing between slices depends on length of LV, typically 6-12mm.

5. A grid-tag is applied with spatial SAT pulses throughout the FOV using a SPAMM technique. Tag separation of 7mm, TE 3.1 msec with matrix 256x160, Nex 1, flip angle _ 12°.

6. "Number of cardiac phases to reconstruct" se to 30.

7. Maximum 10 views per segment. **If HR >65 decrease to 6-8. If HR<55 consider increase to 12-14 to achieve breath-hold of 14 secs or less**

8. 2 long axis-tag views in HLA (4 chamber view) and VLA (2 chamber view)

Cine phase-contrast sequence

1. Short breath-hold (<14 secs) FIESTA Cine sequence acquired in oblique sagittal plane to demonstrate the full length of the aorta.

2. Axial Short breath-hold (<14 secs) FIESTA Cine to measure distensibility with the following parameters: 30° flip angle, 5-mm slice thickness, 280x280-mm field of view (or smallest possible), 6.7 repetition time, 256 x256 matrix.

3. Phase contrast sequence (PCMRI) is set up FREE- BREATHING (4-6 mins depending on RR) with the following parameters: 30° flip angle, 5-mm slice thickness, 280x280-mm field of view, 6.7 repetition time, 256 x256 matrix, 2 excitations, and **through-plane velocity encoding starting at 200cm/s**, with **1 view per segment and "No of views to reconstruct" 100**.

References

Maceira et al. Normalized left ventricular systolic and diastolic function by steady state free precession cardiovascular magnetic resonance. J Cardiovasc Magn Reson 2006; 8: 417-426.